THE NATURE AND CAUSES OF COASTAL LANDSLIDING ON THE MAUNGATAPU PENINSULA, TAURANGA, NEW ZEALAND.

A thesis submitted in partial fulfilment of the requirements for the Degree of Master of Science in Earth Sciences

at the

University of Waikato

by

GERARD ANTHONY BIRD

'Upokokohua, haere atu i oku whenua!'

A frontal view of the landslide scar behind the Anglican church on Te Hono st., Maungatapu (Site 1).

ACKNOWLEDGEMENTS

I would like to acknowledge the assistance of the following people in the preparation of this thesis.

Firstly, thanks to my supervisor, Professor M.J. Selby, for suggesting the research topic, and for his helpful suggestions and criticisms of the draft text.

To Craig Law for his help and advice in starting the study, and for introducing me to the art of 'crashing' the PDP 11/70. Also to Lyn Prentice for his invaluable help in the writing of JANBU.SMP.

To David Lowe, Peter Singleton, and Kieran Bird for their help in the field, Mr & Mrs C.F. Whiteman and Mr & Mrs W.H. Nielson for the use of their land, and to Mr & Mrs J.G. Corston for their five star accommodation.

To Dr W.A. Pullar for his advice on stratigraphy, and to Dr I. Smalley for his enthusiasm.

To Tony Petch and Tony Phipps for their comments, to my mother for proof reading, to Elaine Norton for typing the tricky bits and to Mrs Christobel White for her oddfellows and Courier 10 golfball.

And finally to Lynda, without whom this thesis might not have been started (and to the staff of the Turquoise Lounge, without whom it might have been finished a little earlier).

ABSTRACT

Lengths of cliffed coastline in Quaternary sediments around Tauranga Harbour, and particularly on the Maungatapu Peninsula, have been subjected to major landsliding episodes during and after rainstorms in recent years. This study is intended to broaden the database concerning coastal landsliding by documenting a descriptive and analytical study of the landslides, and to provide information useful for those attempting to control the effects of the landslides.

A field mapping project was undertaken, associating patterns of landslide scars, marine erosion and groundwater seepage from cliff faces. More intensive studies at three sample sites included surveying, soil strength and physical index testing, hydraulic conductivity determinations and groundwater table observations. A number of working hypotheses, concerning the nature and causes of the landslide events, are erected and tested using the results of these descriptive studies. The hypotheses are further evaluated in factor sensitivity studies, using a simplified Janbu slope stability analysis program, which was written as part of the study.

It has been found that the landslide events occur as parts of one of two cliff evolutionary sequences observed on the Maungatapu Peninsula. Where the rate of basal erosion by tidal currents and wind driven waves exceeds the rate of cliff crest retreat due to various cliff face modifying processes, the cliff segment gradually steepens. Failures in the material above an impermeable clay bed in the Pahoia Tuffs are triggered by high pore water pressures. Critical pore water pressures occur when long wet periods, culminating in medium to long return period storms, produce high seepage flows through the sandy material above the impermeable clay bed. The failures initially occur in a rotational manner, apparently causing the liquefaction of a bed of low bulk density silty sand lenses within a denser sandy mud matrix. Subsequent movements are therefore rapid and translatory, producing elongate annular debris lobes extending from the cliff base.

The results of the study are then applied in formulating coastal management strategies, and in suggesting appropriate site stabilisation techniques.

TABLE OF CONTENTS

LIST OF FIGURES

Figure

Figure

LIST OF TABLES

LIST OF SYMBOLS

a	area, shear force distribution factor
a_r	area of head of triaxial ram
B.D.	bulk density
C	a constant
Cy	clay
C'	effective cohesion
d	depth
D	vane width
dx	width of slice
e	strain
E	normal interslice force (in Morgenstern and Price method)
F	factor of safety
f_o	shape correction factor
f(x)	arbitrary mathematical function
h	height
H	vane height
hc	depth of tension cracking
H_T	height above failure surface of line of thrust (in Morgenstern and Price method)
K	hydraulic conductivity
L	length
L.L.	liquid limit
n	sample group size
N_1	effective cohesion
N_2	effective internal friction angle
N_3	height of groundwater table above failure surface
P.D.	particle density
P.I.	plasticity index
P.L.	plastic limit
Q,q	normal force on slice side, due to free water in a tension crack
q_u	unconfined compressive strength
q_{ur}	unconfined compressive strength of remoulded material
r	unknown constant, regression coefficient, radius
S	sand
S_t	sensitivity
T	torque, interslice shear force (in Morgenstern and Price method)
u	pore water pressure
V	degrees of freedom
W,w	weight

x	independent variable
y	dependent variable
Y	measured dependent variable
$\bar{y}$	average dependent variable
$\bar{Y}$	average dependent variable, predicted by equation
z	silt, height of groundwater table above failure surface
α	slope angle
α_T	angle of line of thrust (in Morgenstern and Price method)
β	an angle
γ	unit weight
γ'	effective unit weight
θ	direction of interslice forces (in Morgenstern and Price method)
σ_1	major principal stress
σ_2	intermediate principal stress
σ_3	minor principal stress
σ_r	σ_2 and σ_3, when these are equal
ϕ'	effective angle of internal stress

CHAPTER ONE

Introduction

Landslide: "The group of slope movements wherein shear failure occurs along a specific surface or combination of surfaces."

Schuster (1978)

INTRODUCTION

During the period 19-20 March, 1979, the Tauranga basin experienced heavy rain, peaking in intensity between 1630 and 1800 hours on the 19th, with a total of 75 mm precipitation being recorded at Tauranga airport over this 90 minute period. As a result of the storm, more than 100 landslides were reported within the Tauranga City area (Unpublished T.C.C. report). Most of these slides were shallow debris-flow type events (Varnes, 1975) occurring in road or section cut-and-fill sites. Several of the landslides, however, were of a distinctive nature, being relatively large and deep seated and occurring in more or less undisturbed coastal cliff sites along the Maungatapu peninsula.

These landslides occurred in the upper part of the cliff profiles, typically producing a cliff edge retreat of 0.3 to 2 metres across arcuate crowns, and had a distinctive shelf-like feature at 6 to 8 metres below the main scarp (fig. 1.1). Recent landslide scars of similar form may be observed about the harbour on the Matapihi, Te Puna, and Pahoia peninsulas, as well as on Motuhoa island (fig. 1.2). A series of landslides similar in form but on a larger scale, with about three times the scarp height and cliff-edge retreat, were noted on Omokoroa peninsula following intense rain during August 1979 (Gibb, 1980). This group of distinctively shaped landslides observed along the coast of the Tauranga Harbour, and more particularly the Maungatapu peninsula, is the object of this study.

REASONS FOR STUDY

An important feature to be observed in the geomorphological literature of the past twenty years is the ever increasing emphasis on practical applications (eg. Coates, 1976; Cooke and Doornkamp, 1974; Hails, 1977; Jones, 1980, amongst others). This is consequent not only on an awareness of a need for social relevance among geomorphologists, but also on the advent of logical positivist thinking within the field. Mainstream logical positivism holds that phenomena may be explained on the

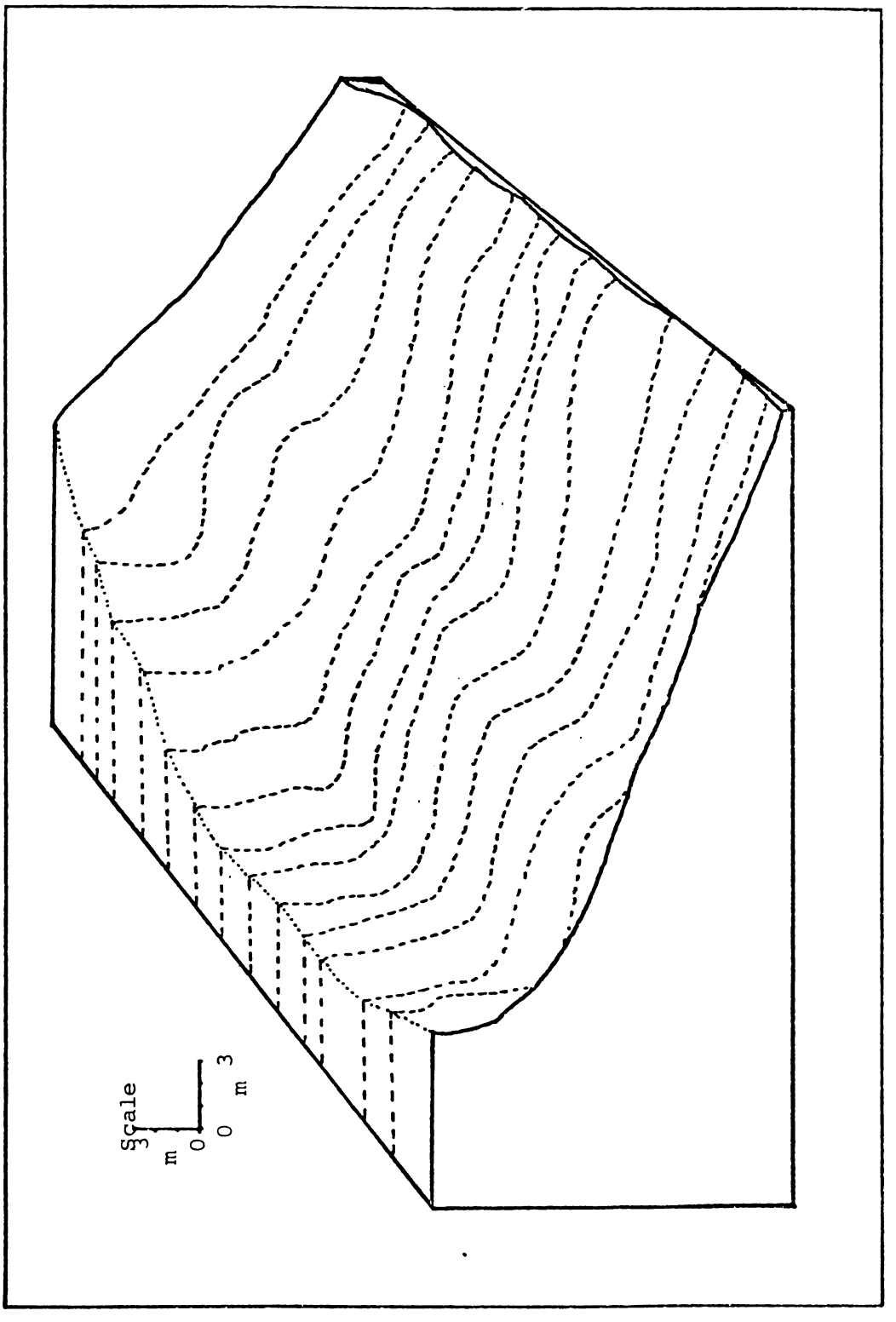

Figure 1.1. Block diagram of site 1.

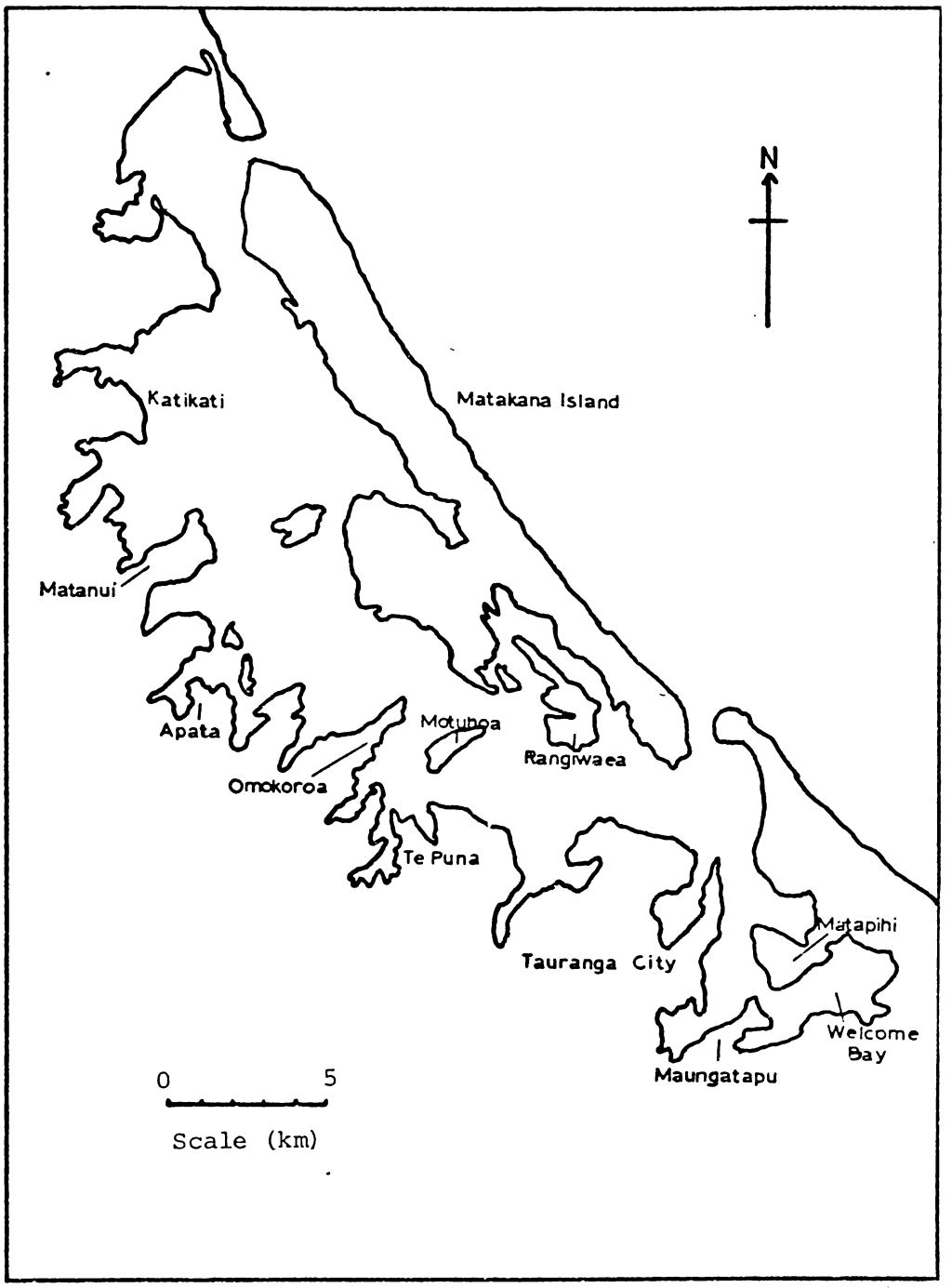

Figure 1.2.Locality map of the Tauranga Basin.

basis of regular observations of association. The search for causal mechanisms behind such empirically observed relationships is a functionalist derivative of this central tenet (Kraft, 1953). This rise in "process-realist" thinking (Keat and Urry, 1975) as a basis for geomorphological theory has brought implicit changes in attitude to spatial-temporal scales of study as well as modifying the aims and objectives of geomorphology. This mode of thinking became apparent in the "quantitative revolution" of the 1960s and 1970s.

In the field of slope stability studies this change in aims has manifested itself, in part, as an awareness of the need to reliably quantify the stability of slopes. In many, if not most cases, this is still not possible (Peck, 1967). Hovland (1977) has suggested that the establishment of a database of analytical case studies would be necessary to achieve this end. The present study is intended to extend the present, rather limited, quantitative database concerning coastal landslides. The spatial-temporal scale connotations of the problem in this context will be considered in the discussion of methodology below.

On a more pragmatic theme it may be noted that, while individual landslides are not perhaps as destructive as other natural catastrophes such as earthquakes or major floods, they are somewhat more widespread and frequent. Hence landslides are probably responsible for greater

financial loss than any other single geological hazard. Schuster (1978) estimated landslide related losses in the U.S.A. exceed US$1000 million p.a.. In New Zealand recent landslides have caused millions of dollars worth of damage to roads and buildings, with events such as those which occurred at Omokoroa and Abbotsford gaining widespread publicity. There is consequently an increasing local awareness of the need to gain a better understanding of landslides as rectifiable or predictable engineering phenomena (e.g. Taylor et.al., 1977).

The coastline of the Tauranga harbour is a popular location for holiday and retirement homes, and cliff-top sections commanding good views are in strong demand. Large numbers of expensive dwellings now appear on the ever-increasing length of subdivided cliff coastline. Recent publicity attracted by the landslides distributed along this coastline has therefore generated a desire for an ablity to predict their occurrence and/or mitigate their effects.

AIMS OF STUDY

The problem then may be defined as being in the field of applied geomorphology, concerned primarily with a process, through, and with, its causes and effects. The reasons for the study are:

i) to increase the body of information concerning the nature of coastal landslides;

ii) to decrease the vulnerability of local residents to individual cliff failures.

The aims implicit in these directions are:

i) development of an understanding of the landsliding process, its nature, causes and effects;

ii) development of a physical model of landslide prediction and/or development.

METHODOLOGY

The achievement of these overlapping aims involves three main steps (modified from Skempton and Hutchinson, 1969);

1) detailed description of the failures;
   a) classification by movement, rate, and type;
   b) quantification of the properties of the materials involved;
   c) determination of space-time patterns and associations;
2) establishment of a failure model utilising this data;
3) evaluation of the significance of relevant variables using the model, followed by comparison with the initial data.

Two interrelated assumptions implicit in this outline must be considered. The first involves investigative scale; the second is concerned with the place of working models or hypotheses in the project design.

Schwartz (1968) made a threefold division in timescales when considering beach erosion, listing microscale (minutes), macroscale (one week to months), and megascale (tens of thousands of years). This division illustrates the philosophical dichotomy in geomorphology, discussed previously, which has had its most marked effect on investigative scales.

Early work in geomorphology was almost entirely concerned with landforms at the landscape scale (Mark, 1980), but the trend towards quantified, process oriented studies has brought a move towards small scale studies.

Model developement therefore proceeds on two levels. At the landslide site scale, factors promoting or opposing movement are investigated. On the landscape scale, spatial and temporal disparities in processes are related to postulated slope evolution sequences. Process models are thus approached from both "cause" and "effect" directions.

A further group of microscale studies distinguishes data obtained from small samples, often concerning events on the scale of millimetres or less. The familiar question of the statistical significance of microscale results and models to site-scale modelling is discussed in Chapter Four.

This question is analagous to the problem of developing site-scale process-response models from landscape scale investigations. A major drawback is experienced in the difficulty of gaining adequate temporal coverage for full macroscale investigation (Carson and Kirkby, 1972). Estimates of adequate time periods for such studies range from one hundred years (Brunsden and Jones, 1980), to tens of thousands of years (Schwartz, 1980), depending on the local geology. Savigear (1952) suggested the use of study locations where space may be substituted for time; however this is rarely practical. If one assumes the spatial distribution of a variable to be the same as its temporal distribution (Harvey's, (1969) ergodic hypothesis), a realistic approximation of long term coverage may be obtained. The implicit assumption, that all slopes within stipulated groups follow the same evolutionary sequence, albeit possibly at different rates, must be recalled as a possible source of error in susequent arguments.

In summary:

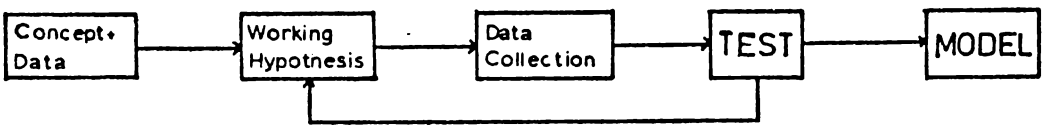

Rather than obtaining all data which may appear pertinent to a problem, according to previous experience, it is usual in geotechnical investigations, as in other

scientific work, to use a system of multiple working hypotheses. The most readily ascertained (usually descriptive) data are first obtained and, within constraints imposed by these data, a series of reasonable hypotheses, as to the nature of the problem, may be erected.

On the basis of these hypotheses, a directed data collection programme may be initiated, with constant re-examination of the hypotheses in the light of new information (fig. 1.3). A combination of the concepts discussed above, applied to a slope stability investigation such as this may be expressed as in fig. 1.4:

The earth science literature concerning the study area, as well as that discussing investigations similar to the present study will be reviewed in Chapter 2. Landscape and site scale studies will be presented in Chapter 3, while microscale and quantitative site scale investigations will be discussed in Chapter 4. Quantitative evaluation of suggestions based on data thus obtained will be carried out utilising a slope stability analysis model in Chapter 5, and the results will be summarised and related to practical applications in Chapter 6.

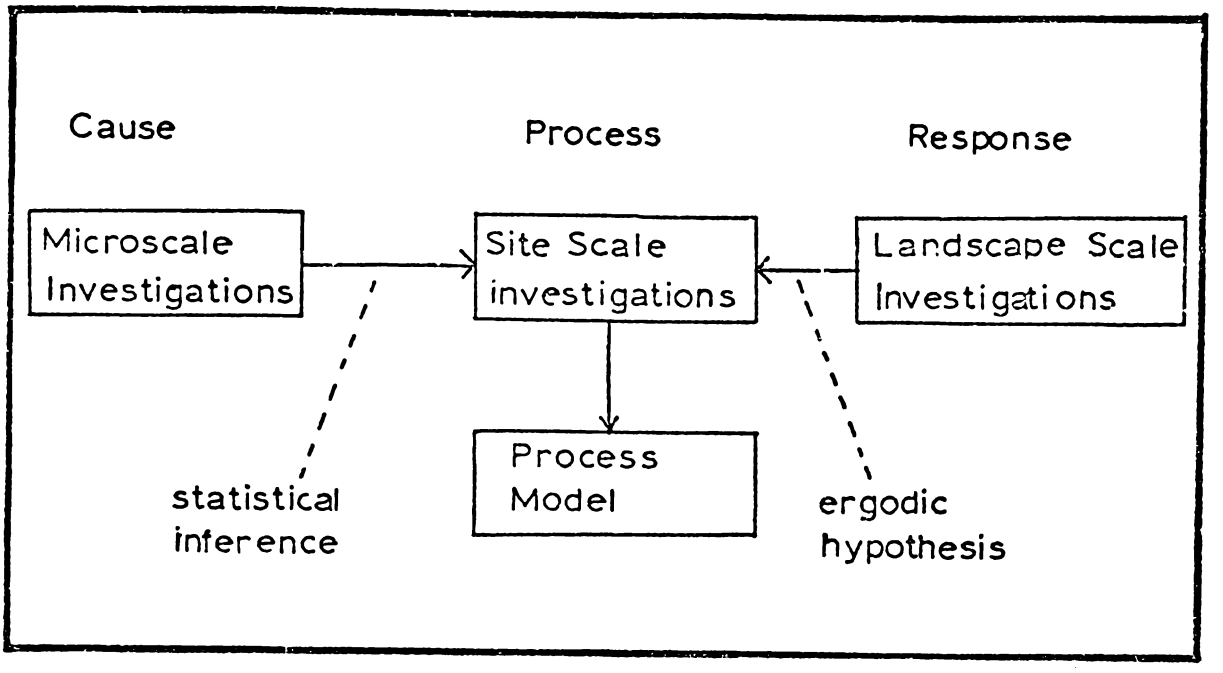

Figure 1.3. Conceptual framework of geomorphological investigations.

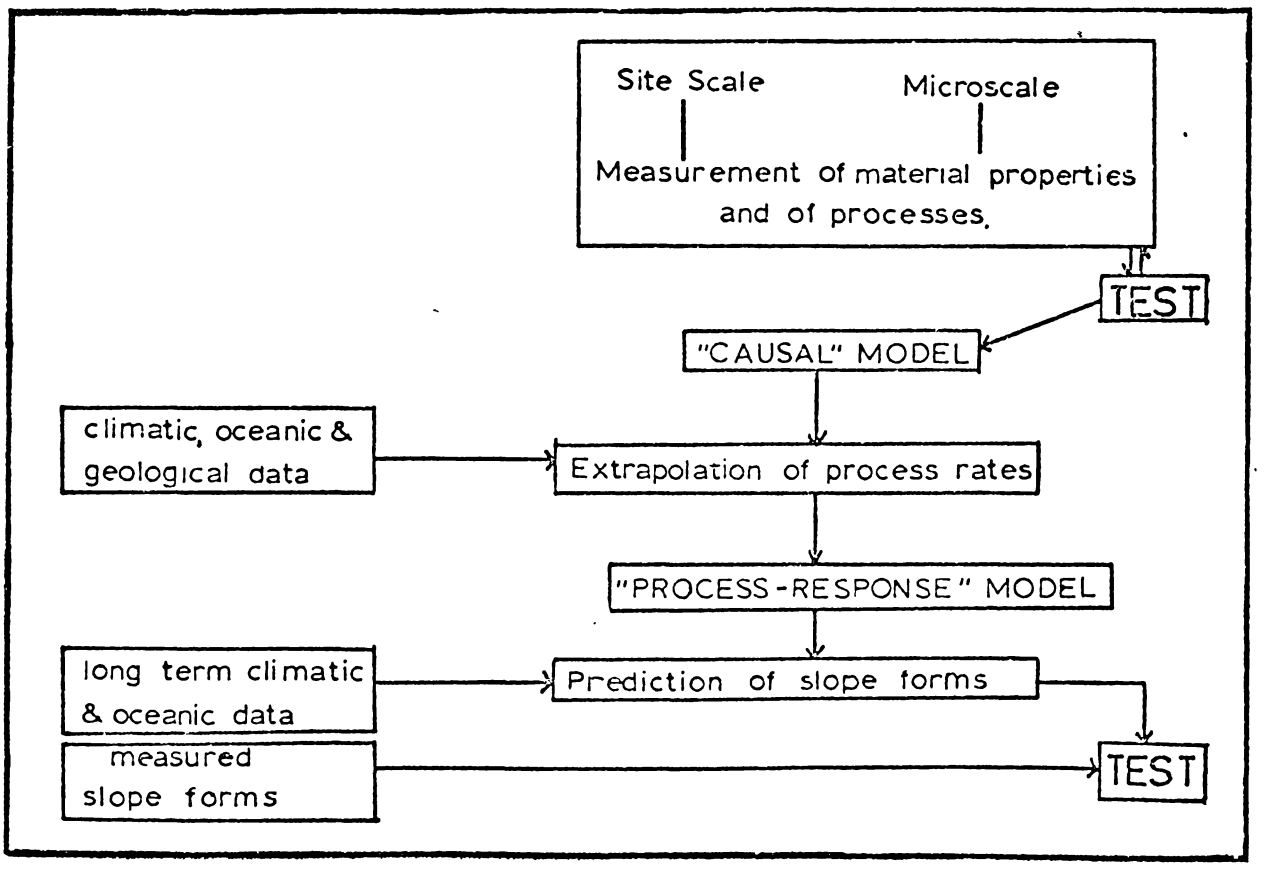

Figure 1.4. Development of predictive models.

CHAPTER TWO

Study Area Description and Literature Review

GEOLOGY

The Tauranga basin is a downfaulted north-easterly dipping faulted block (Henderson and Bartrum, 1913). It is assumed to be tectonically stable (Chappell, 1975; Kear and Waterhouse, 1961), although suggestions of subsidence have been made (Schofield, 1968; Wellman, 1962), supported by observations of infilling of the Waikareao estuary (White, 1979). The upper Cenozoic geology of the basin is dominated by the influences of the nearby Indian-Pacific plate boundary magmatic arc. Geological mapping has only been carried out on a regional scale thus far, although more detailed work is at present under way (Houghton pers.comm.) (fig. 2.1).

The stratigraphic column of the Tauranga basin may be broken down into four main sections (fig. 2.2):

i) a Mesozoic greywacke basement,

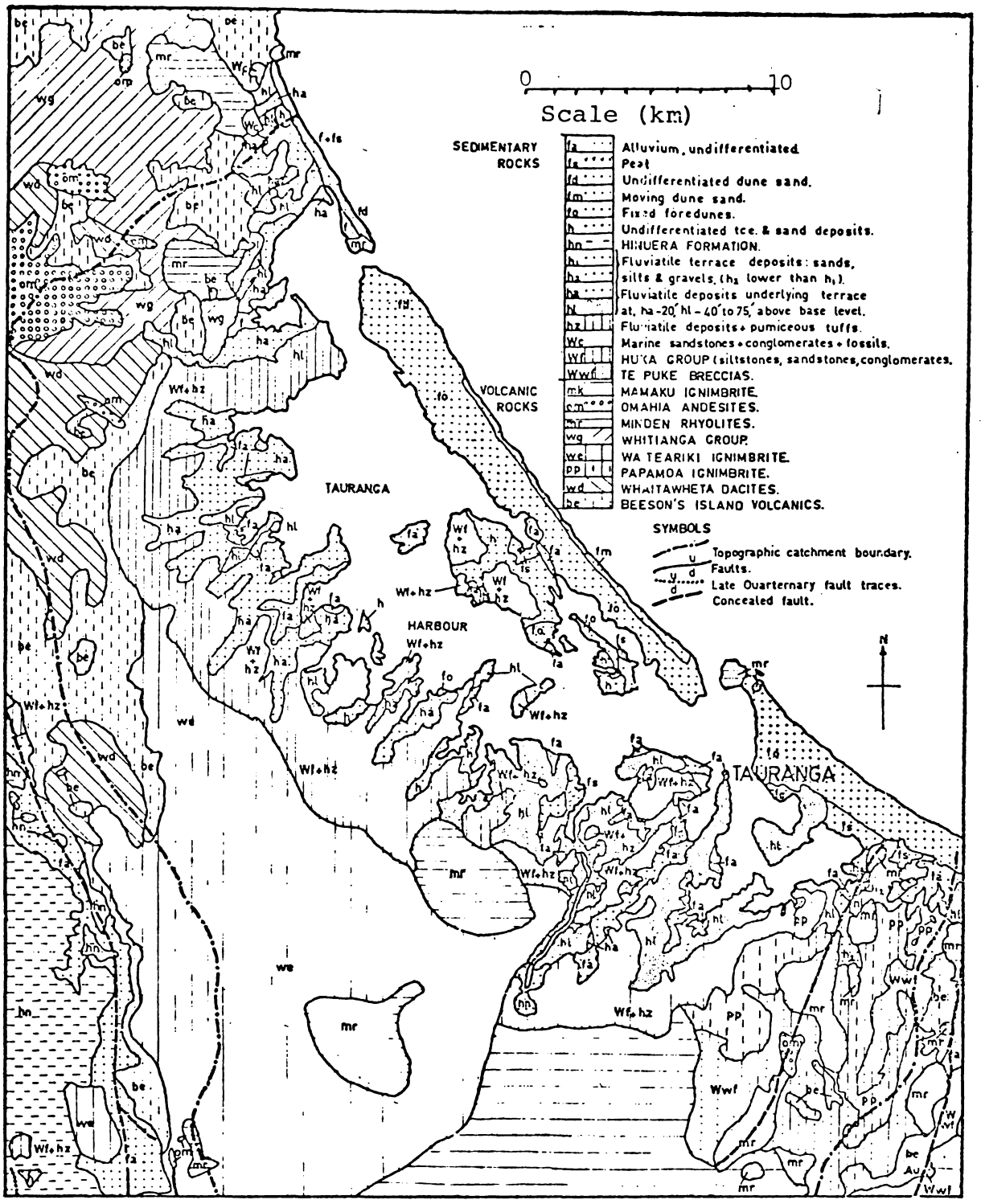

Figure 2.1. Geology of the Tauranga Basin.

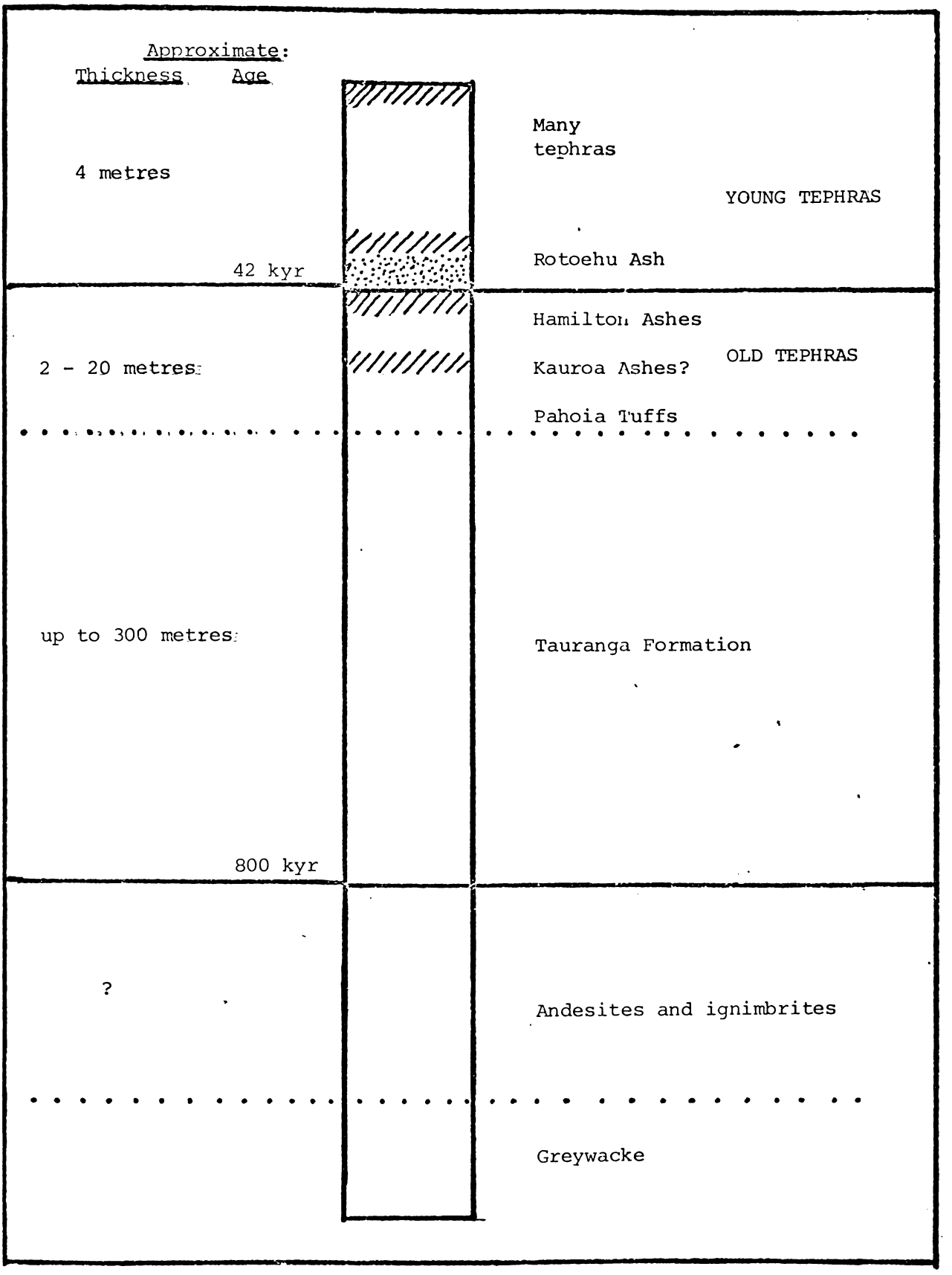

Figure 2.2. Stylised stratigraphic column of the Tauranga Basin.

ii) Miocene and Lower Pleistocene volcanic rock cover,

iii) an onlapping cover of Mid to Upper Pleistocene sediments, tuffs and tephras,

iv) a blanket cover of Upper Pleistocene and Holocene tuffs and tephras.

The basement rock in the Tauranga basin consists of north-easterly dipping Jurassic greywackes of the Waipapa terrane (Sporli, 1978), bounded to the west by the Hauraki Fault, and to the south by the Taupo-White Island depression. No structure other than folding has been observed in the greywacke.

Over this basement lies a series of Mio-Pliocene dacites, rhyolites and ignimbrites. Outcrops of Lower Pleistocene Minden rhyolite occur at Mount Maunganui and Bowentown Heads, and two ignimbrites; the Wai-Te-Ariki (Healy et al., 1964) and the Aongatete (Houghton pers.comm.), are believed to extend under much of the Tauranga basin.

Above the volcanic rock lies a sequence of late Quaternary rhyolitic-pumiceous alluvial and estuarine sediments. Davies-Colley (1976) considers that these sediments were deposited in a

wide bay resembling the modern harbour. These were first noted by Cox (1887) as the brown "Tauranga sands". Henderson and Bartrum (1913) described the Tauranga beds as poorly consolidated bedded sediments, ranging from clay and lignite to conglomerates, usually pumiceous in composition, and often current bedded. Healy et al. (1964) in their regional map separated the Pleistocene sediments by morphogenetic criteria, suggesting no group names and no correlations with sedimentary groups observed in other areas. Kear and Schofield (1978) proposed the term "Tauranga Group" for the "mainly pumiceous, terrestrial, estuarine and marine sediments deposited since [a marked lithological and time break at the beginning of the Pliocene in the northern North Island] and found in the Bay of Plenty" and nearby lowlands. The Tauranga Group of this definition is a correlative of Brothers' (1954) Kaihu group, plus Holocene age sediments.

Terrestrial sediments of rhyolitic provenance dominate the Tauranga Group. These were derived from the Coromandel ranges during the Waitotoran stage, and largely from the Rotorua-Taupo region in subsequent times (Kear and Schofield, 1978). Pumiceous tuffs and tephras and reworked tuffs and

tephras are also common. Some workers identify local formations of similar nature as being distinct from the Tauranga Group, for example the Athenree Formation of Kear and Waterhouse (1961)

The tephra column above the Tauranga Group may be loosely grouped in two sections:

i) older (pre-Rotoehu Ash) tuffs and tephras,

ii) younger (post-Rotoehu Ash) tephras.

Together these total between ten and twenty meters of cover in the southern Tauranga basin (Pullar, 1972).

The stratigraphy of the older group of tuffs and tephras is not well defined, owing to problems caused by poor exposure and incomplete sequences left by erosion. The situation is further complicated by difficulties associated with identifying the highly weathered tephras, with their largely secondary mineralogy and lack of prominent disinguishing characteristics (Pullar pers. comm.).

Chappell (1975), in investigating upper Quaternary warping and uplift rates in the Bay of Plenty, defined and traced Upper quaternary tephras along the coast. He identified the

Hamilton Ash beds under the Rotoehu Ash, the Little Waihi Formation, consistng of pumiceous tephras immediately under the Hamilton Ash and some undifferentiated pumice beds under the Little Waihi Formation. It was suggested (Chappell, 1975) that the portmanteau term of "Pahoia tuffs" (Pullar, Birrell and Heine, 1973) used for "tephras under the Hamilton Ash beds" (Chappell loc.cit.) probably included most of the Little Waihi Formation and the undifferentiated pumice beds. Selby et al., (1971) at the northern end of the Tauranga basin, recognised a sequence of weathered rhyolite, unidentified red ash, Kauroa Ash beds and Hamilton Ash beds , with a post 42kyr B.P. tephra cover. Pullar, Birrell and Heine (1973), Birrell et al., (1977) and others, however, only recognise "undifferentiated brown tuffs" beneath the Rotoehu ash at the southern end of the Tauranga basin. These undifferentiated tuffs probably include an unidentified brown ash, some of the Hamilton Ash beds, and perhaps some of the Kauroa Ash beds (Pullar, Birrell and Heine, 1973).

Directly beneath these undifferentiated brown tuffs lies a series of strongly weathered white tuffs, the previously mentioned Pahoia tuffs.

Kirkman and Pullar (1978) noted a minimum of twelve beds, each containing a basal ash and associated paleosol,within the Pahoia tuffs. Aside from one distinct pink bed, all the beds were observed to be white or pale yellow in color, with many small manganese concretions giving a distinctive speckled appearance.

Kirkman and Pullar (1978) state that the base of the Pahoia tuffs is marked by a further group of undifferentiated brown tuffs, although they did not observe these in their study. From observations at a cutting near Pahoia School, it has been suggested that these chocolate coloured beds may be of Kauroan age (Pullar pers.comm.). This again reflects the uncertainties surrounding interpretation of the stratigraphy of the older tephra column.

The younger (post Rotoehu) tephra column consists of a collapsed column of tephras from the Rotorua, Taupo and Mayor Island eruptive centers (Hogg, 1979). The detailed composite stratigraphic column presented by Hogg (1979) sums up present knowledge of the younger tephras. The stratigraphy of these thin tephras is complex, and for most practical purposes it is only worth noting the distinct Rotoehu ash marker bed with a

cover of younger ashes, together totalling about three meters depth at the southern end of the basin (Pullar 1972).

Since the last major rise in sea level, coastal dune and estuarine deposits have added to the stratigraphy of the outer regions of the Tauranga basin. These sediments are believed to have been derived mainly from eroded material, which was deposited and reworked on the continental shelf during the last major low sea level, and subsequently moved onshore during the sea level rise (Davies-Colley, 1976).

PHYSIOGRAPHY

The downfaulted, northeasterly dipping Tauranga basin block is bounded on three sides by volcanic ranges, and on the fourth by the sea (fig. 2.3). To the north and west lies the Whakamarama plateau, to the west and south-west the Kaimai ranges, and to the south and south-east the Mamaku plateau. The surrounding hills dip beneath the flat-lying sediments of the Tauranga Group, once continuous to at least Rangiwaea and the inner portion of Matakana island (Henderson and Bartrum, 1913). Marine and fluvial erosion of

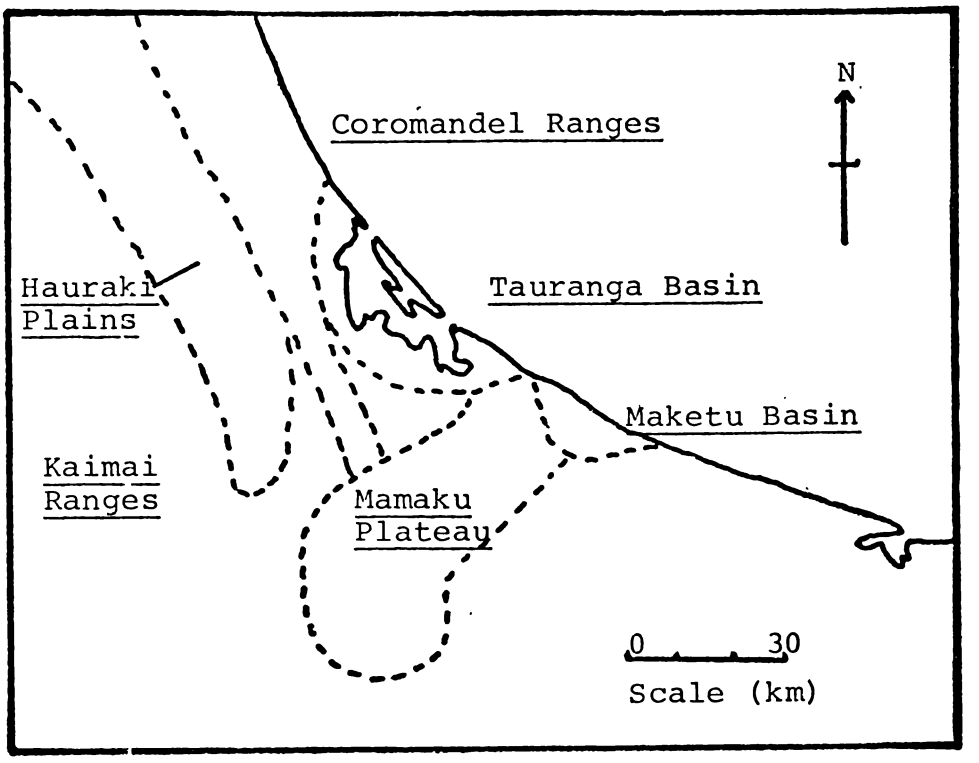

Figure 2.3. Physiography of the Tauranga Basin area.

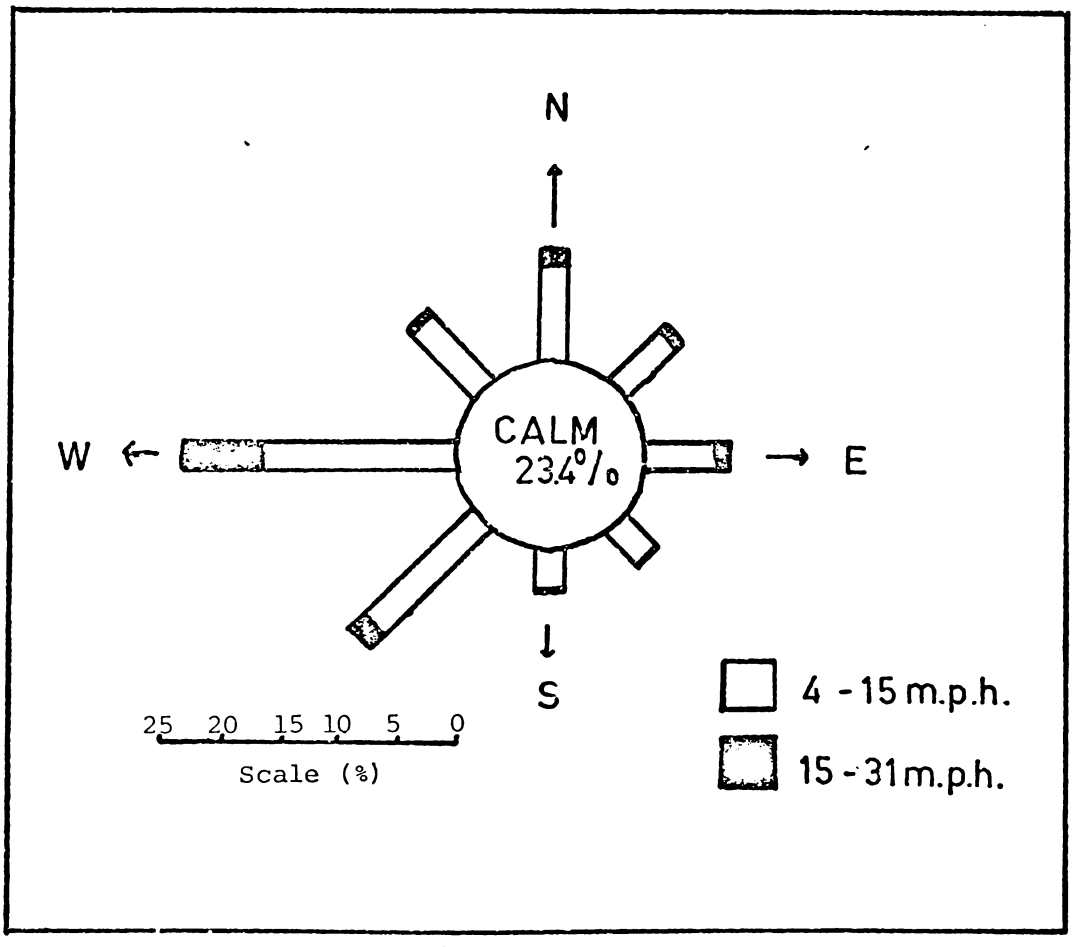

Figure 2.4. Baillie wind rose for Tauranga Airport, 1952 - 1960.
(After deLisle, 1962)

these sediments eventually formed a tidal basin dotted with flat lying islands, with the coastline running roughly through Katikati, Apata, Omokoroa, Tauranga and Maungatapu (Wallingford Report, 1963). Stream downcutting during the last glacio-eustatic low sea level, followed by streambed aggradation, gave rise to the present inner harbour coastline; a series of long, narrow, fingerlike peninsulas, extending in a north-easterly direction into the harbour, with wide tidal flats between.

A series of glacio-eustatic terraces may be observed along the coast of the Tauranga basin, inside and outside of the harbour. Four terraces were observed and named at Waihi beach (Kear and Waterhouse, 1961 and 1971; Selby et al., 1971) and correlations with terraces further south have been suggested (Chappell, 1975). The terrace heights at Waihi were estimated at 1.8 - 3.0 meters a.s.l., 5.2 meters a.s.l., 14.6 - 14.9 meters a.s.l., and 33.5 - 35.0 meters a.s.l. (Selby et al., 1971). The digitate peninsulas within Tauranga Harbour form part of this terrace system.

The present coastal lagoon form of Tauranga harbour was brought about by the last major

geomorphic event in the basin, the cyclic progradation of a succession of beach ridges on a line continuous with the main sweep of the Bay of Plenty coastline. The initiation of the Matakana Holocene barrier system probably occurred about 4 to 7 kyr B.P. (Pullar and Cowie, 1967) as the last glacio- eustatic sea level rise slowed. It was possibly due, in part, to the drowning of the present harbour behid a series of ancient dune ridges, although certainly the onshore movement of material from the continental shelf maintained the necessary supply of sediment. This material was probably eroded at times of lower sea level, reworked on the shelf, and moved onshore by the rising sea level, providing, along with littoral drift, the sediment supply for the Matakana Barrier island as well as the Bowentown and Mount Maunganui tombolos (Davies-Colley, 1976).

The processes modifying the geomorphology of the Tauranga basin at present may be considered in three broad groups.

i) The first group consists of the shallow landsliding and fluvial erosion of the ranges and foothills surrounding the basin, together with the associated terrestrial and estuarine deposition. The highly permeable nature of the young ashes

permits little or no surface drainage, and hence no observable fluvial processes on the flat-lying land near the coast.

ii) The second group of processes is comprised of the erosion and accretion of the barrier island and tombolo features.

iii) The third group consists of processes associated with the erosion of the fingerlike peninsulas inside the harbour. Henderson and Bartrum (1913) noted that"tidal currents are planing away the the points of land and filling in the bays". Captain Arthur Crapp (quoted in Henderson and Bartrum, 1912) of Omokoroa observed two meters of cliff retreat in forty years and stated the erosion of Matakana island was even more rapid, It is not clear, however, if this referred to the older portion of the island, or to the sand dune portion.

CLIMATE

The topography of the areas bordering the Tauranga basin is a major factor in determining local weather patterns, modifying the weather producing systems which move in from the Tasman Sea. The inland ranges create a partial wind and

rain shadow, sheltering the Tauranga basin from the shower type precipitation associated with the passage of unstable air masses following cold fronts (de Lisle, 1962). Despite the relatively low number of days on which rain falls, however, the average annual rainfall is not less than that of adjacent areas. This is due to the exposure of the coast to the passage of frontal depressions and tropical cyclones from the north, in spring and late summer respectively. Heavy rainfalls result as the moist north and north-easterly winds rise over the land.

Table 2.1 Rainfall records in the Bay of Plenty

Station	Return Period (Years)	Fall Duration 1 hr	12 hrs
Waihi	2	33	117
	10	56	211
	50	76	292
Tauranga	2	32	90
	10	64	147
	50	93	198
Rotorua	2	25	69
	10	41	94
	50	56	117

The rainfall pattern of the Tauranga basin is

thus characterised partly by infrequent heavy rainfalls, illustrated by the comparison of depth-duration-frequency figures for two Tauranga basin meteorological stations, and nearby inland Rotorua (table 2.1).

The storm which affected the Tauranga basin on the 19th and 20th of March was a tropical cyclone, which produced a short duration, heavy rainfall. Light rain, averaging 5 mm per hour, fell between 0500 hours and 1630 hours on the 19th. An intense period of rain followed this, with 75 mm falling between 1630 and 1800 hours, with a further 15 mm falling in the following 90 minutes. Intermittent light showers were followed by a further fall of 45 mm between 0130 and 0230 hours on the 21st. The heaviest rainfall in the storm thus approximately equalled the 10 year return period, 1 hour storm, while the 48 and 72 hour rainfalls recorded over this period were the highest rainfalls ever recorded during March at the Tauranga airport. The monthly total was the second highest monthly rainfall recorded since 1898, and the highest, at 504 mm, since 1910 (Met. Office records). The mass movement episodes thus appear to be associated with long periods of heavy rainfall and storm peaks, rather than short,

intense, high return period storms.

The prevailing wind is south-west to westerly (fig. 2.4) at Tauranga airport and almost all the strong (>15 m.p.h.) winds, which might be expected to drive waves, are westerlies. Although the region is one of the least windy areas in New Zealand, the harbour current dynamics are believed to be influenced to a considerable extent by winds (Wallingford Report, 1963).

The Tauranga basin is mild and sunny, with monthly mean temperatures seldom falling below 9 degrees C, and a mean daily range of only 9.5 to 10.5 degrees C throughout the year (de Lisle, 1962).

SOILS

The soils of the Tauranga basin are derived from weakly to moderately weathered accumulations of rhyolitic ash. In the southern portion, where the top few inches of cover are dominated by the younger Taupo and Kaharoa Ashes, and pieces of unweathered pumice are still visible in the profile, the soils are classified as moderately leached yellow-brown pumice soils. North of a line drawn between the Maungatapu and Tauranga

City peninsulas, where older ashes assume prominence and little unweathered pumice is visible, the soils are classified as moderately leached yellow-brown loams (Gibbs and Pullar, 1961).

COASTAL LANDSLIDES - INTERNATIONAL LITERATURE

Early investigations of coastal cliff processes and morphology tended to be descriptive in nature. Usually concerned with long term processes and regional land forms, most work centred on the origins of spectacular hard rock cliffs. Theories were put forward relating the genesis of these features to wave attack during marine encroachment (Darwin, 1891) and during static sea levels (Johnson, 1919).

The same relatively academic approach, concerned with the genesis of landforms such as steep cliffs and shore platforms, may be observed in more recent work (e.g. Mclean and Davidson, 1968; Cotton, 1969). A leaning towards more practical applications is evident in much of this work, however, with emphasis on process distribution and intensity. Typically coastal mass movement events are related to the intensity

of marine erosion (Mclean and Davidson, 1968; Sunamura, 1973; Gelinas and Quigley, 1973), rainfall events (McGreal, 1979), or other causative factors.

The expertise available in the field of coastal geomorphology is now commonly focussed on specific problems, with the same stimulus and with similar changes in research orientation as those found throughout geomorphology today, as discussed in Ch. 1. Such applications generally involve a projected estimate of the stability of a given length of coastline for a stated period (Hutchinson, 1980). The interpretation of "stability" used in such studies is generally that of susceptibility of the cliff edge to mass movement induced retreat. Expressed in more abstact terms, the dominant orientation of modern marine and lacustrine cliff stability studies, is towards an understanding of the relationships between process and morphology.

Recognition of mass movement generating processes is relatively simple on the landscape scale (for example, the discernment of a relationship between mass movement incidence and areas of interrupted littoral drift by Hutchinson et al., 1980). An integration of form and process

is also relatively simple over a long period of time (e.g. The correlation of mass movements with lake level changes, found by Quigley and Gelinas, 1976). Brunsden and Jones (1980) suggest a span of one hundred years is sufficient to observe consistent process-form relationships in soft mudstone. This term must, of course, vary with the type and intensity of processes occurring. It is notable that the scale at which most attempts are made to quantify process-form relationships is somewhat smaller than considered in the studies mentioned above.

Bryan and Price (1980) found a different type of approach was necessary in studies of cliff stability as it affected suburban housing. They found that "a fundamental problem in analysing cliff recession as a basis for control measures [was] determination of the relationship of crest and toe retreat". This reflects an interest in the stability of small lengths of coastline over a relatively short period. It is the application of long term and large scale studies to short term, small scale problems that is the chief concern of much coastal cliff stability work today.

Site-specific studies aimed at elucidating local patterns applicable to individual sites are

common (e.g. Norrmann, 1980; Hutchinson et al., 1980). Hutchinson (1973) made the first attempt at setting up a general theory of coastal cliff evolution oriented towards short term small scale studies. Hutchinson (1973) defined three types of coastal margin in London Clay, dependent on the relative rates of basal erosion and weathering (where weathering is taken to include downslope transport processes such as sheet wash). Coasts where 1) erosion is in balance with weathering, 2) erosion exceeds weathering, and 3) erosion is non-existent were defined. These coastal types were associated with distinctive types of evolution; constant self - parallel retreat, cyclic landsliding, and degradation to a low slope angle respectively. Hutchinson (1973) also recognised the modifying effects of geology and groundwater configurations on this scheme. Studies elsewhere have served to illustrate the evolutionary models established for Hutchinson's (1973) type 1 (Prior and Renwick, 1980), type 2 (Quigley et al., 1976), and type 3 coasts (Nash, 1980). A similar three part coastal evolution model with the same erosional versus degradational process rate basis was erected for Northern Lake Erie coasts (Gelinas and Quigley, 1973; Quigley

and Gelinas, 1976). This model utilised quantitative estimates of wave erosivity, and considered the modifying effects of geology. Quigley et al. (1976) further considered the interdependence of retreat rates and landslide types, allowing for other modifying influences. Kilgour et al. (1976) discussed situations where the effects of geology modified the influence of erosion rates on the nature of cliff evolution. This work constitutes a series of steps towards a "unifying theory"; a basis for the study of coastal cliffs and individual landslides, and the major feature of present coastal cliff research.

Many coastal cliff erosion studies are somewhat less ambitious, attempting merely to provide basic information and a database of case studies. The quantification of average cliff retreat rates by field, map and aerial photograph measurement provides essential information for planning and subsequent detailed erosion studies (e.g. Gibb, 1979; Keller, 1979). Similarly basal erosion rates and series of cliff profiles are monitored, usually for the purpose of long term research.

Landslide classification, based on systems such as those proposed by Sharpe (1950) and Varnes

(1975), has been utilised, often in conjunction with estimates of relative volumetric importance (Hutchinson, 1965; Davidson, 1965; Prior and Eve, 1973; McGreal, 1979). These classifications are useful for description and as a basis for the comparison of work.

The application of engineering techniques of measurement and analysis to the study of coastal mass movements is well advanced. Strength and index testing methods are the same as those used in any geotechnical study, and many of the commonly used methods of slope stability analysis have been applied to coastal cliffs (McGreal, 1979; East, 1974; Bromhead, 1978; Quigley and DiNardo, 1980; Hutchinson et al., 1980; Prior and Renwick, 1980).

It is worth noting that one major gap exists in the literature concerning coastal mass movements and coastal cliff evolution. There is little or no information recorded concerning the processes (other than basal erosion) which act to degrade abandoned cliffs, to cause retreat, and to modify the form of type 1 and 2 cliffs between mass movements.

CHAPTER THREE

Field Investigations

INTRODUCTION

The first step towards a complete description of the nature of a process, and the evaluation of its causes and effects, is a description of its field characteristics. A full description of a mass movement process would include the description of:

i) the materials involved,

ii) the geotechnical nature of the area surrounding each failure,

iii) the nature of the non-mass movement processes affecting the area,

iv) the morphology of the mass movement scars,

v) the rate and nature of the mass movement events,

vi) the space-time distribution of the events.

Field landscape scale studies have been augmented by the use of geological maps, aerial photographs and historical literature. In order to extend the study over the greatest possible length of coastline and the largest number of mass movements, landscape scale sudies included as much of the harbour coastline closely resembling the Maungatapu coast as possible. Detailed site investigations

were confined to three sites on the Maungatapu peninsula. The use of three sample sites can provide reasonable confirmation of results while still remaining within the time limitations of an M.Sc. thesis. The three test sites are located, one on the north-eastern tip of the peninsula, and two on the north-western side (fig. 3.1). Map references for the sites are (N.Z.M.S. 1):

Site 1: N58 663560

Site 2: N58 659562

Site 3: N58 659560.

Where geotechnical techniques are to be applied, the erection of an idealised soil profile is necessary as a basis for representative soil sampling and subsequent mathematical modelling (Blakeley, 1974). Qualitative field description will be presented at this point, the physical characteristics of the materials will be discussed in Chapter 4.

Two brief definitions:

The term "soil" is used here in the engineering sense of "a natural aggregate of mineral grains that can be separated by such gentle mechanical means as agitation in water" (Terzaghi and Peck, 1948).

The most convenient reference point during field work was the level surface of the Maungatapu peninsula terrace at about 14.5 metres a.s.l.. Heights used in soil column and morphological description therefore use this level as a

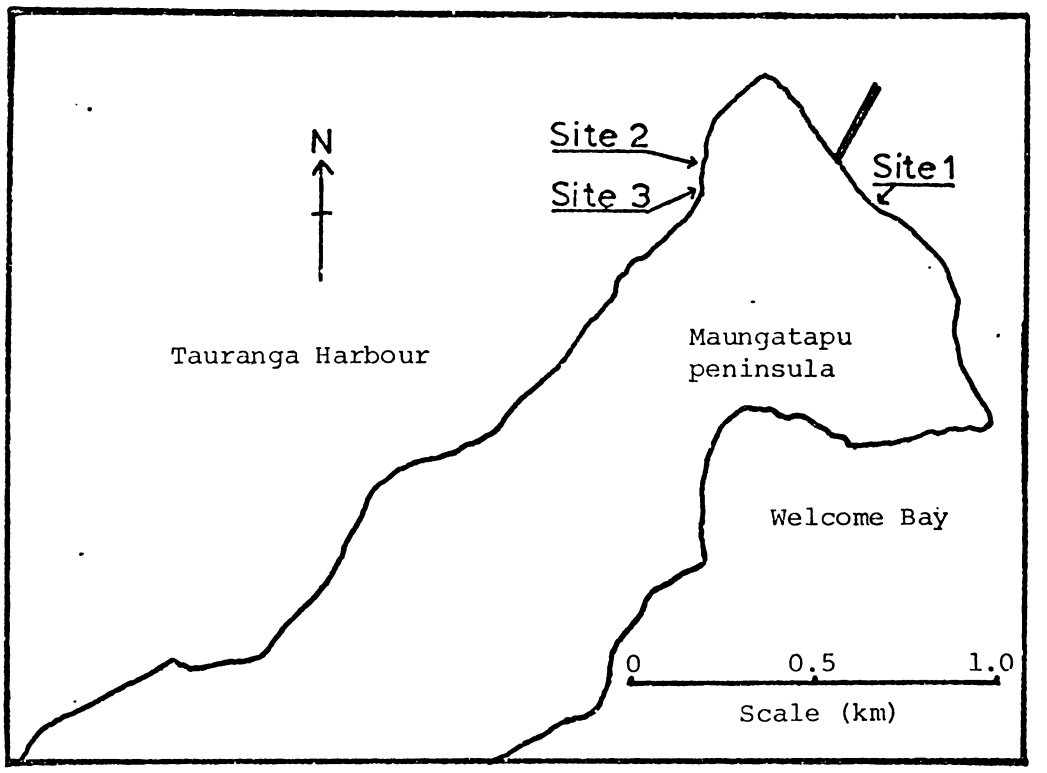

Figure 3.1. Location of the three representative sites.

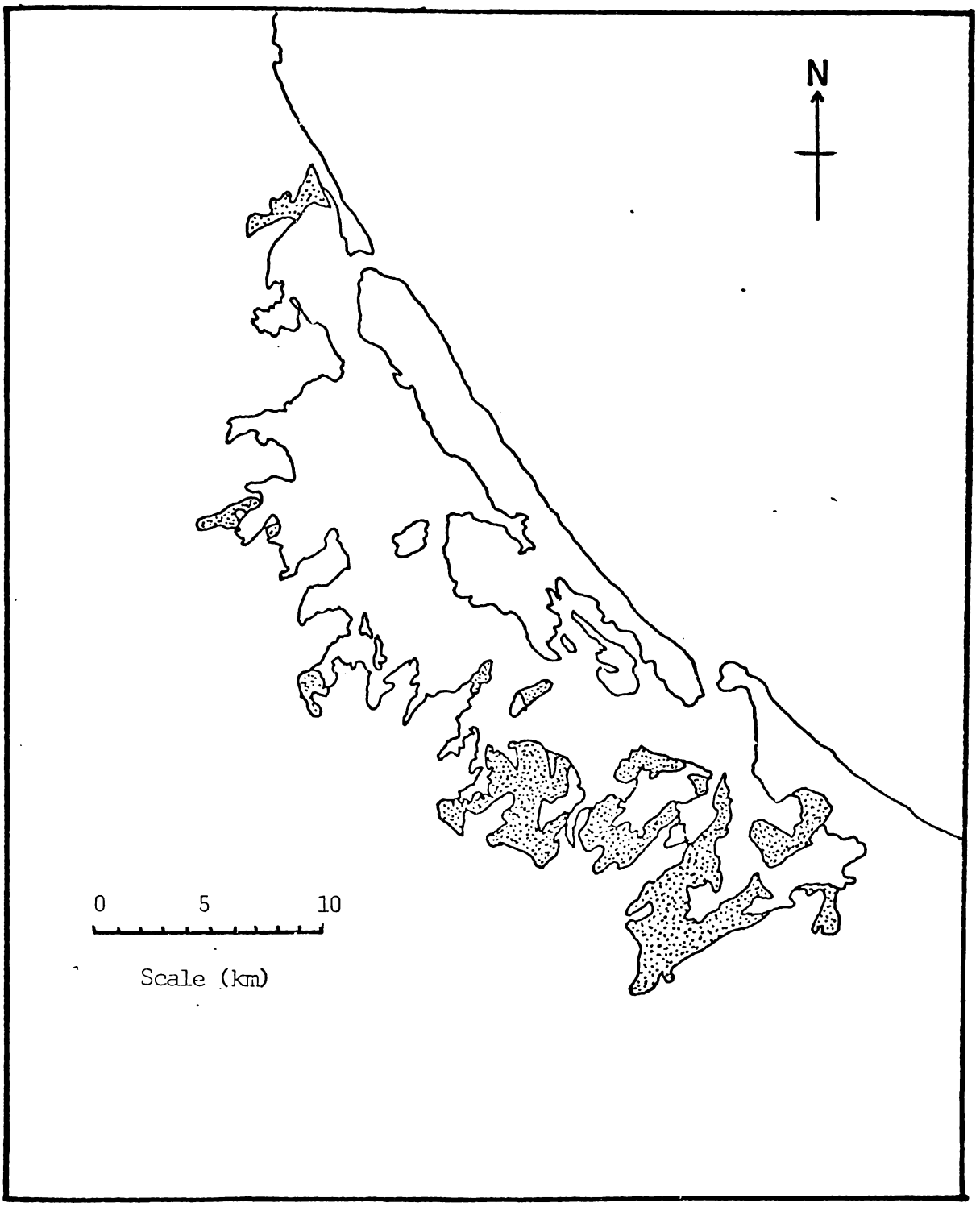

Figure 3.2. Distribution of areas of similar elevation and with similar stratigraphy to that of Maungatapu peninsula.

datum.

SITE SCALE INVESTIGATIONS

STRATIGRAPHY OF THE MASS MOVEMENT SITES

As discussed in Chapter 2, the late Quaternary stratigraphy of the Tauranga basin is not well defined, owing largely to the highly discontinuous nature of the tephra and sediment deposits in the region. A preliminary survey showed that an idealised soil profile could be drawn up for the Maungatapu peninsula, and be applicable to other coastal terraces of the same elevation. Fig. 3.2 shows the distribution of the areas of similar elevation and stratigraphy to the Maungatapu peninsula, and to which the idealised soil profile applies. The survey also indicated the gross differences between the stratigraphic columns of sites on the lower (14.5 metre) and higher (38-40 metre) terraces on which landslides such as the Bramley Drive, Omokoroa events occurred. Exposures at Bramley Drive show the tephra columns observed elsewhere to be extremely collapsed and discontinuous. This is evident to such a degree that extension of any other than elementary results or conclusions from Maungatapu to mass movement problems om terraces of different elevation is questionable.

The idealised soil profile presented in fig. 3.3 was first drawn up at test site 1, then checked and found

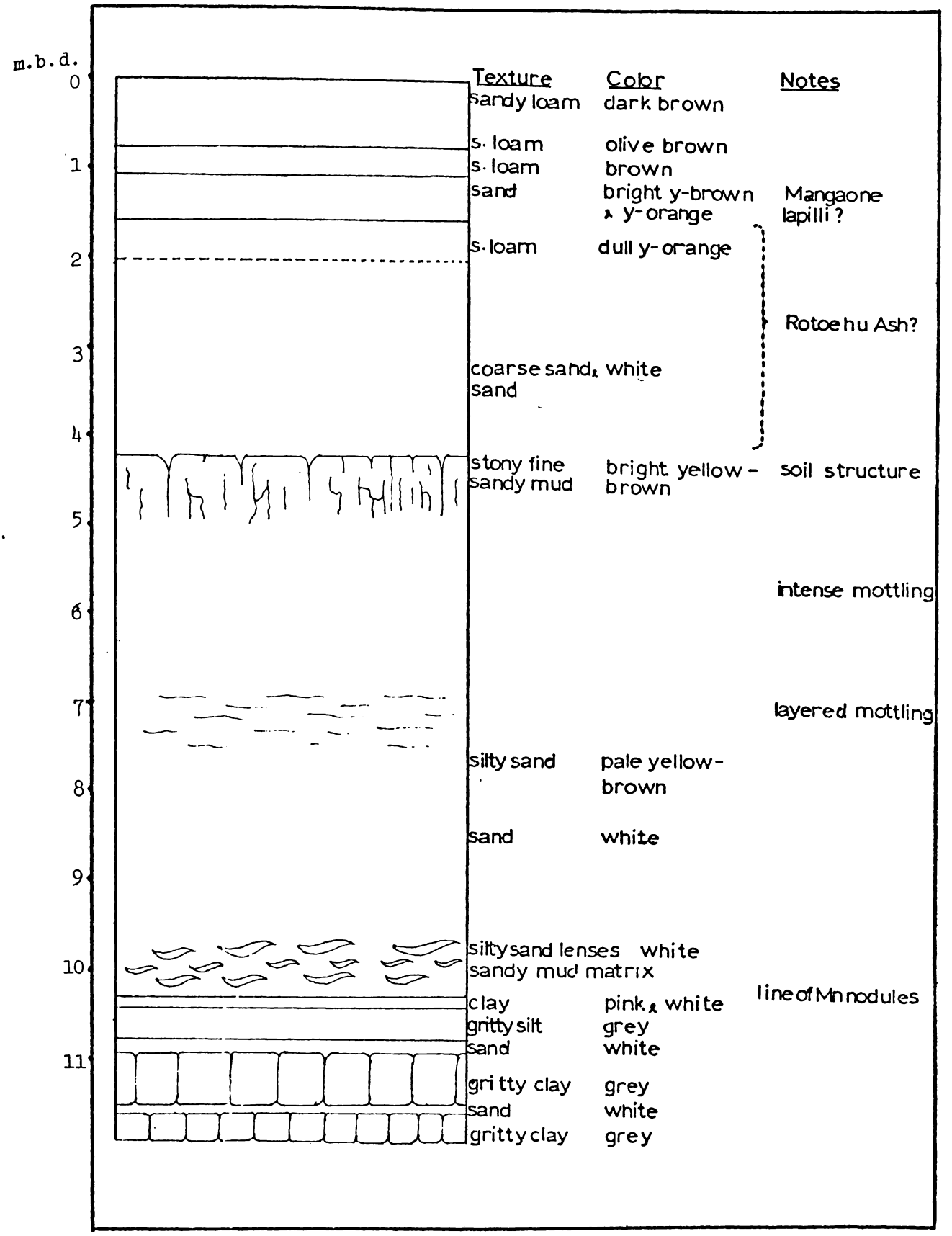

Figure 3.3. Idealised soil profile.

consistent at sites 2 and 3, before being compared with the rest of the peninsula and profiles elsewhere about the harbour. A pedological soil profile described at site 1 (sites 2 and 3 were disturbed) showed the upper portion of the profile consists of a typical yellow-brown pumice soil (Gibbs and Pullar, 1961). The soil is developed on a collapsed column of post 20,000 Kyr tephras, present on all the terraces about the harbour. Differentiation of the column into separate tephas and paleosols is irrelevant to the purposes of this study.

Beneath the white sandy Rotoehu Ash lies an orange and yellow-brown mottled tuffaceous material, with a red, clay rich paleosol in the upper portion which appears similar to a strongly weathered tephra, however moderately to strongly weathered rounded rhyolite and pumice pebbles are distributed throughout. This deposit may be interpreted as consisting partly of Hamilton Ash age tephra, which has been alluvially reworked, or which fell into water in which coarser material was being transported and/or deposited at the same time. Below the orange mottled material, first brown, and then white colors dominate, and the texture changes to a silty sand. It is suggested this sandy material may possibly be a tephra flow or distal ignimbrite, or simply a fluvial deposit, and should be grouped in the upper portion of the Pahoia Tuffs (Pullar, pers. comm.). The series of silts, sands and clays below this, and the 3

metre sequence of tephras and paleosols below this again, may also be classed with the Pahoia tuffs according to Pullar (pers. comm.). At the base of the weathered tephras lies a firm to hard white silt, which resembles a distal ignimbrite, or reworked ignimbritic material (Lowe, pers. comm.). This material probably represents the top of the Tauranga Group in the area.

Investigation of a large number of landslide scars showed that the distinctive shelf form, mentioned previously, is consisently associated with the upper portion of the Pahoia Tuffs. A more detailed consideration of this section of the soil profile would therefore appear to be of value.

Exposure of the white silty sand varies from between 7.0 and 8.0 metres below datum at the top, to a consistent 9.8 metres b.d. at the base, with the upper limit depending largely on the extent of brown staining from the yellow-brown silty sands above. The textural change from silty sand to sand appears to be at a relatively constant stratigraphic level (7.0 m.b.d.), and intense red-brown mottling is confined to the relatively clay-rich material above this point, however yellow-brown staining and some little mottling may extend down as far as 8 m.b.d.. At this level the silty sand is loose, however it becomes somewhat firmer and denser in the metre below, where the color changes from white to a pale grey and texture fines from

sand to silty sand, and to sandy mud in places. Between 9 and 9.8 m.b.d. lenses of loose silty sand appear in a matrix of denser sandy mud. These lenses may be distinguished by their light color when nearly dry, as the denser sandy mud matrix retains sufficient moisture to be slightly darker an hour or two after exposure at relatively dry sites. Although the well sorted nature of the material doesn't allow further observations of bedding structures, the irregular lensoidal forms observed suggest a flow deposition origin, supporting Pullar's suggestion of tephra flow or alluvial deposition.

Beneath these lensoidal sands the material becomes finer (gritty silt) and denser for about 10 cm, at which point a 2mm thick line of manganese nodules makes a sharp boundary to 8 cm of white clay and 1 cm of distinct pink clay. Below this clay bed a series of blocky grey gritty clay beds of 30 to 60 cm alternate with 8 to 20 cm thick, loose sandy beds. The line of manganese nodules above the clay bed implies the existence of reducing conditions, probably with slightly alkaline pH (Mason, 1966). This supports the idea that the clay bed, being of much finer texture than the material above, and having no vertical cracking as the lower gritty clay beds do, should provide a barrier to drainage. Kirkman and Pullar (1978), in tracing the loosely defined Pahoia Tuffs further south-east in the Bay of Plenty, used a distinctive 1 inch pink clay marker

for reference. It is possible that this bed correlates to the pink clay bed observed at Maungatapu. The pink and white clay beds together were used as a reference point during field work, and are hereafter referred to as the clay marker bed.

SITE DESCRIPTIONS

The second stage in the study of a mass movement process is the description of some of the individual mass movements which most conspicuously constitute that process. Descriptive data concerning rates of movement, modes of failure and so forth may be obtained from witnesses. Verbal and sketched morphological descriptions may be qualified by classification within a stipulated system, and/or quantified by surveying. Features outside the scars which appear relevant may also be noted by geotechnical mapping. In this investigation such site scale investigations were carried out on the three representative sites mentioned earlier. The morphological and classification terminology used follows that of Varnes (1975).

Mass Movement Scar Morphology

The mass movements in question occurred in the upper 10 metres of the 14.5 metre cliffs found along the sections of the Tauranga harbour coastline shown in fig. 3.2. Beneath

flat-lying arcuate crowns, near vertical (80 to 90 degree) main scarps (section 'a' fig 3.4) drop 7 to 8 metres to near horizontal (15 to 25 degree) shelf-like features (section 'b' fig. 3.4). It is this distinctly biplanar surface of rupture which characterises the group of mass movements being studied. The main scarps show changes in angle down their length, related to differences in strength, for example the relatively resistant red paleosol in the upper tuff which juts out several cm below the less cohesive sandy Rotoehu Ash.

The shelf feature usually has a maximum width, in cross section, of 3 to 5 metres the center of the scar, lying within the 1.5 to 2 metres of lensoidal silty sands above the clay marker bed, which is commonly exposed near the outer edge. In a cliff formed in isotropic material the least stable surface will pass through or near to the base of the cliff. The non-basal intersecting form of the mass movement scars therefore indicates a major irregularity in either the restraining or disturbing forces near the failure plane. From the evidence presented thus far, this irregularity could be any of;

i) Unusually strong material beneath section 'b',

ii) Unusually weak material at the level of section 'b',

iii) A major irregularity in the pore-water pressure regime at the level of section 'b'.

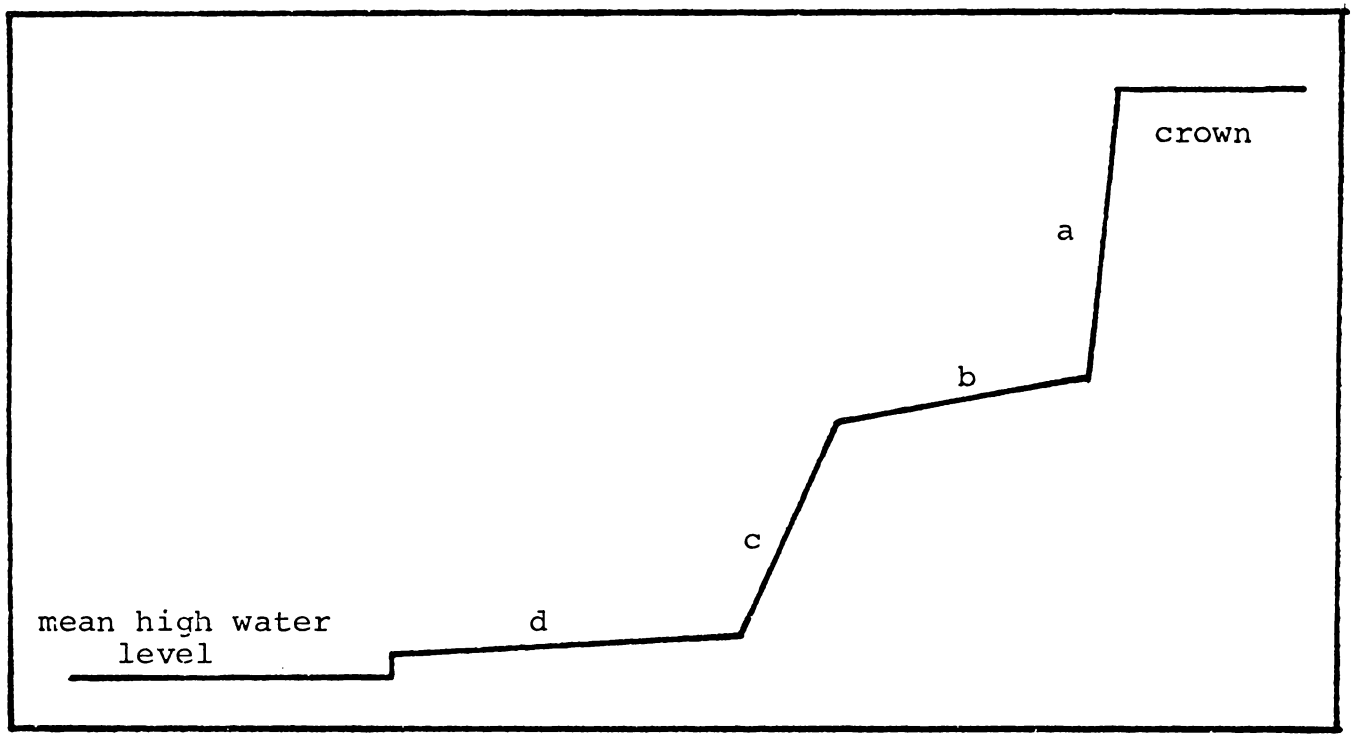

Figure 3.4. Idealised slope profile.

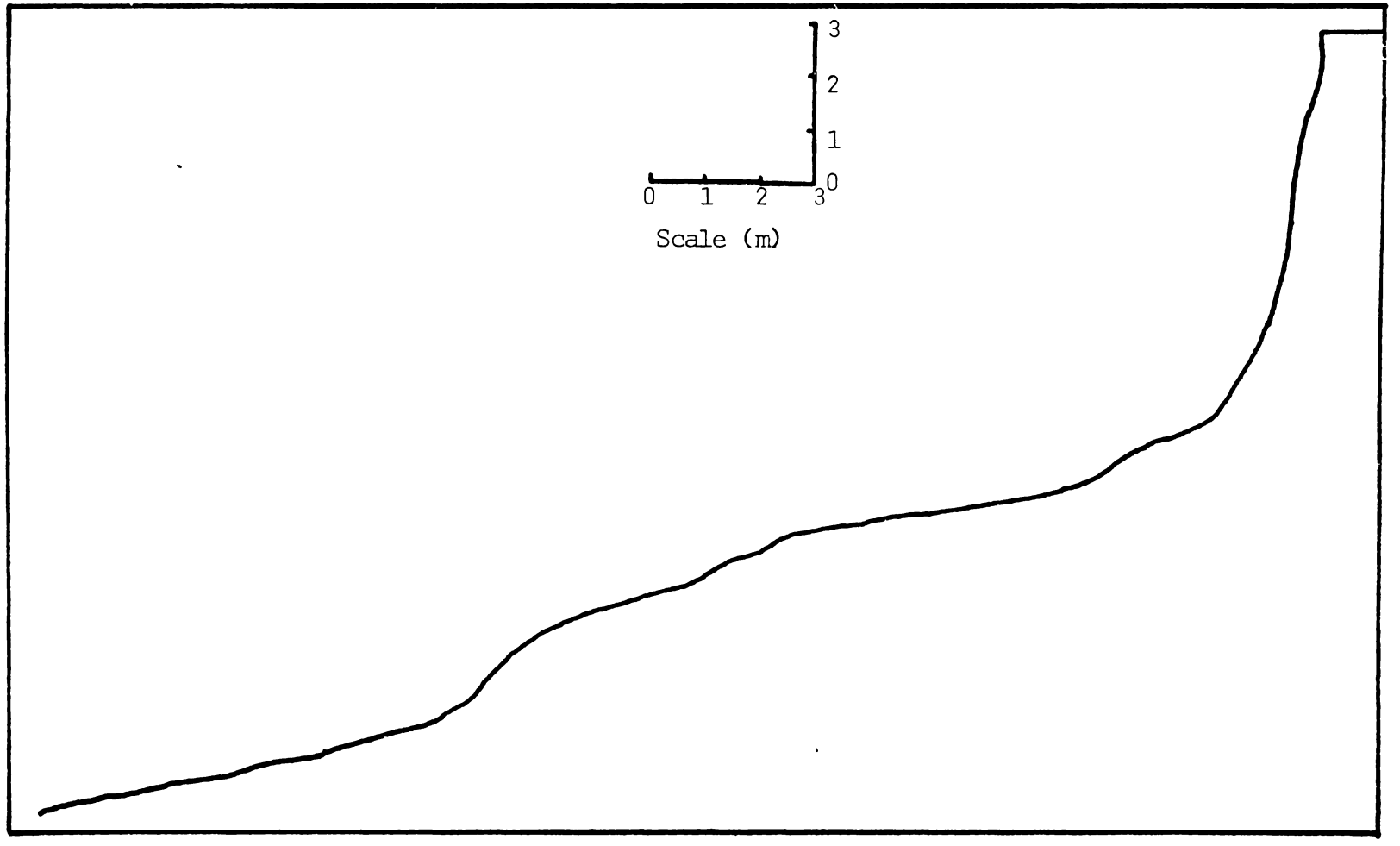

Figure 3.5(a). Surveyed profile of site 1.

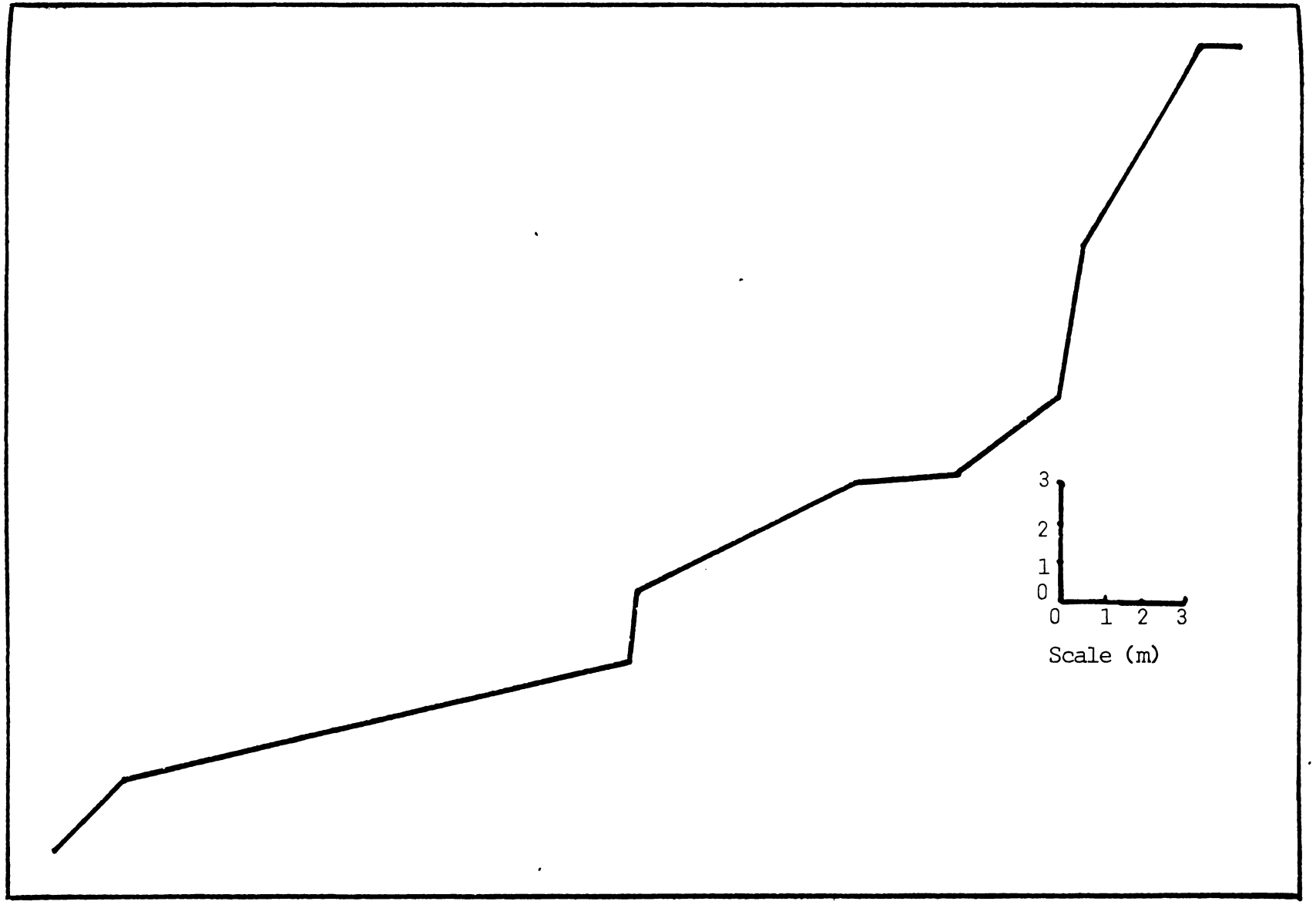

Figure 3.5(b). Surveyed profile of site 2.

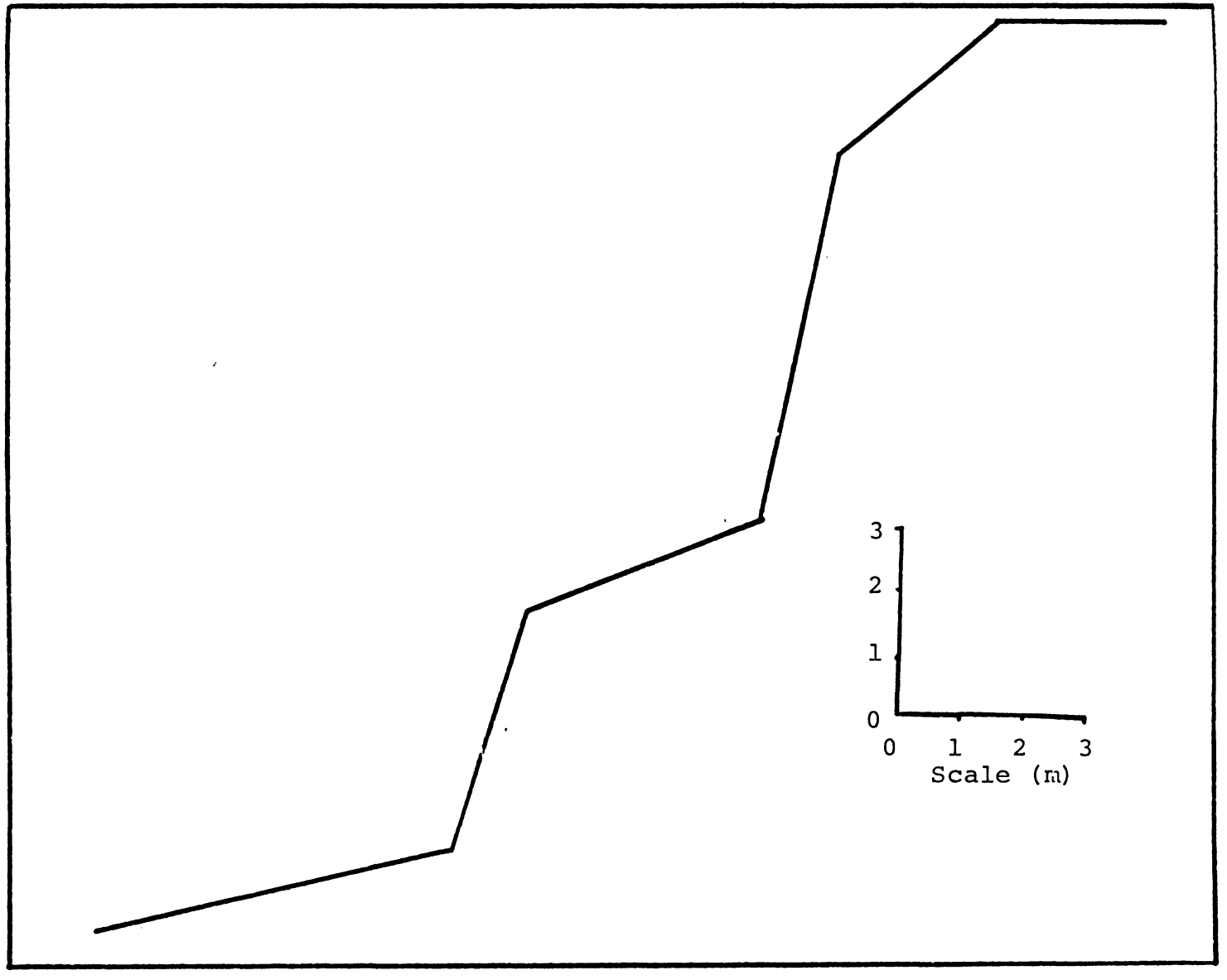

Figure 3.5(c). Surveyed profile of site 3.

The distinctively squared-off, biplanar nature of the surface of rupture renders option 1 unlikely, as such a feature on its own would probably produce an arcuate failure, exiting above the firm bed. The second and third options are more likely to produce this biplanar type of rupture surface.

Some differences in morphology may be observed at the three representative sites (fig. 3.5). There are some differences in scale, but all are of the same magnitude. The volume of displaced material was estimated at approximately 220 cubic metres at site 1, 100 cubic metres at site 2, and 200 cubic metres at site 3. Sites 2 and 3, which have experienced only one recent failure, have steep 'c' sections, dropping to an old beach, now buried by about 2 metres of displaced material. The displaced material forms an elongated foot, which may extend up to 30 metres beyond the former cliff face, directly after failure. Site 1 is different in that it has experienced at least two failures in the past decade (Mrs. W. H. Nielson, pers. comm.). The shelf thus extends for 10 metres from the base of the main scarp ('b') and, in places, the clay marker bed is exposed up to 4 metres from the outer edge. The upper few cm of shelf left after the earlier slip(s) appears to have been scraped off by the passage of displaced material from the later slip(s), resulting in this exposure. The second major difference between site 1 and sites 2 and 3 is

that the relatively large amounts of displaced material from two or more past mass movements bury section 'c' to a far greater extent at site 1. Some caution is therefore necessary in interpreting surveyed cross sections of this site for stability analyses. Surveying of site 1 was carried out using a Jacob's staff and tape, the other two sites with a tape and Abney level. Central cross sections were used for stability analysis.

None of the Maungatapu peninsula mass movements were observed by eye witnesses, however several residents have reported hearing loud thumps and feeling vibrations at the time of failure. One of the Bramley Drive, Omokoroa, events was observed by several people who reported an extremely rapid failure, producing waves of over 1 metre in height (Gibb, 1979). A similar rate of movement may be inferred for the Maungatapu mass movements from the accounts of noise and vibration, and from the length and low angle of repose of the displaced material toes.

Examination of several debris toes showed that much of the displaced material reaches the base of the cliffs in a relatively intact state. This is shown by the presence of trees which have been rafted down from the crown, still in an upright position (fig. 3.6). It is possible that the trees may have had a local stabilising influence on the soil mass, allowing rafting to occur. The observation, independent of any tree roots, of a large piece of intact

Fig. 3.6. Intact brown tuffs and tree rafted in a vertical position from high on the cliff face.

Fig. 3.8. Debris fan at site 3, exhibiting annular zonation.

Fig. 3.7. Intact tuffs beside *in situ* Tauranga Formation sediments.

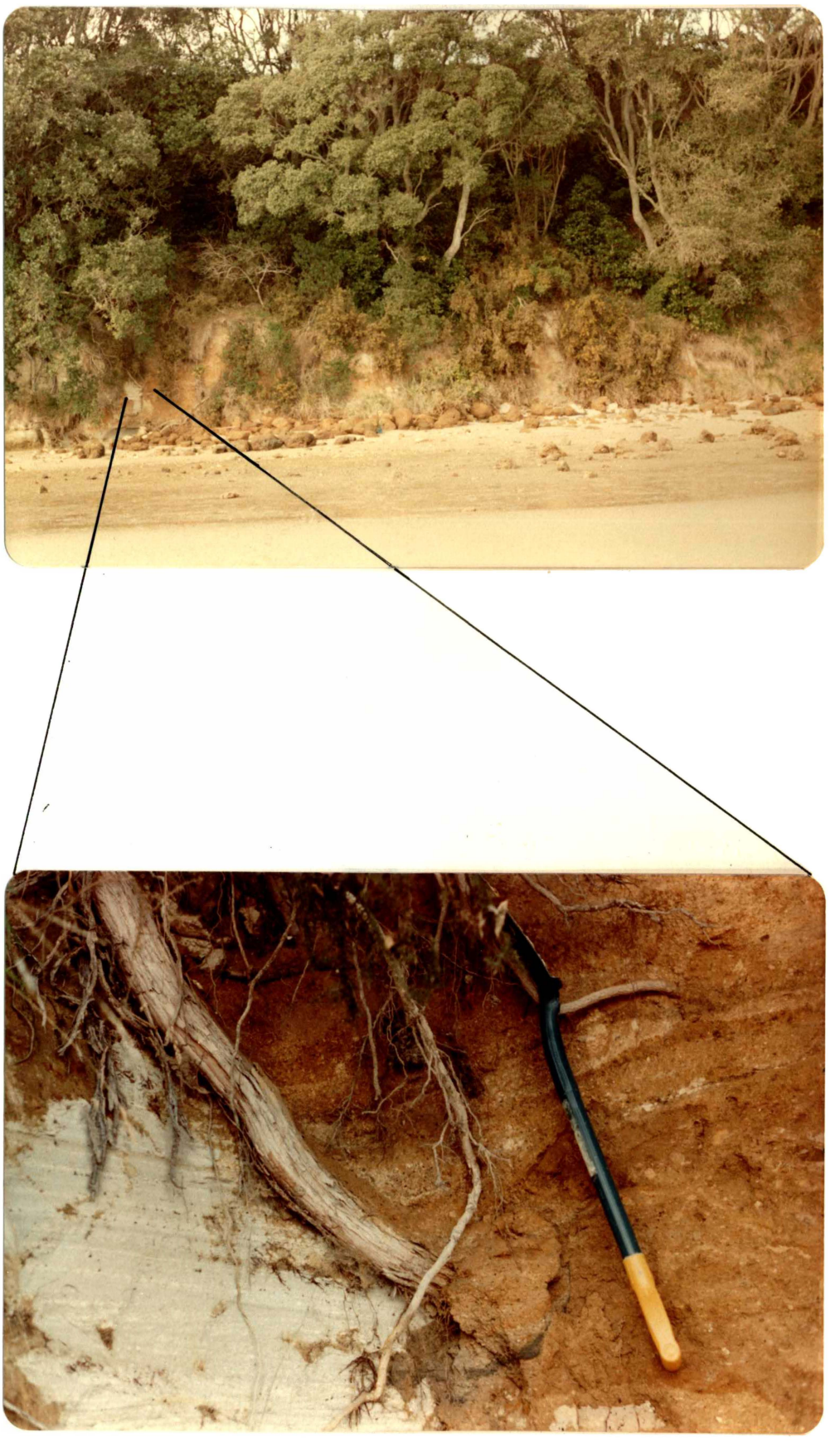

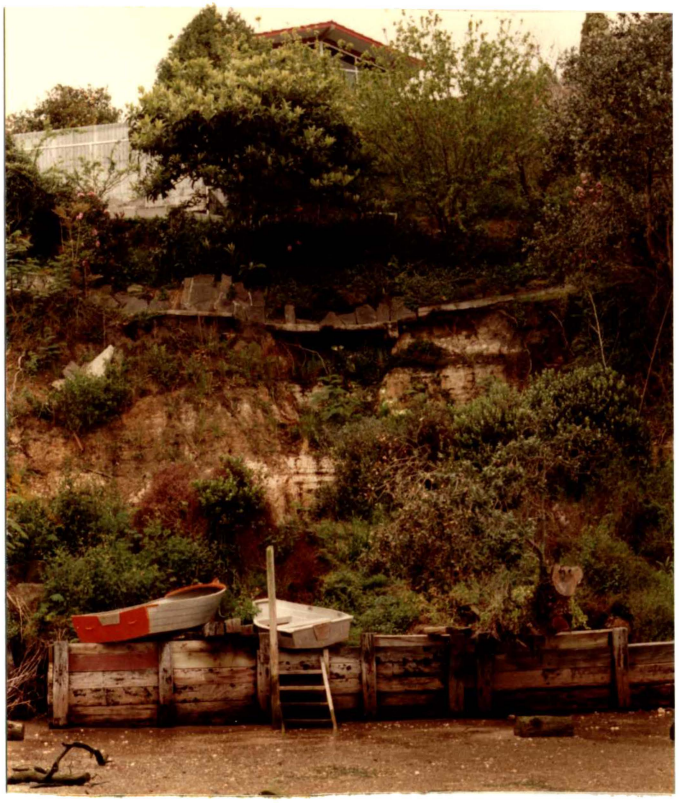

Fig 3.9(a). Site of failure behind anchored concrete path.

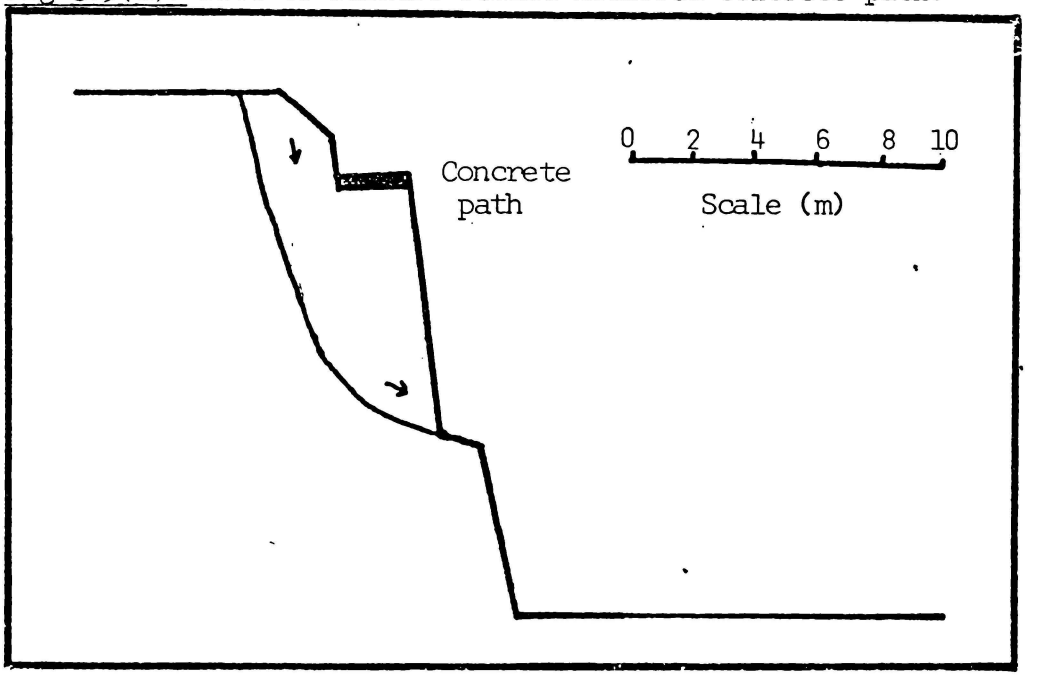

Figure 3.9(b). Movement of displaced mass beneath and behind concrete path.

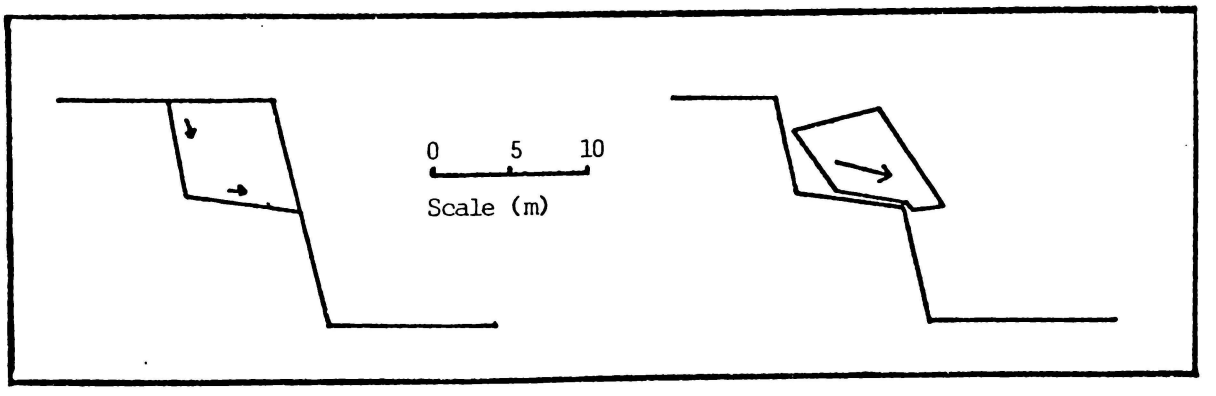

Figure 3.9(c). Initial rotational, and subsequent translational movement.

displaced material from about 5 to 5.5 metres below datum at the stratigraphic position of the uppermost Tauranga Group sediments (15 m.b.d., see fig. 3.6) indicates that rafting is not dependent on such external influences. These inact blocks are found as part of long, lobate debris fans, extending up to 30 metres from the base of the cliffs (fig. 3.7). These fans exhibit roughly annular zonation (fig. 3.8). The outer ring usually consists of logs and debris placed at the base of the cliffs as a seawall. The second ring is made up of white silty sands from above the clay marker bed. Small pieces of the clay marker bed, from the outer edge of the shelf, have been observed near the outer edge of this ring. The third ring is made up of the pale yellow-brown sands from above the white sands. The central portion consists of the firm reddish and yellowish brown tuffs interpreted as being of Hamilton Ash age, covered and surrounded by reworked younger ashes. Pieces of intact turf are often found in this zone.

The concentric zonation observed in the displaced material implies a rotational-type failure, with the foot pushing outwards and the upper material moving down in a relatively non-turbulent manner, allowing the rafting of undisturbed blocks of incoherent young ashes. This impression is strengthened by observations at a scar about ten years old, midway along the north-west side of the Maungatapu Peninsula (fig. 3.9). A reinforced concrete

path across the face of the cliff has had a landslide occur behind it, leaving it anchored by its ends only. Figure 3.9(a) appears a little deceptive, in that the unsupported path has subsequently swung in towards the cliff face. This observation implies that the head of the displaced material initially experienced little or no outward movement, while the biplanar form of the surface of rupture indicates that the initial movement of the foot must have been almost entirely outwards. As might be expected, the top few cm of the sands on all of the shelf features show signs of intense reworking. However, beyond 1 or 2 metres out from the base of the main scarp, almost no material from the upper soils is mixed in. This implies that while materials may have fallen from the upper soils onto the proximal section of the shelf following failure, the head of the displaced mass was not brought into contact with the lower surface of rupture during movement. As complete translation of the displaced mass from above the surface of rupture is evident in all observed cases, a fully rotational mode of movement cannot be assumed. The near horizontal orientation of intact segments of turf, and the near vertical orientation of trees suggests that movement is largely translational in nature, with little overall rotation. In summary, field evidence indicates a rapid, rafting mass movement mechanism, initially rotational, and subsequently more translational in nature.

GEOTECHNICAL MAPPING

A standard technique for determining factors which may be related to a mass movement process is that of producing detailed geotechnical maps of the area surounding individual slip sites. Such maps usually record hydrological data (e.g. springs, streams and poorly drained areas), geology, plant indicators of mass movement, recent scars, and surface forms such as joints, depressions and bulges (Rybar, 1973). A geotechnical field mapping program of this nature was carried out around each of the three representative sites. A limited mapping program, utilising field work and stereo-air photo analysis, was also carried out for the entire coastline of the Maungatapu Peninsula and some of the similar coasts nearby. The results of this program will be presented and discussed later.

The individual mapping exercises proved of little use, due largely to a lack of any notable features on the terrace surface. The highly permeable nature of the upper tephras result in no sign of drainage patterns being observable at ground level, and the very few surface irregularities observed in the vicinity of the representative sites proved to be man-made, and apparently not associated with mass movement. The appearance of tension cracks about the crowns of the failures was the only notable feature observed at the site scale. These cracks were not associated with progressive failure, only appearing after mass movement had

occurred. These cracks were observed to result in small toppling failures of the upper ashes during the months following mass movement.

Investigations of cliff morphology at and near the failures proved to be most productive when considered in a large scale context. These studies were therefore conducted as a part of the larger scale mapping program.

Studies of seepage rates proved useful on both the landscape and site scales. Briefly, the main facts noted at individual sites were:

i) Spring seepage occurred consistently above the clay marker bed, from the white sands, and sometimes from the yellow-brown sands above.

ii) Total seepage from the face of each scar varied from 0.5 liters per minute to tens of liters per minute, depending on the amount of antecedent rainfall.

iii) Seepage rates are generally higher at the scar faces than on either side.

Landscape scale studies, however, showed that there appeared to be no definite relationship between seepage rates and mass movement incidence. The presence of vegetation and refuse dumped over the cliffs made a complete survey difficult, however it appeared that seepage was continuous over almost the entire coastline. Seepage rates did vary somewhat, with very low rates occurring on the margins of slip site 1, along a high section of coast marking a

topograhic high in the surface of the Tauranga group sediments, and at a few other points about the peninsula. At these points flow may be so low as to be observable only as a distinct dampness of the silty sands above the clay marker bed. Recent mass movement scars are all found within areas of relatively heavy discharge, however there doesn't appear to be a distinct "sufficient cause" empirical relationship, as much of the coast exhibits seepage rates just as heavy, with no recent slip scars visible.

Local site scale disparities in seepage rates suggest a concentration of drainage, due possibly to irregularities in the surface of the relatively impermeable clay marker bed. Surveying of the upper surface of the clay marker bed with an Abney level in areas of drainage rate disparities revealed no such irregularities. This implies either that the hypothesised uneven areas are located inland of the sites investigated, that the irregularities are too small to be detected with an instrument as imprecise as an Abney level, or that the seepage disparities are due to some other cause. Gibb (1979) noted that an ancient depression in the surface of the Tauranga formation appeared to provide a drainage concentration effect at the landslide sites at Bramley Drive, Omokoroa, similar to that suggested here. At a few places on the peninsula, gullies extend back from the coast for up to 200 metres. It is possible that these gullies represent areas of past sub-surface drainage

concentration. The gullies have all now been modified during subdivision, so it is not possible to determine the amount of seepage occurring through them at present.

It is worth noting that during subdivision of the Maungatapu Peninsula, as at present, householders were required to provide their own storm-water drainage systems for houses and many sealed areas such as driveways. The standard method of drainage employed was to dig seepage holes, and to allow direct drainage into these. The drains were all dug to a "16 foot level", coincident with a dark brown coloured bed, according to local tradesmen. This practice appears to result in the discharge of storm-water approximately 1 metre below the base of the Rotoehu ash (see fig 3.5), that is, below what is apparently the finest, and least permeable bed above the clay marker bed. Household water is discharged at the same level. Although septic tank outfalls could not be located more accurately than to plus-or-minus 3 metres, there appeared to be no discernible association of these, or of storm-water outfalls with individual mass movements. Single outfalls may be found within 10 metres of all the slip scars, but outfalls draining similar areas of roof and driveway may be found closer to stable faces than this. Roads are the only areas where storm-water drainage is not directed to below the base of the Rotoehu Ash. The road drainage system is reticulated to discharge points not far above mean high water mark.

The effects of subdivision on drainage patterns may be estimated by first quantifying the areas affected by road drainage, and by roof and driveway drainage. Random samples of areas of the peninsula were examined on aerial photographs, using a planimeter, and the following percentages were calculated:

Roads: 8%

Drained, sealed: 16%

Unaffected: 76%

About half the driveways observed were not connected to seepage holes, but drained onto lawns. This is taken into account in the above figures. As no surface runoff occurs on the peninsula, urbanisation resulted in a loss of about 10% of the precipitation available for seepage, while a further 15% joins the groundwater cycle somewhat more quickly. The volume of effective precipitation increase afforded by town water supply reticulation can only be estimated, as the area is not metered. Domestic water supply records show an addition of approximately 5% onto the annual precipitation for the subdivided portion of the Omokoroa Peninsula.

NON MASS MOVEMENT PROCESSES AND FEATURES

During site scale investigations, a number of features and small scale processes were observed on and about the

slip sites investigated. These processes constitute a part of the geomorphic process or set of processes affecting the cliffs, of which the mass movements are the most conspicuous element.

Starting at the terrace level, one striking feature of the mass movement scars is the vertical, and often overhanging nature of the upper main scarp ('a'). Several processes have been observed actively modifying this form. The most dramatic is that of the toppling of large blocks of the upper tephras, from 10 to 100 cm thick, and 1 to 3 metres across. The bases of all the blocks observed were within the loose, sandy, orange Mangaone Lapilli. Toppling occurred after the appearance and growth of a tension crack over several months, commonly to one side of the main scarp (fig.3.10). All the failures observed occurred within a few months of mass movement. The long term effect of these toppling failures is to bring about a retreat of the cliff edge, decreasing the average slope of the cliff.

A similar cliff edge retreat is produced by a slower frittering of the loose sandy beds of the Rotoehu Ash and Mangaone Lapilli by the wind. During the summer very dry aggregates of the loose to friable upper soil and paleosols may also be seen blowing away, and slumping off as the support of the sandy beds below is removed. Slaking due to regular wet-dry cycles may also play some part in the attrition of these soils. The cumulative effect of these

Fig. 3.10(a). 1.2 metre deep crack behind the block which toppled.

Fig. 3.10(b). The block, a few minutes prior to failure.

Fig. 3.11. Spalling failure at the centre of site 3.

Figure 3.12. Effect of spalling-type failures on bluff morphology.

frittering processes is to produce a rounded, retreating cliff edge.

Further down the scars, a group of surface seepage related processes may be observed. At site 3, seepage appears to be particularly concentrated at the center of the main scarp base. Where this springing occurs a process of removal of the loose yellow-brown sand was observed, notably during and after rainstorms. The movement of the material resembled millimetric debris flows as small rivulets moved large amounts of light, pumiceous material. As a consequence of this removal process, a spalling falure occurred at the center of the base of the main scarp (fig 3.11). It seems probable that this process of undercutting and spalling will result in the slumping of a block of the upper tuffs and tephras, causing a retreat of the cliff crown, and butressing the lower portion of the main scarp (fig 3.12). The toppling process affecting the upper soils, and the seep/spall/topple process active further down were not observed often enough to enable quantitative estimates of their effects on cliff morphology. Any morphological effects that the frittering processes affecting the upper soils may have had were insufficient to be measured over a period of 12 months.

Another feature consequent on seepage, and observed on all the mass movement scars, was the incision of deep channels in the shelf ('b') features by seep-supplied

rivulets. Site 3 exhibited a single rill channel 30 cm deep and 20 cm across, and extending 4 metres back from the edge of the shelf, which was formed by a single major stream, as well as several minor channels formed by smaller rivulets. Sites 1 and 2 had a more even spread of seepage across the base of their main scarps, and consequently a wider distribution of rill erosion. The difference in times of exposure to erosion between site 2's shelf and the outer portion of site 1's shelf appears to show a development sequence. The rills become steadily more deeply incised at the outer edge of the shelf, and cut back towards the main scarp, steadily degrading their channels to a terminal form in which a steep drop from the base of the main scarp to 2 or 3 metres a.s.l., is followed by a very gentle drop to sea level. Block slumps and falls of the order of tens of cm wide and deep, occur in the blocky silts and sands along the edge of the rills as they are incised, and as they develop meanders near sea level, late in their development. The rill channel sides generally stand at an angle of 55 to 70 degrees, indicating their temporary nature. Site 2 shows rilling to an average depth of 20 cm over about 5% of the shelf area; a total of perhaps 0.2 cubic metres removed after 18 months exposure. Site 1, after 5 to 10 times this exposure period, shows rilling to an average depth of 30 cm over about 30% of the surface area, a total volume of about 3 cubic metres. Site 3 experienced a loss of about 0.4

Fig. 3.13(a) Passive erosion: western side of debris lobe.

Fig. 3.13(b). Passive erosion:eastern side of debris lobe.

Fig. 3.13(c). Flat lying debris toe protected by a wooden seawall.

Fig. 3.13(d). Active erosion of Tauranga Group sediments.

cubic metres from its single major rill. Converted to rates of erosion (cubic metres eroded per metre of slip frontage per annum), all three sites return similar values of 0.02 (sites 1 and 2) to 0.04 square metres per annum (site 3). The long term effect of this rilling process on the slip morphology is to remove the distinctive shelf form. Assuming the rates estimated above are representative and consistent, shelf removal by this process alone would take on the order of 500 to 1000 years.

The long, lobate mound of displaced material experiences reworking in the form of minor slumping, wash erosion by rain, and alluvial reworking by the seep-supplied streams. The main process affecting the debris lobes, however, is the removal of material by wave erosion. Immediately after mass movement, the debris lobes slope to the intertidal mud flats. Within weeks wave attack produces small cliffs tens of cms high. These miniature cliffs are formed more quickly, and retreat noticeably more rapidly on the north and north-west sides (fig. 3.13). Removal of the material by slow longshore drift in a 2 to 3 metre zone, obvious due to its cloudy color, occurs for 2 to 3 hours either side of high tide. All the debris lobes observed lay well above the high tide mark.

The erosion of the debris lobes may be described as passive erosion: removal of material not resulting in an actual decrease in stability, but further predisposing the

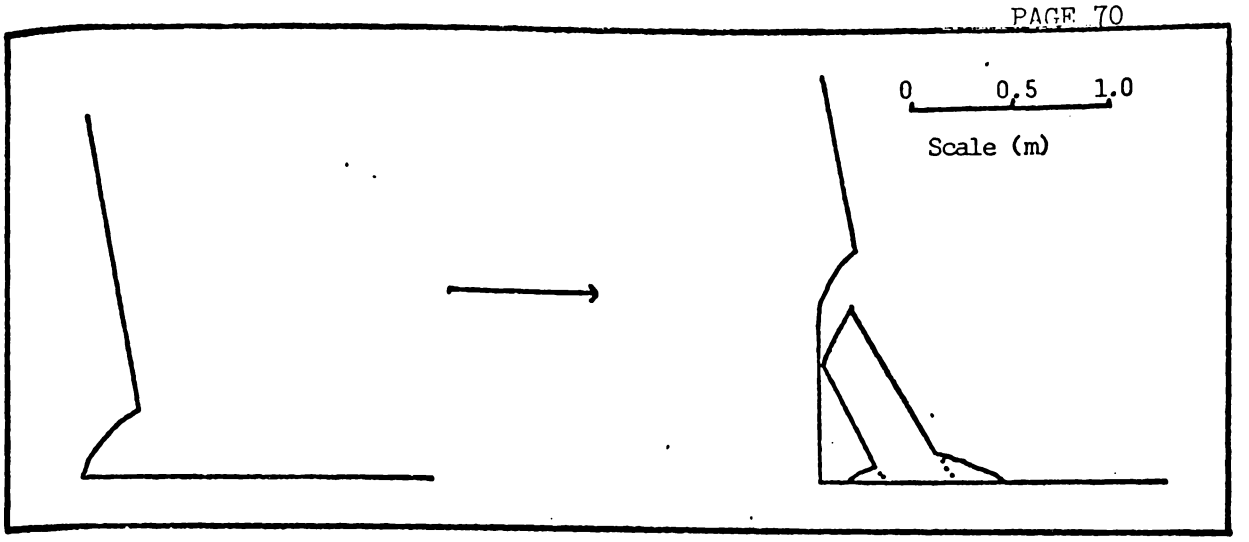

Figure 3.14. Collapse-fall failure at the bluff base.

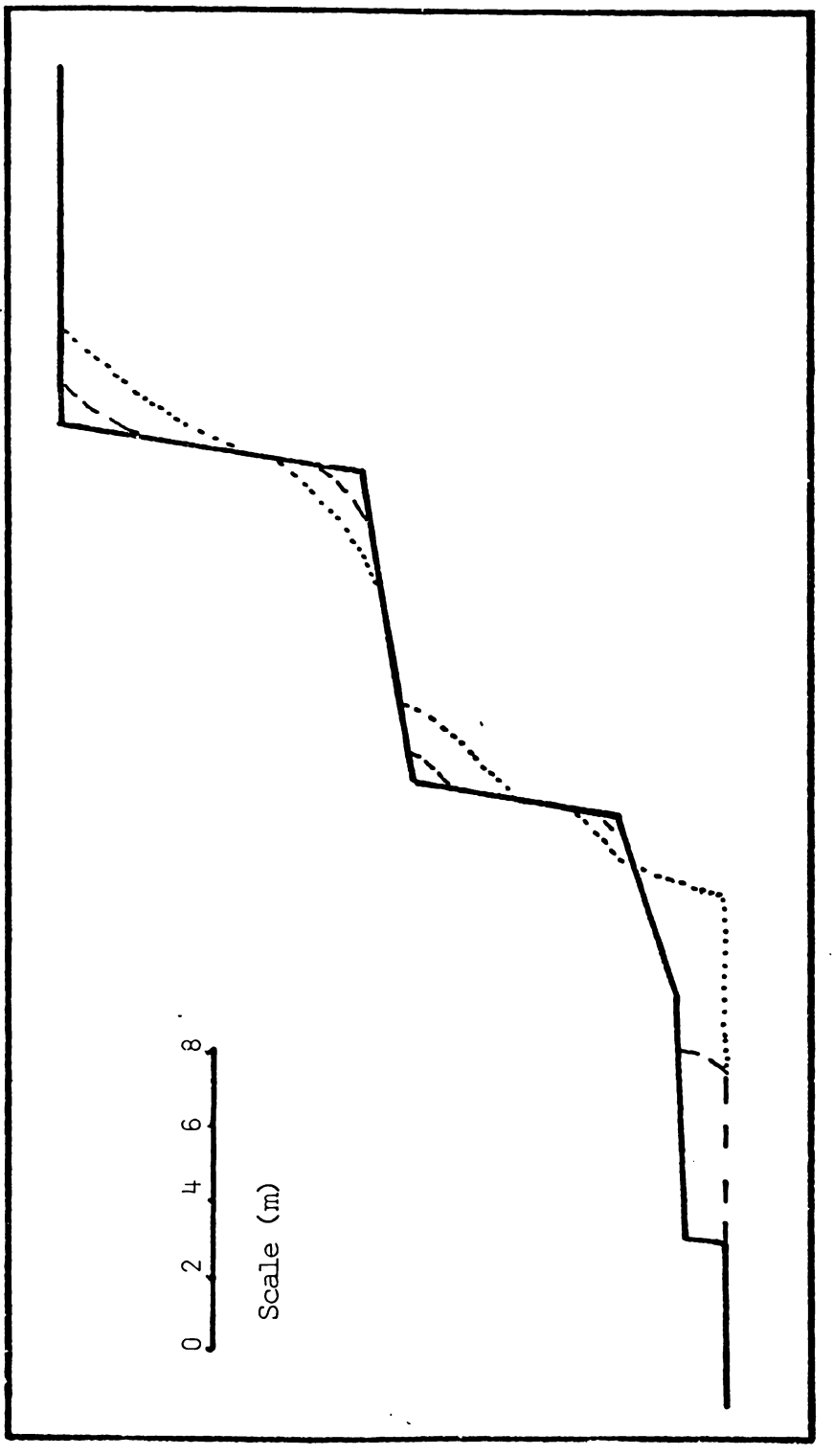

Figure 3.15. Cumulative effect of slope modifying processes.

cliff to such a loss. On the removal of the protecting mass of the debris lobe, wave attack would result in active erosion: removal of material resulting in a decrease in the cliff's stability. Commonly a rather nebulous distinction, this is one worth making here, as the debris lobe and intact cliff are sufficiently different in composition and thickness for a large change in horizontal toe retreat rates at the active-passive erosion boundary. More significantly, there is no loss of buttressing effect during passive erosion, due to the uncommonly low rest angle of the debris lobe; hence this distinction marks a major boundary in the cyclic evolution of the stability of a cliff under wave attack.

Active erosion is far less obvious than passive erosion along the coastline of the harbour, reflecting its slower horizontal progress. It is usually manifested as a process of undercutting, followed by collapse-fall failures (Lash, 1971, fig. 3.14). The large, usually intact, block is broken down by further wave attack, however this process is relatively slow, hence it is common to find cliffs which have developed steep basal sections with many small 'boulders' of sediment at their bases. The rate of basal erosion is dependent on the flux of eroding energy at the exposed face. As Maungatapu Peninsula lies within a largely enclosed tidal basin, the main energy souces available are tidal currents and wave erosion. The relatively minor

influence of the former (Wallingford report, 1963) would be dependent on the mean depth of the water at the exposed face through a tidal sequence, and the distance of the exposed face to the nearest tidal channel. The wave energy flux would likewise be dependent on the mean depth of water at the eroding face, and also the waves' local directional distribution. In an enclosed area such as Tauranga harbour, the directional distribution of wave energy is dependent, not only on the directional distribution of wind energy, but also on the fetch over which this energy may be transferred to the water. A wind stress analysis is usually necessary to determine the true dominant wind energy direction, as a wind-rose type analysis fails to take into account the increase of wind stress at a rate between the square and the cube of the velocity.

i.e. $\text{wind stress} = (\text{wind velocity})^{2-3}$

However such a procedure is rendered unnecessary in this case by the gross differences in wind energy direction indicated by the velocity classed wind rose (fig. 2.4) of deLisle (1962). For the purposes of this study it is sufficient to note that the principle wind stress direction is from the west (resultant 273 degrees, Healy et. al., 1977). Within the Tauranga harbour then, one might expect to find basal erosion most commonly on faces exposed to the west with a more than minimal fetch in that direction, and possibly in areas close to tidal channels.

In summary the processes observed acting on the mass movement scars, and the harbour coastline in general, have the following effects (fig. 3.15):

i) rounding and recession of the square crown, and lowering of the main scarp angle;

ii) removal of the shelf feature;

iii) removal of the displaced material, and undercutting of the cliff edge.

LANDSCAPE SCALE INVESTIGATIONS

INTRODUCTION

Qualitative evaluation of factors significant in the genesis of mass movements may be carried out by investigating the areal distribution of mass movements and factor associations at this scale, as well as by the more site specific methods already discussed. It is usually appropriate to carry out such large scale work as a mapping exercise. By locating mass movement sites on a map, one is not only able to elucidate areas of event concentration, but also to record possibly relevant data, such as vegetation type, changes in geology or general geomorphology, aspect, distances from erosive water channels, and anthropic features such as roads and house sites.

COASTAL CLIFF CLASSIFICATION

Preliminary field investigations, together with small scale aerial photograph analysis, showed that the coastal cliff morphology of the Maungatapu peninsula could be loosely grouped into three classes:

type 1: steep; steep 'c' and/or 'e', sharp 'a'/'b'/'c' breaks;

type 2: moderately steep; 'c' varies from steep to moderately steep, less distinct 'a'/'b'/'c' breaks;

type 3: low angle; smooth slope.

Note: Angles are defined from the edge of the terrace to 2 metres above high water mark.

When viewed on aerial photographs, particularly large scale ones, it is possible to subdivide the type 1 cliff group on the basis of steepness, a division not readily observable in the field. Subtype 1A (very steep) profiles generally possess a near vertical main scarp ('a'), and profile segment 'c' is generally steep (40 degrees or more). A subtype 1B (steep) profile is closer to those of type 2, commonly exhibiting greater rounding of the crown, and hence a slightly lower 'a' angle. The slope breaks between sections 'a', 'b' and 'c' are also less obvious.

The terrace edge above a length of type 1 cliff coastline consists of a series of linked arcs, usually square or slightly rounded in vertical section, above

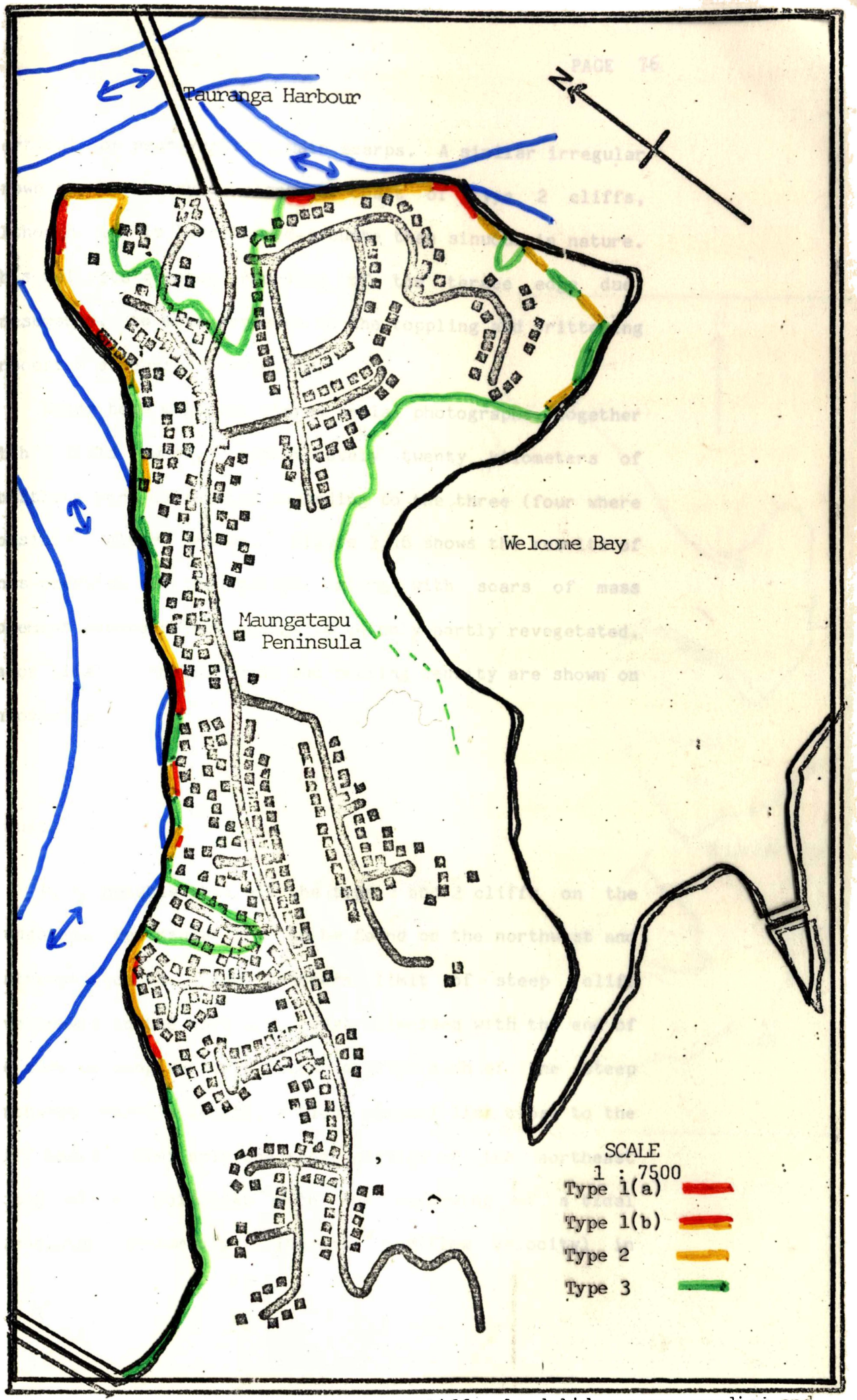

Fig.3.16. The distribution of typed cliffs, landslide scars, roading and housing densities on the Maungatapu Peninsula.

vertical or near-vertical main scarps. A similar irregular crown may be observed along a coast of type 2 cliffs, although it is less linked-arcuate than sinuous in nature. This reflects greater rounding of the terace edge due, presumably, to more exposure to the toppling and frittering processes discussed previously.

Using both mono and stereo aerial photographs, together with field work, approximately twenty kilometers of coastline were classified according to the three (four where possible) class scheme. Figure 3.16 shows the results of this exercise on Maungatapu, along with scars of mass movement events recent enough to be only partly revegetated. Major tidal channels, roads and housing density are shown on an overlay.

Results

It is notable that all the type 1 and 2 cliffs on the Maungatapu Peninsula are to be found on the northwest and northeast coasts. The southern limit of steep cliff development on the northwest coast coincides with the end of the zone of long westerly fetch, and for much of the steep northwest coast's length, a tidal channel lies close to the cliff bases. Similarly the steep portion of the northeast facing cliffs coincides with the narrowing of a tidal channel (and presumably an increase in flow velocity) in

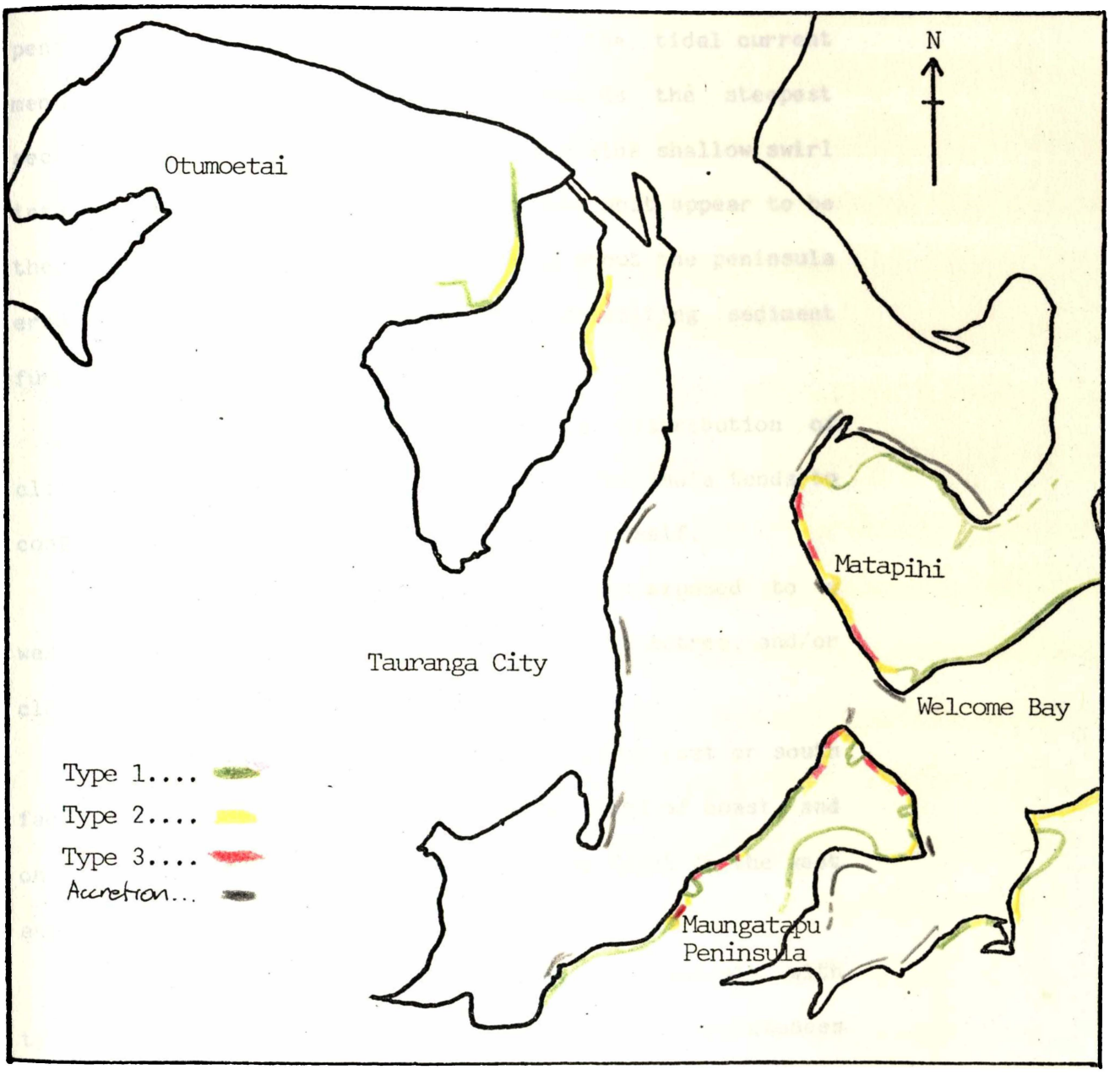

Fig. 3.17. The distribution of some typed coastal cliffs near the Maungatapu Peninsula.

close proximity to the cliffs. Accretion occurs on almost all of the south and southeast facing coastline, an area where no discrete tidal channels may be observed. Accretion may also be observed along the northeastern tip of the peninsula, apparently in the lee of the tidal current mentioned above, which swings in towards the steepest section of the coast, and then out in a wide shallow swirl into Welcome Bay. Aerial photographs show what appear to be the most heavily laden littoral currents about the peninsula eroding these steep cliffs, and then depositing sediment further along the coast and in Welcome Bay.

Examination of fig. 3.17 showing the distribution of cliff types on coasts near the Maungatapu Peninsula tends to confirm the observations made on Mangatapu itself.

i) Type 1 and 2 cliffs occur on coasts exposed to a westerly fetch of greater than 200 to 300 metres, and/or close to a tidal channel.

ii) Type 3 cliffs occur most commonly on east or south facing coasts, in the lee of exposed sections of coast, and on coasts with less than 200 to 300 metres fetch to the west and no nearby tidal channels.

iii) Accretion is associated almost exclusively with type 3 cliffs, and is found only in the circumstances described in ii) above.

It seems probable that the group of cliffs classified as types 1A, 1B and 2 represent an evolutionary sequence of repeated landsliding. The sequence would involve:

i) mass movement,

ii) removal of debris toe,

iii) rounding of crown,

iv) oversteepening and retreat of 'c',

v) removal of outer 'b' by rill erosion,

vi) mass movement.

The form of a cliff at any one time would be dependent on the time since the last failure, and the relative rates of basal erosion, rilling and upper slope attrition. If basal erosion occurs rapidly, one might expect a type 1A cliff with almost no 'b', immediately prior to failure. If basal erosion is relatively slow, the cliff might be expected to be more eroded in the upper section with a rounded crown, a low angled 'a', and an abbreviated 'b'. According to this model, failure could be expected from a cliff of either type 1A or 1B morphology. Cliffs of type 3 represent a state where basal erosion has ceased to be a significant geomorphic factor. The processes of rill erosion, wind attrition, toppling and creep would remove the angular crown and shelf features. Slope wash, creep and possibly shallow translational landsliding processes would then produce a smooth slope, subject to 'normal' hillslope processes.

Similar erosion-rate dependent coastal cliff evolution

models have been suggested for cliffs in London Clay (Hutchinson, 1973) and glacial moraines and clay till (Gelinas and Quigley, 1973; Quigley and Gelinas, 1976). These comprehensive models suggest a third state; one where basal erosion removes material at the same rate as it is supplied by downslope transport processes. This results in a bilinear slope profile; a steep feeder slope above a low angle, and often short, accumulation slope, retreating parallel to itself. It seems likely that a slope experiencing equal toe and crest retreat rates on the Maungatapu Peninsula would exhibit different morphology, owing to local geology. The differences in cohesion between the lower and upper soils would result in a biplanar cliff profile, with a steep lower section retreating by undercutting and toppling, and a lower angled slope in the upper non-cohesive sands retreating by slope wash and similar processes. Several cliffs were observed which arguably showed this morphology, however it is equally possible that these profiles were in transition from type 2 to type 1 morphology, or experiencing an increase in basal erosion rates. It is possible that the dynamic nature of erosion and erosion rates results in few or no areas having sufficiently balanced erosion to develop this (merely postulated) morphology.

Anthropic Effects

Areas of dense housing appear to be associated with

recent failures or, more accurately, with areas of type 1 and 2 cliffs. It is probable that this association is a function of the financial rewards furnished by developing flat-lying sections, some with a cliff-top view, which lie close to the main road. The preservation of a large strip of land for motorway development, together with the lower popularity of sloping sections with southerly aspects is probably responsible for the coincidence of low density housing with type 3 cliffs.

Cliff Type - Mass Movement Associations

Recent mass movement scars are found only in areas of type 1 cliff morphology and, more commonly, type 1A morphology. This apparently supports the suggestion made earlier, that cliff evolution probably involves many transitions of failure - type 1A - failure, failure - type 1B - failure, failure - type 2 - type 1A -failure, and failure - type 2 - type 1B - failure, with the latter two involving slower basal erosion rates. The definition of type 2 cliffs makes no mention of 'a' or 'c' slope angles, or 'b' length, hence this group covers all cliffs which have degraded due to a period of aggradation or protection from active basal erosion by the presence of a debris toe. Type 1 cliffs, with their postulated faster evolutionary cycle, might therefore be expected to be associated with a greater number of failures.

The scalloped cliff crowns found along all the

cliff-type 1 and 2 coastline, indicate that cyclic landsliding is universal in areas of basal erosion. There does, however, appear to be another factor or factors controlling landslide cyclicity. A number of cliffs exhibit apparently critical type 1A and 1B morphology without any observable recent failure scars. Basal erosion has produced very steep 'c' sections, sometimes continuous with 'a' sections, and this morphology appears to have been maintained for a minimum of 35 years, according to aerial photograph analysis, and probably very much longer. The most obvious group of such cliffs occurs on the northern tip of the northwest side of the peninsula, coincident with a section of coastline exhibiting very little seepage above the clay marker bed. This association appears to hold true in the other isolated cases observed. The length of 'dry' coastline is found where an old topographic high in the upper surface of the Tauranga Formation occurs, elevating the impermeable clay marker bed's surface, and limiting the area drained at the cliff face. As discussed earlier, no such explanation can be offered for other, more localised, areas of low seepage on the evidence available.

Basal erosion appears to be a necessary, but not sufficient, condition for mass movement. The appearance of cliffs which bear evidence of past mass movements, exhibiting little seepage at present, leads one to conclude either that 'high' seepage rates are not necessary for

failure, or that 'high' seepage rates are necessary, and that they did occur at these cliffs at some time in the past. Elucidation of this point requires investigation of the reasonableness of the occurrence of high seepage rates at points which now exhibit low seepage rates, of the efficacy of seepage rate variation as a mass movement triggering mechanism, and of the possibility and efficacy of any alternative mass movement triggering mechanisms. Possible mechanisms which may be suggested by referring to similar mass movements reported in the literature are:

i) critical stress reached through increasing soil density as % saturation increases,

ii) critical strength loss as % saturation increases,

iii) mobilisation of sensitive beds,

iv) external stresses - structures, traffic or seismic vibrations.

The presence of sensitive soils was suggested to be of significance in the occurrence of the mass movements on the Omokoroa Peninsula (Smalley et al., 1980; Gulliver and Houghton, 1980). The presence of sensitive material has been found to affect the nature of mass movement, favoring high speed failures and retrogressive landslides, after failure conditions have been reached. The mobilisation of a sensitive material does not, in itself, constitute a mass movement trigger. Vibrations, induced seismically or anthropically, have been recognised as the trigger of many

failures (Schuster and Krizek, 1978). Seismically induced vibrations are not a likely trigger mechanism in this case, considering the pronounced temporal association of mass movement events with intense rainfall events. It is also unlikely that anthropically induced vibrations are significant in causing failure, as much of the coast is too far away from any source of vibration, not to mention the fact that failures occurred long before the area was settled. One short length of coastline on the southeast side of the Matapihi Peninsula, is within 15 to 20 metres of the Tauranga to Mt. Maunganui highway. The vibrations induced by passing trucks are very noticable at this point, resembling a low magnitude seismic tremor. It is possible that in a situation where one or more factors reached near-critical levels, the stresses imposed by traffic induced vibrations might cause a failure which otherwise might not have occurred. Validation of this suggestion would require a long term monitoring program, or dynamic strength testing, and/or a detailed study using stability analysis techniques which account for dynamic stress. The limited areal application of any results renders such an investigation impractical.

SUMMARY

Field work at the site and landscape scales has

revealed the following points.

i) The mass movements are rapid, initially rotational and then largely translational in nature, displacing 100 to 200 cubic metres of material up to 50 metres in an often partly intact form.

ii) The failure surfaces are biplanar in form, with the lower, near horizontal failure plane ('b') passing through usually saturated lensoidal silty sands in a sandy mud matrix, above a relatively strong and impermeable clay bed.

iii) Each mass movement event is part of a cliff evolutionary sequence.

iv) Basal erosion by tidal currents and north or northwesterly wind driven waves preconditions the cliffs to failure.

v) A mechanism associated with heavy rainstorms triggers each individual mass movement.

CHAPTER FOUR

Quantitative Analyses

INTRODUCTION

The understanding of most natural phenomena involves the erection and testing of many qualitative and/or quantitative models of facets of the phenomena. When natural materials are involved, the quantitative elucidation of the materials' physical properties, or the parameters of variation of these properties is necessary for this process of model evolution. At the same time it is necessary to provide standardised physical descriptions of the materials involved, so that the study results may be used and compared in other situations. Throughout the laboratory investigations, standard methods were used wherever possible, hence detailed discussions are entered into only where test modifications mean that a single reference to a standard test is not sufficient to fully define the procedures used.

Following the consideration of field investigations, a number of points of interest remain unresolved. The biplanar, non basal-intersecting nature of the surface of rupture remains unexplained, and possible mechanisms for providing the rapid, rafting, highly translatory mode of

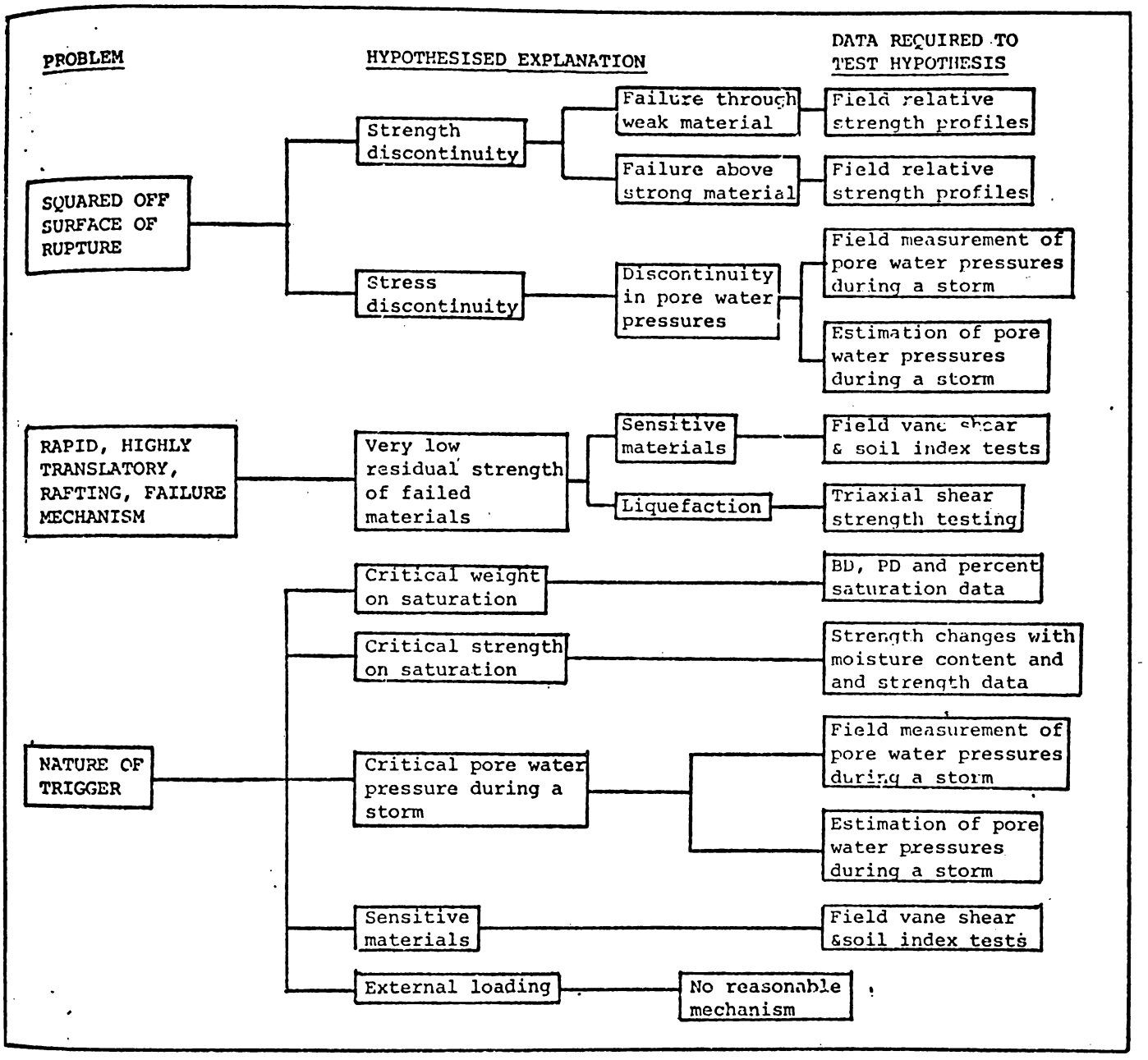

Fig. 4.1. Directive flow plan for quantitative investigations.

failure have yet to be validated. The plausibility of several possible mass movement triggers must be evaluated, and finally investigation of the effects of reversible land-use changes and possible remedial measures using the same data would prove beneficial. Alternative explanations for the unexplained features and the possible consequences of changes to the local environment may be suggested, and the information required to test these hypotheses may be catalogued (fig. 4.1). It therefore appeared that quantitative evaluation of poorly understood aspects of the nature, causes and effects of the mass movements required the following data;

i) strength profiles of the cliffs indicating the relative peak and residual strengths of the materials in which the cliffs are formed,

ii) the variation of these strengths with moisture content changes,

iii) profiles of field moisture contents, bulk densities and particle densities,

iv) values of cohesive and frictional strength for materials which may then appear to be of critical importance,

v) the behaviour of the strength tested materials at failure,

vi) field piezometric data recorded during a mass movement event, or some other estimate of pore-

water pressures during a mass movement event.

Full description of the failures requires the use of various index tests to classify appropriate materials:

i)Atterberg limits,

ii) particle size analysis,

iii) mineralogical investigation.

LITERATURE REVIEW

The literature concerning laboratory and field techniques for obtaining the data listed above is voluminous. A brief cross section of the available literature presenting selections of appropriate techniques is presented below.

General reviews (e.g. Skempton and Hutchinson, 1969; Zaruba and Mencl, 1969; Blakeley, 1974; Schuster and Krizek, 1978) which consider the methodology of site investigations give good coverage of the most commonly used geomorphological and geotechnical investigative techniques. Voight's (1978, 1979) cross section of thoroughly researched case studies provides a database of practical slope engineering experience, giving examples of the applications and limitations of many relevant methods of investigation. More detailed discussions concerning techniques relevant to this study may be found in recent, more specialised reviews. Standard index testing procedures are outlined by Akroyd (1964), the Association for Testing and Materials (A.S.T.M.,

1978), Kezdi (1979), and the New Zealand Standards Association (N.Z.S.4402, 1980), amongst others, while theoretical treatments of soil mechanics aimed at the interpretation of such data are presented by Yong and Warkentin (1975), Mitchell (1976), Wroth and Wood (1978), Lambe and Whitman (1980) and many others.

Strength testing, mentioned briefly in most soil mechanics texts, is given detailed consideration in a number of publications. A few writers have attempted to consider techniques applicable to all soils (e.g. Skempton and Bishop, 1950; Bishop, 1966; Wilun and Starzewski, 1972 a and b; Lambe, 1973), while others limit discussion to clay soils specifically (A.S.C.E., 1960; Roscoe and Poorooshasb, 1963; Skempton, 1964) or granular soils (Bishop et al., 1950; Anagnosti, 1967) specifically. As the field of soil strength measurement is as subject to change as any other area of modern technology, most relevant advances and standards are still to be found in unreviewed short papers and technical notes. Where relevant, such publications will be mentioned in later discussions.

FIELD TECHNIQUES

Three of the areas requiring quantitative evaluation: 1) relative strengths of contiguous beds, 2) cohesive and frictional strength parameters of the materials (these

latter values can be used in stability models, and in this sense, are said to be 'absolute' strength values), and 3) piezometric observations, may be carried out in the field.

Relative Strength Determination

Relative strength determination may be carried out as easily in the field as under laboratory conditions, and the avoidance of disturbance during sampling and transport means that field values may better represent the true in situ shear strength. There are four commonly used methods for obtainng measurements of in situ shear strength; the standard penetration test, the pressuremeter test, the vane shear test, and the quasi-static cone penetrometer test (Tavenas, 1971; E.S.O.P.T., 1974; Schmertmann, 1975). The ready availability, direct data output, and rapidity of both the manual vane shear and the manual quasi-static cone penetrometer tests recommend them as suitable for use.

The vane shear test directly evaluates both in situ strength and sensitivity; however it has the disadvantage of being limited in application to fine grained materials (Arman et al., 1975). A lack of understanding of the nature and distribution of shearing during vane shear testing has resulted in a recent tendency to avoid the vane shear test, however it is still considered perfectly valid as a 'strength index' test (Schmertmann, 1975; Blakeley, 1974). The Geonor vane shear was callibrated in the laboratory to check the validity of field results (Appendix 2). The

manufacturer's callibration appeared accurate to 5%.

Cone penetrometers are widely used to estimate shear strength through the dependent parameters of cone bearing capacity and soil - steel friction. Simple models provide strength index numbers based on the force required to drive a standard 60 degree head into the soil. Both the vane shear and the penetrometer tests used provide strength index values, the vane shear in units which invite comparison with other field and laboratory derived values of unconfined shear strength. The penetrometer, on the other hand, is supposedly usable through a range of textures up to sand size, and hence is more appropriate for use in the materials being investigated.

The vane shear was used in the horizontal position, thrust 10 to 15 cm into vertical cuts in cliff exposures. Values of unconfined compressive strength obtained in this manner (whether with vane shear or penetrometer) provide the best basis for comparison of the strengths of soils which are naturally found under differing normal loads. Residual strengths were determined after 50 rotations of the vane, and sensitivities calculated using the definition of Terzaghi (1944):

$$S_T = \frac{q_u}{q_{u_r}}$$

where q_u = unconfined compressive strength, and q_{u_r} = unconfined compressive strength of samples remoulded at

constant water content.

In order to obtain an estimate of the relative densities of some of the sandy materials, similar peak and residual strength determinations were carried out, rather than determining large numbers of bulk density and particle density values. It was thought that, as sand strength is dependent to a large extent on the degree of packing, loose sands would provide initially low strength values and would pack down during the 20 rotations used for 'remoulding' to give an extremely low second value. Denser materials might be expected to give a higher initial reading, and a less marked loss in strength on remoulding. Packing indices were calculated in the same manner as Terzaghi's sensitivity numbers. It was originally intended that an attempt be made to evaluate both entire strength profiles, and variations within the profiles with seasonal moisture changes. Accordingly initial work was aimed at evaluating the variability of readings obtained for individual beds. Coefficients of variation at site 1 were found to be about 0.15 (vane) and 0.15 to 0.40 (penetrometer) for 15 trials of 20 readings taken within 1.5 metre horizontal spreads. Three partial profiles of soil strength taken within 2 to 3 metres of one another at site 1 show intra-bed differences of the same order as the inter-bed differences (fig. 4.2). Similar differences were observed in comparing full profiles from sites 1 and 2 (fig. 4.2). Similarly fig. 4.3 shows

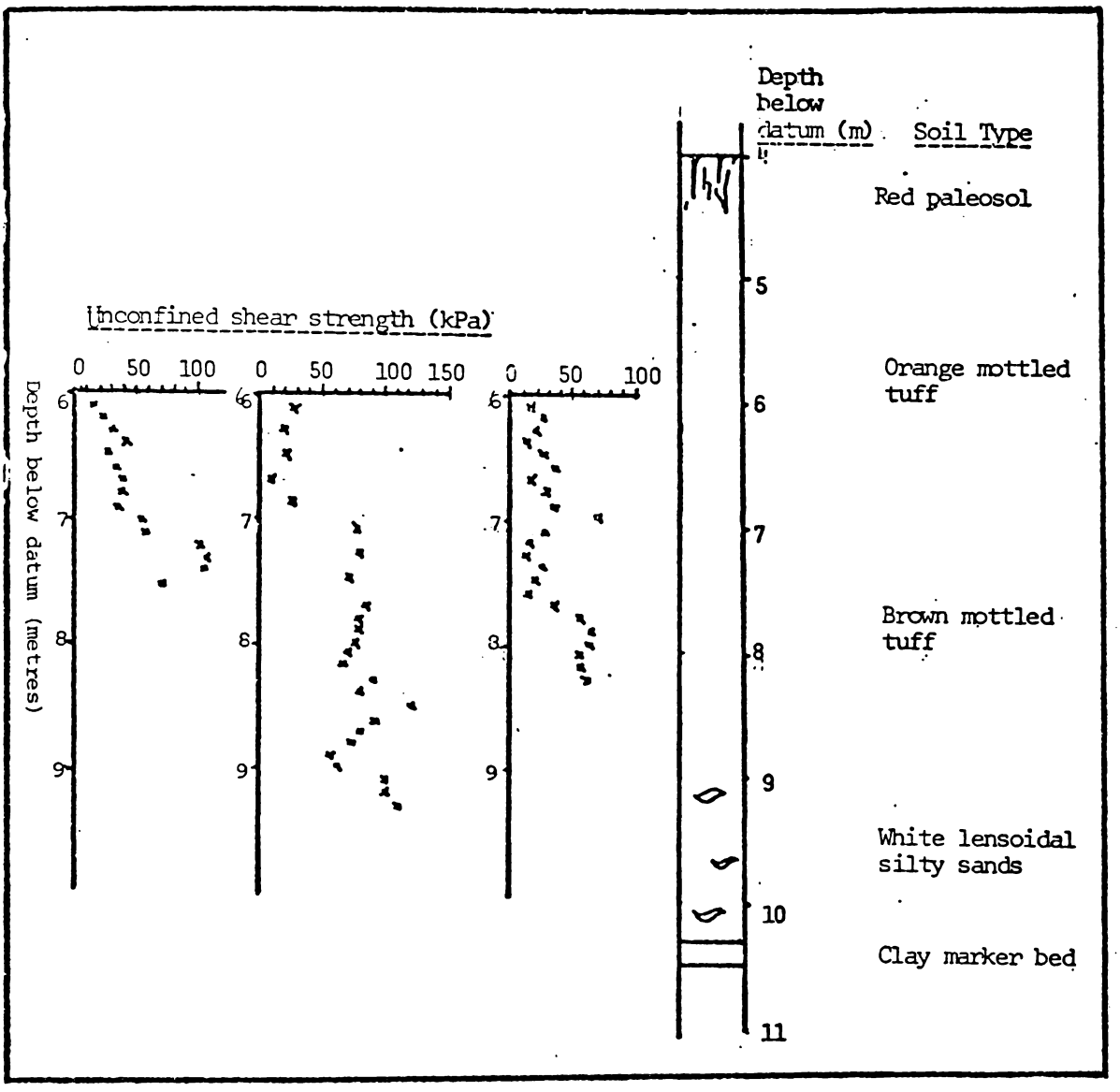

Figure 4.2. Partial vane shear strength profiles obtained at test site 1

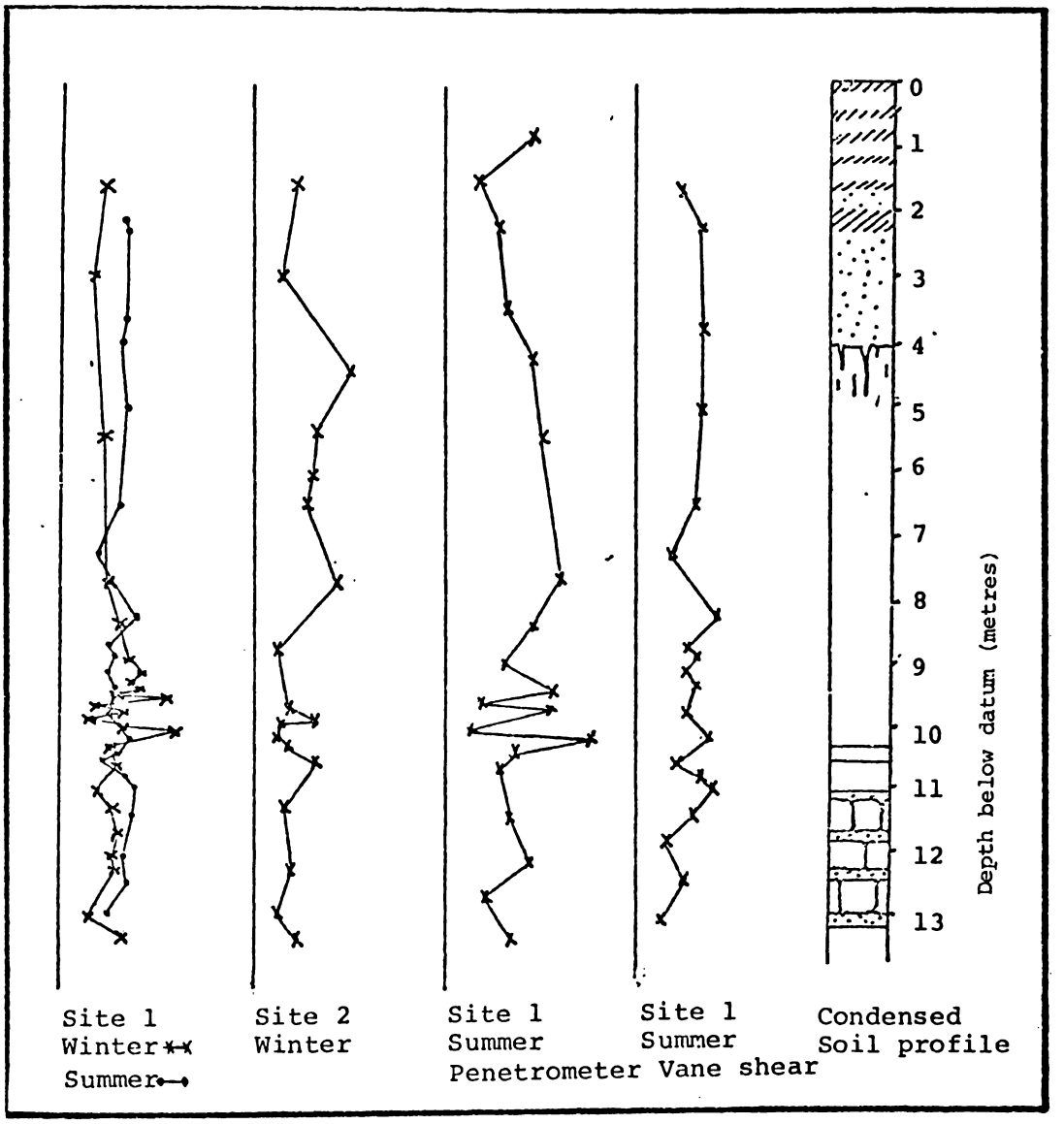

Figure 4.3. Field relative shear strength data.

the disappointing lack of distinction encountered on comparison of summer and winter profiles from site 2. Oven dry moisture contents were generally 50 to 100% higher in the winter, reflecting the large seasonal differences in soil moisture contents which might have been expected to cause some seasonal variation in soil strengths. Unfortunately the penetrometer was not available for use during the summer, hence a parallel seasonal evaluation was not possible. The similarity of the coefficients of variation of the penetrometer data to those of the vane shear data indicate this probably would not have provided any further information. Any soil shear strength changes with moisture contents appear to be of sufficiently small magnitude to be obscured by natural soil variability and instrumental error.

When the relative strength data (fig. 4.3) are examined, it must be noted that the measurements at about 9 to 10 metres below datum were taken in the lensoidal silty sands with the finer matrix giving higher values than the loose, coarser matrix. Profiles b and c probably show a disproportionately high number of low readings, as it is often difficult to distinguish between the two materials in field exposures. Bearing this in mind, three facts may be noted. First, and most important, is the lack of any major strength discontinuity in the strength profiles. The only area where strength disparities appear is within the

lensoidal silty sands. As already noted, this material consists of a strong and apparently continuous matrix with pockets of weaker material within it. It is therefore likely that the 'bulk' strength of the material is not significantly different from that of the other soils in the profile. The clay marker bed appears to be stronger than average. A slight trend towards lower strengths below the clay marker bed may also be noted.

Secondly the soils are all quite weak. This may be illustrated by considering the strength values obtained for central yellow-brown loams and central yellow-brown loams by Rogers (1978). Typically these soils exhibit unconfined compressive shear strengths in the range 130 to 180 kPa, below the A horizon. A third feature of the relative strength profiles is the similarity of the trends observed with the vane shear and the penetrometer. This apears despite the suggested inappropriateness of the vane shear test in coarse materials, and the different units of measurement applied. Some small part of the irregularities in the vane shear test results may possibly be attributed to its theoretical inapplicability to testing coarse materials.

It seems, however, that the similar coefficients of variance obtained for individual beds, and the similarity of the features observed with both instruments tend to indicate natural material variability as the source of the poor moisture - strength change results. It is possible that

large numbers of readings, statistically analysed, may show changes in strength with increasing moisture content, however it is questionable whether a change of such a magnitude is likely to be great enough to significantly affect cliff stability.

Sensitivity

There are two commonly used definitions of sensitivity. Terzaghi's (1944) definition (defined earlier), based on unconfined compressive strength data, can utilise readings made by vane shear, penetrometer, and many other types of field apparatus. Most workers, however, (see e.g. Soderblom, 1975) utilise definitions based on relative strength numbers obtained by the drop - cone method:

$$S_T = \frac{H_1}{H_2}$$

where H_1 = undisturbed strength index number,

and H_2 = remoulded strength index number.

Sensitivity values were initially determined in the field, using the Geonor vane shear apparatus. The remoulded strengths of the more sensitive clays proved to be very close to the limits of precision of the vane shear, hence both these low values, and the derived values of sensivity are somewhat unreliable. Attempts were made to overcome this problem by taking undisturbed samples back to the

laboratory and determining unconfined compressive strengths with a Wykeham - Farrance Model 123500 Laboratory vane shear apparatus.

Samples were taken with 200 mm by 35 mm internal diameter (area ratio 17.9%) and 40 mm by 60 mm internal diameter corers (area ratio 11.3%). The sample cores were retained in their corers and packed in polystyrene foam for transport. It was thought that the long cores would be better suited to transport, as they were backfilled or trimmed flush at the ends, and then sealed with rubber caps which were the only part of the corer to touch the polystyrene packing, thus further isolating the samples from disturbance. The short corers, on the other hand, probably produced significantly less disturbance during sampling, owing to their smaller area ratio; however, it was thought the lack of end restraints and insulating packing mounts made transport disturbance more likely, hence both types of corer were used. The long cores appeared to be unaffected by transport. A few of the short, large diameter cores had shifted within their corers, and one appeared to have been somewhat disturbed in transport. These samples were discarded. The lack of apparent disturbance of the samples was reflected by the similarity of the laboratory derived strength and sensitivity values to those obtained in the field (Table 4.1). Remoulded strength determinations were carried out after remoulding with a spatula for one minute.

TABLE 4.1 Sensitivity and rapidity results

Sample	Vane shear			Penetrometer			Rapidity
	q_u	q_{ur}	S_t	H_1	H_2	S_t	number
Clay marker bed - lower	45 ± 5	≃0.5	100	250	>1.2	>200	4
Clay marker bed - upper	87 ± 10	≃1	90-100	25	>1.2	> 20	5
Grey gritty clay bed	111 ± 22	≃1	25-30	160	>1.2	>130	3

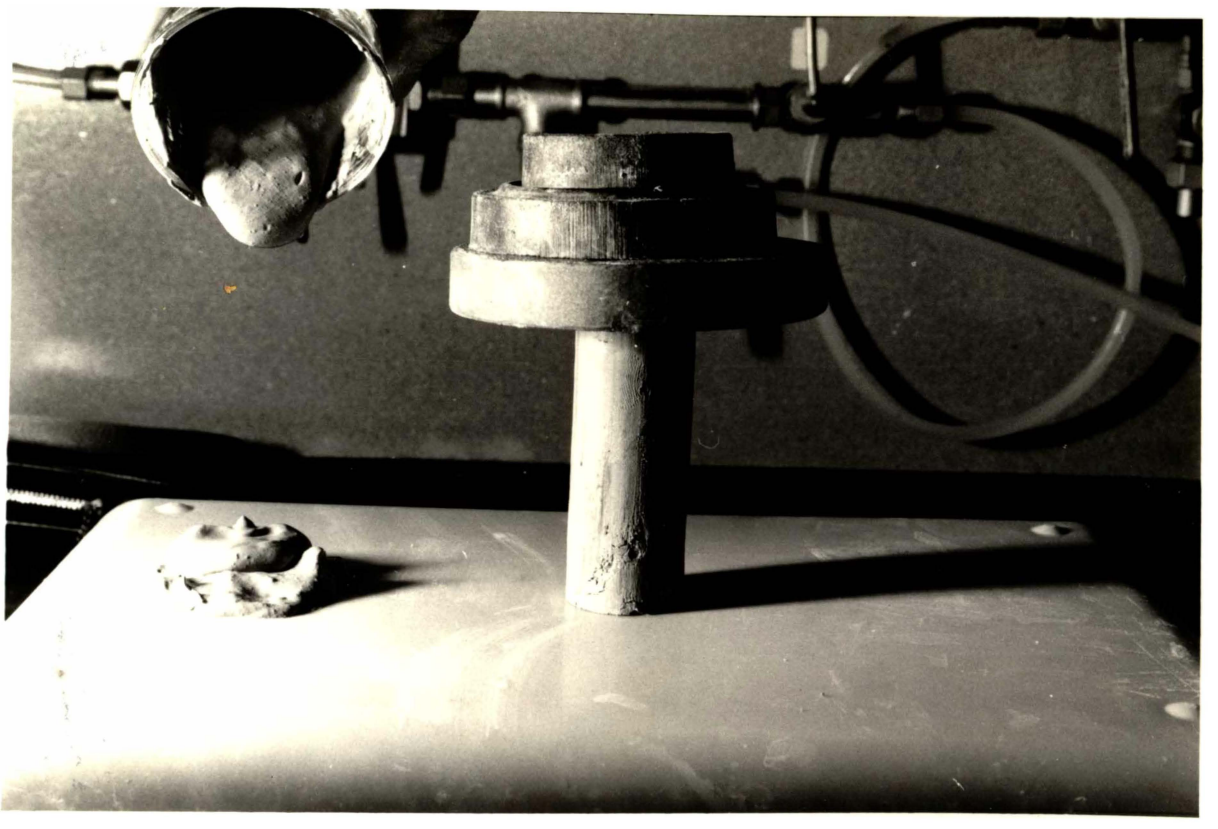

Fig. 4.4. Remoulded and undisturbed samples of the clay marker bed.

The problem of instrument sensitivity was not overcome by laboratory determinations, as the more sensitive laboratory vane shear apparatus also proved insufficiently precise to define adequately the remoulded clay strengths. The degree of this problem is reflected in fig. 4.4, showing two long core samples of the clay marker bed, taken from sites 5 cm apart. The fluid sample was remoulded for one minute with a spatula at field moisture content. Attempts were therefore made to determine sensitivity values using the drop-cone penetrometer method. Relative strength numbers were obtained with a standard 80 gram, 60 degree stainless steel head, using standard drop - cone penetrometer methods. Residual values were determined on samples remoulded for one minute with a spatula. H (strength index) values were then obtained from the conversion chart presented by Kezdi (1980). The resistance of the remoulded clays was so low that the penetrometer went byond its maximum reliable reading (23 mm) and hit the bottom of the sample dish within 0.5 to 1.0 seconds of clutch release. With only one head available, the drop - cone penetrometer therefore proved as unsatisfactory as the vane shear apparatus. A lighter cone such as that used in the Swedish penetrometer (Kezdi, 1980) may have made this method more suitable.

The sensitivity values obtained by laboratory and field vane shear, and laboratory penetrometer all rely on an inadequate measure of residual strength, and cannot be

considered as better than approximations. Table 4.1 shows both the combined laboratory and vane shear and the cone penetrometer sensitivity values. Values of plasticity index are shown in Appendix 1: these are low values, typical of low activity, sensitive clays. Sensitivity values of 100 to 200 are therefore recorded directly beneath much of the low angle part ('b') of the failure plane, and, perhaps more significantly, along the failure plane itself for the outer 50 to 150 cm of section 'b'. It is therefore important to further consider the significance of these sensitivity values.

Quick clays, soils significant in slope stability due to their sensitivity, were originally defined as those having sensitivity numbers over a certain value. For example Holmsen (1946, in Soderblom, 1975) defined a quick clay as having a sensitivity of greater than 50. More recently this type of definition has been extended to include a measure of the strength of the remoulded material. Odenstad (1951) specified a penetrometer sensitivity of greater than 50, together with a remoulded strength index number of less than 1, while the Laboratory committee of the Swedish Geotechnical Society (1973, reported by Soderblom, 1975) suggested a vane shear sensitivity of greater than 30, together with a remoulded unconfined compressive strength of less than 0.4 kPa. The samples investigated appear to conform to both of these types of criteria. However, as the

remoulded strength test values were unreliable, a further type of classification of sensitive materials, that of Soderblom (1975), was employed. Soderblom's (loc. cit.) method of rapidity number determination gives an estimate of the amount of energy input requred to produce the drop in strength indicated by a sensitivity number. This involves dropping an undisturbed core sample 10 mm 200 times, using Casagrande's liquid limit device, and then classifying the degree of disturbance on a scale of 1 to 10. Soderblom (loc. cit.) defined a quick clay as one with a sensitivity of 50 or greater, and a rapidity number of 8 or greater. The results (table 4.1), consistent over three samples for each value shown, indicate that an extremely large amount of energy would have to be applied in order for any of the sensitive materials to be liquified. It appears highly unlikely that even a major earthquake would be sufficient to trigger mobilisation of the sensitive clays, and in the absence of any such external source of energy, the sensitivity of the clays appears to be of little significance in mass movement instigation.

Sand Density

During field determination of the sensitivity of several of the clay beds, similar peak and remoulded strength determinations were carried out on the sandier materials in the profile as discussed earlier. The results of this investigation are shown in table 4.2. Strengths are

TABLE 4.2 Packing and strength indices of sandy materials

Sample	Packing index	Strength index
Silty sand, 30cm above marker bed	100-200	2
Sandy mud, 30cm above marker bed	30	12
Mottled brown sand 40cm above marker bed	25	2.3
Mottled brown sand 55cm above marker bed	20	2.5
Mottled brown sand 150cm above marker bed	20	2.0
Orange mottled tuffs	30	4.5

given as vane readings (1 unit equals about 2 kPa) to indicate their index nature. The test appeared to be satisfactory in that it tended to confirm observations made visually. The results show that most of the sandy materials in the profile are of roughly equal density, having similar packing indices, with a range in peak strengths which appears to be related to texture (and presumably cohesion) variations. The lensoidal silty sands appear to be far less dense than the surrounding matrix of sandy mud. Shearing of this material under saturated conditions could conceivably result in the generation of large positive pore water pressures as the lenses of silty sand collapse within the finer and, presumably less permeable, matrix. Almost all of the sandy materials sampled from below 6 m.b.d. had moisture contents well in excess of their liquid limits, suggesting many of the materials could exhibit low residual shear strengths , if sheared quickly.

Piezometric Observations

Field observation of critical piezometric conditions is the most useful method to use as a basis for modelling hillslope hydraulics. In general, these critical measurements are very difficult to make. Amongst others, the following problems occur;

i) difficulty of locating points where critical conditions might occur,

ii) likelihood of encountering critical conditions

within the necessarily limited period of observation,

iii) 'high point' values only may be recorded, as monitoring of rates of rising requires data logging equipment,

iv) Technical difficulties of obtaining correct piezometric values in nonhomogenous and/or anisotropic media.

Initial auger investigations revealed problems with bore-holes collapsing below 4 metres below datum. It became obvious that a cased bore would be necessary to monitor piezometric conditions below this depth. The property owners at all three sites were reluctant to allow the necessary drilling equipment onto their sections, and considering the possibility that little or no effective monitoring might be achieved, it was decided to abandon this side of the investigation. Several soak holes of 3.7 to 4.3 metres depth were located 15 to 30 metres behind sites 2 and 3. These had been dug out and lined with steel drums, and were believed to have relatively undisturbed bases (i.e. no coarse sand or gravel added). As the base of these soak holes roughly coincided with the top of the clay rich red paleosol at 4.0 metres below datum, it is possible that dessication during summer may have caused some shrinkage cracks to appear, thus locally altering the drainage regime for short duration storms. For longer duration storms,

however, it appeared likely that these soak holes would provide a reasonable estimate of the groundwater table height, should it rise to within 4.3 metres of the ground surface. Accordingly these soak holes were checked daily during and after heavy rainfalls by a section owner. At no point was a free water table observed. Laboratory tests relevant to investigations on the hydraulic regime about the test sites will be discussed later.

LABORATORY STUDIES

SOIL PHYSICS AND ENGINEERING INDEX TESTS

Soil index tests are used in the quantitative description of soils, for the purposes of soil classification and comparison, and in order to provide a basis for explaining soil behaviour. Index tests were conducted on samples of most of the materials involved in the mass movements, as an adjunct to the initial investigation, and as part of subsequent detailed laboratory work. The data obtained using the following tests are listed in appendices, and is presented during later discussions, where relevant.

Moisture content determination

Determinations were carried out on loose field samples

transported inside two sealed plastic bags, and on sub-samples of laboratory test cores. The weight of water was determined by oven drying at 106 degrees C, and moisture contents were calculated as:

(N.Z.S. 4402, test 1)

Atterberg limits

Atterberg limit determinations quantify a soil's remoulded strength / moisture content relationship, and are important in predicting and interpreting soil behaviour. Tests were conducted on loose double bagged samples, which were wetted from field moisture content, and then slowly dried over the test period. Determinations of both liquid and plastic limits were conducted using Towner's (1973) drop-cone penetrometer method, which is more rapid and consistent than the older (New Zealand Standard) Casagrande methods.

Density

Bulk density measurements were conducted on double bagged 40 mm by 48 mm internal diameter core samples in field moist and oven dry states. Results were generally low, with densities ranging from 0.75 g/cm^3 for a sand, to 1.35 g/cm^3 for a clay. Particle density determinations were carried out according to N.Z.S. 4402 test 8(B), using 50 ml

density bottles, and de-airing by shaking with teepol rather than by vacuum. Percent porosity and fully saturated bulk densities were calculated from these figures (Appendix 1).

Particle Size Analysis

Loose double bagged samples were subsampled to determine their natural moisture content, and were then disaggregated using an end over end shaker, and analysed according to N.Z.S.4402, tests 9 (A and D). Results are shown in Appendix 1 .

Mineralogy

Prior to particle size analysis, a check was made for the presence of allophane in each sample using sodium flouride solution and titrating with dilute hydrochloric acid (Perrot, Smith and Inkson, 1976). Other than this, semiquantitative mineralogical analyses were carried out by X-ray diffraction studies on powdered samples in comparison with a quartz standard (Nelson and Cochrane, 1970). Determinations were carried out on fine silt and clay size fractions, and bulk samples. Results showed little variety between the samples. In general, the clay fractions were completely dominated by halloysite, while the sand fractions were dominated by feldspars and sometimes quartz (table 4.3). The only remarkable feature revealed by the mineralogy work was the striking difference between the mineralogy of the <2 m and the <10 m fractions. The fine

TABLE 4.3 Dominant Mineralogy

Sample	<2μm	2-64μm	>64μm
Clay marker bed	halloysite	feldspar	quartz, cristobalite, feldspar
Silty sand and sandy mud	halloysite	feldspar	feldspar, cristobalite, quartz
Mottled tuffs	halloysite	feldspar	feldspar
Blocky grey gritty clay	halloysite	feldspar	feldspar, cristobalite, quartz

TABLE 4.4 Strength data obtained by direct shear testing

	cohesion (kPa)	ϕ' (degrees)	r^2
	0	41.6	.9316
Loose orange sandy tephra	1	40	.9683
Rotoehu Ash paleosol	0.2	41.6	.9215
Loose sandy Rotoehu Ash	0.3	37	.8984
Red paleosol	5.6	31	.9368
Orange mottled tuff	8.7	32	.9211
Brown mottled tuff	6.1	33	.9877

silt fractions were strongly dominated by feldspars and highly crystalline halloysite (narrow, high peaks), while the clay size fractions had no primary minerals, and only moderately crystalline halloysite, reflected by the production of low broad XRD peaks.

STRENGTH DETERMINATION TECHNIQUES

Field investigations have revealed a need for two types of strength investigation. The biplanar nature of the surface of rupture indicates a special condition, or set of conditions at failure, within the strata of lensoidal silty sands. Field strength and density investigations have shown that these materials have certain properties which are unique within the profile.

Accurate laboratory shear strength testing of soils may be stated as having two aims. Firstly, one may obtain an accurate, representative estimate of the soil's shear strength under given conditions. Secondly, testing may be used to determine the mechanical behaviour of the material at, or near failure, in terms of the stress paths followed and the rate and mode of failure. Ideally a form of strength testing combining elements of both should be used in every case. However, constraints, imposed by time, limit the use of such tests to situations where they might be expected to be of maximum value. Elsewhere more rapid

tests, supplying less information on soil behaviour, must be used. A shear strength testing programme was therefore proposed, as outlined below, and carried out at test site 1. Statistical checks, together with apparently reasonable results from initial stability analyses seemed to indicate that the programme was adequate, hence it was extended unchanged to sites 2 and 3.

Failure occurred within all the tephra and sedimentary beds above the clay marker bed, consequently the establishment of a failure model required strength data input from all these materials. Data concerning behaviour prior to, and during failure was also required for the metre of lensoidal silty sands which appeared to be of particular importance. Strength testing of the latter was therefore carried out in a Wykeham-Farrance triaxial shear apparatus, while the other materials were tested in a Wykeham-Farrance shear box.

Direct Shear Testing

The particular direct shear apparatus utilised has been employed with some success in testing local clays (e.g. Rogers, 1978; Bridson, 1980), and similar machines have been used in testing a variety of materials elsewhere (e.g. Skempton and Hutchinson, 1969). Theoretical objections have been raised as to the accuracy of the direct shear test when used in the testing of soils with highly developed structure (Sowers and Sowers, 1961; Lambe and Whitman, 1979). The

soils under consideration do not have highly developed structures, often being single grained. It appeared that the degree of in situ strength variation shown by field testing would probably render instrumental error insignificant. Considering the time constraints within which the study was conducted, it therefore appeared reasonable to use the direct shear box for testing all the materials except for lensoidal silty sands.

Samples were taken with 200 mm by 60 mm internal diameter stainless steel corers. These were inserted horizontally into the failure scarp, ensuring that the shear plane imposed during testing would be parallel to the observed failure. The cores were trimmed or backfilled flush with the corer end, capped, and transported in polystyrene foam cases. In the laboratory, 40 mm was discarded from each end of each core. Individual samples were extruded by hand and cut to length for testing in the circular direct shear box. Samples from below 7 m.b.d. were assumed to have failed under saturated conditions, hence tests were conducted on saturated, consolidated samples. For the other soils in the upper 7 metres of the profile, it was difficult to determine testing conditions which could be both representative of in situ conditions and consistent between samples. At first samples were prepared by 24 hours of consolidation under saturated conditions, draining for 1 hour, and then testing under drained

conditions. It was thought this would best represent conditions above the water table during, or after a heavy rain storm. However checks showed that results obtained using this method were not significantly different from values obtained from fully saturated tests. As the latter tests are somewhat more simple and more consistent in nature, all subsequent tests were conducted at full saturation. The tests were conducted under a range of normal stresses appropriate to the sample depth. A 'central' normal load value was estimated by referring to the bulk density profile, and normal loads of up to 50 % above and below this value were applied:.

For example, for a sample of Rotoehu Ash:

Sample depth : 2 metres

Average field moist unit weight: 11.5 kNm^{3}

Normal load : 23 kPa

Tests conducted at: 14.90 kPa

18.36 kPa

21.83 kPa

28.76 kPa

For the deeper samples, more tests were conducted at the lower end of the normal load scale, in order to provide an approximation of effective cohesion and internal friction angle, should the suggestion of a water table above those sample depths require testing during stability analysis.

The extra tests did not produce any significant difference in strength parameters compared with those derived from the initial normal load range used. It is probable that a large number of tests might reveal such a change in strength parameters as different normal load ranges are considered (Lambe and Whitman, 1979).

Evidence discussed in Chapter 3 indicates that the failures occurred rapidly. Trials were therefore conducted in order to determine the maximum rate at which direct shear tests could reasonably be conducted. The maximum rate of 1.22 mm min^{-1} was found to be too fast for dial gauge accuracy, and for accurate reading of the dial gauges. Tests were therefore carried out at 0.61 mm min^{-1}, the second fastest rate available. Rogers (1978) found that tests at this rate produced stress - strain curves and peak shear strength values esentially similar to those from tests as slow as 0.00065 mm min^{-1} on clay samples. The tests were otherwise conducted according to the methods presented by Akroyd (1964) and Chandler and Rogers (1978, unpublished). A total of 38 direct shear tests was carried out.

Proving ring shear stress values were subjected to an area correction to allow for the displacement of material at either end of the sample during strain. This correction to a consistent area shear strength is achieved by multiplying the dial gauge shear stress reading by a factor of

The area of displaced 'arc' produced by the displacement 'h' of two circles of radius 'r' is equal to the area of central displacement produced by displacing two semicircles of the same radius 'r' by the same distance 'h'.

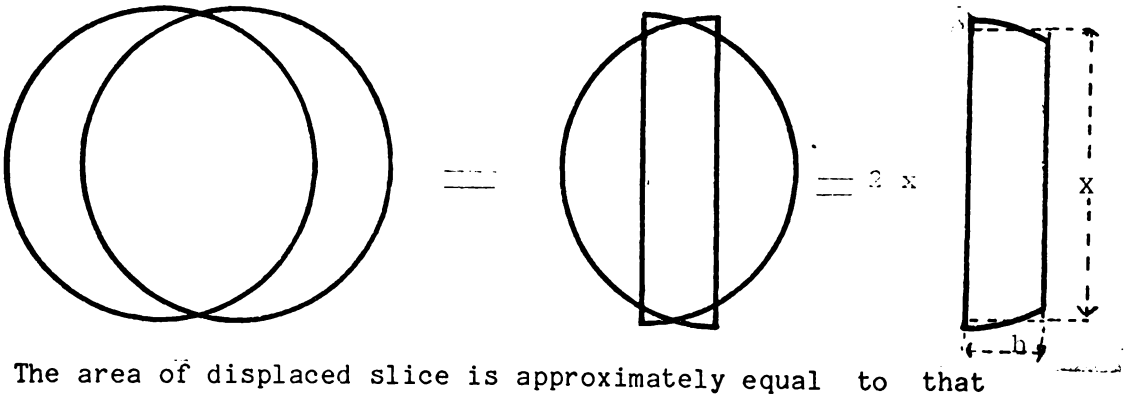

The area of displaced slice is approximately equal to that of a rectangle 'h' wide, by 'x' long. Now, for any circle:

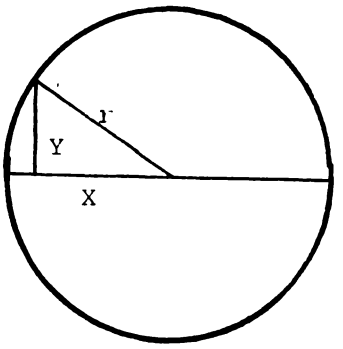

$$r^2 = y^2 + x^2$$

$$x = r^2 - y^2$$

For the semicircle slice, 'r' = 30 mm, and y = h/2

$$x = \sqrt{900 - h^2/4}$$

$$\text{slice area} = h\sqrt{900 - h^2/4}$$

$$\text{correction factor} = \frac{2828.57}{2828.57(mm^2) \times h \sqrt{900 - h^2/4}}$$

For ease of use, this correction factor has been tabulated and graphed. The graph is available in Geomechanics manual No. 4 (Law, 1980; unpublished).

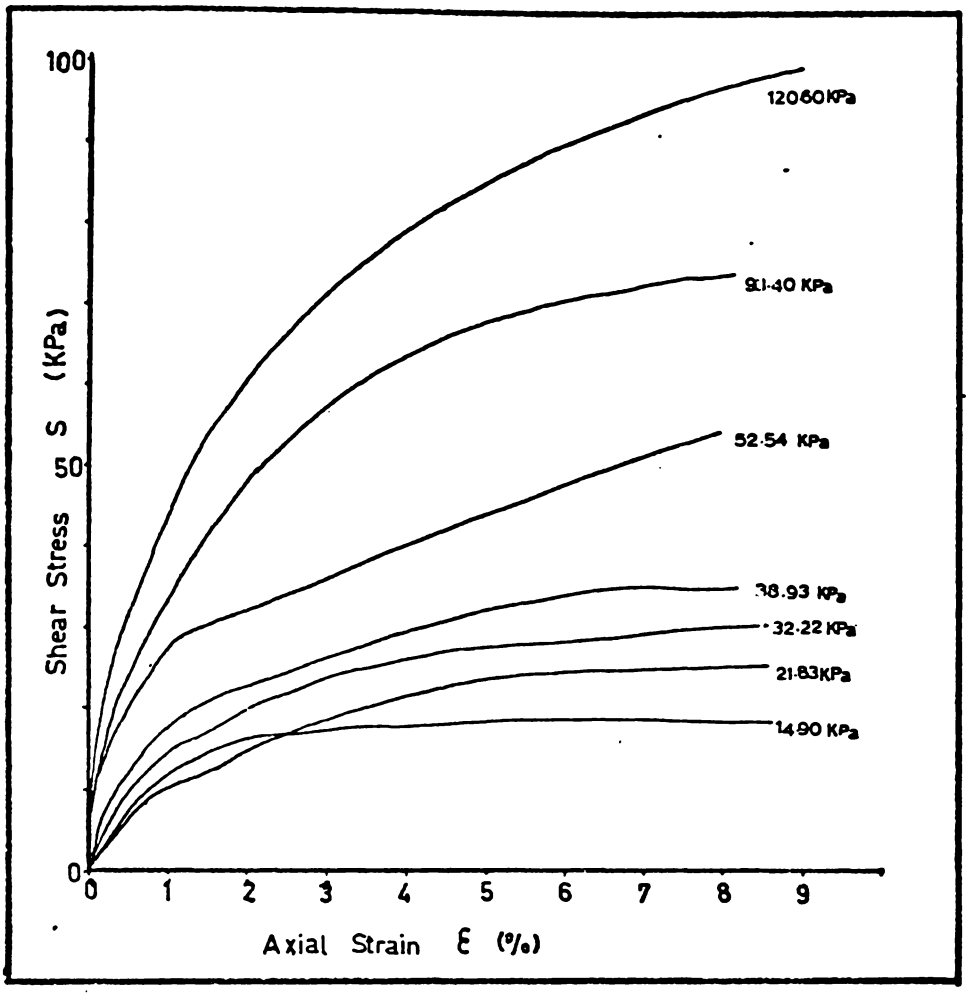

Figure 4.5(a). Direct shear box stress-strain results for orange mottled sands.

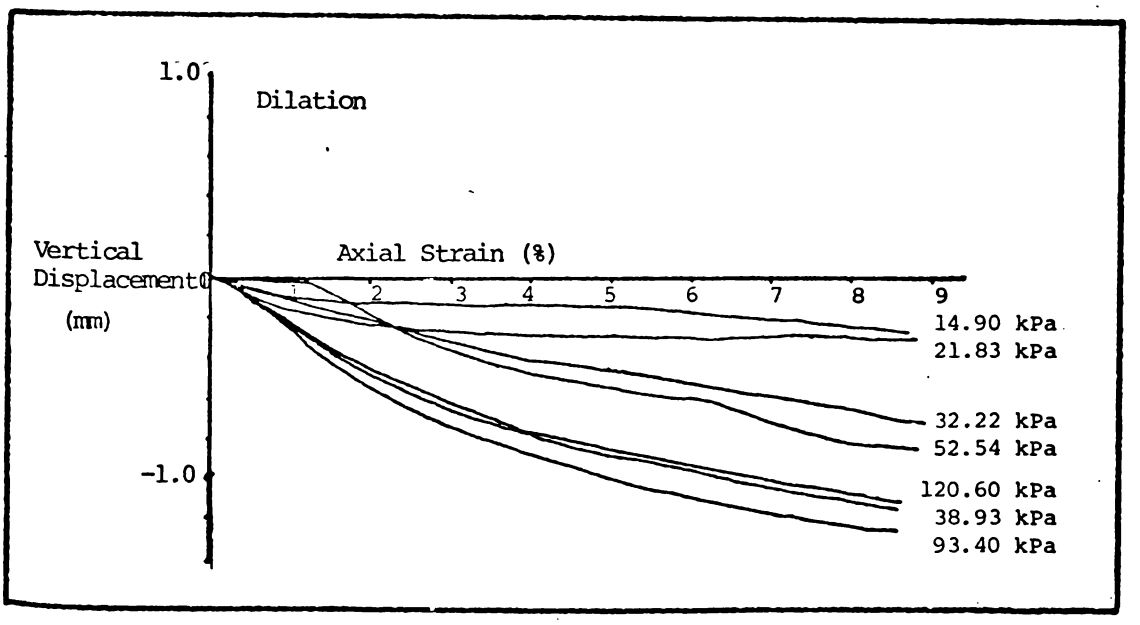

Figure 4.5(b). Direct shear box vertical displacement results for orange mottled sands.

Results

As the nature of the materials tested varied little, all soils being granular, behaviour under shear was similar for all the sample groups. All direct shear results are therefore shown in Appendix 1, while detailed results are presented for one group only. The orange mottled tuff lying between 5.5 and 7.5 m.b.d. was sampled at 7 m.b.d. at site 1 at the base of the main scarp. Vertical displacement-strain and stress-strain graphs obtained (fig. 4.5(b)) are typical of those derived from all the materials tested in the direct shear box. Stress-strain relationships in granular materials depend largely on the initial density of the material. The stress-strain curves shown in fig. 4.5(a) are typical of loose sands, yielding in a non-brittle fashion, and hence no peak stresses are observed. This is reflected in the negative dilatancy (net volume loss) shown by all samples (fig. 4.5(b)). As strain continues, the incremental volume change tends towards zero, and void ratio tends to a constant value; this is the critical state of Hvorslev (1937; quoted in Yong and Warkentin, 1975). The degree of negative dilatancy increases with increasing normal load, owing to more grain crushing and denser packing during displacement.

Failure envelopes were fitted by linear regression analysis using the BMD package program P1R.CTL on the PDP 11/70 computer facility. It is possible that a better fit line could be found, particularly in the low normal stress

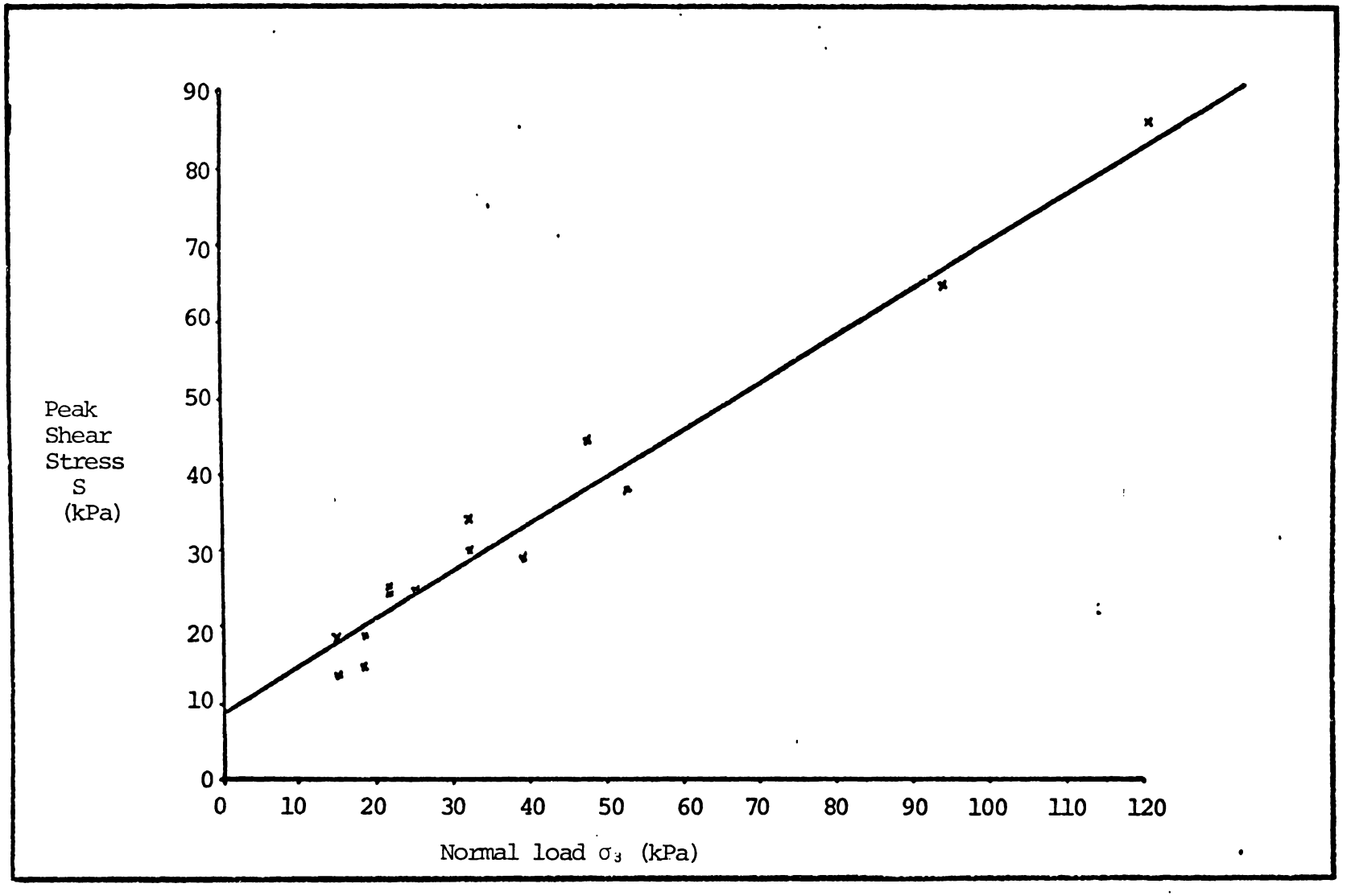

Figure 4.6 Direct shear box strength results.

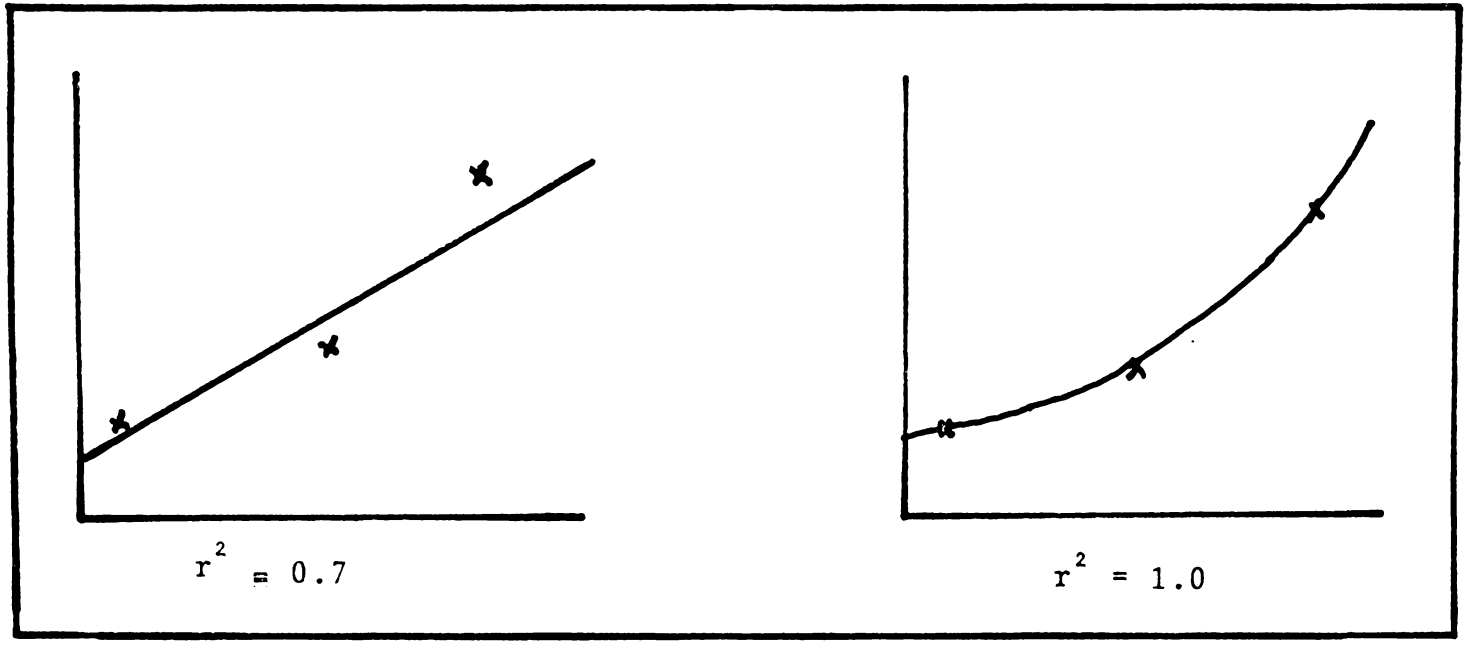

Figure 4.7. Inaccuracies caused by using curvilinear regression analysis where 'n' is low.

part of the failure envelope, as a number of workers (e.g. Sowers and Sowers,1961) have found that curvilinear relationships exist here. However it seemed that a curvilinear analysis would probably prove less accurate in the more relevant high stress portion of the failure envelope, considering the low number of data points used in each regression analysis (fig. 4.7). Table 4.4 sums the results of the direct shear tests analysed in this manner.(fig. 4.6).

NOTE:

$$r^2 = 1 - \frac{\Sigma (Y - \bar{Y}_x)^2}{\Sigma (Y - \bar{Y})^2}$$

$$= \frac{\text{equation explained variation}}{\text{total variation}}$$

where Y = measured dependent variable

and Yx = dependent variable, predicted by equation, using the independent variable x.

The strength of association of the two variables, x and y, is directly indicated by r^2. While r indicates whether a relationship is direct or inverse, it gives an inaccurate assessment of the strength of association (Lapin, 1975). The use of r in discussing the strength of association indicated by regression analysis results is incorrect, and should be avoided.

Triaxial Shear Tests.

The triaxial shear test permits the control of stresses along the three principal axes, and does not impose a plane of failure on the sample. Field failure conditions may thus be approximated more closely than in the direct shear test

and, as discussed previously, the characteristics of failure may be observed more closely. The triaxial apparatus utilised, together with practical details of its operation, is discussed in Akroyd (1964) and Chandler and Rogers (1978, unpublished), while the theory of testing is discussed in detail by Bishop and Henkel (1962), with recent literature reviewed by Chandler and Rogers (loc. cit.).

Field evidence appeared to indicate that an understanding of the strength characteristics of the lensoidal silty sands could be of paramount importance in understanding the nature of the mass movements. Extreme care was therefore taken in all phases of strength determination. Large numbers (85 including test runs) of tests were conducted on overlapping samples from all three sites. Triaxial shear strength tests were also conducted on samples of the clay marker bed, in order to evaluate the possible effects of this bed on the morphology of the mass movements.

Samples were collected from the base of the main scarps, generally after carefully removing 30 to 50 cm of material to avoid material affected by mass movement or rill erosion. Cores were obtained in standard 200 mm by 35 mm (internal diameter) corers. The method of advance trimming, found useful in work on clays, favoured by some local workers (Rogers, 1978; Daji, 1980) proved impractical, as the loose saturated silty sands comprising much of the

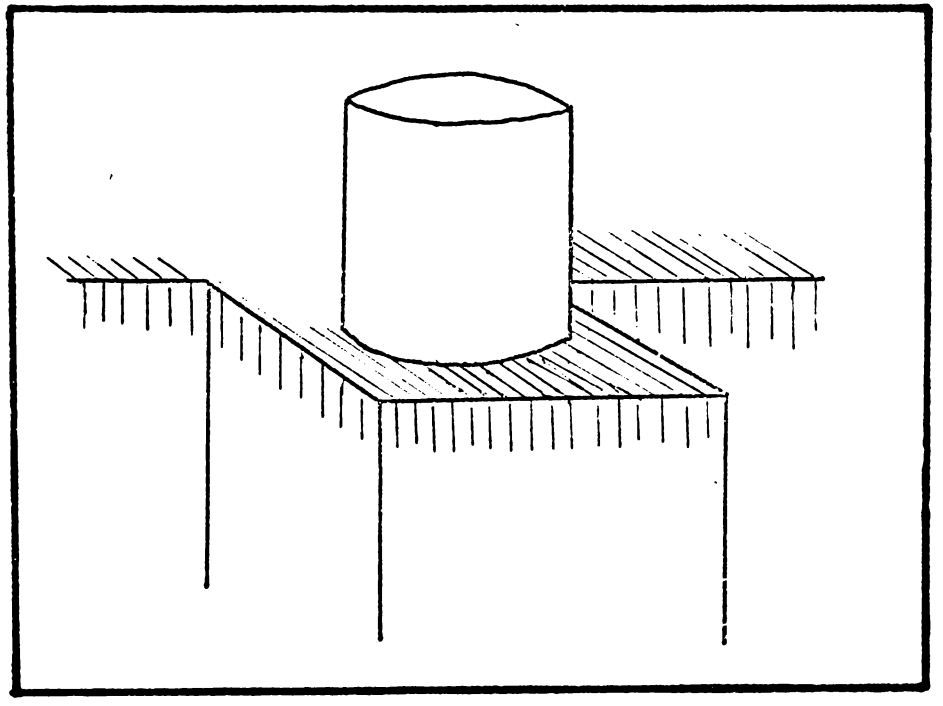

Figure 4.8. Obtaining triaxial test samples from a small monolith.

samples collapsed and flowed away on disturbance. Core sampling was therefore carried out by forcing oiled corers vertically into prepared monoliths as slowly as possible. A consequence of using this technique was that core samples were usually obtained from several cm behind described faces, and in the lenscidal sands, which were very difficult to describe in the saturated state anyway, this resulted in 'blind' sampling. Samples could consequently only be accurately described after testing. "Identical' samples were taken within centimetres of each other, and proved remarkably consistent, considering the common lack of resemblance to the described monolith faces. Despite all the care taken, sample compression of 10 to 20 % was impossible to avoid, due to the high (17.9 %) area ratio of the triaxial corers. Attempts were made to remedy the situation by sampling in small monoliths (fig. 4.8) in order to allow the sideways displacement of the material, hence mitigating the effects of the high corer area ratios within the corer itself. This proved unsuccessful, as did attempts at varying the coring rate (including hydraulic extrusion from larger cores in the laboratory), and creating a vacuum above the sands by withdrawing a rubber plunger during corer insertion. The most obvious solution of obtaining thinner walled corers proved to be impossible until after testing was completed, owing to a lack of any tubing strong and thin enough, and capable of holding a

cutting edge. The problem of compaction proved to be of major significance during testing.

The cores were trimmed to 20 cm lengths, capped with rubber caps and transported in polystyrene cases. It is significant that, while samples of the lensoidal silty sands transported in lower area ratio corers were observed to shake down as much as 15% during transport, producing wet and slick upper surfaces, the 200 mm by 35 mm core samples exhibited this behaviour in only half a dozen cases. This indicates that:

i) High area ratio core sampling caused compaction within the core, and not merely beneath it.

ii) The loose silty sands are easily disturbed, and hence even perfectly obtained samples would have been unlikely to survive transport undisturbed.

The triaxial core samples appeared to be saturated in the field and were transported under watertight conditions. As sample preparation included consolidation, which generally involves some water loss, it was thought preferable that the samples should gain rather than loose water during storage, hence the cores were stored submerged in water with the apparently watertight rubber end-caps in place.Tests were conducted within 10 days of sampling to avoid any reaction between sample and corer. It is worth noting that the odour of the extruded cores tended to confirm that reducing conditions (indicated in the field by a total lack of

mottling) were preserved throughout sampling and transport.

- - Test Conditions

Consolidated undrained tests with pore water pressure measurements were carried out in the manner outlined by Chandler and Rogers (1978, unpublished). Details of test conditions were decided on in the manner outlined below.

While field evidence pointed towards rapid failure, it was thought that testing would be best carried out at a slow rate, bearing in mind the difficuty of assessing sample textures and hence drainage rates until after the completion of testing. Initial trial runs revealed problems with the stability of pore water pressure readings, presumably due to the presence of dissolved air or highly elusive air bubbles in the triaxial machine system. Slow strain rates thus proved necessary in order to obtain accurate pore water pressure readings. All the tests referred to in the statistical analysis below were conducted at a rate of 0.030 mm min (0.043 % strain per minute). Trial runs also showed that the volume change monitoring apparatus had perished seals which were not replaced until very late in the testing programme. Testing was therefore confined to undrained tests with pore pressure measurement.

A major feature of many of the tests discussed later was the observation of high positive pore water pressures. Such observations tended to support the possibility that liquefaction played some part in the failure mechanism,

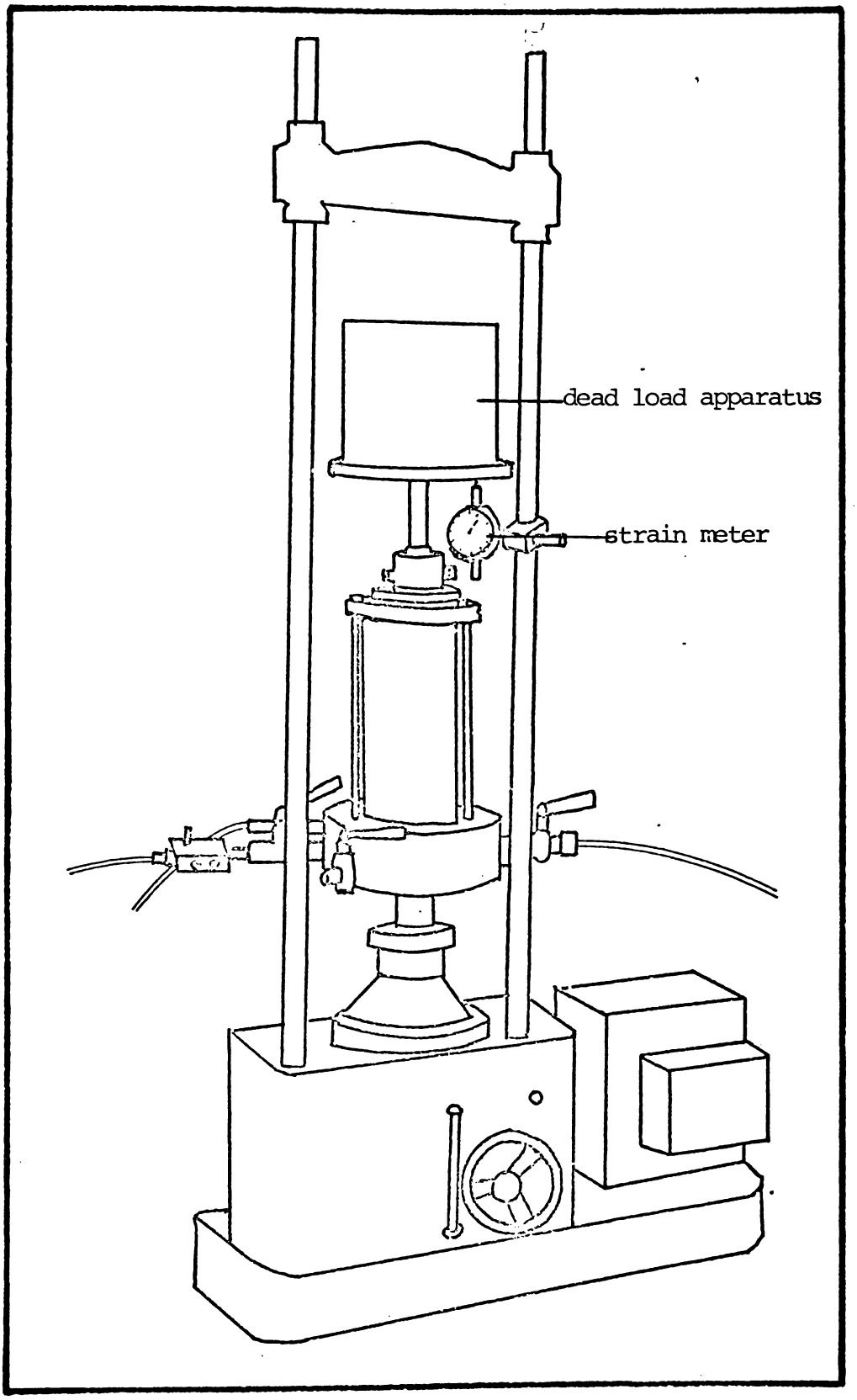

Figure 4.9. Triaxial apparatus modified for dead-load testing.

suggested on the basis of the rapid long distance rafting nature of the failure, and the presence of collapsible silty sands within a finer matrix along part of the surface of rupture. It was important that this possibility should be considered and tested in the triaxial strength testing programme. Casagrande (1970, reported by Green and Ferguson, 1970) has suggested that strain rate controlled undrained testing of sands susceptible to liquefaction may give strength results which err well on the unsafe side. This suggestion was based on the concept of the development of 'flow structure'; the orientation of grains in such a way as to offer minimum resistance to deformation after yielding has initiated rapid movement.

- - Stress Controlled Testing

In order to test the possibility of liquefaction occurring and, at the same time, test the validity of the strength values obtained using low strain rate tests, it was necessary to conduct stress controlled undrained testing. This was attempted both by incrementally increasing dead loads on the ram, and by incremental reduction of the cell pressure (σ_c) under constant dead loading. The triaxial apparatus was modified to allow for dead loading, strain measurement and rate of strain estimation (fig 4.9). Incremental dead loading was first accomplished by adding 100 ml aliquots of water to a large basin. For tests at higher cell pressures, 1 and 2 kg weights were necessary, as

no basin large enough to hold sufficient water would fit in the machine frame. In order to investigate the effects of a stress path more akin to that found in the field during rainstorms (decreasing σ_1 and σ_3 [σ_r] as water table rises, constant σ_1) the second type of test was utilised. Dead load was applied with water for low σ_1 tests, and weights for high σ_1 tests. As a consequence it was only possible to attempt to maintain a truly constant σ_1 during low σ_1 tests of this type. The magnitude of σ_1 for a given load w (including weight of loading plate and ram, 0.530 kg) may be calculated thus:

$$\sigma_1 = \frac{w - a_r\sigma_3}{a} + \sigma_3$$

where w = dead load.

a_r = ram area (1.1310 cm^2).

a = sample area at any one time $= a_0 \frac{1}{1 - e}$

e = strain

It was therefore possible to adjust w to compensate for changes in σ_3 and a at each loading increment, thus maintaining a relatively constant σ_1.

As the stress controlled tests were partly intended to provide a check on the validity of the strain controlled tests, the samples were prepared and consolidated in the same manner as for the strain controlled tests. Consolidation, in the case of the increasing σ_1 tests, was conducted under the same σ_3 as applied during testing. The

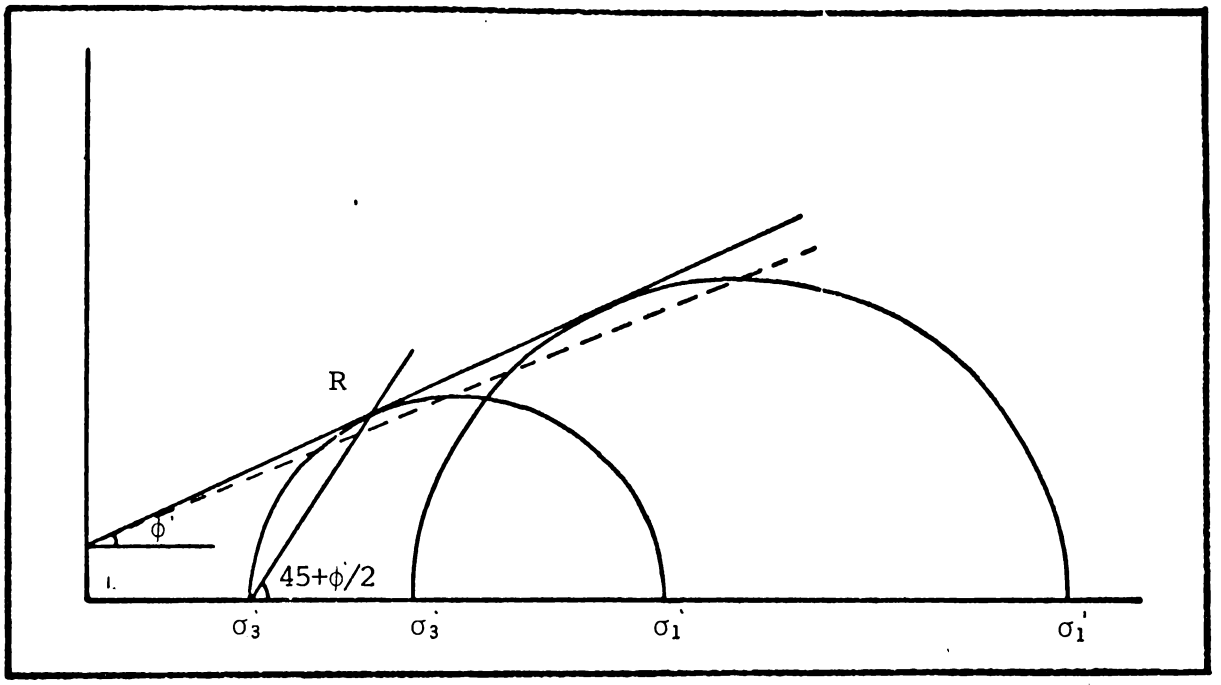

Figure 4.10. Linear regression analysis used to approximate the Mohr-Coulomb envelope.

decreasing σ_3 tests, on the other hand, required an estimate of the likely σ_3 at failure. This value was obtained using the Mohr - Coulomb equation derived from the strain controlled tests. The choice of appropriate consolidation pressures will be discussed further in the discussion of results below.

The calibration of proving ring 5729 was checked, and the factory gauge factor confirmed at 3.8455 N per division. The BASIC PLUS program TRIAX.BAS was then used to calculate % strain and deviator stress from the test readings. Linear regression analysis, finding the best fit line by the least squares method, was utilised to approximate the Mohr - Coulomb failure envelope for each data set. The following procedure was employed in these determinations. Initially the coordinates of the tops of the Mohr circles were analysed to give an approximation of ϕ' (fig. 4.10). This ϕ' value was then used to graphically find a value for R. The coordinates for R were then used to reapproximate ϕ'. A consistent value for o was always reached within three iterations of this process.

- - Results of Strain Controlled Testing.

One of the main problems associated with testing small samples of non-homogenous material is that of relating the test results to one another. The 7 cm test samples were cut from 10 cm halves of between 4 and 7 20 cm cores taken within a few cm of each other. After destructive testing

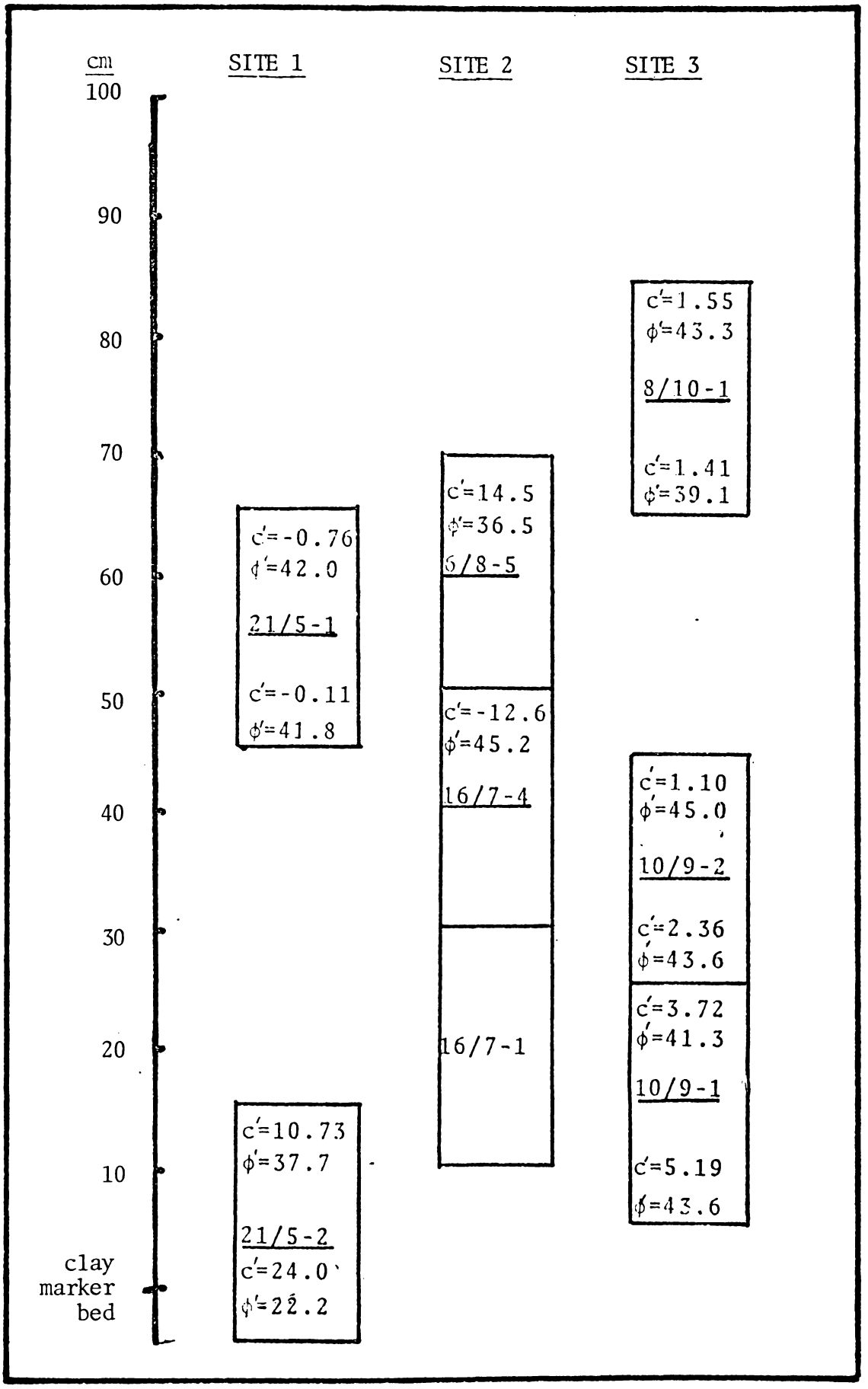

Figure 4.11. Stratigraphic relationships of the triaxial samples, and the strength parameters derived from them. (c' in kPa, φ' in degrees)

TABLE 4.5 Triaxial data merged in stratigraphic groups

Sample Groups	C' (kPa)	ϕ' (degrees)	r^2
21/5-1a & 21/5-1b	- 0.2	41.8	.9786
10/9-1a & 10/9-1b	13.7	41.9	.9528
10/9-2b & 10/9-1a	8.4	42.4	.9526
21/5-2b & 10/9-1b	-65.	53.7	.8906
21/5-2a & 10/9-1a	13.0	39.4	.9429
10/9-2a & 10/9-2b	0.4	44.5	.9852
10/9-2a & 16/7-4	- 5.6	45.0	.9461
10/9-2a, 10/9-2b & 16/7-4	- 4.5	45.0	.9654
21/5-1b & 16/7-4	- 9.2	44.7	.9908
6/8-5, 8/10-1a & 8/10-1b	10.1	37.6	.9783
8/10-1a & 8/10-1b	7.8	38.8	.9168
21/5-1a & 8/10-1b	9.0	36.7	.9668
21/5-1a, 8/10-1b & 6/8-5	8.3	38.1	.9767
8/10-1b & 6/8-5	10.0	36.7	.9801
21/5-2a, 10/9-1a & 16/7-1	15.0	39.7	.8949

these cores were quickly described, and moisture content and bulk density (based on pre-testing volume) were determined. As samples were taken 'blind' it was surprising to find that in all but two cases the samples appeared similar enough to provide a set of 'identical samples'. The strain controlled test results were therefore initially grouped in the order they were tested, as groups of 3 to 7 'identical' samples from a 10 cm stratigraphic location. The relative positions of the samples at the three test sites, and the c and o parameters obtained by linear regression are shown in Fig. 4.11.

The strength parameters obtained using this type of analysis are not very useful for two reasons. Firstly the small number of data points from which the values are obtained produces relatively unreliable results, indicated by the three negative cohesion values reported. The second reason is that the large numbers of differing strength values are a little difficult to rationalise into a form which may be utilised in an analytical model. Rationalisation of the strength data was attempted by merging data groups from similar stratigraphic levels. This produced no improvements in the regression coefficients or standard error values for the derived shear strength parameters, as might be expected if the data were indeed related (Table 4.5).

Examination of the bulk density data for the test cores

Fig 4.12. Triaxial shear samples from tests 45 (sandy mud, brittle failure) and 59 (silty sand, plastic failure).

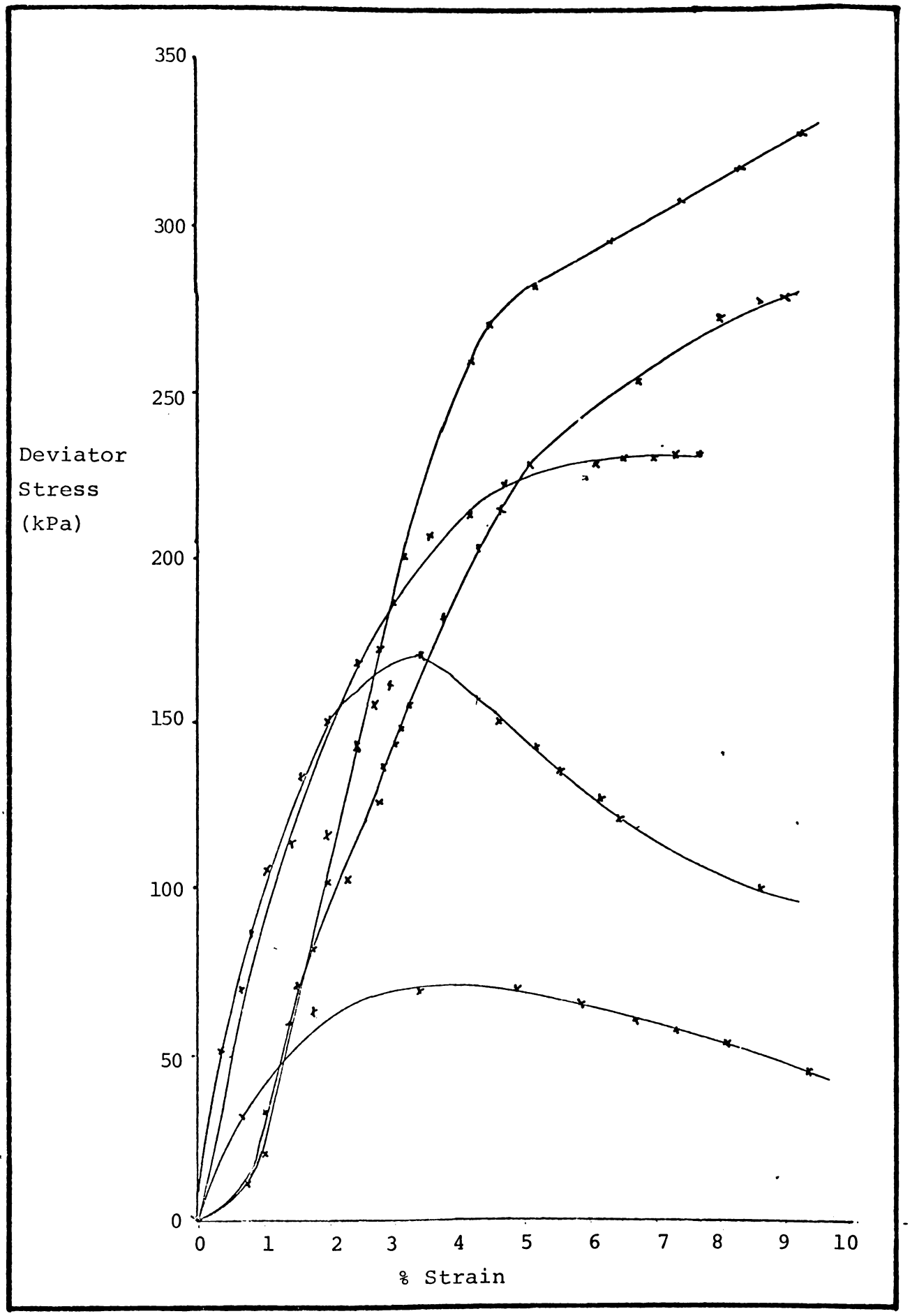

Figure 4.13. Deviator stess curves for high bulk density samples.

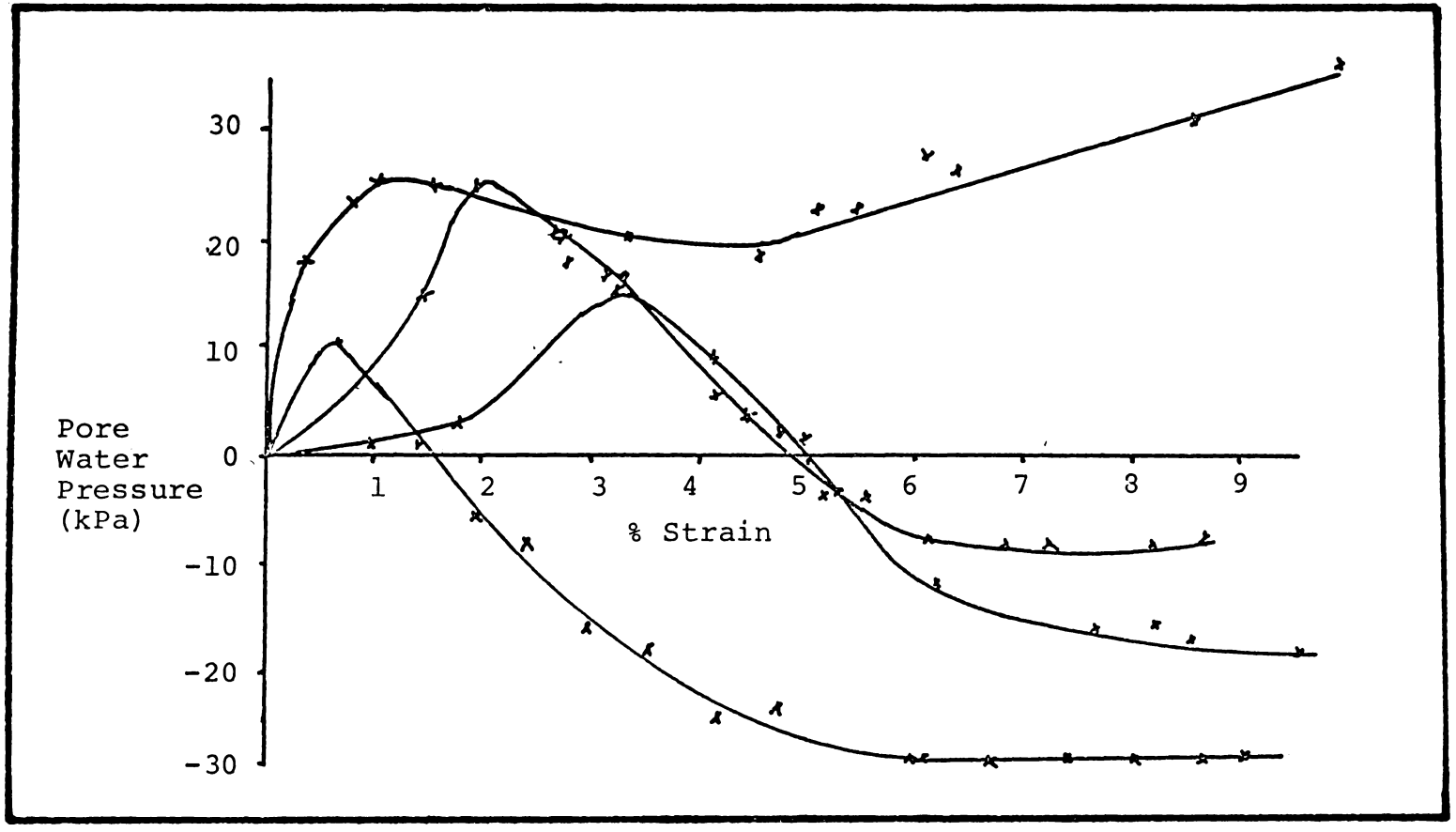

Figure 4.14. Pore water pressures recorded during triaxial shear testing of high bulk density samples.

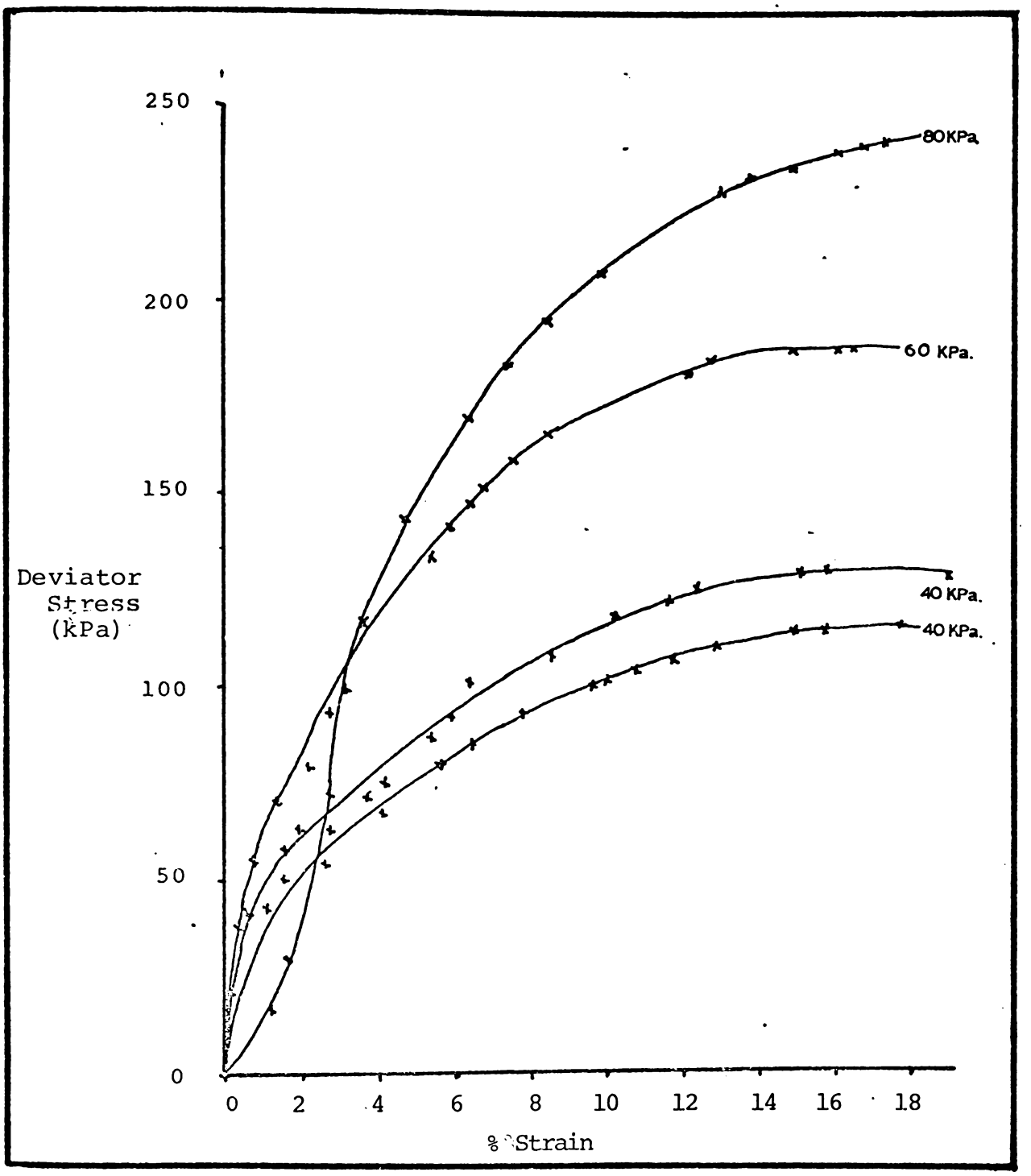

Figure 4.15. Deviator stress curves for low bulk density samples.

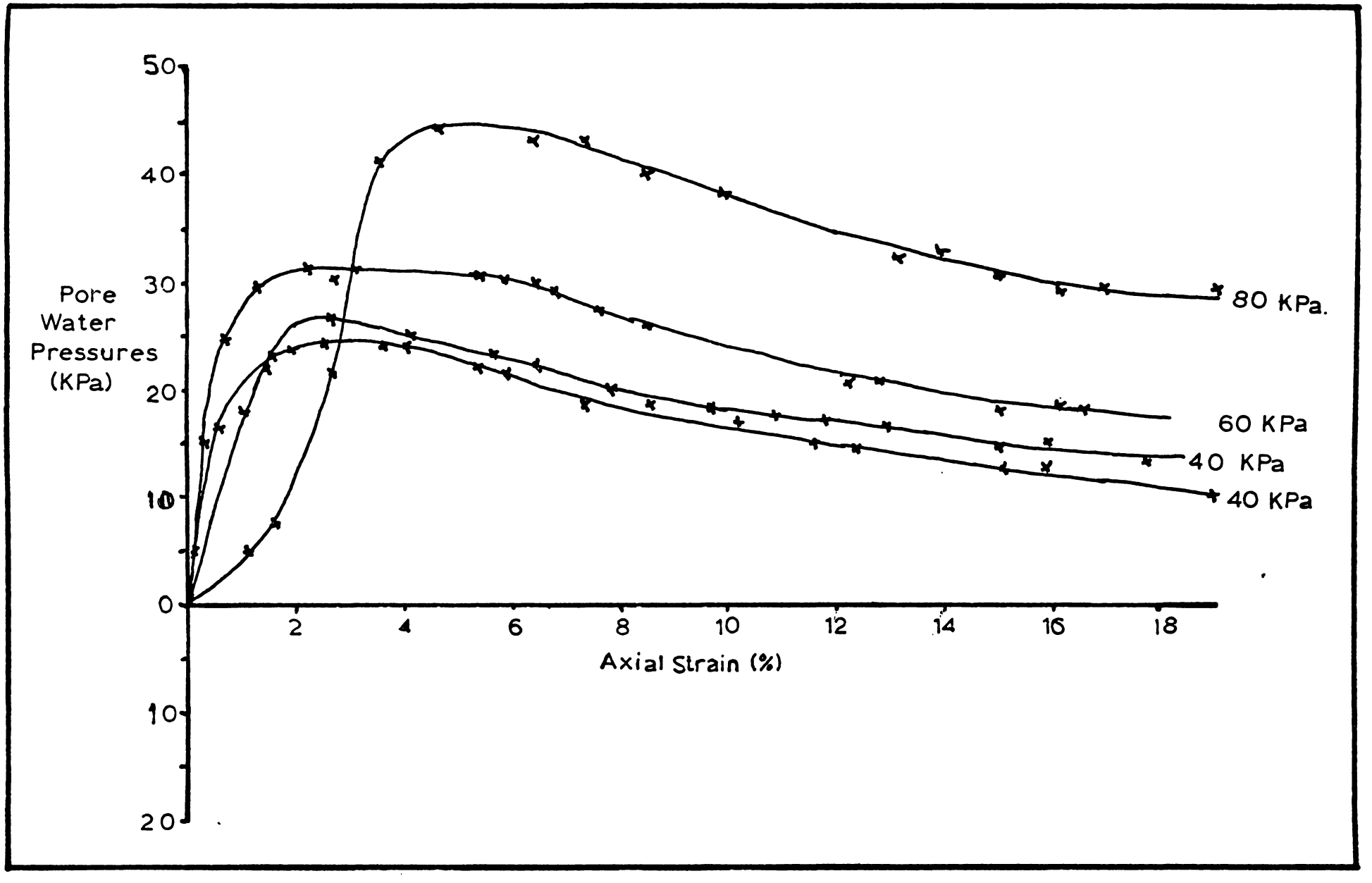

Figure 4.16. Pore water pressures recorded during triaxial testing of the low bulk density samples.

revealed a distinct bimodality, with groups at 1.123 + 0.014 g/cm^3 and 0.965 + 0.024 g/cm^3. The modes of failure associated with the two groups were quite different, with the lower bulk density samples (e.g. test 59) failing by bulging, and the higher bulk density samples (e.g. test 45) undergoing brittle failure (fig. 4.12). This difference in failure type is further reflected in the deviator stress vs strain and pore water pressure vs strain curves (figs. 4.13, 4.14, 4.15 and 4.16). The low bulk density samples failed in the manner of loose sands, yielding in a plastic manner, tending to an asymptotic value of deviator stress, and exhibiting high positive pore water pressures. Conversely, the high bulk density samples failed in a brittle manner, giving a peak strength value and exhibiting dilatory behaviour, causing negative pore water pressures. It is believed these two sample groups represent the lenses of loose silty sand and the sandy mud matrix respectively. Routine particle size analysis on samples 45 and 59 showed that these were indeed their textures. The two data groups delimited by these observations were then subjected to linear regression analysis, and 5% confidence intervals were calculated using student t tables.

When the data points and best fit lines were plotted (fig. 4.17&18 the similarity of the two data groups, indicated by the overlapping confidence intervals, was striking (table 4.6). To quantify the differences between the two best fit

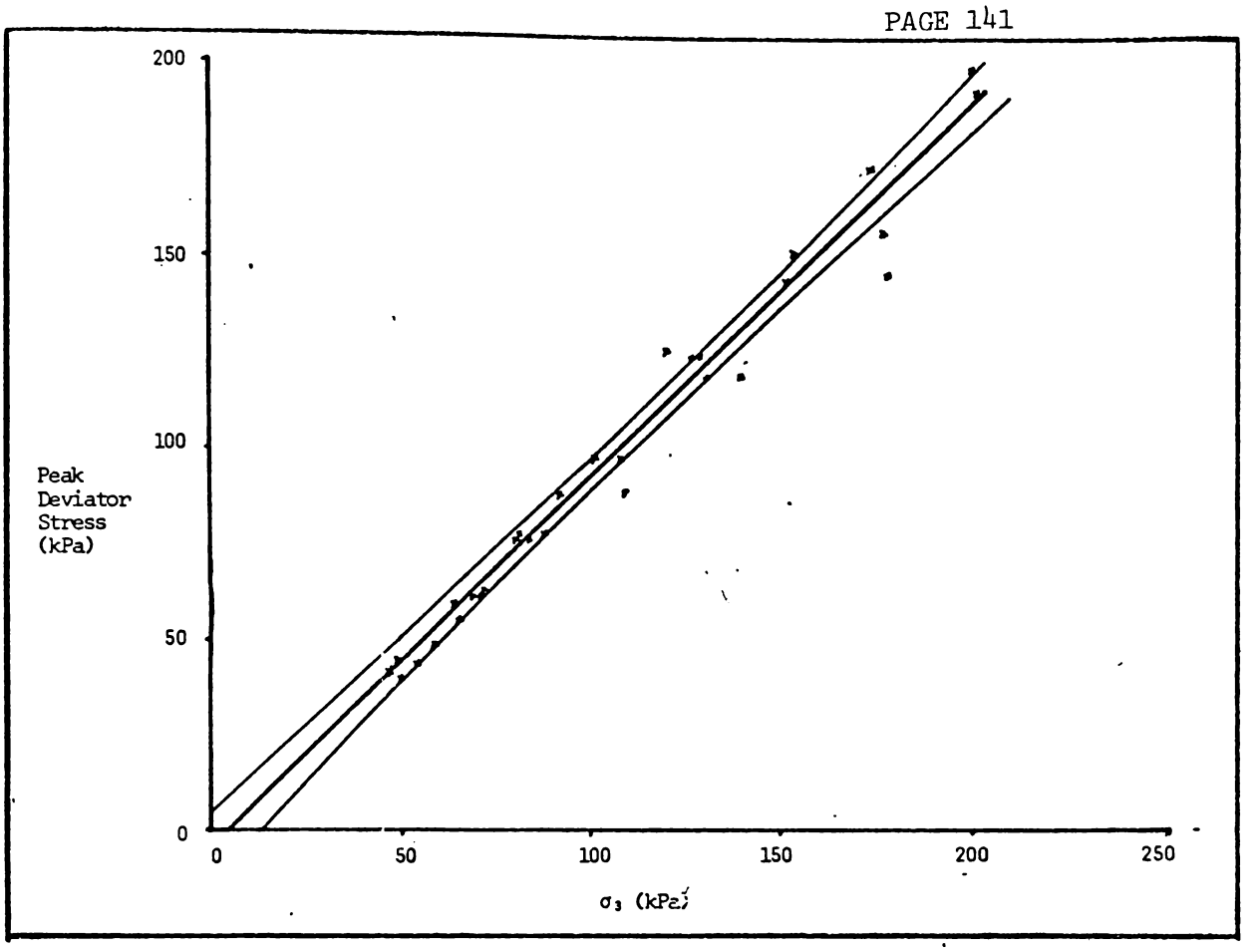

Figure 4.17. Best fit linear regression line and 95% confidence intervals for the low bulk density data.

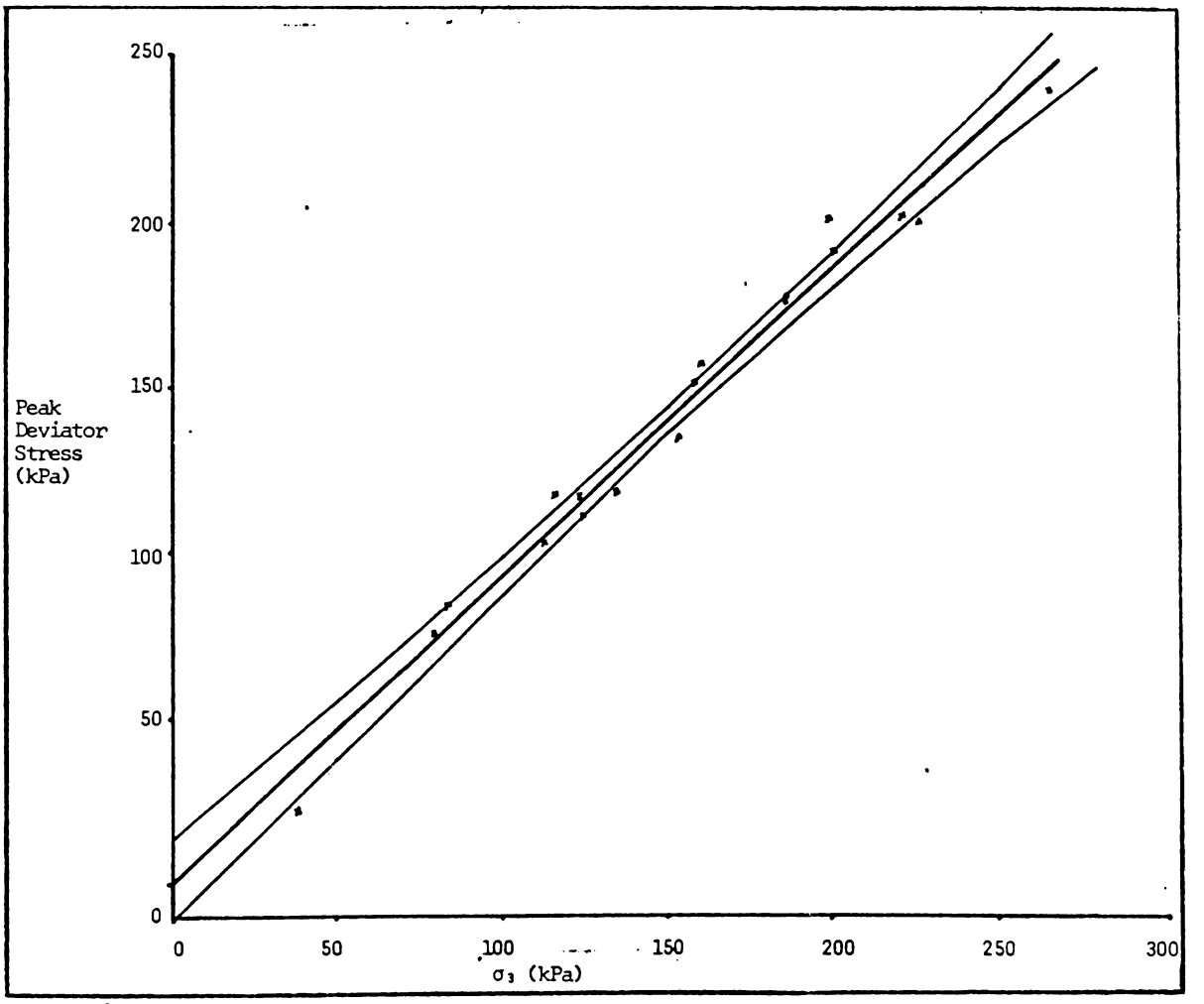

Figure 4.18. Best fit linear regression line and 95%confidence intervals for high bulk density data.

Table 4.6 Triaxial data merged according to bulk density.

Low Bulk Density Data.	High Bulk Density Data.
$r^2 = 0.9704$	$r^2 = 0.9797$
$n = 29$	$n = 18$
$\beta = 0.96432 + 0.06878$	$\beta = 0.92874 + 0.07569$
$(\phi' = 44.0 + 1.9)$	$(\phi' = 42.9 + 2.1)$
$c' = -3.19 + 8.10$ kPa	$c' = 0.69 + 12.23$ kPa

failure envelopes, the program DIF.CTL (Appendix 3) was written and utilised in conducting comparisons of best fit lines for the high bulk density and low bulk density groups. For degrees of freedom v = 2 (number of variables in each group) and v = 43 (number of cases read - number of variables in both groups), an F statistic is considered significant if it is >3.22 at the 5% level of significance, or >2.44 at the 10% level.

i.e. $P(F > 3.22) = 5\%$

$P(F > 2.44) = 10\%$

Note: F statistics are not normally used at greater than the 10% level of significance.

The F ratio produced by comparison of the two groups was 0.308. Therefore at the 10% significance level the slopes and/or intercepts of the best fit lines do not differ beyond chance. The two data groups were therefore amalgamated, and subjected to a least squares regression analysis. This resulted in an increase in prediction confidence, expressed

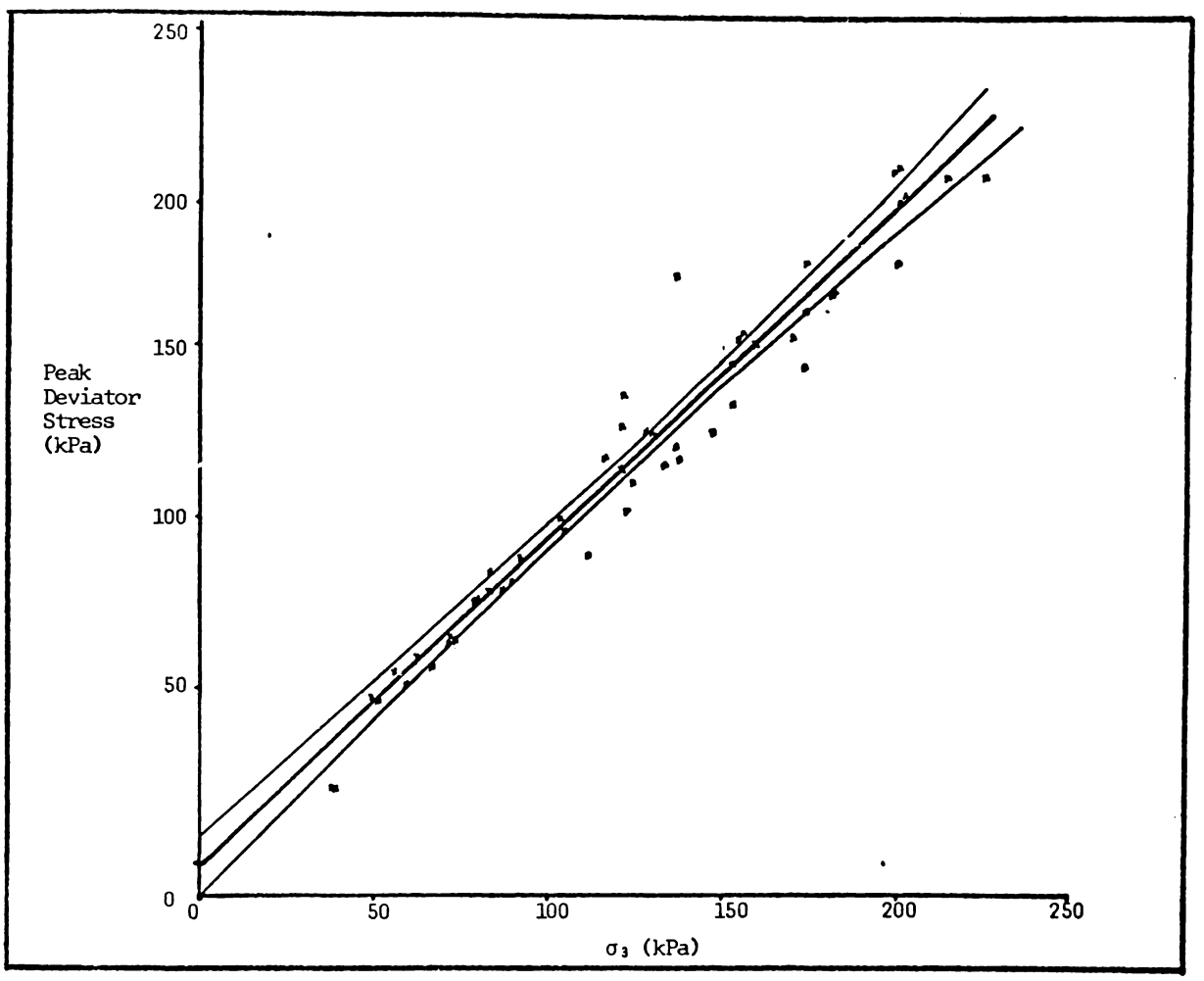

Figure 4.19. Best fit linear regression line and 95% confidence intervals for all data.

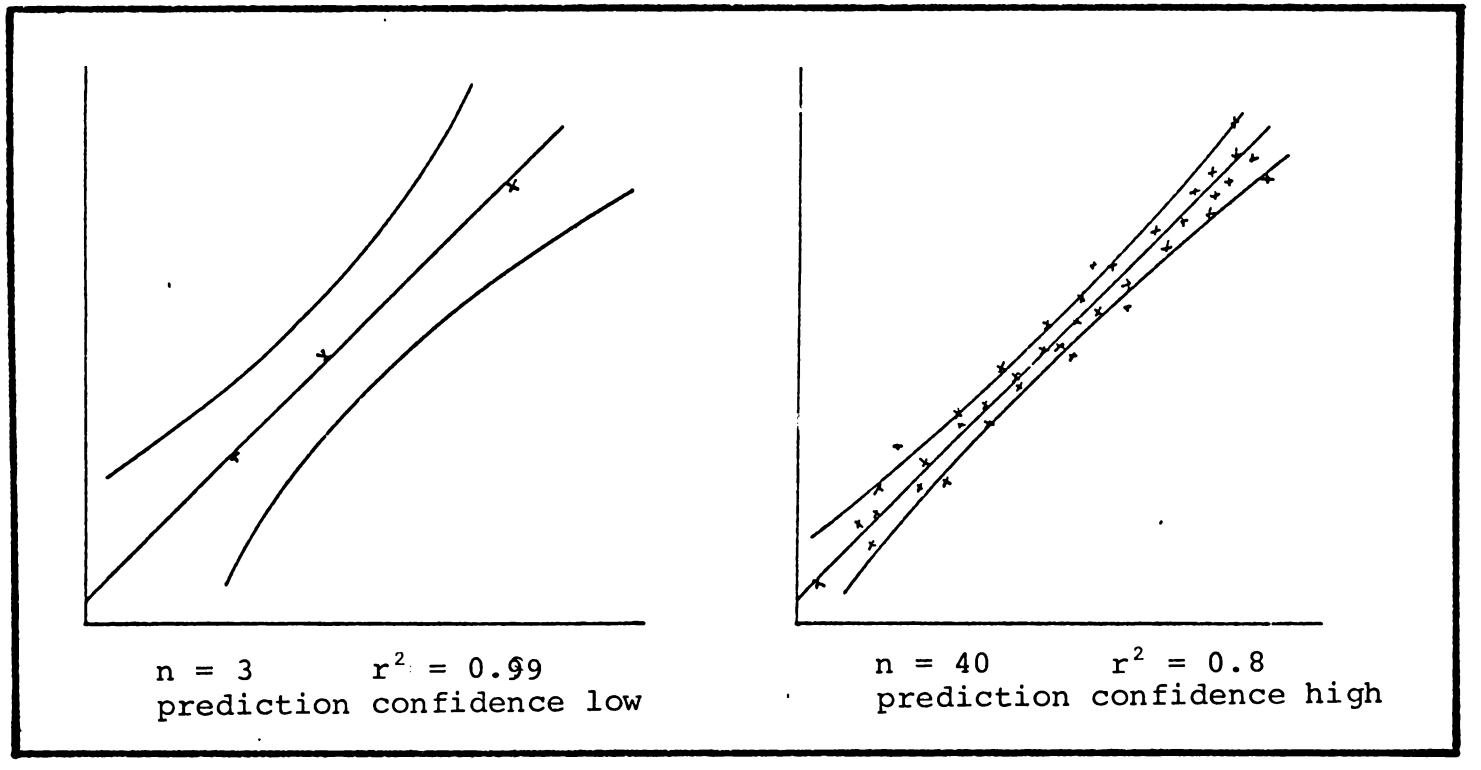

Figure 4.20. The relationship between sample size, regression coefficient, and prediction confidence for two hypothetical subsamples of a population.

as a contraction of the confidence envelopes (fig 4.19).

TABLE 4.7

All Data Grouped

$r^2 = 0.9548$

$n = 51$

$\beta = .94434 + 0.0625$

$(\phi' = 43.36 + 1.85)$

$c' = -0.78 + 8.42$ kPa

This example illustrates the importance of understanding the relevance of statistical parameters to applied situations. Merely determining the respective correlation coefficients of the two data groups individually and then merged, would have resulted in the rejection of data amalgamation as erroneous. However the true reliability of a predictive model such as the Mohr-Coulomb equation is indicated, not by the sample correlation coefficient, but by the predictive confidence interval. Increasing sample numbers (n) and thus more closely approximating the assumed normal population, may reduce r^2, especially if n is low, however the predictive confidence will increase, as C.I. is proportional to n (fig. 4.20).

Despite the differing modes of failure of the two data groups, this analysis reveals that the lensoidal material, through which sub-horizontal failure occurred, may be considered as a single soil with well defined strength

parameters (Table 4.7). Where possible, a statistical analysis of the form described above is considered preferable to an analysis of variance of c' and ϕ' values derived from small (3 - 5 data points) sample groups. The use of the latter type of analysis (e.g. Pender, 1979; Law, 1980), necessitated by the testing of large variable masses of material, often involves a high risk of error due to the unreliability of individual c' and ϕ' values.

A portion of the unreliability of strength parameters derived from laboratory testing of clays has commonly been attributed to the effects of different σ_1 values on the mode of failure (e.g. Chandler, 1978; Law, 1980). It is suggested that high σ_1' values cause a levelling off of the Mohr-Coulomb failure envelope, which is assumed to be linear in standard regression analysis. As the sample population available for analysis in this study is relatively large, an ideal opportunity was thus available for a statistical check of the influence of this effect on a granular material. At the same time a further check would be provided on the reliability of the strength parameters used in subsequent stability analyses. The data was therefore subjected to a least squares regression analysis, using up to fifth order polynomial functions. Within the relatively limited range involved, low order polynomial functions can closely approximate exponential, trigonometric or any other curvilinear function. The package used (BMD P5R) may

therefore, in this case, be considered capable of any curvilinear regression analysis. In essence, the lowest order polynomial which does not yield a significant F statistic value may be regarded as providing the best fit line. Results (table 4.8) indicate that the best fit line is an order 1 polynomial function; i.e. it is of the form $y = mx + c$. Consideration of the residual plots (fig 4.21) shows further that there is no appreciable clustering of the residuals, indicating no consistent deviation from the failure envelope produced by rectilinear regression analysis.

Triaxial shear results for the clay marker bed were taken from only 5 samples, as the material did not appear to be very variable. Also, because the clay itself did not appear to be involved in failure, a high degree of precision in measuring its strength did not appear essential to forming an understanding of the nature of the failures. Slow test rates were considered appropriate, due to the slow drainage rates of the fine textured samples. Stress-strain curves (fig. 4.22) show that failure was slightly brittle, with a tendency towards more plastic failure at higher normal loads. The development of discrete failure planes was not observed; bulging type failures were the norm. In contrast to the coarser samples, pore water pressures were low, usually slightly negative at failure, hence total and effective shear strength parameters were nearly identical.

TABLE 4.8 Results of polynomial function goodness-of-fit test

Degree of polynomial	F
0	198.24
1	0.47
2	0.46
3	0.69
4	1.36

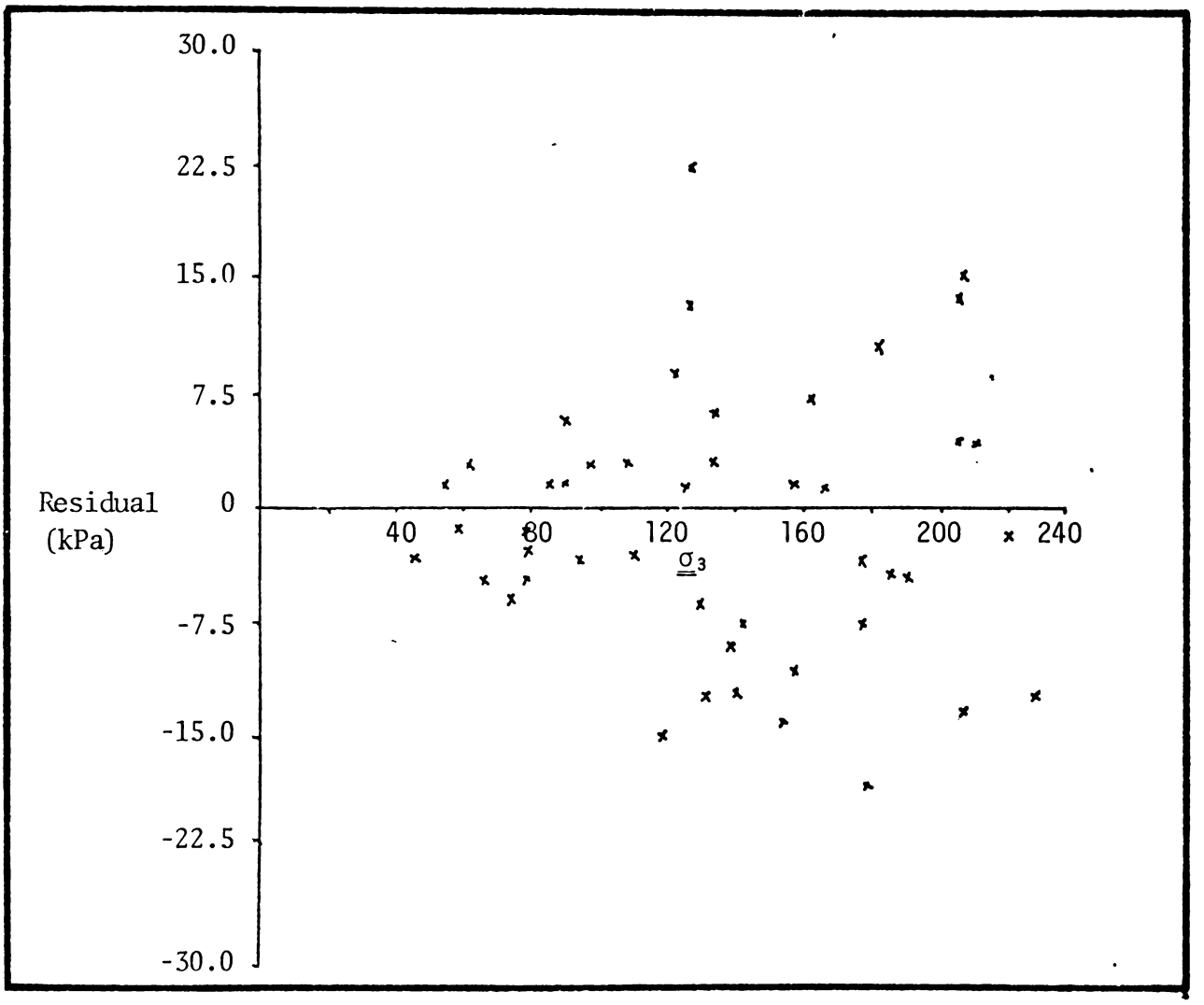

Figure 4.21. Linear regression residuals plot for all triaxial data grouped.

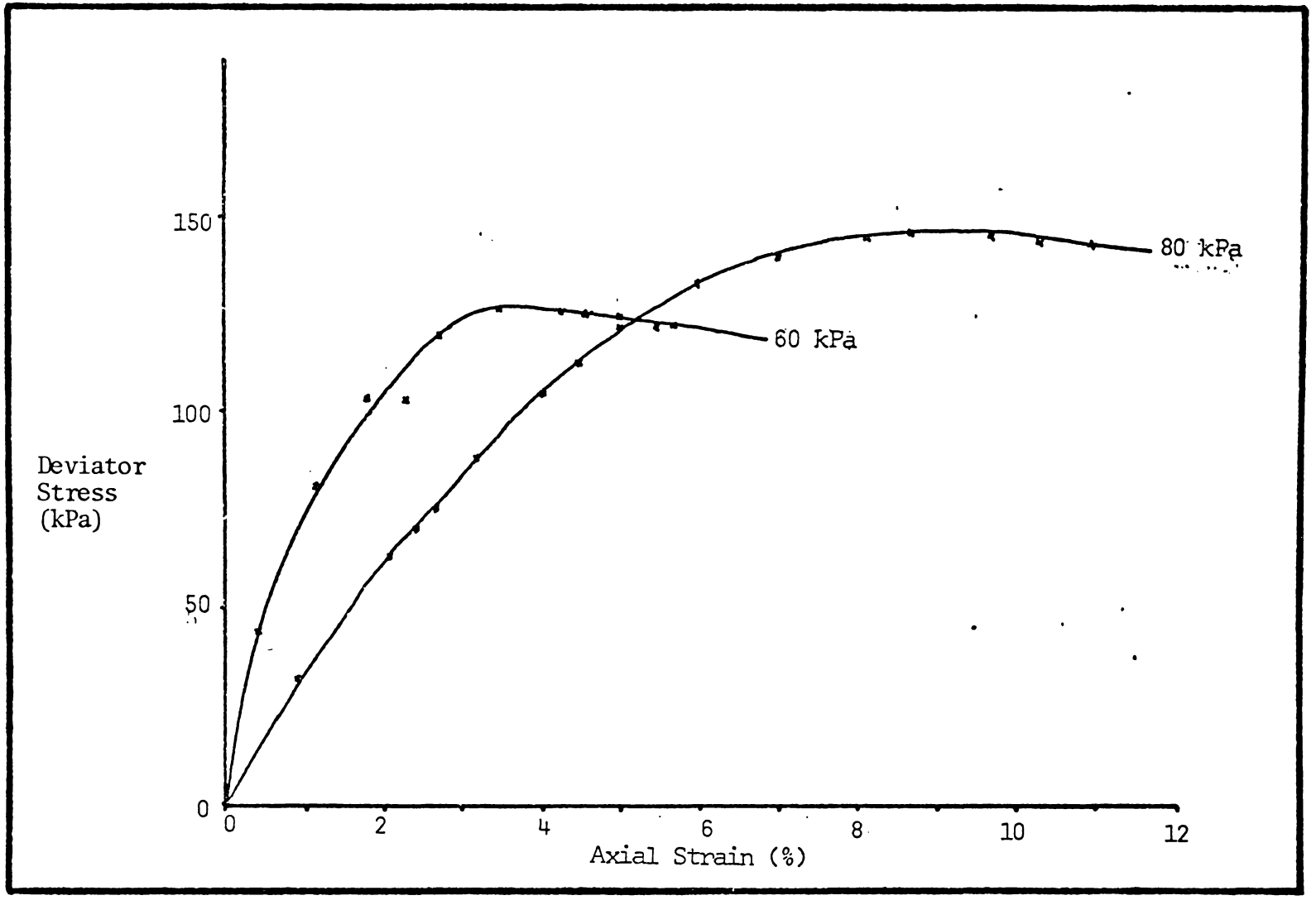

Figure 4.22. Deviator stress vs. strain curves for the clay marker bed.

Linear regression analysis yielded effective shear strength parameters of c' = 24 kPa and ϕ' = 22.2 (r^2 = .6456). The relatively low angle of internal friction is consistent with the clay's low plasticity index and activity (1.1 and 0.02 respectively). The halloysite which comprises most of the clay fraction is therefore indicated as having extremely low surface activity, a possible clue to its sensitive behaviour. The large amount of very fine feldspar observed may also be of some significance (table 4.3). Further investigation into this material could be of some importance in understanding the nature of sensitivity, as suggested by Smalley et al. (1980) for similar materials found in the Omokoroa area.

- - Results of Stress Controlled Testing

The aims of stress controlled testing were twofold;

i) to test the possibility that liquefaction occurred at or about failure,

ii) to test the validity of strain controlled test results.

Evidence was produced to provide some support for the suggestion that liquefaction occurred, and at the same time apparently validating the strain controlled test results. Generally, however, the test program was not successful owing, largely, to compaction of the loose silty sands during sampling.

Four tests of the increasing σ_3 type were carried out,

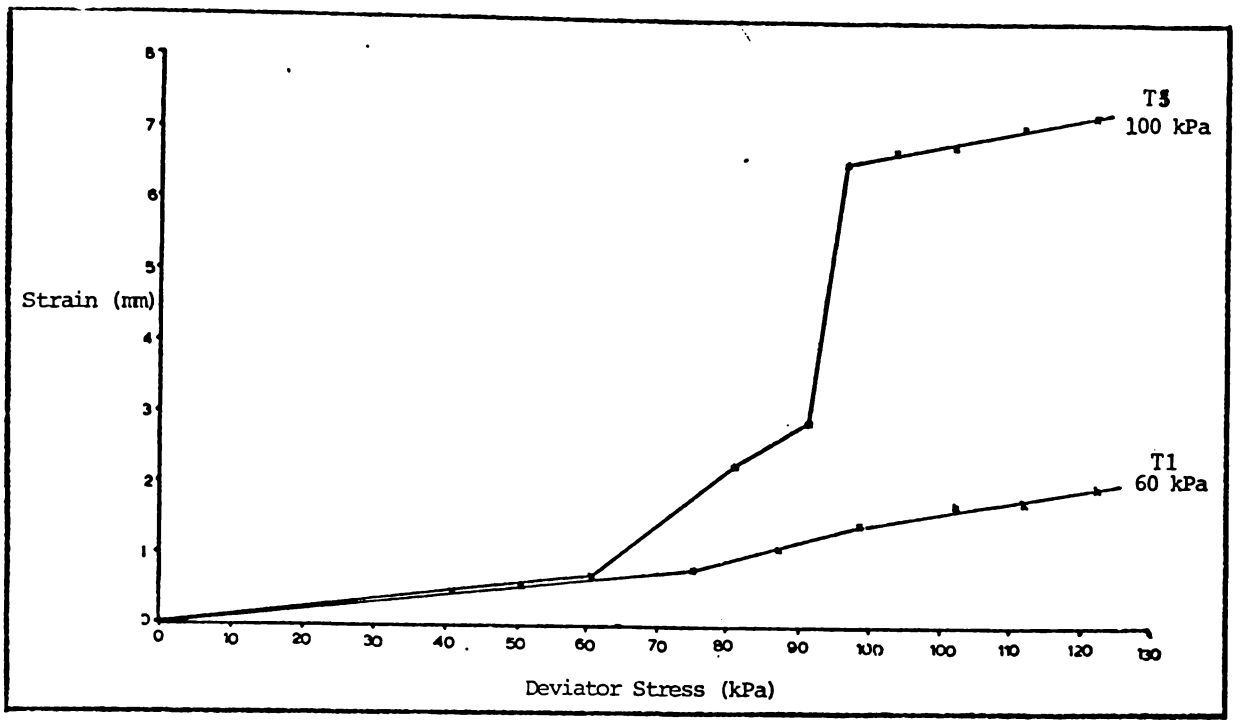

Figure 4.23. Stress controlled tests; strain curves.

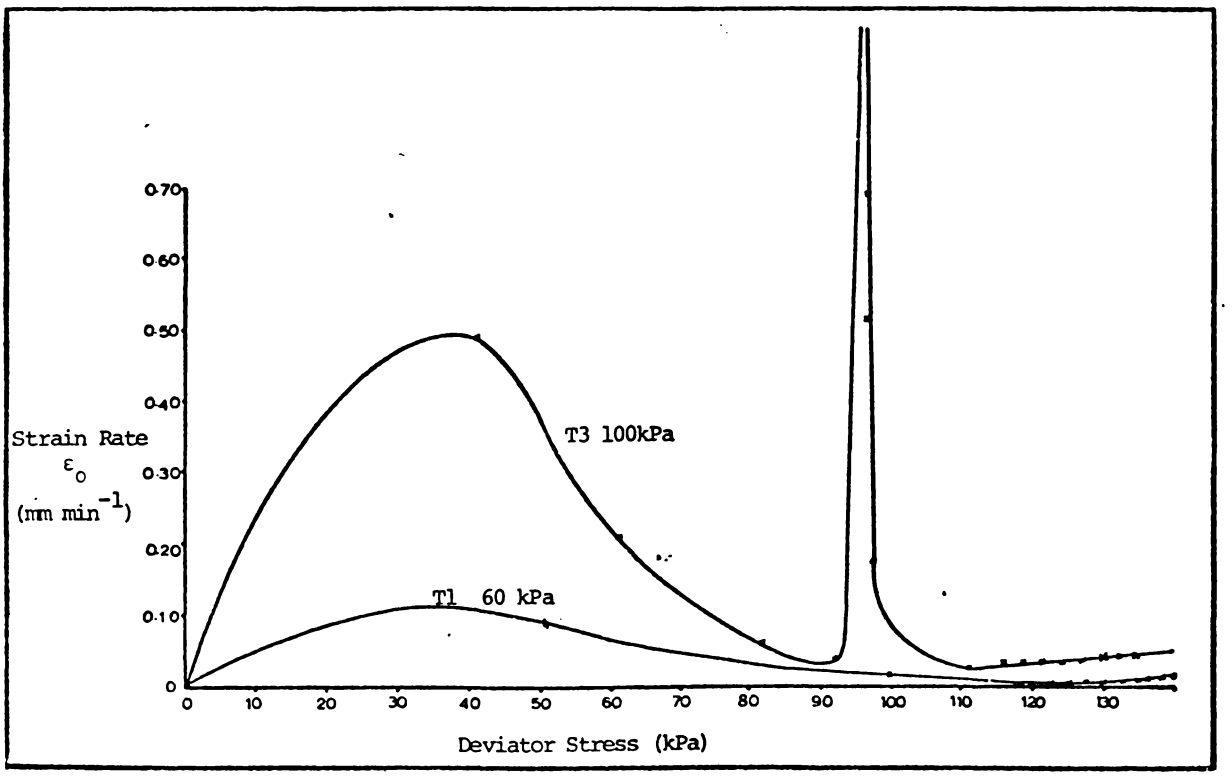

Figure 4.24. Stress controlled tests, strain rate curves.

together with three of the decreasing σ_3 type. The increasing σ_1 tests were conducted under σ_3's ranging from 60 to 120 kPa. Test results are presented in figs. 4.23 and 4.24. As loading intervals were not regular, the strain rate curves are not derivative functions of the strain curves.

Three of the samples tested responded in the manner illustrated by the lower curve (fig. 4.24). An initial period of consolidation was followed by a steady decrease in strain rate to greater than 60 to 140 kPa (depending on σ_3) when a slight increase was observed. Strain never exceeded 3 % during testing, despite the application of normal stresses 20 to 50% in excess of those predicted to be sufficient to cause failure, according to the Mohr-Coulomb equation established by strain controlled testing. One sample, however (T3), produced a distinctive strain rate - deviator stress curve. The initial consolidation period was unusually short, with rapid consolidation being followed by a long period of very little movement up to a σ_1 of 92 kPa. On the addition of a further 5 kPa of deviator stress, rapid failure occurred, causing almost 4 mm (6%) of strain in a few seconds. Following this, the strain rate slowly increased in a manner akin to the other three samples.

The test results are interpreted in the following manner. The initial consolidation was probably due to the settling of the uneven ends of the core samples. The three

samples which experienced little deformation were probably compacted during sampling to the extent that they behaved in the manner of dense sands, failing slowly. Pore water pressures were not monitored during testing, as it was necessary to maintain regular strain readings for strain rate calculations, hence this suggestion cannot be confirmed.

It appears that sample T3 experienced a liquefaction type failure of small magnitude, despite compaction during sampling. It is not apparent why only this sample failed rapidly. Possibly this was due to differences in sample compaction, or to differences in composition which weren't apparent on post - test examination. It appears significant that the failure occurred at a deviator stress of between 92 and 97 kPa. The value predicted by the Mohr-Coulomb line produced earlier was 92.7 + 3.3 kPa. While not a conclusive piece of evidence, this does tend to validate the results of the strain controlled tests.

As discussed earlier, a major source of uncertainty in the decreasing σ_3 type tests was the area of sample consolidation. As test T3 offered some validation of the strain controlled test Mohr-Coulomb line, it was decided to consolidate samples at o values corresponding to the deviator stress to be applied, according to this equation. A deviator stress of approximately 60 kPa was applied in three tests, with consolidation being carried out at 50, 60

and 70 kPa. Drainage valves were closed, σ_3 increased to 100 kPa, σ_1 applied, and then σ_3 incrementally decreased. Strain and pore water pressures were maintained throughout the tests. In all three cases negative pore water pressures were recorded over the entire period of testing. The samples could not, therefore, be regarded as representative of the previously observed behaviour of the lensoidal silty sands. Post-testing examination showed the samples to be indistinguishable from other tested samples by eye or hand textural examination. It may be that these samples were, in fact, slightly different. It appears more likely, however, that compaction occurred during sampling or preparation, and caused the subsequent dilative behaviour.

Triaxial shear tests thus showed the lensoidal silty sands to have an effective cohesion of 0.8 + 8.4 kPa, and a ϕ' value of 43.4 + 1.9 degrees. Failure probably occurs rapidly under natural conditions, and it is postulated that structural collapse of pockets of low density silty sands during strain produces local liquefaction. Support for this suggestion of liquefaction is given by Atterberg limit values which show that the material for at least 1.5 metres above the clay marker bed has moisture contents in excess of their liquid limits (Appendix 1). It is notable that the moisture contents referred to were determined on samples taken 8 days after the last significant rainfall, hence they probably err on the low side, compared with failure

conditions. The amount of energy required to remould the silty sands was minimal, however, 30 to 60 seconds of heavy work were necessary to remould the sandy mud matrix. As disturbance of the material as a whole would be necessary for the silty sands to collapse, it appears unlikely that liquefaction of the silty sands occurred as a result of any shock loading. It appears most likely that liquefaction occurred after movement was initiated. Strain occurred, causing collapse of the open structured silty sands, thus substituting a fluid support for the matrix support, causing rapid rafting movement.

An interesting parallel may be drawn between these failures and those observed in sensitive clays. The behaviour of sensitive clays at failure resembles that of the silty sands studied here. The 'sensitivity' of the silty sands, shown by sudden failure in one stress controlled triaxial test, is high, and failure occurs at relatively low strains in both materials as a result of local structure loss (see e.g. Smalley, 1976). The failures found in sensitive materials, particularly where only one part of a stratigraphic sequence is 'quick', often closely resembles the biplanar form evident in the Maungatapu failures. It is worthwhile, therefore, to recall the statement made earlier in this chapter that, except in circumstances such as under seismic shock conditions, the presence of a sensitive soil may be important in determining

the nature and/or form of failure, but not as a direct causative factor in mass movement incidence.

HYDRAULIC CONDUCTIVITY

In any practical study of slope stability, the three most important variables to be considered are the soil strength, the slope morphology, and the hydraulic conditions. Field investigations indicated that variations in the hydraulic regime appeared to be significant in determining the distribution of mass movement events, when other preconditions existed. In the absence of any field piezometric data, it appeared necessary to obtain laboratory evidence to provide a reasonable estimate of the hydraulic regime about the failures during heavy rainfall.

Determinations of hydraulic conductivity were therefore conducted on samples taken from all three sites, and mean values were determined for each bed sampled (fig. 4.25). Sampling and testing were carried out using 100 mm by 102 mm (internal diameter) cores (area ratio 12.1 %). Cohesive materials were sampled using the advance trimming technique, while sandy materials were sampled by forcing cores into prepared flat surfaces. Both vertical and horizontal samples were taken but, surprisingly, considering the sedimentary origin of the materials, no appreciable anisotropy was observed. This was more likely due to the low numbers of samples tested than to the nature of the

TABLE 4.9 Hydraulic conductivity results.

Sample	Depth (m.b.d.)	No. of tests	K (mm/s)
Loose orange sandy ash		7	$1.5 \pm 1.3 \times 10^{-1}$
Rotoehu Ash paleosol		6	$4.1 \pm 0.1 \times 10^{-2}$
Red paleosol	4.1	3	$2.7 \pm 3.4 \times 10^{-2}$
Orange mottled tuff	5.0	17	$6.6 \pm 2.2 \times 10^{-3}$
Brown mottled tuff	7.0	20	$1.9 \pm 0.5 \times 10^{-2}$
Yellow brown sand	8.2	5	$1.2 \pm 0.3 \times 10^{-3}$
Yellow brown sand	9.2	9	$3.8 \pm 0.5 \times 10^{-4}$
White silty sand	9.8	22	$2.1 \pm 1.3 \times 10^{-4}$
Clay marker bed	10.2	11	$3.5 \pm 1.9 \times 10^{-5}$

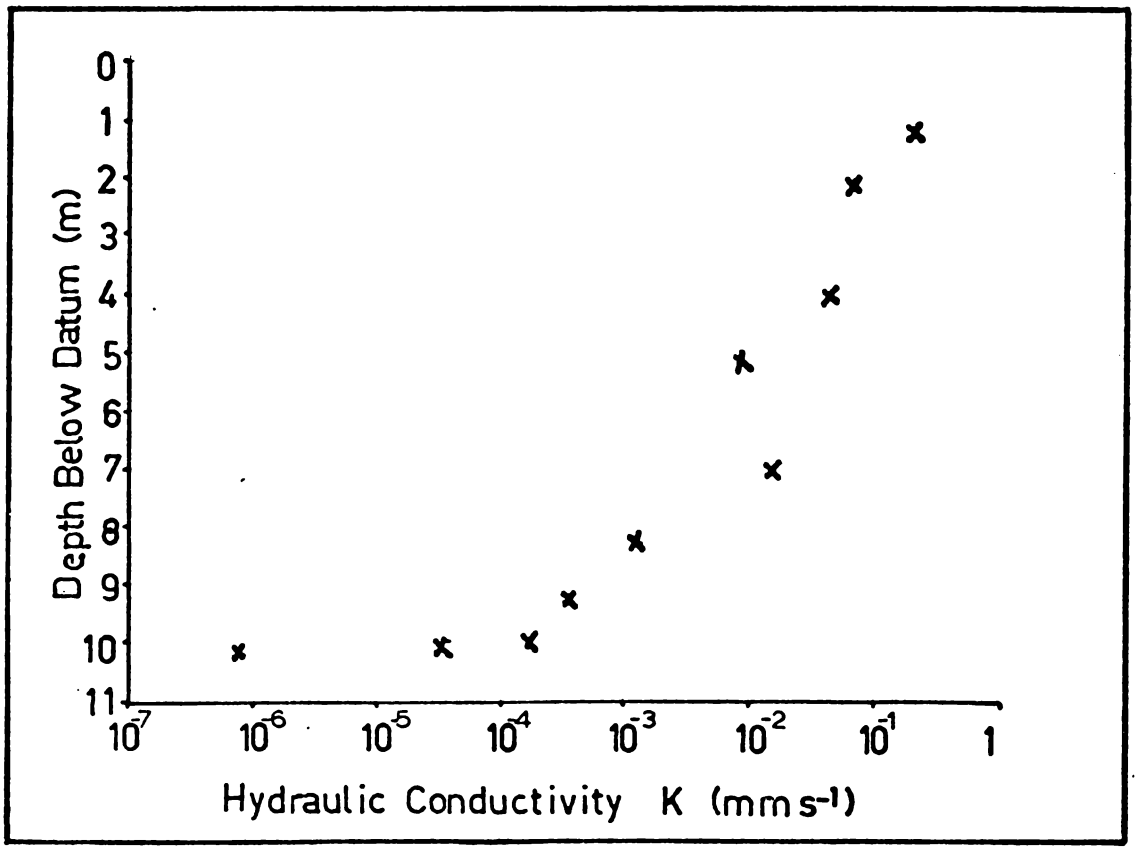

Figure 4.25. Hydraulic Conductivity results.

soils. Hydraulic conductivity determinations were carried out with a constant head (1.18 m) permeameter, using large sealing rings to eliminate boundary effects (Hawley and Northey, 1981). A problem which made itself obvious during testing of relatively coarse samples was that of blowouts; the induction of 'quick' conditions by a hydraulic head of greater than critical value. In granular materials, usually those near fine sand in texture, the application of a hydraulic gradient in excess of about 1 is usually sufficient to promote this condition (Capper and Cassie, 1976). As a hydraulic gradient of about 12 was applied during testing, it proved necessary to retain many samples with a fine mesh wire disc at each end. The mesh did not appear to limit the flow of water.

A total of 103 tests was conducted, the results of which are presented in table 4.9 and fig. 4.25. The most notable feature of the results is the large decrease in hydraulic conductivity below 7.5 to 8 m.b.d.. This reflects the field observations of consistent surface seepage from the material above the clay marker bed, and reports of seepage from as high as 7.5 m.b.d. during the 24 hours after the March 1979 failure at site 1.

The hydraulic conductivity values found in the 1.5 metres above the clay marker bed indicate that the fine sandy mud matrix is probably continuous, surrounding lenses of the looser silty sand which, if continuous, would give a

much higher K value. This provides further reason to consider the soil as a single structural unit.

The conductivities reported for the clay marker bed are so low that it would taken some years for water to permeate through. In other words there is an isolation of the local meteoric groundwater system above the clay marker bed. This would obviously result in a major discontinuity in the hydraulic regime, with positive pore water pressures occurring above the clay marker bed and not below, during heavy rainfalls.

SUMMARY

Referring to the flow chart presented at the start of the chapter (fig. 4.1), it is possible to evaluate the questions posed by field investigations in the light of laboratory data, and to determine what uncertainties remain. Two hypotheses have been eliminated through data collection. Firstly, the near horizontal section of the failure plane did not pass through an unusually weak bed, and secondly, sensitive soils were not responsible for triggering the failures, nor for their distinctively biplanar forms.

Evidence was found which threw some doubt on the suggestion that a critical strength loss occurred on saturation. It also seems doubtful that the appearance of the sub-horizontal section of the failure surface was due to

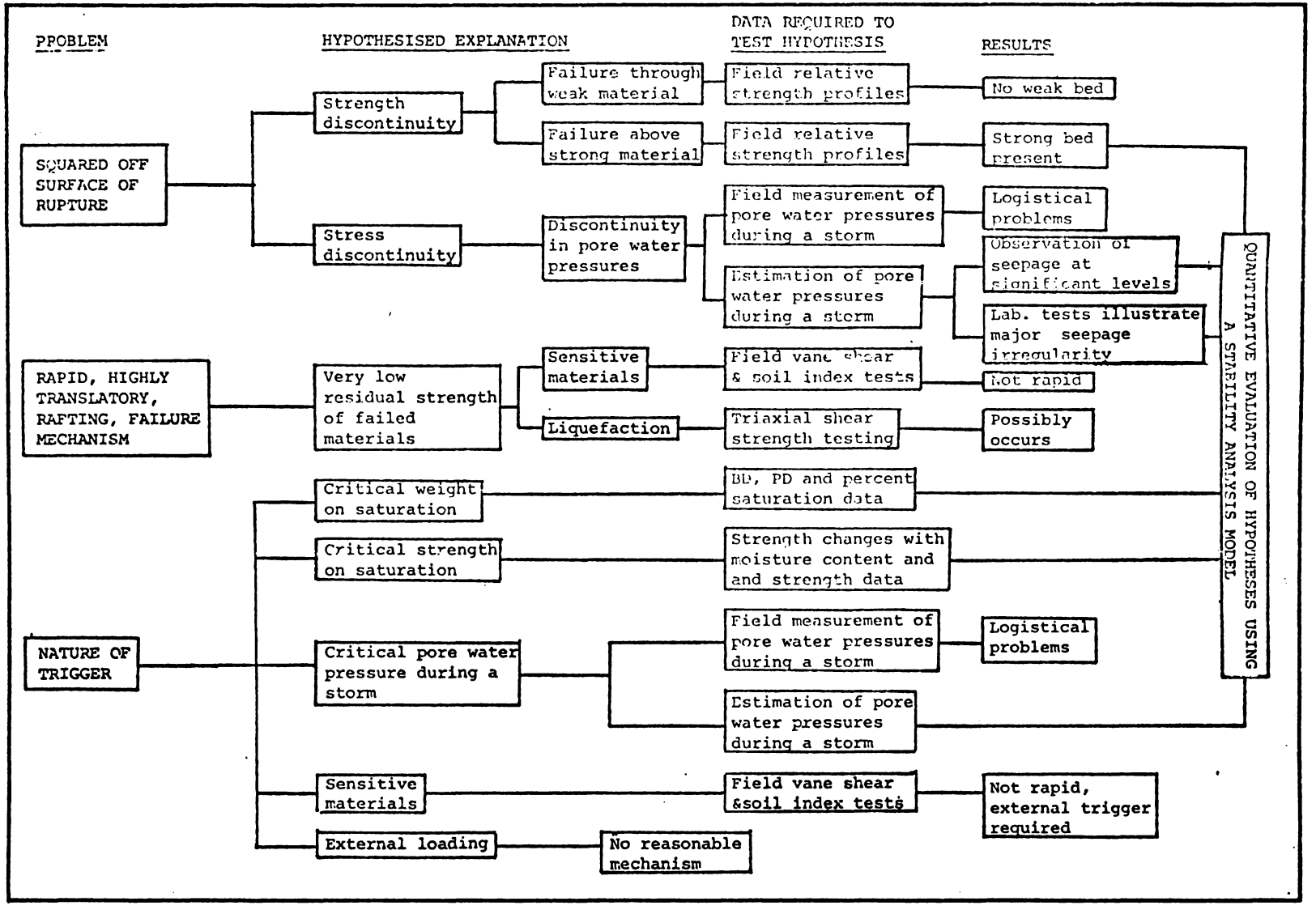

Fig. 4.26. Directive flow plan and results of quantitative investigations.

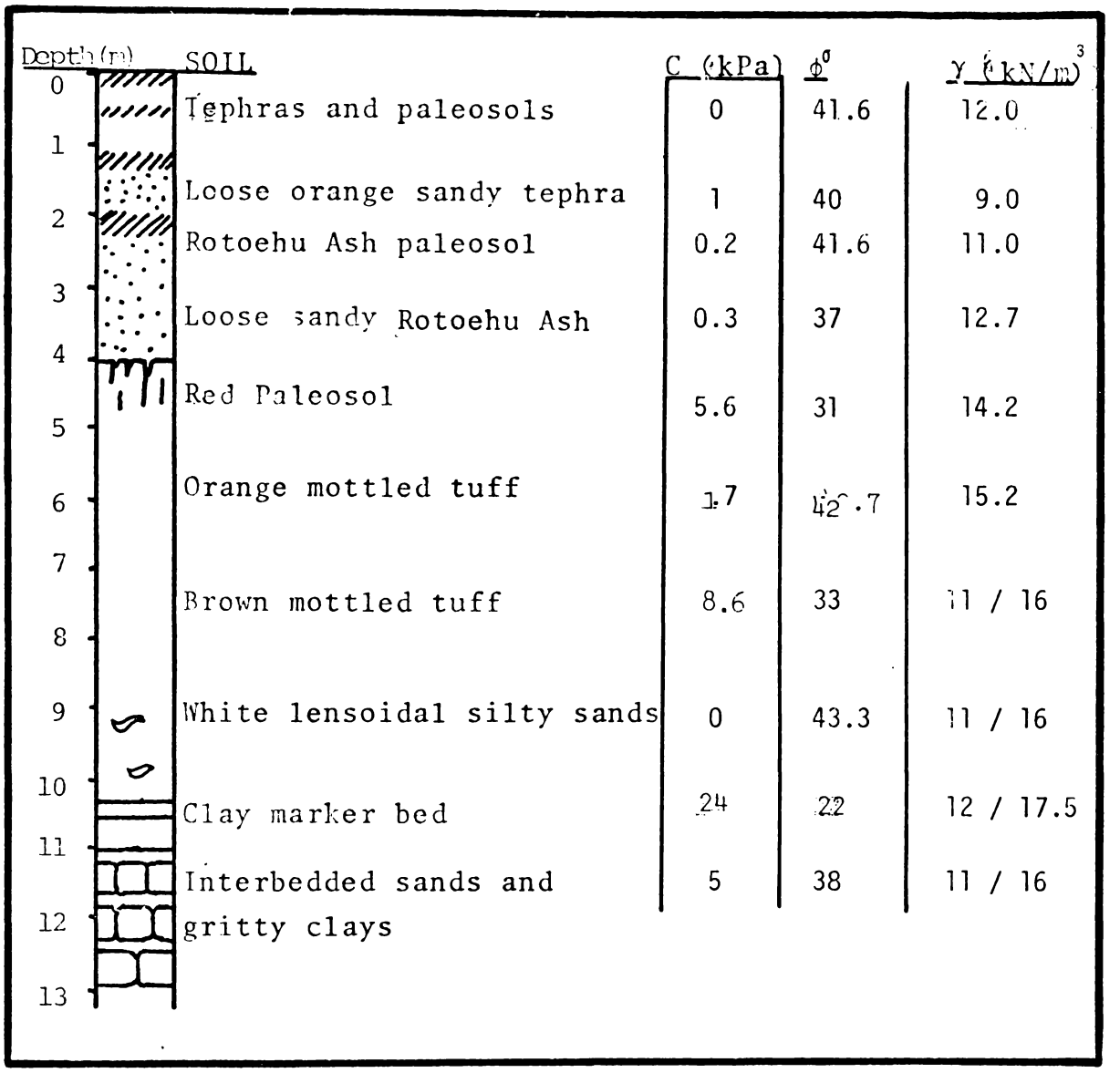

Figure 4.27. Idealised soil profile. Note: Where two values are given for γ the first value is dry unit weight, the second is saturated unit weight

the presence of an unusually strong bed directly beneath. A revised version of fig 4.1 (fig. 4.26) shows that several hypotheses remain which may be best tested by utilising a quantitative slope stability model.

In conclusion, the quantitative data assembled in this chapter are condensed into an idealised soil profile, suitable for use in a slope stability modelling situation (fig 4.27).

Note: The strength of the materials below the clay marker bed is only needed for estimating the effect of the clay bed's strength on overall stability. As these materials are many and varied, it was not practical to get accurate values by shear box testing, hence the strength values shown were estimated by comparing field descriptions and vane shear values with those obtained for similar materials tested in the triaxial or direct shear apparatus.

CHAPTER FIVE

Stability Analyses

"The greatest uncertainties in stability problems arise in the selection of the pore pressure and the strength parameters. An elaborate mathematical treatment of the analysis can lead to a fictitious impression of accuracy and the engineer can loose sight of the real uncertainties in the problem"..... T.J.Kayes (1974)

INTRODUCTION

The first need for a method of quantitatively analysing the stability of natural and man-made slopes became apparent in early nineteenth century Europe, with the boom of railway and building excavations accompanying the industrial revolution. Collin (1846, quoted in Tavenas et al.,, 1980) was the first to attempt a study of the nature of mass movements for this purpose. Based on Coulomb's (1773, quoted in Kayes, 1974) concepts of soil strength, Collin (loc. cit.) suggested that the stability of a soil mass could be represented in terms of a factor of safety 'F', where

$$F = \frac{\text{Restraining Force}}{\text{Disturbing Force.}}$$

In 1916 Pettersen (1955) put forward the Swedish Circular Arc method of analysis, which was developed as a method of slices by Fellenius in 1927 (Pettersen, 1955). In this type of analysis, the soil mass under investigation is divided into vertical slices and an overall factor of safety is reached by separately considering the equilibrium of each slice. The flexibility of the method of slices, allowing the investigation of complex and varying geometry and soil parameters, has resulted in its utilisation as the basis of many of the methods of stability analysis used today. Wright (1969) estimated that twelve methods of slices have since been developed.

SELECTION OF ANALYSIS MODEL

The six most commonly used methods, according to Fredlund and Krahn (1977), are:

i) Fellinius' method,
ii) Bishop's Simplified method,
iii) Spencer's method,
iv) Janbu's Simplified method,
v) Janbu's Rigorous method,
vi) Morgenstern-Price method.

A factor of safety may be derived by summing forces in two directions or by summing moments. However these summations

together with failure criteria, are insufficient to render the problem determinate without further information concerning the normal force distribution. All the methods commonly used today close this information gap by making an assumption about these forces. The Fellinius method assumes interslice forces may be neglected. The simplified Bishop method neglects interslice shear forces, assuming interslice forces may be adequately defined by a normal or horizontal force (Bishop, 1955), while Spencer's method assumes all net interslice forces are parallel (Spencer, 1967). Janbu's Simplified method uses a horizontal force equilibrium equation to derive F, hence the interslice forces sum to zero. The interslice shear forces are then accounted for by a correction factor, which is determined according to the cohesion and angle of internal friction of the failed materials, and by the geometry of the failure surface (Janbu et al., 1956). Janbu's Rigorous method assumes that a "line of thrust" defines the points at which interslice forces act, and interslice shear forces are used in determining normal forces. The interdependent unknowns of F and interslice shear forces are therefore initially assumed and then approximated through an iterative procedure (Fredlund and Krahn, 1977). The Morgenstern-Price method assumes that some arbitrary mathematical function describes the direction of interslice forces ($\theta = rf(x)$, where $f(x)$ is assumed at each interslice boundary and r is unknown). The magnitude

of these forces is calculated in a similar manner to that used in Janbu's Rigorous method (Duncan and Wright, 1980). The Fellinius, Simplified Bishop and Spencer methods assume circular failure arcs, and hence are not suitable for back analysis of non-circular mass movements. A modified form of Spencer's method may be utilised for non-circular failure surfaces (Spencer, 1973; Wright, 1975). Duncan and Wright (1980) found that "although there is no mathematical proof that the values of F calculated by Janbu's, Spencer's [modified] and the Morgenstern-Price methods are rigourously correct, from a practical point of view there is no doubt that they may be considered to be correct for all practical purposes".

In addition to these methods, the Rankine wedge method is also theoretically suitable for the analysis of the Maungatapu mass movements. This method of stability analysis has been applied with some success locally (East, 1974) and overseas (Boutrup and Lovell, 1980); however some experience is necessary in utilising the technique, as care must be exercised in selecting the inclination of interwedge forces (Chowdhury, 1978). This is especially critical in the case of short deep failures such as occur at Maungatapu, where factors of safety may err (on the low side) by twenty to thirty percent or more when compared with a more "correct" Morgenstern-Price analysis (Hamel, 1977; quoted by Chowdhury, 1978). The Rankine wedge method carries the

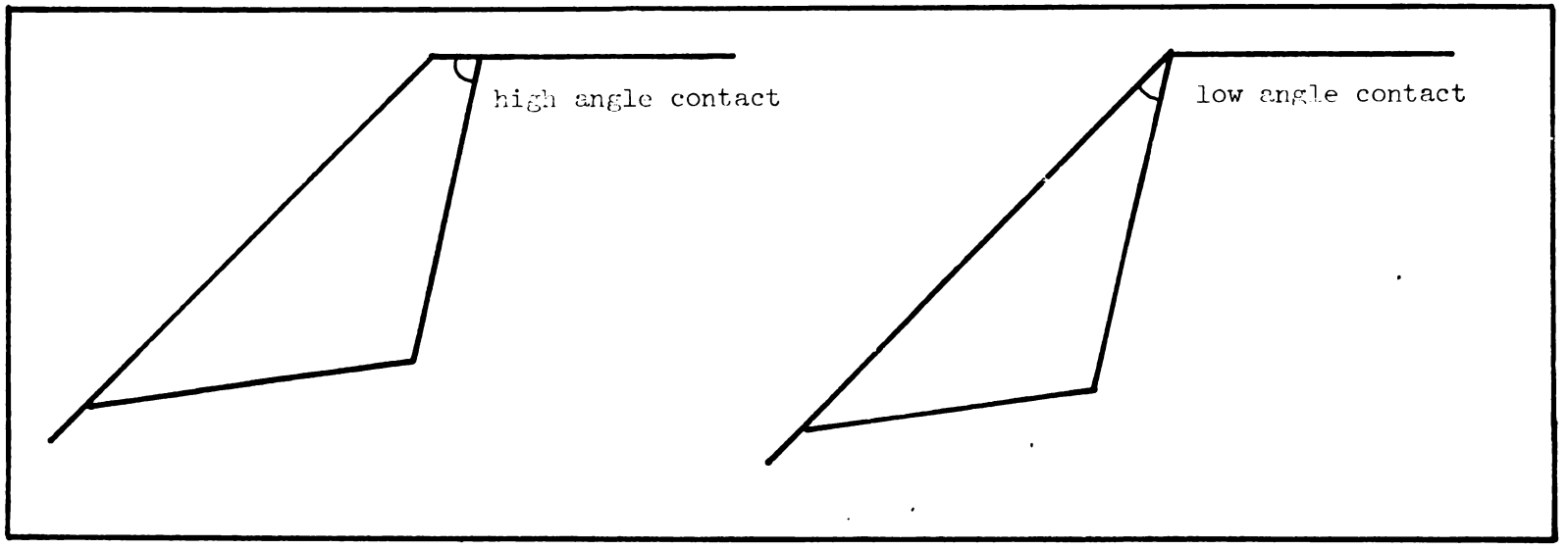

Fig. 5.1. The upper slope - failure surface contact, which may be regarded as high angle or low angle.

further limitation of being able to utilise only one set of strength parameters per wedge, while interwedge force definition uncertainties mean that a minimum of wedges is desirable.

Janbu's simplified and rigorous methods, Spencer's modified, and Morgenstern and Price's methods are not subject to such limitations where complex failure surfaces are involved, and generally produce factors of safety differing by less than five percent (Duncan and Wright, 1980). It is therefore commonly recommended (e.g. Tavenas et al., 1980, Whitman and Bailey, 1967, Wright et al., 1973) that Janbu's Simplified method, by virtue of its simplicity, is the most suitable for the analysis of non circular failures such as the Maungatapu features.

However Boutrup et al. (1979) found that this method produced factors of safety seriously in error when used in the analysis of failures where deep surfaces of rupture make a high angle upper-slope contact, coincident with high values of cohesion in the area. As it is arguable (fig. 5.1) that the geometrical portion of this condition is satisfied in the Maungatapu failures, it seemed advisable to provide some means of checking the results produced by Janbu's Simplified method before proceding with vital analyses. Accordingly BASIC PLUS programs were written (Appendix 3) to perform Janbu's Simplified and Rigorous analyses. Only minor (<2%) differences were observed in the

factors of safety produced by the rigourous and simplified programs.

Janbu's Simplified method of stability analysis therefore appeared theoretically and practically suitable for use as a model within which the significance of soil, geometrical and pore-water pressure parameter variations could be evaluated. A further BASIC PLUS program was written, utilising the original Janbu's Simplified method program as a basis for the iteration of values of soil cohesion, bulk density, internal friction and water table heights (Appendix 3). The effects of geometry may also be tested using this program.

FAILURE SURFACE MORPHOLOGY

One aspect of the Maungatapu peninsula mass movement investigation which could not be studied using the simple JSITER.BAS program was that of the unusual failure surface morphology. Adequate investigation of hypotheses concerning a feature such as this requires the generation of a number of alternative surfaces and the comparison of factors of safety found for these surfaces under conditions varied according to the nature of the hypothesis. The generation of such surfaces manually (as would be necessary if JSITER.BAS were used) is impractical because of the lengthy data preparation and input required. While it would

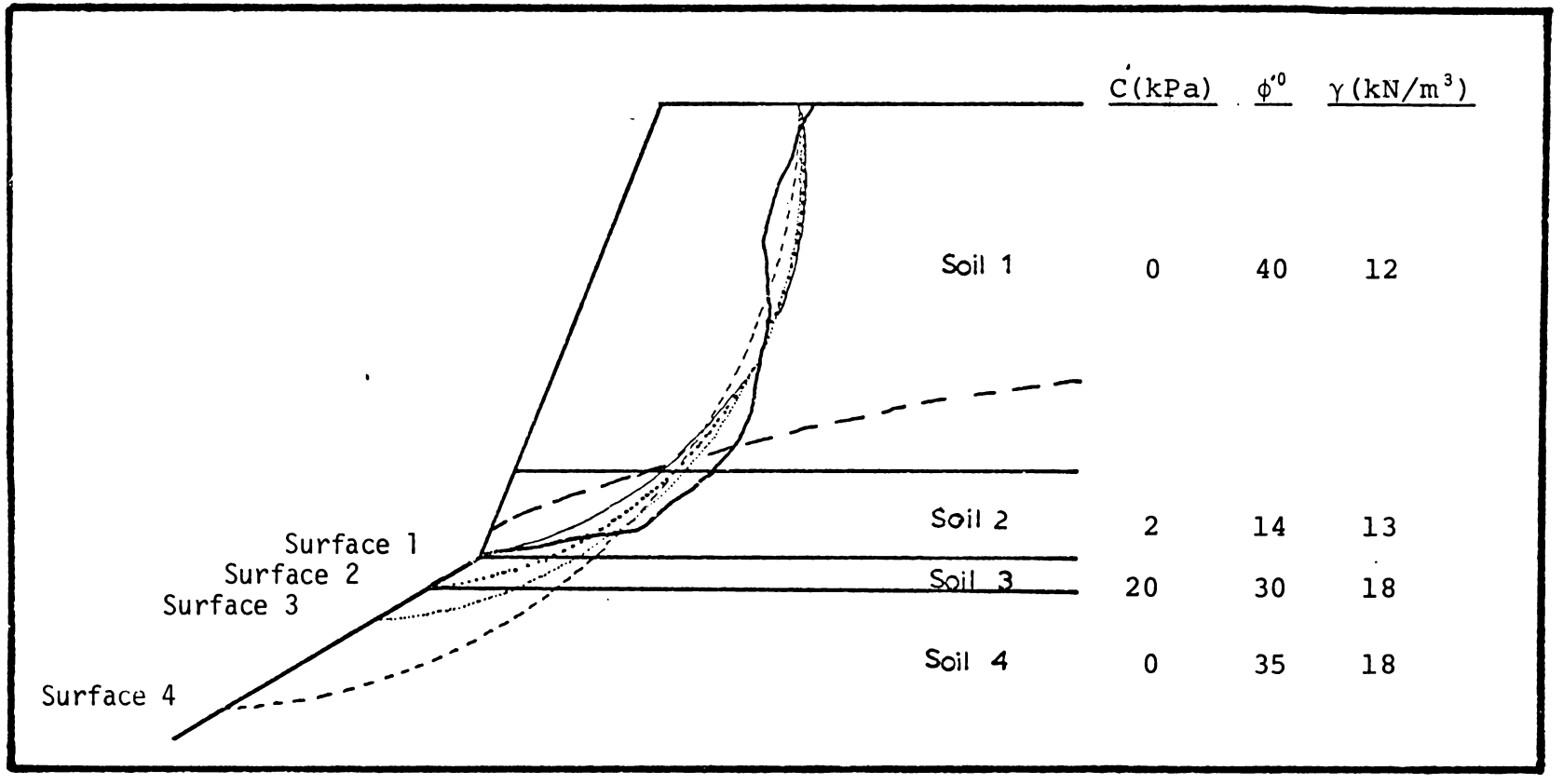

Figure 5.2. Investigation of the effect of the presence of the clay marker bed using multiple failure surfaces.

possibly be better to generate irregular surfaces using a mechanism such as Carter's (1971) Fibbonacci series generator, the only surface generator available on the University of Waikato computer facility produced circular arc surfaces, and utilised a Bishop's Simplified stability analysis. Duncan and Wright (1980) showed that while Bishop's Simplified method is not as rigorous as Janbu's or Morgenstern-Price's methods, it consistently produces similar (<5% difference) factors of safety, and for all practical purposes may be considered to be just as accurate.

The only hypothesis concerning the failure surface morphology which required testing in this manner, was the suggestion that the slightly higher strength of the clay marker bed may have been sufficient to cause a non basal-intersecting failure. Such a test would produce results relatively unaffected by the type of analysis used, as long as feasible alternative failure planes were utilised. The use of the Bishop's Simplified search option FORTRAN IV program STAB.FOR (Geomechanics Manual 5, Law, 1980, unpublished) thus apeared reasonable.

STAB.FOR is only capable of handling four sets of soil data, hence the idealised soil profile (fig. 4.27) was condensed to four soils with "average" properties (fig. 5.2) and STAB.FOR was then run, first utilising the soil profile shown in fig. 5.2, and then with soil 2 extended over the volume "occupied" by the clay marker bed (soil 3).

The surveyed geometry of site 1 was used, the upper failure plane entry point was specified, and a water table was postulated according to work discussed below.

The results are illustrated by the factor of safety values obtained for the four surfaces shown in fig. 5.2. While the presence of the clay marker bed significantly increased the factor of safety for any surface passing through it (e.g. 0.55 cf. 0.80), a basal or near basal-intersecting potential failure surface remained significantly less stable than a failure surface exiting above the clay marker bed (0.80 cf. 0.98). It must be noted that surface 4 does not represent the least stable case. It is chosen over a lower line (with a lower F) as it is closer in form and upper slope contact point to the three upper surfaces, minimising irrelevant influences on the value of F,and also because of the uncertainties surrounding the lower pre-failure geometry.

The presence of the clay marker bed, therefore, probably contributed to the biplanar nature of the failure surface morphology. However it was not sufficient to cause the formation of this feature on its own.

SOIL PROFILE RATIONALISATION

In preparing site specific soil profiles, the idealised soil profile obtained from field and laboratory studies (fig.

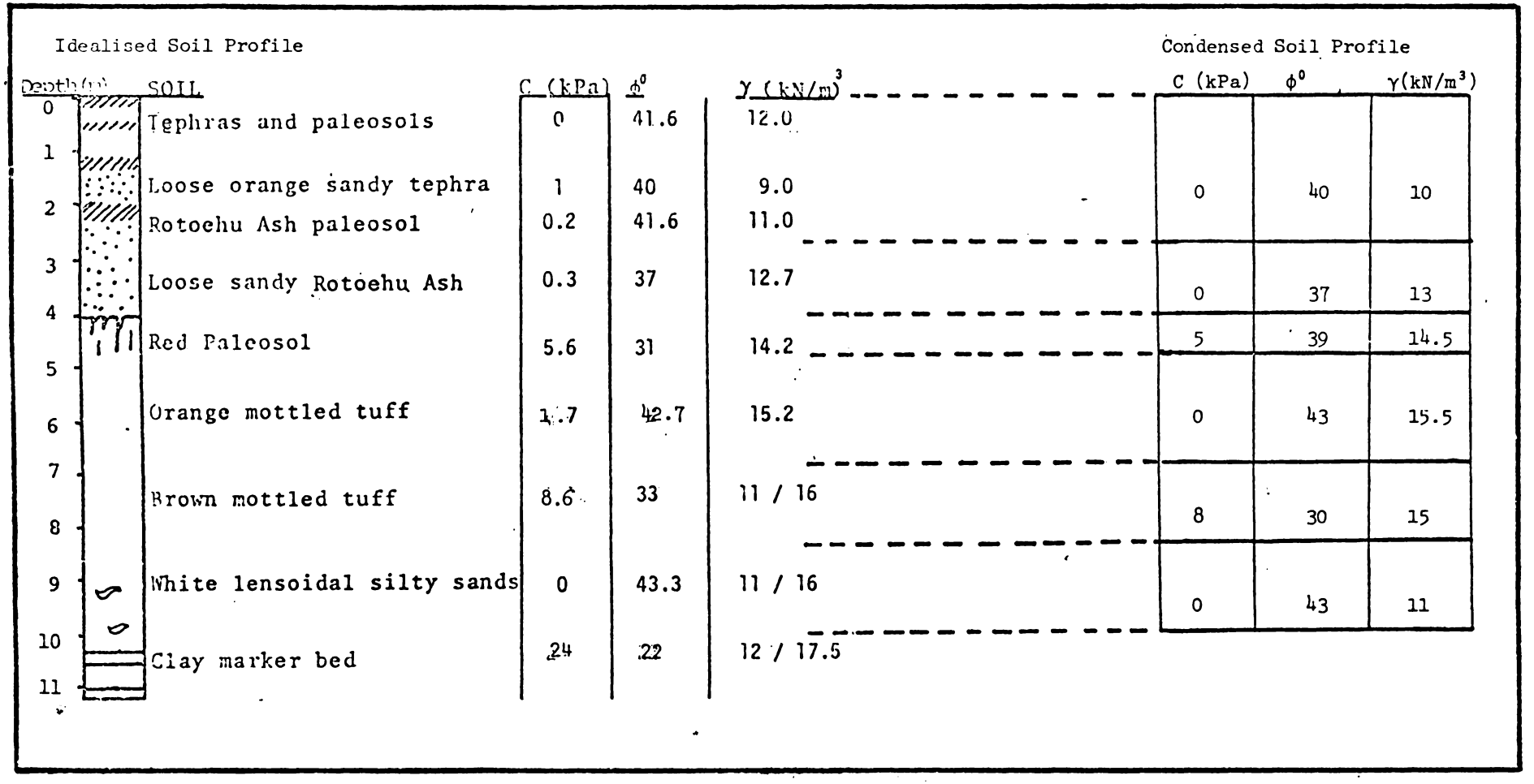

Fig. 5.3. Condensation of idealised soil profile to a test case soil profile.

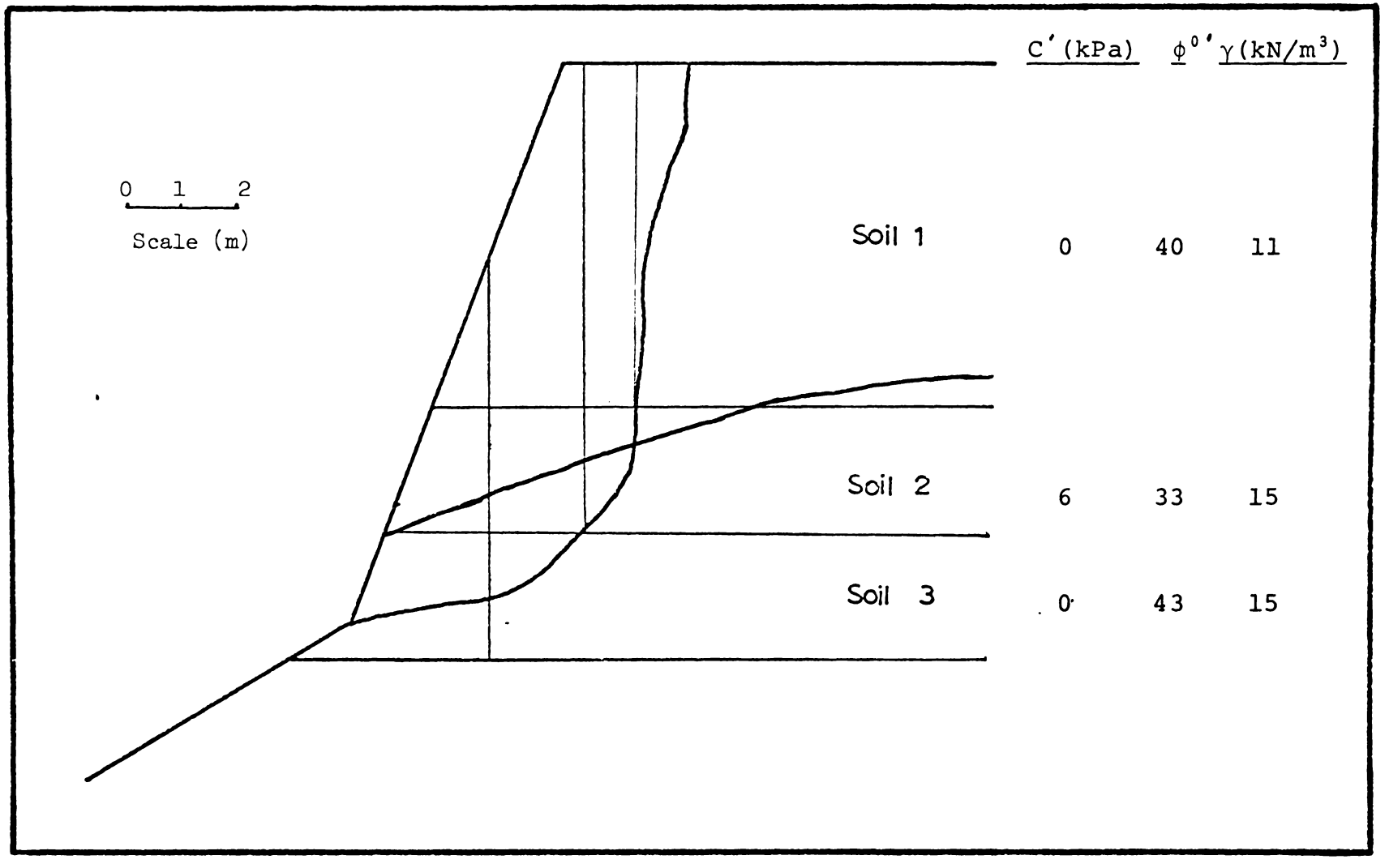

Figure 5.4(a). Test profile for site 1.

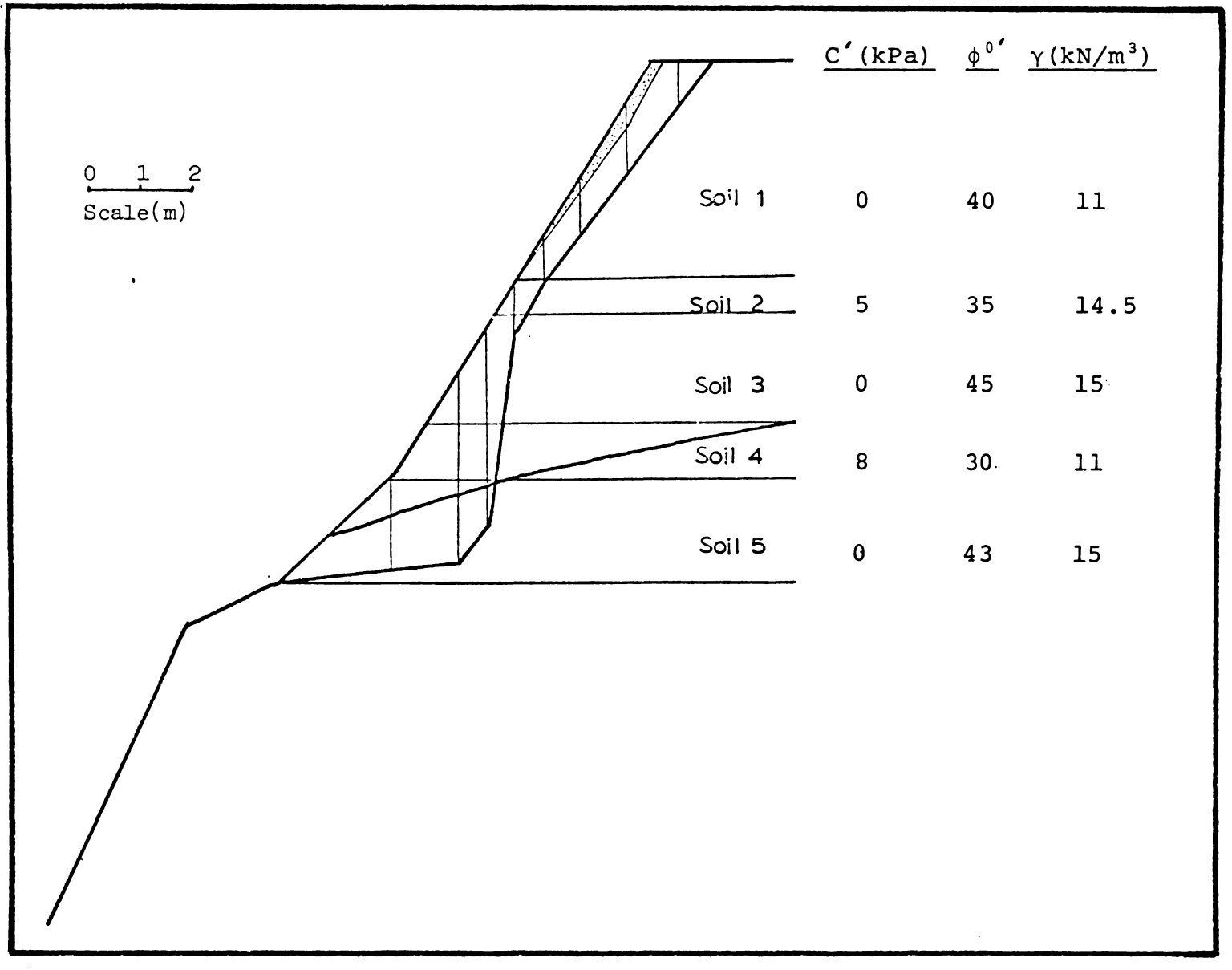

Figure 5.4(b). Test profile for site 2.

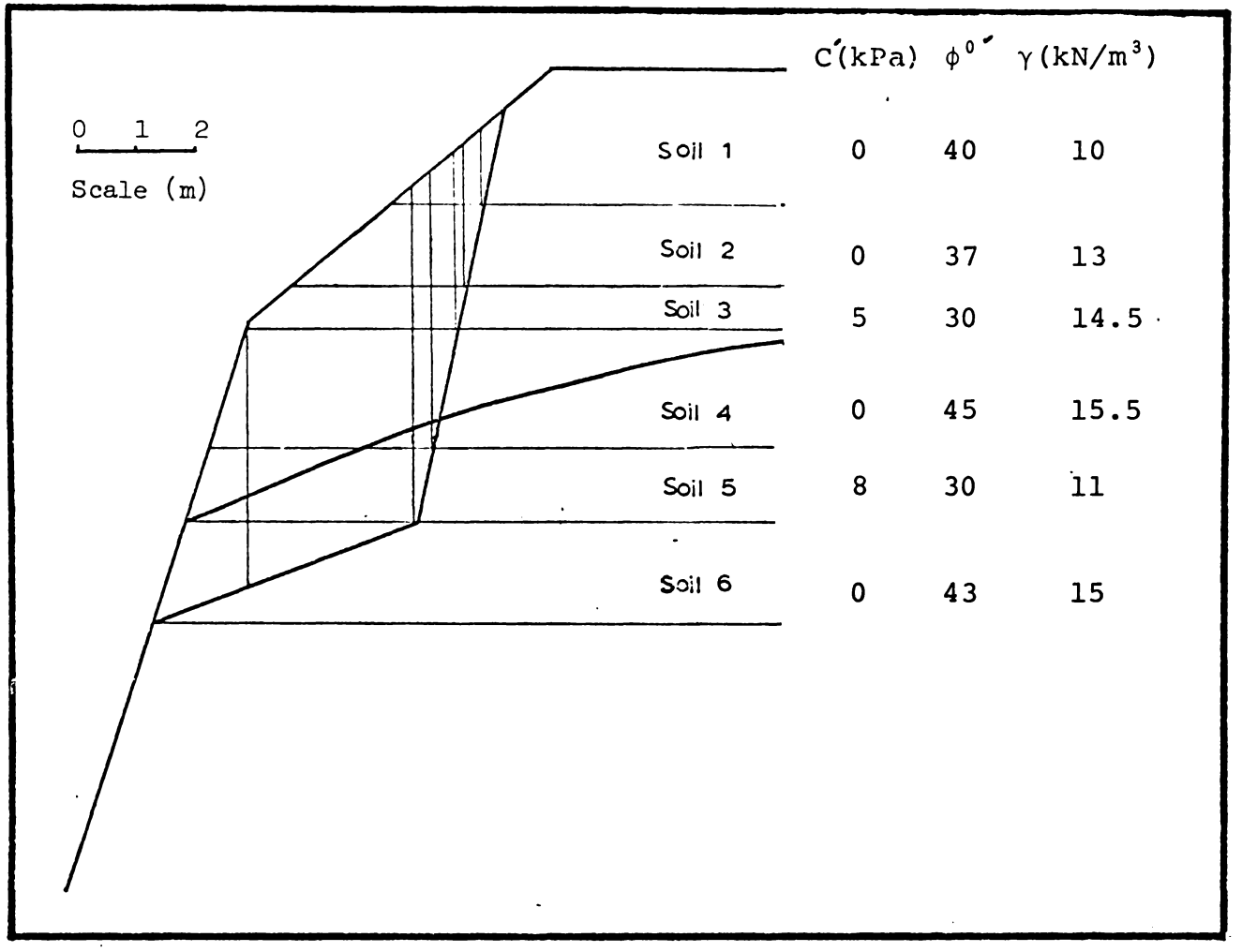

Figure 5.4(c). Test profile for site 3.

4.27) was placed alongside diagrams of the surveyed failure surfaces, and the displaced soil mass was divided into vertical slices according to the failure surface morphology and major changes in the soil parameters. Within the confines of these slices, soil properties were then rationalised to a few sets of values, in order to simplify calculations (e.g. fig 5.3). The test profiles produced in this manner are shown in fig. 5.4.

The morphology of the displaced mass at site 2 (fig. 5.4b) appears a little unusual compared with the other two sites. The thin layer of material from the upper four metres of the profile which was involved in movement, consisted largely of fill deposited on a cut surface. The failure surface did not occur at the fill/in situ soil boundary but occurred within the in situ soil. The estimated dimensions of the fill are shown in fig. 5.4b (C.F. Whiteman, pers. comm.). It is thought that the presence of the fill did not affect stability notably (see discussion of bulk density variation effects below). The pre- failure morphology of site 3 exhibited a bevelled edge, cut down several years before as part of a landscaping project.

PIEZOMETRIC DATA RATIONALISATION

Field evidence indicated that surface seepage occurs from

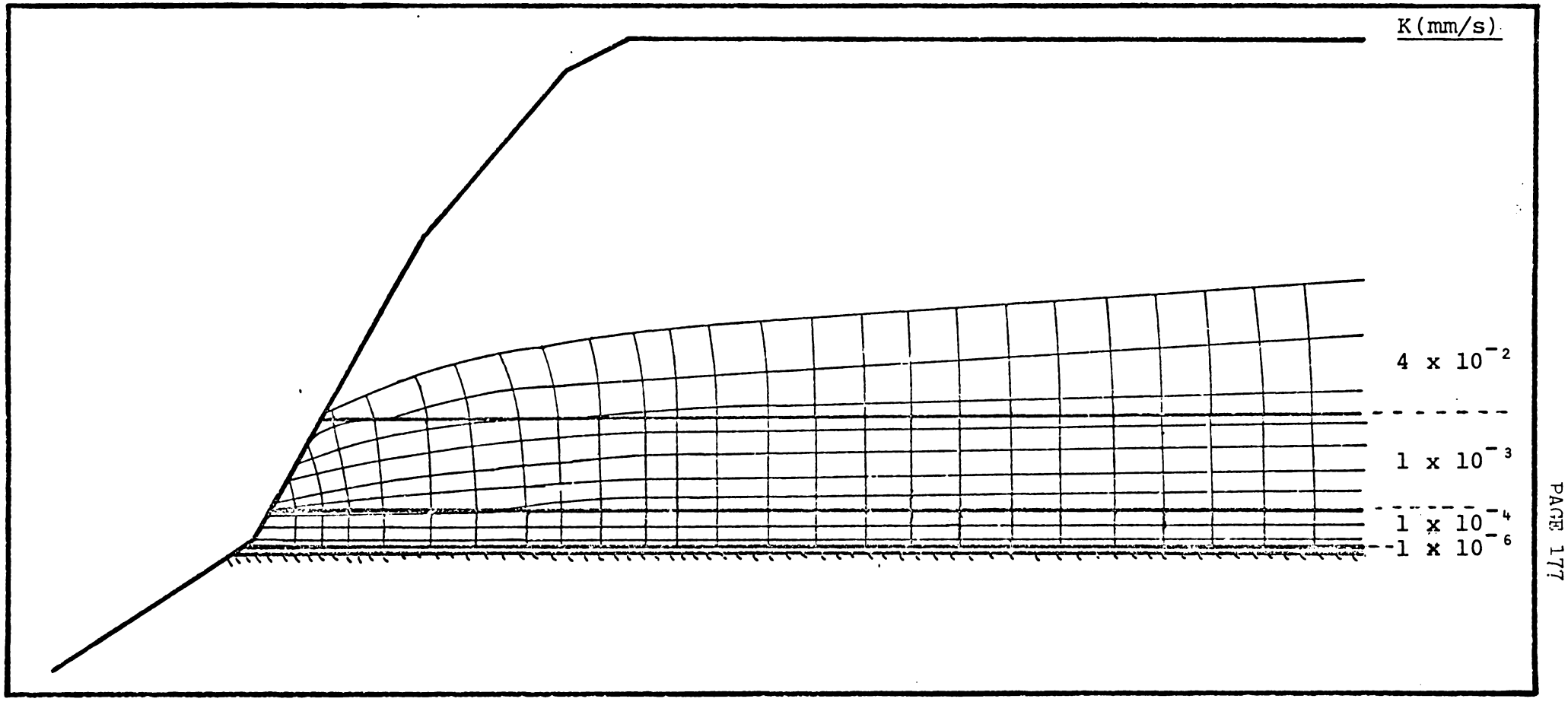

Figure 5.5. Flow net drawn from hydraulic conductivity data for an idealised soil profile.

the exposed surface of rupture in the 2 to 3 metres above the clay marker bed, for a considerable period after failure. Laboratory hydraulic conductivity tests have shown that this is due to a marked decrease in the hydraulic conductivity of the materials in the metre or so above the clay marker bed. The clay marker bed may be kregarded as impermeable over periods of less than years. To simplify illustration of the effects of the hydraulic regime, the values were condensed to give three 'average' soils. The hydraulic conductivity values assigned to the soils were 4×10 mms^{-1}, 1×10 mms^{-1}, and 1×10 mms^{-1}, plus the clay marker bed at 1×10 mms^{-1} (fig 5.5).

A flow net was drawn up, utilising these soils, a seep point at 2.5 metres above the clay marker bed, and a moderately curved phreatic surface (fig. 5.5). Although this is only one of a number of equally feasible scenarios, it indicates a factor common to all; the pore pressure distribution indicated is different from that which would be postulated under hydrostatic conditions. Seepage forces, applied to the soil through frictional drag, transfer pressure (related to the loss in total head) from pore water pressure to effective stress (Lambe and Whitman, 1980). In general, seepage flow causes a decrease in slope stability, most marked where flow is parallel to, or out of a slope. This effect is illustrated by the factor of safety equations derived for an infinite slope. If the slope is

cohesionless, for hydrostatic conditions:

$$F = \frac{\tan \phi}{\tan \alpha}$$

and for seepage parallel to the slope through the entire profile:

$$F = \frac{\gamma'}{\gamma} \times \frac{\tan \phi}{\tan \alpha}$$

where α is the slope angle. The value of $\frac{\gamma'}{\gamma}$ is commonly 0.5 (Chowdhury, 1978). Seepage parallel to the slope in an infinite slope in cohesionless material can thus halve the slope's factor of safety. In the slopes under consideration, seepage does not occur through the entire profile and hence the effect will not be as dramatic. The direction of flow (and hence seepage force, assuming the soil is isotropic) is out of the slope, a situation which results in a greater destabilising effect than flow parallel to the slope. The important conclusion is that there is a significant force affecting slope stability during periods of high rainfall that is effective above, but not below the clay marker bed.

In stability analyses employing the method of slices, seepage forces are accounted for by calculating a pore water pressure resultant at the base of each slice. This is obtained from a flow net which, to be accurate, must be based on a series of piezometric observations. As discussed previously, no such observations could be made in this study. To provide working estimates of pore water pressures

for stability analysis, a moderately curved phreatic surface (similar to that in fig 5.5) was postulated for each site. and estimates of pore water pressures were based around these. Such assumptions are commonly made in situations where steady state seepage is thought to occur (Fredlund, 1978). This case, with transient seepage conditions, is one step further removed from this idealised situation. It must therefore be noted that the effective stresses calculated on the basis of this assumption probably give a conservative estimate of the effect on stability of any given phreatic surface level. More significantly, and less certainly, it is possible that this assumption would not accurately represent the nature of the dynamic phreatic surface height - factor of safety relationship. This is because an assumption of hydrostatic conditions implies a linear phreatic height - pore water pressure relationship exists at any one point, which is not necessarily valid under transient seepage flow conditions. It is probable that this error would again be on the dangerous side (overestimating F). The results of the stability analyses below, concerning phreatic surface heights, must therefore be considered as probably optimistic.

SENSITIVITY ANALYSES

Initial analyses were conducted using the idealised

profiles shown in fig. 5.4, with a moderately curved phreatic surface emerging as a spring 8 metres below datum. The phreatic surfaces were then lowered vertically until a factor of safety of 1 was obtained. This produced upper seepage limits at between 8.2 and 9 metres below datum (1.3 to 2.1 metres above the clay marker bed) at the three test sites (fig 5.4), agreeing well with post-mass movement field observations. The program JSITER.BAS was then used to obtain solutions for the factor of safety equation, iterating soil parameters over reasonable ranges. Cohesion and internal friction angles were iterated in two groups; in the slices with near horizontal bases, and in the slices with near vertical bases. This grouping was necessary to examine the relative importance of strength variations in the lensoidal silty sands and in the other materials which were suggested to be less important in failure. Bulk density variations were initially evaluated one soil at a time, but the effects were so small that coincident variation was used to produce effects which could be illustrated graphically. The effects of variations in the hydraulic regime were estimated by vertically moving the phreatic surface. The limitations of this approach have already been discussed.

The solutions obtained are shown in the form of factor of safety versus parameter graphs (figs. 5.6 to 5.8). Two questions must be considered in sensitivity analysis; what

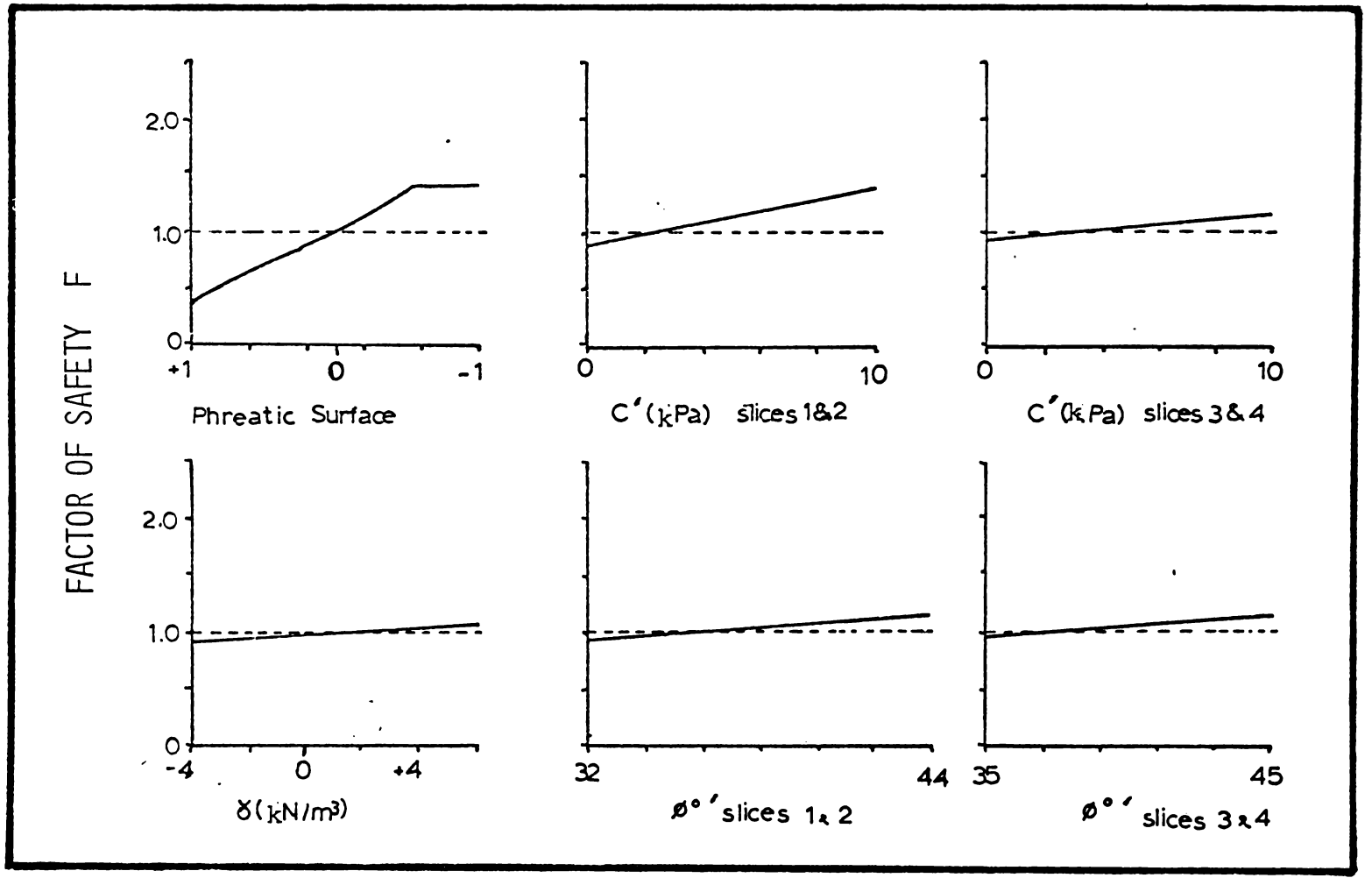

Figure 5.6. Effects of changes in soil and pore water pressure parameters on the factor of safety F for test site 1.

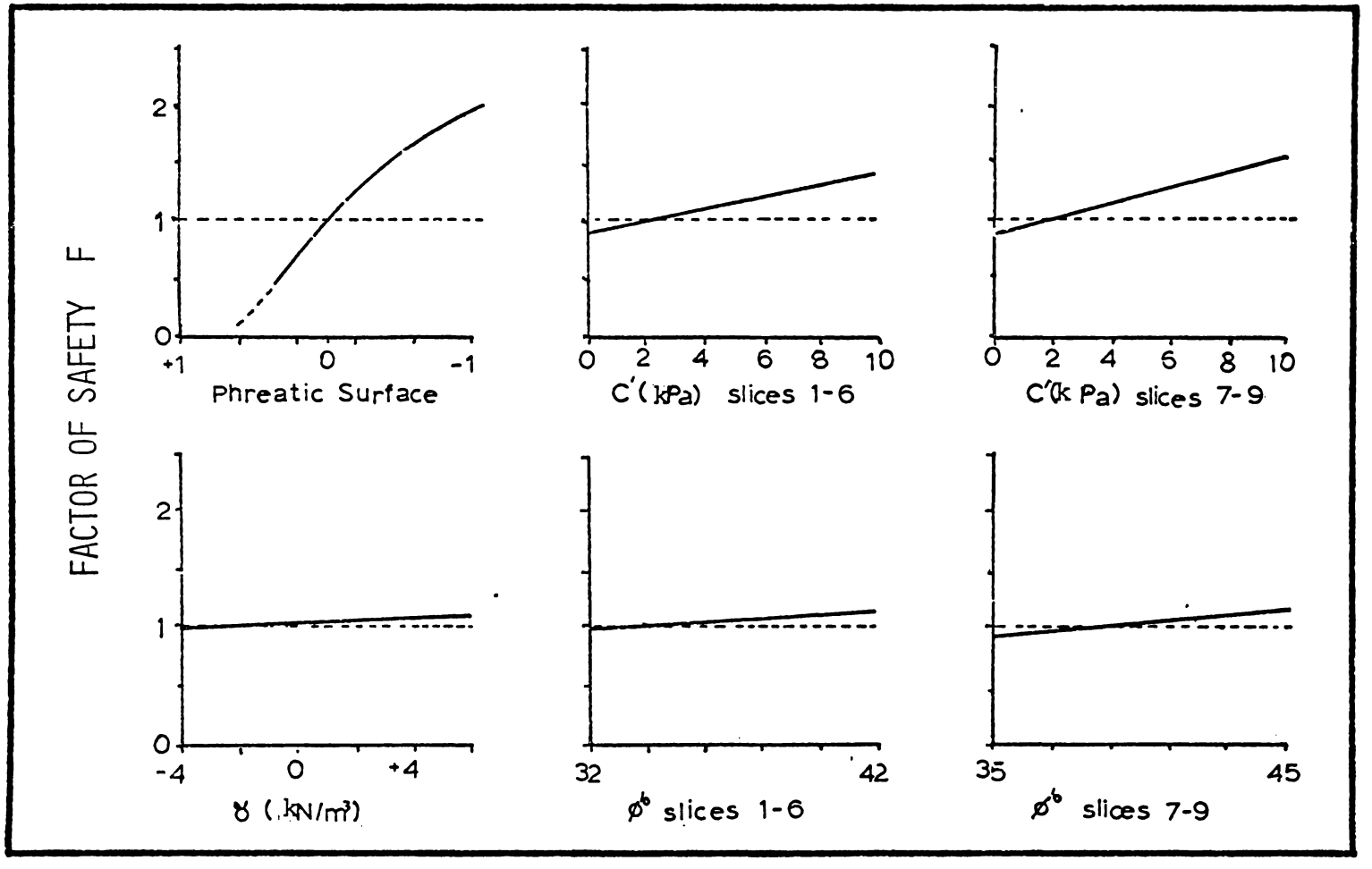

Figure 5.7. Effects of changes in in soil and pore water pressure parameters on the factor of safety F for test site 2.

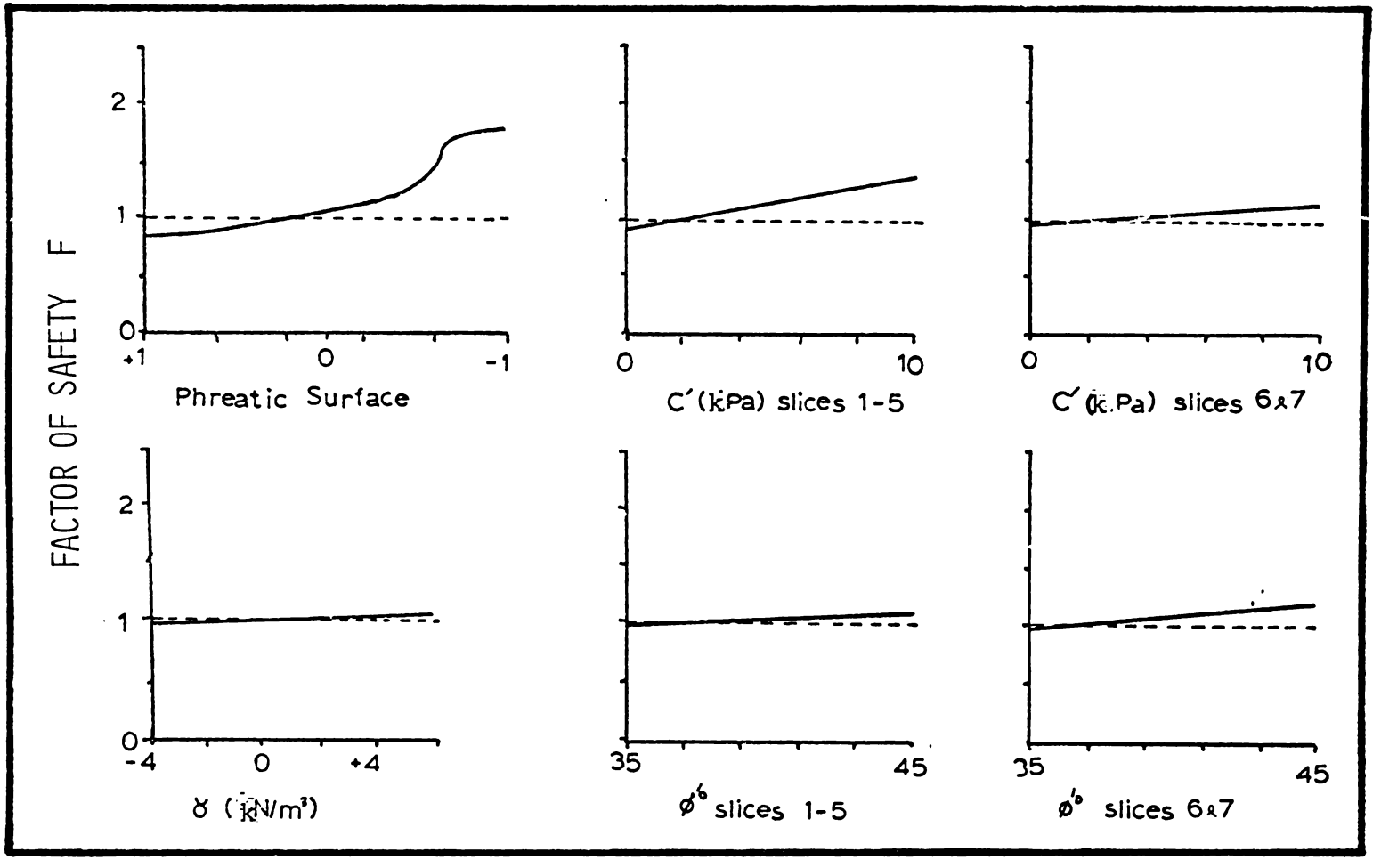

Figure 5.8. Effects of changes in soil and pore water pressure parameters on the factor of safety Ffor test site 3.

is the magnitude of likely variation, and what will the effects of a change of this magnitude be? The effects of unit weight variation are minimal, and act to stabilise the slope during a rainstorm, the opposite of the effect postulated. For an 'average' soil above the clay marker bed:

Dry unit weight : 10.0 kN/m^3

Field moisture content : 30%

Field moist unit weight: 13.0 kN/m^3

Saturated unit weight : 16.2 kN/m^3

(assuming particle density = 2.65 g/c m^3)

Hence the probable maximum increase of unit weight of 3 kN/m would only increase F by 0.05.

Triaxial tests showed the lensoidal silty sand had zero cohesion, with a prediction confidence of 8.4 kPa. It is possible, although highly unlikely, considering field evidence of year round seepage at mass movement sites, that the lensoidal silty sands could dry out sufficiently to gain a few kPa of apparent cohesion, which would be lost on saturation (fig. 5.9). The significance of such effects would be more than marginal, with a possible 5 kPa loss of cohesion producing a significant alteration in the value of F. Such changes in cohesion are not considered likely.

In the upper materials, however, the loss of apparent cohesion on saturation is considered more likely, owing to greater variations in moisture content above the zone of

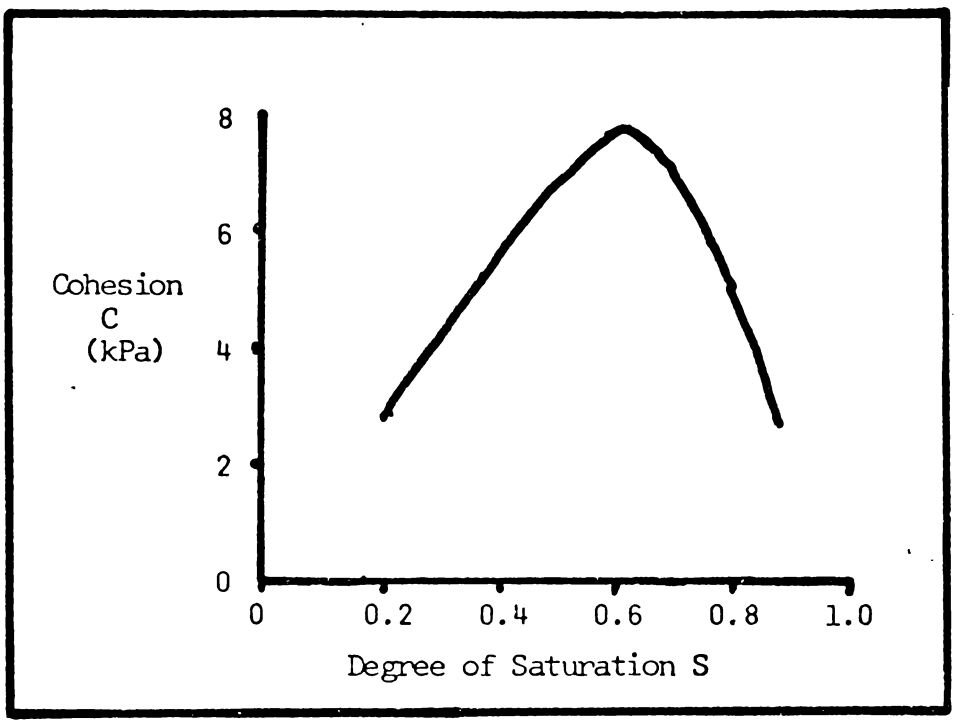

Figure 5.9. Change in effective cohesion with saturation for a medium sand. (after Kezdi, 1979).

seepage. Field strength investigations have indicated that these changes would be very small, probably of the order of 1 or 2 kPa only. Lower test numbers mean there is a greater likelihood that the cohesion values used will be erroneous. There is a greater area of rupture surface in the upper beds than within the lensoidal silty sands, hence despite less critical location, the strengths of the materials through which the near vertical portion of the surface of rupture passes have just as great an effect on stability. This also reflects the initially rotational mode of failure, suggested from field evidence. The loss of apparent cohesion in the upper soils as percent saturation increases probably plays a small but appreciable part in disposing a slope towards failure.

It is not likely that any appreciable pre-failure changes in angles of internal friction occur (Lambe and Whitman, 1980). The prediction interval for the angle of internal friction of the lensoidal silty sands is 1.85 degrees, and somewhat more for the upper soils. The effects of maximum error in one or more of the o parameters is not likely to significantly affect the factor of safety produced.

By far the most critical factor affecting slope stability is that of phreatic surface height, by virtue of significant observable variation, and the significant effects of these variations. It must be noted, once again,

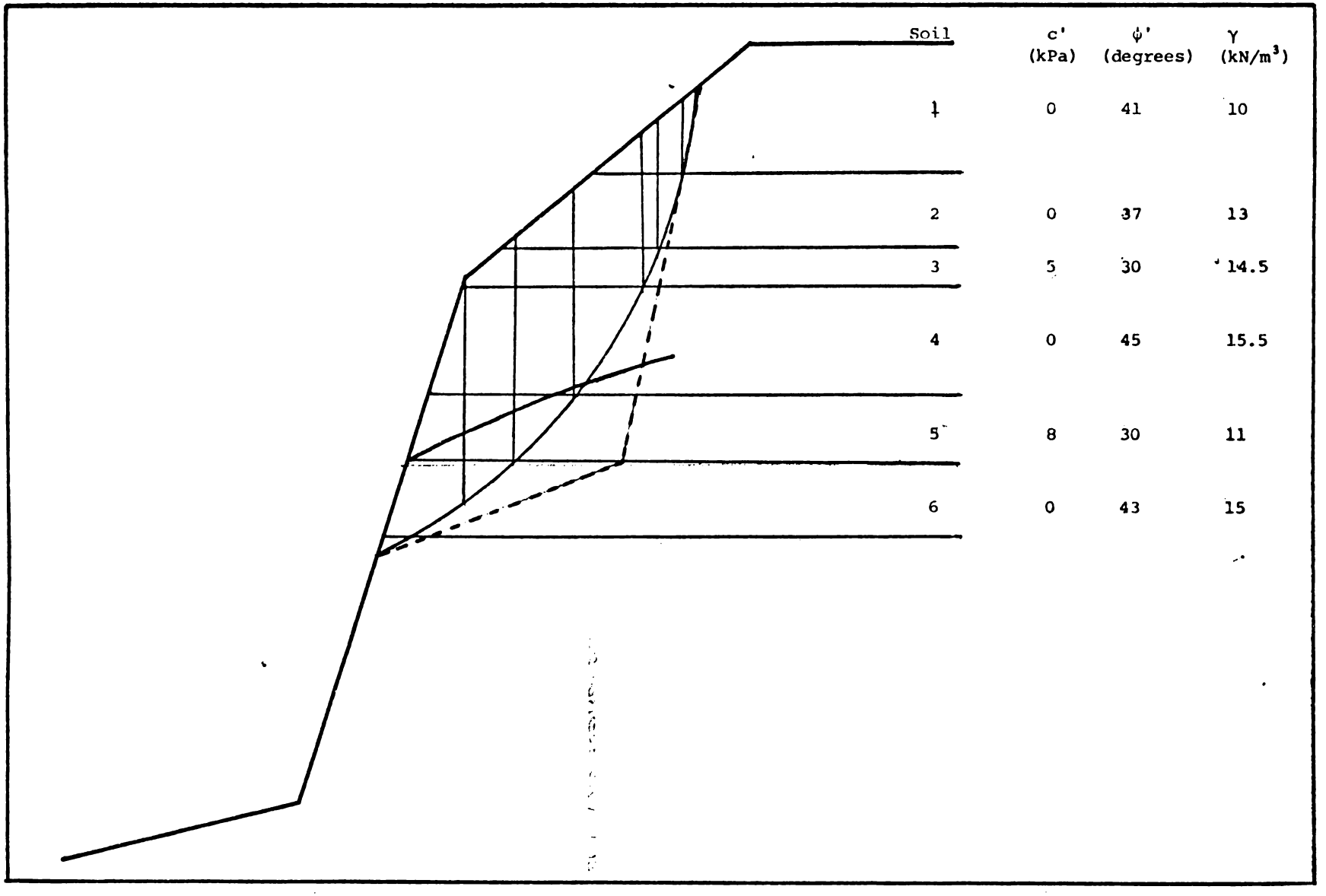

Fig. 5.10 An alternate potential failure surface with a shorter length in the lensoidal silty sand/sandy mud material.

that the piezometric effects considered are based on probably conservative estimates of the transient seepage forces present. Rises and falls of seepage points of 1 metre have been observed during and after storms which did not produce mass movements. A rise in the phreatic surface of only 20 cm can affect the factor of safety by 0.25 or more. This is equivalent to the effect of a decrease in the cohesion of all the upper 8 to 9 metres of soil of 6 kPa, or a decrease in the angles of internal friction of the same soils of 20 degrees.

FAILURE PLANE MORPHOLOGY

The final set of stability calculations was directed towards evaluating the hypothesised relationship of the biplanar failure surface to the presence of weak material above the clay marker bed. The silty sand/sandy mud material at this level has been shown to be cohesionless, lying between two cohesive beds which have lower internal friction angles. It appeared possible that the stability of a potential failure surface which passed through the silty sand/sandy mud soil (fig. 5.10). Analysis with the Janbu simplified program showed the difference in factors of safety for the two surfaces to be negligible (<4%), while soil bulk density and water table height parameters were varied.

SUMMARY

The biplanar nature of the failure surface is due, in part, to the presence of the cohesive clay marker bed, but appears unrelated to the intact strength characteristics of the silty sand/sandy mud above. Increases in soil unit weight with rising percent saturation tend to slightly increase stability. The same rise in soil moisture content probably leads to some losses in cohesion in the upper 8 metres of the soil profile. It is unlikely that significant pre-failure changes in cohesion or internal friction angles occur in the near horizontal portion of the surface of rupture. The critical factor in determining bluff stability, the factor which may be regarded as providing the trigger for mass movement, is that of high pore water pressures at the failure surface.

CHAPTER SIX

Summary and Conclusions

INTRODUCTION

This thesis study was initiated with two major aims:

i) to develop an understanding of the landsliding process observed on and about the Maungatapu peninsula; an understanding of its nature, causes and effects;

ii) to develop a model of landslide development and/or prediction.

In effect, these two aims became condensed into the single aim of relating crest retreat episodes and retreat rates to basal retreat rates.

CLIFF EVOLUTION MODEL

Field evidence discussed earlier was interpreted as indicating a toe retreat/crest retreat system operating by two mechanisms; 1) parallell slope retreat when basal erosion rates are low, and 2) repeated landsliding when basal erosion rates are high. The latter mechanism is active on lengths of coastline which are exposed to erosion by tidal channels passing close to cliff bases, and/or by westerly wind driven waves. Most of the northwest and the

northeast coasts of the Maungatapu peninsula are affected by this mechanism.

The sequence consists of a mass movement, followed by removal of the debris toe, and then erosion of the cliff base by wave and/or tidal current erosion. As this basal erosion occurs, the crest of the cliff and the edges of the shelf feature are rounded by wind and running water attrition. The relative rates of the basal erosion and surface attrition processes determine the form of the cliff at any particular time during its steepening. When a critical form is reached, failure occurs, and the evolutionary sequence begins again. Investigations conducted in the laboratory, and with a computer stability model, were directed towards clarifying parts of this evolutionary model, and towards gaining a further understanding of the nature of the mass movements.

Stability analyses showed that individual failures are triggered largely by the occurrence of high pore water pressures in the lensoidal silty sands/sandy muds above the impermeable clay marker bed. Assuming static groundwater conditions, the ratio of phreatic surface height above failure surface to depth to failure surface which is required to produce failure is only 0.3 to 0.4. As high seepage flow is known to occur from the material above the clay marker bed prior to failures, it is probable that the seepage stresses imposed upon the soil reduce the ratio

required in order for failure to occur. The actual phreatic surface heights required to trigger failure may only be determined with certainty by direct observation. The concentration of mass movement episodes in spring and late summer, the two seasons of heavy rainfall in the Bay of Plenty area, provides further confirmatory evidence for the triggering of mass movements by high pore water pressures. In summary, the pore water pressure rises appear to be generated after long wet periods, which culminate in short, intense rainfalls.

Failure occurs above the clay marker bed, initially rotational, and then subsequently in a translational manner, rafting much of the upper material, in an almost intact form, for up to 50 metres at high speed. It is suggested that this highly translatory movement is the result of the liquefaction of the lensoidal silty sands/sandy muds, due to the sudden undrained compaction of the silty sands during shear failure. The distinctively biplanar nature of the failure surface may possibly have been produced by the extension of this zone of liquefaction back into the cliff. It is also possible that this form was produced by the nearly horizontal water table present (observation of seepage at about 7.5 m.b.d. at the cliff face, while the water table never reached 4.3 m.b.d. at 30 metres behind the cliff face). The cohesionless nature of the silty sands/sandy muds does not appear to be a causative factor.

Both of these features would tend to produce a 'least stable' surface with a long, near horizontal plane, rather than of an arcuate shape. The rapid movement of the failed mass may also be due, in part, to the fact that most of the materials below 5 m.b.d. have moisture contents in excess of their liquid limits during wet periods, and hence would tend to exhibit rather low residual strengths. If any of these materials were subjected to prolonged shear, they would probably have a minimal retarding effect on the landslide's rate of translation.

In summary, the factors which contribute to the instability of a given site are;

i) the presence of an almost impermeable bed in the geological sequence;

ii) the oversteepening of the cliffs by marine erosion;

iii) The generation of high pore water pressures at the failure plane by intense rainstorms.

Contributions of water from domestic sources, and decreases in seepage concentration times, from the use of stormwater soak holes, may also be of importance.

LANDSLIDE MANAGEMENT

The discussions presented up to this point have been

oriented towards one of the two reasons for initiating the study; that of increasing the body of information concerning coastal landslides. At this stage it is possible to apply the results of the study to its second purpose; decreasing the vulnerability of residents to individual landslides.

Management of the landslides must be considered on two time/space scales; the long term coastal erosion scale, and the short term, single potential landslide site scale. If one considers the long term, it is clear that the elimination of landsliding is only possible if basal erosion can be controlled. The control of erosion by conventional beach protection methods such as groynes, sea walls, or beach nourishment is an expensive process, and often very difficult to effect.

It is better, where possible, to apply management systems which design land use according to the limitations imposed by erosion. In the case of Maungatapu, this would involve the definition of a coastal 'no subdivision' reserve zone along lengths of coastline which are in danger of failing, or which, with up to 50 years of erosion, could be at risk. Such a coastal reserve would extend approximately 10 metres back from the cliff edge, and would be redefined every 50 years, or after any periods of major erosion. In the area for which aerial photographs were available, the lengths of coastal cliffs which are considered 'at risk' or

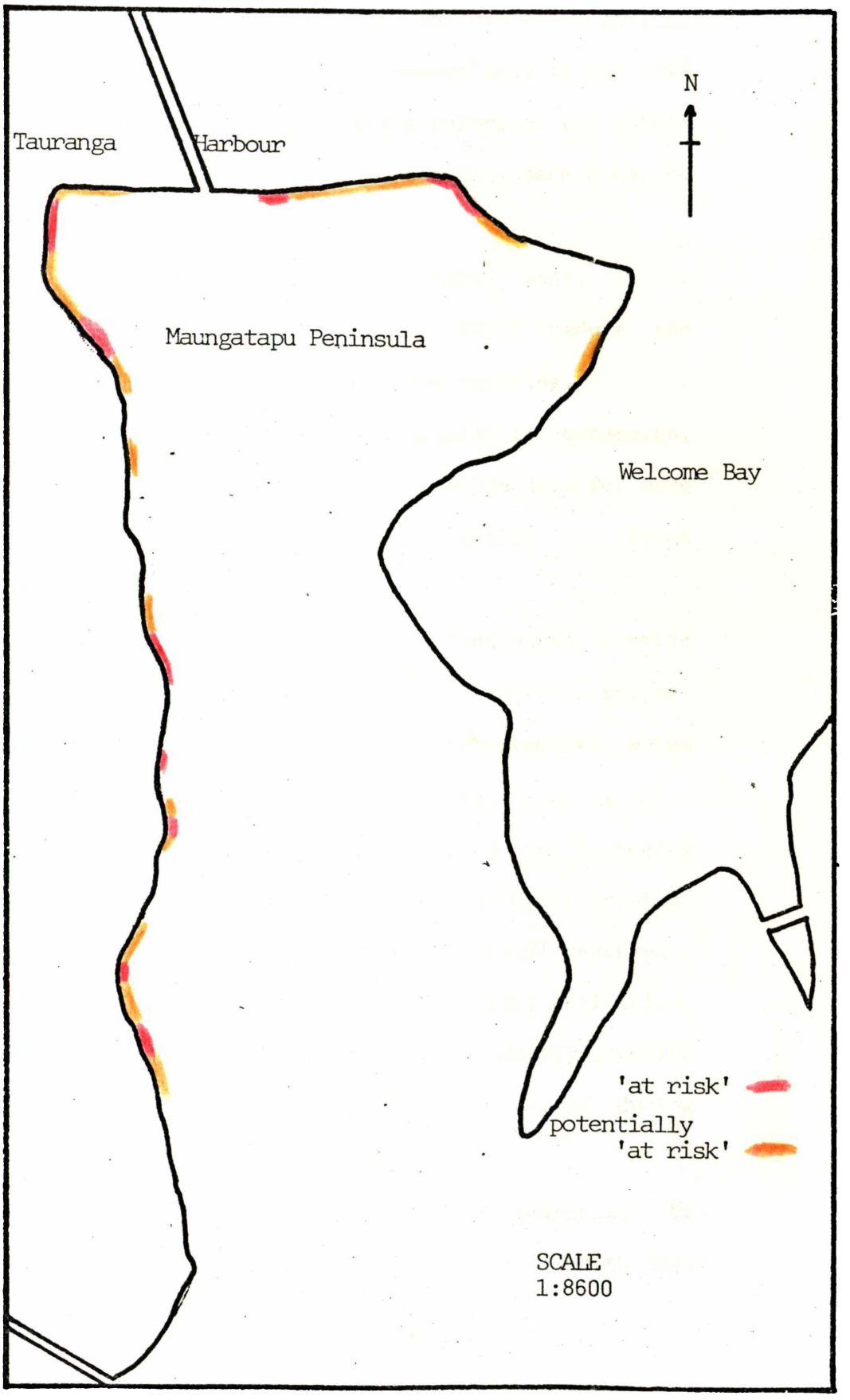

Fig. 6.1. The distribution of 'at risk' and potentially 'at risk' lengths of coastal cliffs on the Maungatapu Peninsula.

'potentially at risk' were mapped, and are shown in fig. 6.1. For sections bordering on the reserve zone in the 'at risk' areas, a geological consultant's report on the site's stability should be required before a building permit may be issued.

Along with the definition of a reserve zone, it is suggested that the following action would reduce the possibility of an unanticipated landslide occuring.

i) Groundwater tables may be monitored in boreholes, preferably near 'at risk' sites, to provide data for more accurate stability analyses, and to give notice of rising groundwater table levels.

ii) Regular inspection of the coastline would provide a check for seepage sources, major basal erosion, and any features such as spalling failures or minor movements which might indicate the onset of further failures.

iii) Surveying of the cliff base at 3 to 5 yearly intervals could be used to monitor rates of basal erosion. This could be of use in defining future 'at risk' reserves.

In addition to these passive, precautionary activities, several steps could be taken towards permanently lowering the water table of the peninsula, particularly during periods of heavy rainfall.

i) Household drainage should, if possible, be connected to a sewage system, rather than eliminated through septic tanks.

ii) Storm water should be reticulated through a drainage system, preferably to near the high water mark, rather than piped directly to several metres below the ground surface. This would both lower the groundwater table, and increase the time for seepage water to reach the cliff face during and after each storm. It would probably also decrease the peak seepage flow, and hence the peak seepage stresses imposed on the permeable materials. In much of Maungatapu this reticulation could be achieved by simply piping household storm water into the road storm water system, providing this doesn't overload the storm drains.

iii) The planting of trees in reserve areas and on private sections would result in an increase in interception and evapotranspiration rates above those given by lawn and flower garden vegetation. While no literature could be found concerning evapotranspiration losses, estimates of interception losses (interception - stemflow) varied from 6 - 10% for 70 - 100 mm storms on scrub vegetation (Drost and Pittams, 1973) to 30% loss for 50 mm storms on hard beech (Aldridge and Jackson, 1973). Provided sufficient trees were planted, an appreciable effect on the groundwater table height should be observed.

SITE PROTECTION

Unfortunately, as much of Maungatapu has already been subdivided, many houses have been erected on sites which may be considered to be 'at risk'. It is quite conceivable that mass movements could affect some of these buildings within their effective lifespan, therefore short term (tens of years) control measures are necessary. Three methods for temporary cliff stabilisation are recommended.

i) A programme of beach nourishment of 'at risk' sites could include the use of stabilising devices such as small groynes. The use of stabilising structures should be approached with extreme caution, however, as these merely transfer erosion along the beach in the direction of sediment drift. As the mechanisms of erosion about the peninsula are not well understood, it would not be wise to risk triggering accelerated erosion in one critical site, in an attempt to protect another site.

ii) Alternatively, it may be cheaper to use gabions to break up waves and/or decrease tidal stream competence. A row of gabions placed 1 to 5 metres out from the cliff edge could provide an effective energy absorbing barrier, without creating the problems of standing wave scour commonly associated with rigid structures such as the seawalls which are presently used. Note the addition of two extra boards to the base of the seawall in fig. 3.13(c). All the older seawalls which don't have boards added in this manner, have had some tens of cm of material eroded from behind them. In

order to further stabilise the material behind the gabions, it is suggested that trial plantings of mangroves or other suitable plants be made in the low energy areas between the gabions and the cliff base.

ii) Drainage of the material above the clay marker beds is recommended for 'at risk' sites, particularly those experiencing appreciable seepage. Drains would probably not need to be large or filtered, hence simple slotted or perforated plastic pipe drains, angled up into the cliff for 10 to 20 metres, depending on flow rates, would probably prove the most useful. Suitable horizontal spacings for the pipe drains would have to be found by trial and error. Two precautions should be taken when using such drains. Firstly, in order to avoid accelerated erosion of the cliff face below the drains, the water drained from the cliff should be piped to near high tide level. In the second place, it should be considered that it is quite possible that the incoherent sandy and silty material which is to be drained, could liquefy and flow out the drains under conditions of heavy seepage flow. Caution should therefore be exercised in the use of pipe drains, with field trials of pipes with very narrow slots or perforations being conducted before use, in order to avoid the possibility of creating artificial tunnel gullies in 'at risk' sites. It is possible that it would be better to turn to the safer, but more expensive approach, of inserting vertical drains to 10

metres depth, at about 10 metres behind the cliff face, and draining these with pumps.

SUGGESTIONS FOR FURTHER RESEARCH

i) Detailed investigations on the mineralogy and chemical and physical properties of the sensitive clays observed in the Pahoia Tuffs could provide useful information in the study of the phenomenon of sensitivity.

ii) Triaxial testing of large core samples of the lensoidal silty sands/sandy muds could provide more conclusive data concerning the suggestion of liquefaction during shear failure.

iii) A comprehensive (possibly thesis-type) study of the erosion and sediment transport systems active about the harbour peninsulas would provide information useful in determining the future evolution of 'at risk' areas, and in evaluating the effects of stabilising structures on cliff evolution.

iv) Groundwater table level monitoring behind an 'at risk' site would provide data for more accurate stability analyses, and would allow more precise groundwater table safety guidelines to be defined.

v) Attempts should be made to improve techniques for the undisturbed sampling of sandy materials, if laboratory analyses are to be assumed representative of the true nature

of the materials concerned.

PAGE

APPENDIX ONE

Data Summary

TRIAXIAL SHEAR TEST RESULTS

Test no.	Sample no.	σ_3 (kPa)	Peak σ_1 (kPa)	P.W.P. (kPa)	Moisture (%)	B.D. g/cm
1	18/4-1a	50	120	2	-	-
2	18/4-1b	50	120	13	-	-
3	18/4-1a	70	143	10	-	-
4	18/4-1b	100	170	24	-	-
5	18/4-1a	100	197	13.5	-	-
6	21/5-1a	60	190	15	-	-
7	21/5-1b	60	275	-5.5	36.3	-
8	21/5-1b	40	152	0	37.4	-
9	21/5-1b	25	117	-10.5	35.2	-
10	21/5-1a	25	109	-2.5	41.4	-
11	21/5-1b	50	190	7.5	38.1	-
12	21/5-1a	80	288	9	28.2	-
13	21/5-2a	60	184	-27.5	41.9	-
14	21/5-2b	60	181	20.5	32.9	-
15	21/5-2a	40	165	-25.5	39.9	-
16	21/5-2b	80	312	-4	32.0	-

Test no.	Sample no.	σ_3 (kPa)	σ_1 Peak (kPa)	P.W.P. (kPa)	Moisture (%)	B.D. g/cm
17	21/5-2a	80	154	-4	49.0	-
18	21/5-2b	40	75	18	33.6	-
20	21/5-2a	40	245	-28	35.0	-
21	21/5-2b	60	134	0	31.9	-
22	21/5-2a	40	197	0	33.2	-
24	21/5-2a	120	480	-16	32.9	-
25	16/7-4a	40	274	-26	-	-
26	16/7-4b	60	273	-15	33.9	-
27	16/7-4b	80	282	7.5	35.5	-
28	16/7-4b	100	484	-12	35.4	-
29	16/7-1a	100	427	-10	32.9	1.198
30	16/7-1b	80	419	-20	37.2	1.200
31	16/7-1a	60	390	-31.5	33.7	1.266
32	6/8-5a	60	234	5	54.7	0.907
33	6/8-5b	40	142	7	60.0	0.868
34	6/8-5a	80	283	4.5	49.3	0.947
35	6/8-5b	40	184	-1	56.6	0.937
36	6/8-5a	100	346	-0.5	50.0	0.901
37	6/8-5b	40	92	21.5	-	-
38	6/8-5a	60	188	-18	-	-
39	6/8-5b	60	188	-17.5	-	-
41	10/9-1a	40	273	-21.5	33.6	1.354
42	10/9-1b	40	286	-16	37.3	1.233
43	10/9-1a	80	402	-16	34.4	1.346
44	10/9-1b	80	467	-20	33.6	1.271
45	10/9-1a	60	333	-11.5	33.8	1.323

Test no.	Sample no.	σ_3 (kPa)	σ_1 Peak (kPa)	P.W.P. (kPa)	Moisture (%)	B.D. g/cm
46	10/9-1b	60	361	-21	35.3	1.272
47	10/9-2a	60	341	-5.5	39.4	1.175
48	10/9-2b	60	301	-4.5	46.3	1.061
49	10/9-2a	40	282	-17	40.9	1.156
50	10/9-2b	40	214	-8	52.2	0.980
51	10/9-1a	80	397	-15	34.0	1.311
52	10/9-1b	100	485	0.5	35.8	1.231
53	10/9-2a	80	424	-7	39.8	1.147
54	10/9-2b	80	350	3	46.0	1.020
55	10/9-2a	100	494	4	38.3	1.160
56	10/9-2b	100	374	23	49.8	0.955
57	8/10-1a	80	241	29	54.1	0.877
58	8/10-1b	80	217	25.5	58.3	0.844
59	8/10-1a	40	130	12.5	-	-
60	8/10-1a	60	187	18	56.5	0.901
61	8/10-1b	60	151	22	60.0	0.842
62	8/10-1a	40	114	15	61.0	0.863
63	8/10-1b	40	136	2	-	-

DIRECT SHEAR BOX RESULTS

Test No.	Sample No.	Normal Load (kPa)	Shear Strength (kPa)	Moisture %
1	10/3-7a	14.90	13.7	-
2	10/3-7b	14.90	18.5	82.1
3	10/3-7c	18.36	14.9	73.6
4	10/3-7d	18.36	18.9	74.2
5	10/3-5a	21.83	24.4	70.2
6	10/3-5b	21.83	25.0	80.1
7	10/3-5c	25.29	24.9	68.5
8	10/3-5d	32.22	30.0	-
9	10/3-4a	32.22	34.2	81.1
10	10/3-4b	47.72	44.5	78.2

Test no.	Sample no.	Normal load (kPa)	Shear Strength (kPa)	Moisture (%)
11	10/3-6a	21.83	20.3	66.7
12	10/3-6a	25.29	22.8	69.0
13	10/3-6a	32.22	26.1	60.5
14	3/5-1a	14.90	16.0	-
15	3/5-1b	21.83	20.2	-
16	3/5-1c	28.76	23.6	-
17	3/5-1d	14.90	13.0	-
18	3/5-2a	14.90	16.1	-
19	3/5-2b	21.83	18.5	-
20	3/5-2c	28.76	25,9	-
21	3/5-2d	21.83	22.0	-
22	3/5-2e	18.36	13.0	-
23	3/5-3a	14.90	12.4	-
24	3/5-3b	21.83	18.0	-
25	3/5-3c	28.76	20.7	-
26	8/10-4a	14.90	9.3	-
27	8/10-4b	14.90	15.3	-
28	8/10-4c	21.83	11.9	-
29	8/10-4d	28.76	11.3	-
30	8/10-4e	35.68	17.4	-
31	8/10-4f	47.72	23.9	-

ATTERBERG LIMITS AND PARTICLE SIZE ANALYSES

(All results except activities are percentages by weight)

Sample	L.L.	P.L.	P.I.	Activity	Moisture	S	Z	Cy
10/7-7a	44	23	21	0.88	58.7	70	6	24
10/7-6a	56.5	29	27.5	1.0	61.4	64	9	27
16/7-7	40	21	19	0.51	59.8	34	35	31
16/7-8	36	31	5	0.20	39.4	36	44	20
3/5-6	63	31	32	0.86	61.0	18	45	37
3/5-5	28.2	27.1	1.1	0.02	42.8	22	17	61

SENSITIVITY AND RAPIDITY RESULTS

(Peak strengths in kPa, obtained with Geonor shear vane)

Sample	Peak Strength	Sensitivity Vane	Sensitivity Penetrom.	Moisture (%)	Rapidity No.
23/7-1	--	-	9	66.4	3.5
23/7-8	40 + 5	35-100	5	39.4	9
23/7-10	48 + 5	25	>4	61.4	10
23/7-11	46 + 5	80	>10	50.3	9
23/7-3	42 + 5	100	>10	52.9	4
23/7-4	87 + 10	90-100	>4	37.5	5
23/7-5	111 + 22	25-32	>10	70.3	3

BULK DENSITY PROFILE

Sample	Depth (m.b.d.)	Bulk Density Oven	Field	P.D.	Moisture (%)
paleosol	1.0	0.73	0.94	2.643	31
Mangaone lapilli	1.3	0.64	0.92	-	44
paleosol	1.7	0.78	1.18	-	51
Rotoehu p/sol.	2.1	0.71	1.09	-	53
Rotoehu - sand	3.0	1.16	1.30	-	12
Red p/sol in tuff	4.3	1.15	1.48	-	29
Red p/sol in tuff	4.5	1.14	1.68	2.596	47
Red p/sol in tuff	5.2	1.04	1.46	-	40
Orange mtld. tuff	6.0	1.06	1.57	2.555	48
" " "	6.8	0.93	1.43	2.544	47
Brown mtld. sand	7.8	0.75	1.21	2.570	51
" " "	8.8	0.90	1.46	2.576	60
White silty sand	9.7	0.98	1.51	2.589	52
" " "	9.9	0.96	1.59	-	60
White sandy mud	9.9	1.02	1.63	-	65

APPENDIX TWO

Callibration of Geonor Vane Shear Apparatus

When first used in the field, the Geonor vane shear apparatus yielded results which varied widely within apparently uniform materials. It was therefore decided to callibrate the Geonor in the laboratory, before utilising it in the field strength testing programme. Weights were suspended from the end of an 11.1 cm arm, and shear strength readings were taken. The torques applied were converted to 'shear strength' readings using equation 1;

$$S = \frac{2T}{\pi D^3 (\frac{H}{D} \times \frac{a}{2})} \qquad \text{(Eqn. 1)}$$

where S = shear strength (Pa)

T = torque (Nm)

H = vane height (m)

D = vane width (m)

a = a factor dependent on the shear distribution assumed at the top and bottom of the failure cylinder.

If we assume that the distribution of shear across the top of the cylinder is uniform (a standard assumption), then a = 2/3. Substituting in known values for D and H (H = 2D), eqn. 1 becomes;

$$S = \frac{6T}{7\pi D^3}$$

W eight (kg)	Torque (Nm)	'Shear Strength' (kPa)	Vane reading	Error %
1	1.09	37.1	35.3	4.85
2	2.18	74.3	70.6	4.98
3	3.26	111.3	105.8	4.95

A consistent, and almost negligible, error of approximately -5% was observed.

APPENDIX THREE

Computer Programs Utilised : Description

1) TRIAX.BAS

A BASIC PLUS program which calculates percent strain and deviator stress values (corrected for membrane and side drain strength additions) from gauge readings. This program is held on tape at the University of Waikato, and interactive use is outlined in Geomechanics Manual 5 (Law, 1980; unpublished).

Authors: Chandler and Rogers, 1978.

2) The Biomedical Statistical Package (BMD)

The BMD programs provide a variety of types of statistical analysis. The packages utilised in this study were P1R and P5R; multiple rectilinear and curvilinear regression analyses by the least squares method. Control programs may be written to utilise these programs in comparing two linear data groups. The following program, DIF.CTL, utilises the linear regression analysis program P1R.CTL to test for significant differences between two data groups.

```
/probl  title is 'linear regression program to test
        differences between triaxial data groups'.
/input  variable=2.
        format = '(f7.2,1x,f7.2)'.
        file is 'dif.dat'
/variablnames are nstres,sstres,add1.
        add=1.
        group=3.
/trans  add1=kase.
/group  cutp(3)=18.
        names are hibd,lobd.
/regres depend = sstres.
        indep = nstres.
/print  data.
        corr.
/plot   variabl = nstres.
/end
```

Authors: Dixon et al., 1979.

3) STAB.FOR

This FORTRAN language program calculates factors of safety by Bishop's Simplified method, on circular surfaces. The program, adapted for the PDP 11/70 from an original Burroughs 6700 program by T.J. Keyes of Auckland University, is fully described in Geomechanics Manual 5 (loc. cit.). The upper slope-failure surface contact point

was specified, and the option of using a grid pattern of test circle centres was chosen. The data file used (STAB.DAT) is presented in Appendix 3(b).

4) Simplified Janbu analysis progams

Manual calculations and operations

The main advantage of the Janbu stability analysis lies in the fact that no simplifying assumptions regarding the shape of the slip surface are made at any stage of the derivation of the factor of safety equation. In order to preserve this advantageous feature, it was decided to retain the division of the mass into slices as a manual operation, thus ensuring minimum simplification of the observed failure mass geometry. Initial manual calcualtions have the further advantage of allowing visual estimation of a 'line of thrust' for Janbu Rigourous analysis. The computer model was therefore designed to simply calculate the factor of safety from a datafile input of failure surface morphology, soil parameters, and slice size parameters.

Profile definition

The morphology of the displaced mass may be found by field surveys. If tension cracks are postulated, their size may be estimated using shrinkage limits, or by calculations

based on the soil strength parameters;

$$h_c = \frac{2c}{\gamma} \quad \text{(cohesive soils)}$$

$$h_c = \frac{2c}{\gamma} \times \tan(45^0 + \frac{\phi}{2}) \quad \text{(frictional soils)}$$

(Chowdhury, 1978)

Soil strength and bulk density parameters may be obtained by field or laboratory analysis. On the basis of this data, the displaced mass may be divided into slices which have a single set of soil strength parameters applicable along the uniformly angled slice base. For each slice the following parameters may then be defined;

i) basal angle in degrees (ALPHA or α_T),

ii) slice width in metres (DELT.X or dx),

iii) water table height above failure surface in metres (N_3 or z),

iv) soil cohesion at slice base in kPa (N_1 or c),

v) soil internal friction angle at slice base in degrees (N_2 or ϕ),

vi) area of soil a, b etc. (H(a) or a_a),

or average height of soil a, b etc. (H(a) or h_a).

The use of soil height or area must be consistent within each profile. Soil height is easier to determine, but is only used if the slices are extremely regular in shape, as area determination will otherwise prove more accurate. A unit weight (γ) value, in kN/m^3 may also be defined for each soil. A correction to allow for interslice forces is made in the Simplified Janbu analysis. The correction factor (f_0)

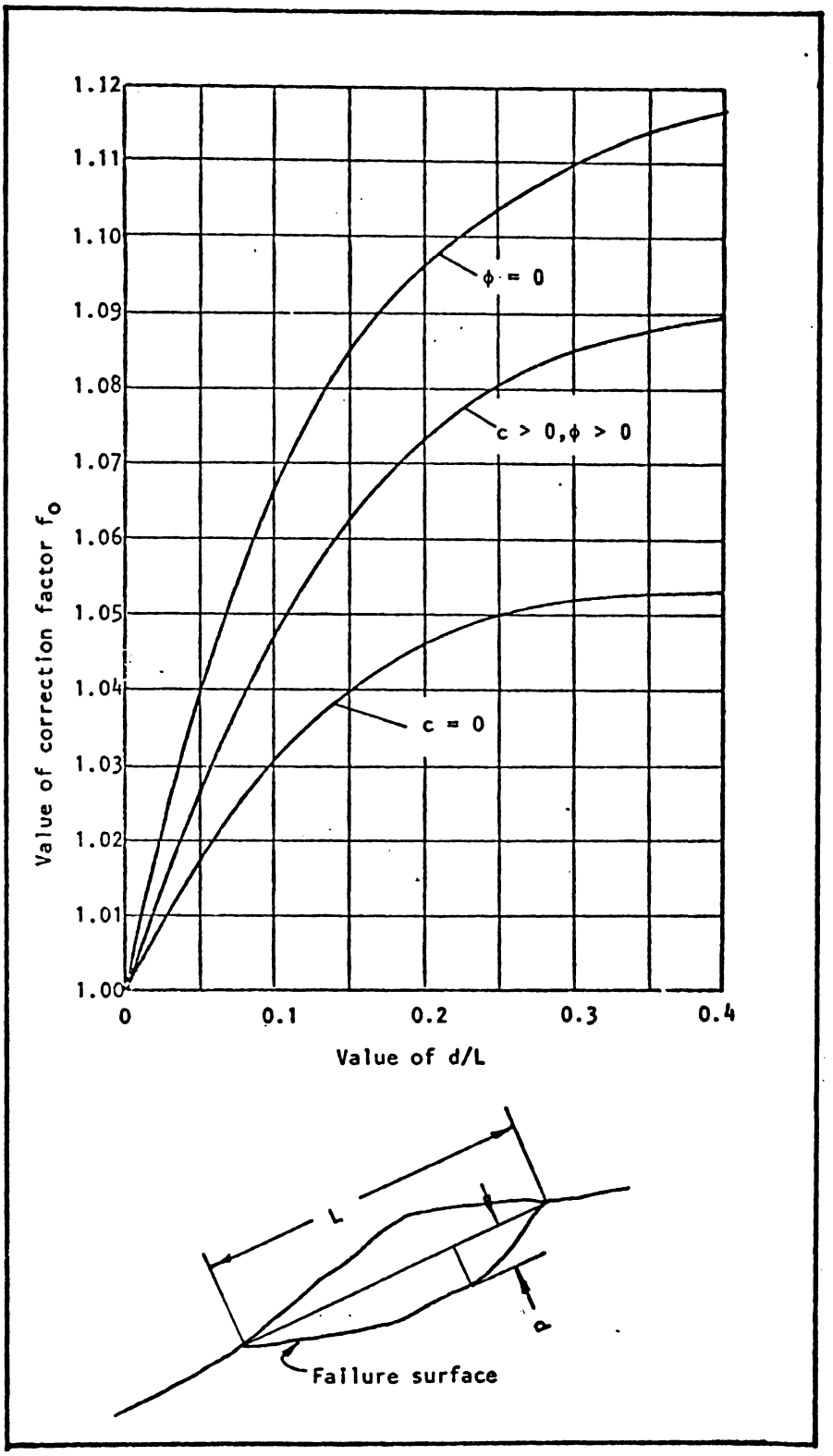

Figure A3.1. Determination of correction factor (f_o). (after Hoek and Bray, 1977)

is determined according to a shape ratio describing the displaced mass, and the average values of cohesion and internal friction for the failure surface (fig. A3.1). Finally, if a head tension crack is assumed and the water table is thought to rise above the base of the tension crack, the water pressure (q) on the edge of the uppermost slice may be calculated (fig. A3.2).

Some of the data may then be entered into data files and accessed automatically for each program run, or be entered manually, using the interactive data loading option. Slice width (dx), basal slope angle (α), and soil heights or areas for each slice are loaded into one file; dx in metres, in degrees, and areas (heights) in square metres (metres). The only formatting requirement is that there be a comma after each data point (see Appendix 3(b)).

Program Operation

An early version of the Simplified Janbu analysis program calculated individual factors of safety. This was incorporated into a more versatile iterative BASIC PLUS program, JSITER.BAS, which is capable of calculating factors of safety for fixed data sets, and for data sets where values of bulk density, cohesion, internal friction angle, or water table height may be varied.

An output file must be named so that output data may be recorded, and the parameter of interest (the parameter to be

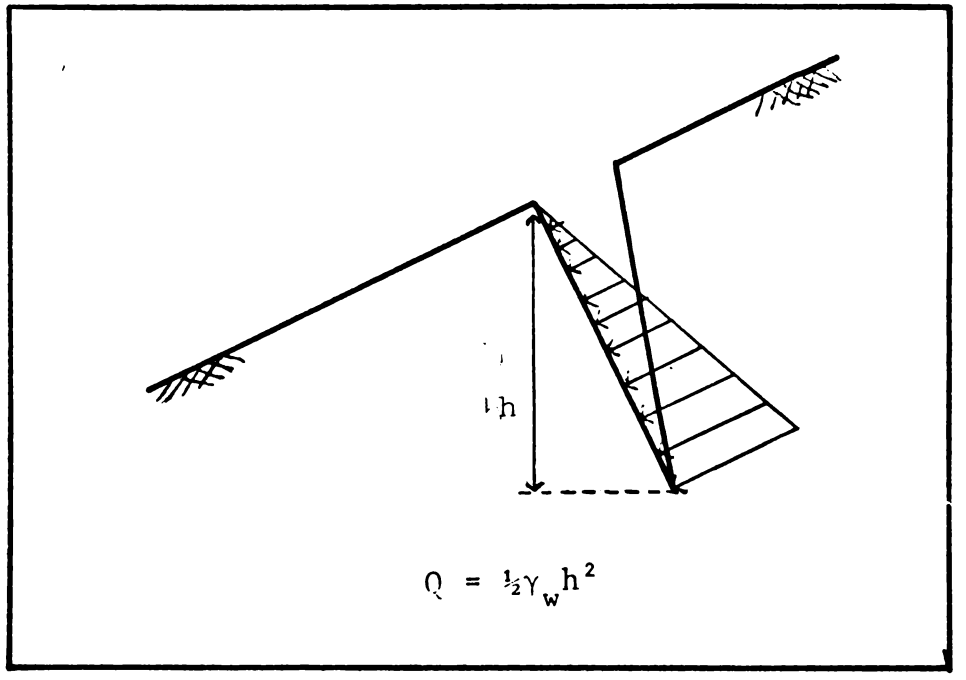

Figure A3.2. Calculation of water pressure in a tension crack.

iterated) may be named in this file. Data is then entered manually, or from a data file, if required. The significance range, or degree of accuracy to which F is to be calculated, may then be stipulated; the default value is 0.03. The parameter of interest is then selected. If cohesion or internal friction angle are nominated, the slices within which these values are to be iterated, the maximum and minimum values, and the increment size, may then be entered. If water table height is nominated, the increment size is entered, and this is subtracted from the watertable heights previously entered for each iteration. If bulk density is to be varied, the soil within which it is to be iterated, its maximum and minimum values, and increment size, are entered.

The program then sums the weights for each slice, which is assumed to be one metre thick, hence:

$$\text{slice weight } W \text{ (kN)} = \Sigma \left[\text{soil area } (m^3) \times \text{unit weight } (kN/m^3)\right]$$

Each factor of safety is then calculated according to the equation;

$$F = f_0 \frac{\Sigma \left[dx \times \frac{c' + (\frac{W}{dx} - u) \tan\phi}{1 + \tan\alpha \times \tan\frac{\phi}{F}} \right]}{\Sigma \left[W \tan \alpha\right]}$$

As F appears on both sides of the equation, an initial F value of 1 is assumed, a second is calculated and, unless the difference between the two F values is less than the stipulated significance range (commonly 0.03), the new F value is substituted in the right hand side of the equation,

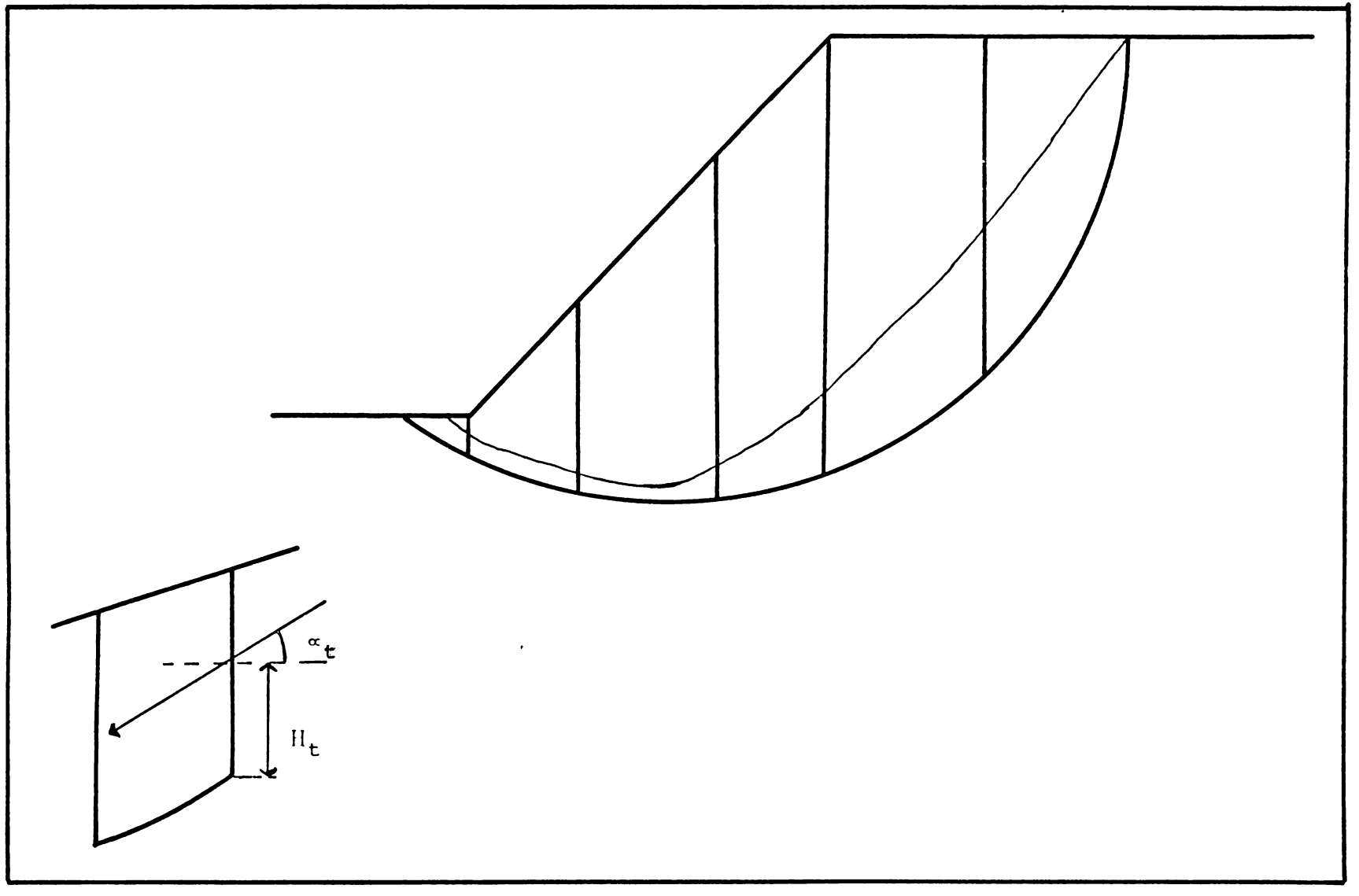

Figure A3.3. Definition of the line of thrust.

failure surface (metres), α_T (degrees), and H_T (metres) parameters, in that order.

Program Operations

The program is non-iterative, owing to limitations on the length of single BASIC PLUS programs, calculating single factors of safety for fixed data sets to within a stipulated signficance range. The use of average slice height or slice area data is optional and, together with α_T and dx, these data may be entered manually or automatically from a datafile. Slice strength data may also be entered manually, or from a datafile. The two input files are checked against each other for size compatability (same number of slices and soils) before calculation of the factor of safety commences.

The factor of safety equation utilised in the rigourous Janbu method is as follows:

$$F = \frac{\Sigma\, dx \left[c + \left(\frac{w + dT}{dx} - u\right) \times \tan\phi \right] \times \sec^2\alpha}{\Sigma \left[(w + dT)\tan\alpha\right] \left[1 + \frac{\tan\alpha + \tan\phi}{F}\right]}$$

where dT is the difference between the shear interslice forces on two successive slices. For any slice, T may be calculated:

$$T = -E \times \tan\alpha_T + h_T \frac{dE}{dx}$$

where E is the normal side-wall force on a slice. The difference (dE) in normal interslice forces between two successive slices is calculated:

$$dE = (w + dT) \times \tan\alpha - \frac{dx\ c + \left(\frac{w + dt}{b}\right) - u) \tan\phi}{F \times \left(1 + \frac{\tan\alpha \times \tan\phi}{F}\right)}$$

and a further F value is calculated. When a final F value is reached, it is printed to the output file, the parameter of interest has one increment added or subtracted, and the process is repeated. The program ends with a series of options; to end the program run, to rerun with different soil strength and/or profile parameters, and to retain or wipe the output file.

5) Rigourous Janbu analysis programs

Manual calculations and operations

Data for the calculation of factors of safety by the rigourous Janbu method are obtained in the same manner as for the simplified Janbu method. In addition to these data, the rigourous analysis requires the postulation of a line of thrust; a continuous line showing the direction of interslice forces at each interslice boundary. This hypothetical line may be sketched in on the scale diagram used for slice definition and slice area calculations. The line of thrust is then defined by two parameters; ALPHAT α_T & HT (H_T) (fig A3.3).

A datafile for slice size data may be prepared exactly as for the simplified analysis. A second datafile, with the same formatting requirements, may be prepared, holding the cohesion (kPa), ϕ (degrees), water table height above

As the values of F and slice E and T forces are interrelated, their initial values must be assumed, and their true values arrived at by a series of approximations. F is initially assigned the value 1, all dT values are set at zero, and the uppermost slice side is assumed to be subject to a normal force (E) of zero, unless a water-filled tension crack is assumed, in which case E = Q. The magnitude relationship of the interslice forces was assumed when the line of thrust was postulated (fig. A3.4). A value of F is calculated to within the defined significance range (eqn. 2), then a value of dE is calculated for the uppermost slice, using eqn. 4. The E value for slice 2 is equal to this value of dE plus the normal force on the upper side of the uppermost slice (Q or zero) (fig. A3.5). For the first slice, T is assumed to be zero, otherwise T is calculated for the slice using the postulated value of α_T, and the calculated value of E. dT is then calculated by subtracting the value of T calculated for the previous slice. The value of dT for the final slice is assumed to be zero minus the value of T calculated for that slice (A3.5). New approximations of H_T and α_T are then calculated for each slice, producing a reapproximation of the line of thrust. The new values of dT are then used to reapproximate F, and the entire process is repeated until the difference in the values of F produced by two successive cycles is less than the stipulated significance range.

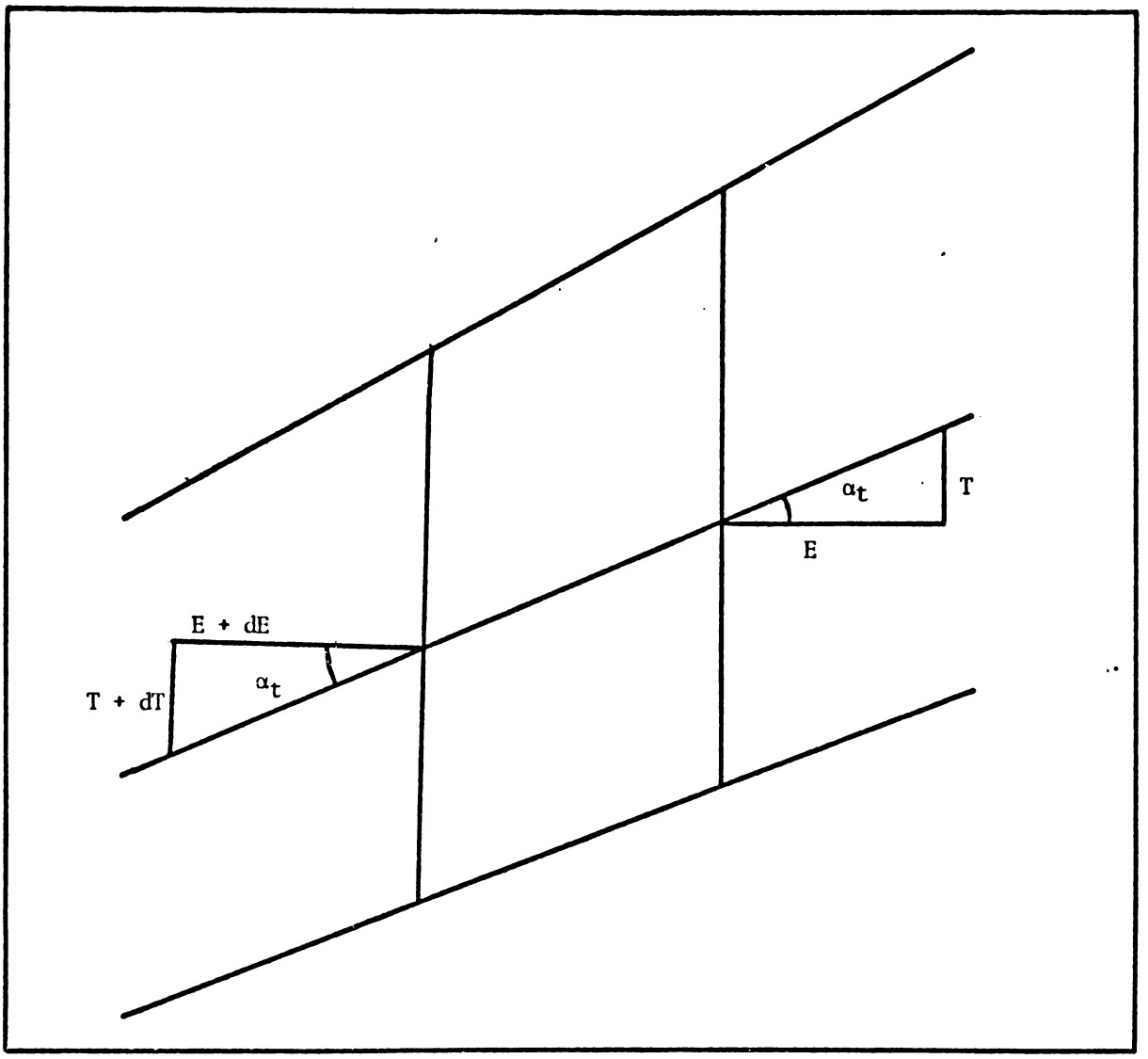

Figure A3.4. Magnitude relationships of interslice forces assumed when α_t values are assumed.

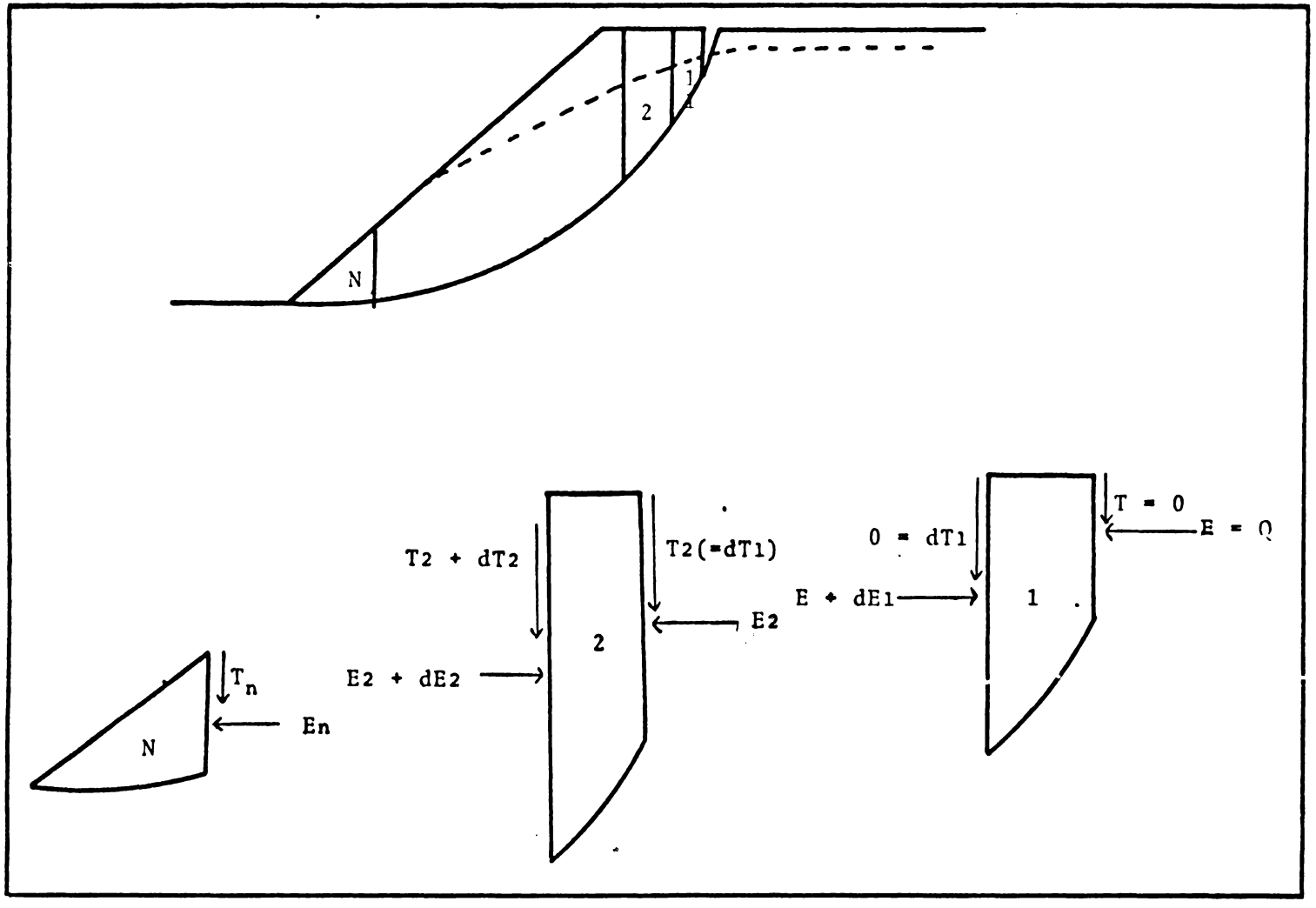

Figure A3.5. Calculation of normal and shear side forces.

The program may then be terminated, or rerun with new strength data, or with all the data changed, and either retaining or overwriting the first output file. The output file contains the final factor of safety, the strength data, the final line-of-thrust parameters, and the name of the slice size file.

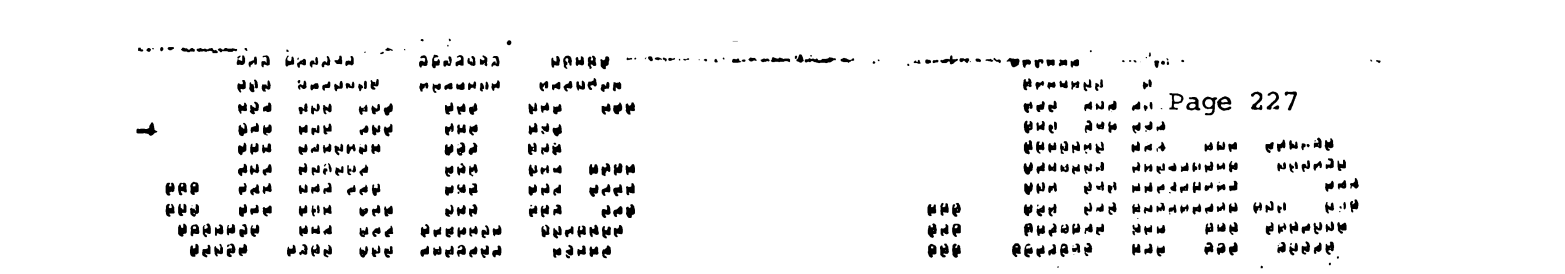

[[[<WAIKATO>#<WAIKATO>#<WAIKATO>#<WAIKATO>#<WAIKATO>#<WAIKATO>#<WAIKATO>#<WAIKATO>#<WAIKATO>#<WAIKATO>#<WAIKA
[[[<WAIKATO>#<WAIKATO>#<WAIKATO>#<WAIKATO>#<WAIKATO>#<WAIKATO>#<WAIKATO>#<WAIKATO>#<WAIKATO>#<WAIKATO>#<WAIKA

JOB = A Printed on 03-Apr-81 at 14:48 for User [45,9]
Copy 1 of 1 /Delete: YES File = SY :[45,9]JRIG .BAS
Record type: STREAM Format type: EMBEDDED

[[[<WAIKATO>#<WAIKATO>#<WAIKATO>#<WAIKATO>#<WAIKATO>#<WAIKATO>#<WAIKATO>#<WAIKATO>#<WAIKATO>#<WAIKATO>#<WAIKA
[[[<WAIKATO>#<WAIKATO>#<WAIKATO>#<WAIKATO>#<WAIKATO>#<WAIKATO>#<WAIKATO>#<WAIKATO>#<WAIKATO>#<WAIKATO>#<WAIKA

```
10      EXTEND \
        ON ERROR GOTO 19000

20      DIM ALPHA(50),DELT.X(50),Z(50),H(50,15),COHES(50) \
        DIM PHI(50),GAMMA(15),ALPHAT(50),HT(50),DT(50),TERSET%(30%)

50      ES=CHR$(155%)

1130    TERSET$ = SYS(CHR$(6%) + CHR$(16%) + CHR$(0%) + CHR$(255%)) \
        CHANGE TERSET$ TO TERSET%
1140    IF TERSET%(9%) = 255% AND (TERSET%(5%) = 81% OR TERSET%(5%) = 133%) THEN
              PRINT ES + '<';ES + '[?21';
5000    PRINT ES + 'H';ES + 'J';ES + '[' \
        INPUT 'output filename';OFILE$ \
        OPEN OFILE$ FOR INPUT AS FILE 1% \
        CLOSE 1% \
        PRINT 'THE FILE ALREADY EXISTS DO YOU WISH TO OVERWRITE <NO>'; \
        INPUT A$ \
        IF LEFT(CVT$$(A$,36%),1%)<>'Y' GOTO 5000
5020    OPEN OFILE$ FOR OUTPUT AS FILE 1% \
        PRINT FNPOS$(1,0);ES + 'J';'output to ';OFILE$
5060    PRINT FNPOS$(1,40);ES+'J';FNPOS$(4,0)
5080    PRINT \
        INPUT 'DO YOU WISH TO USE "H" OR "AREA" __ ';A$ \
        IF LEFT(CVT$$(A$,36%),1%)='H' OR LEFT(CVT$$(A$,36%),1%)='A' THEN
              OP$ = LEFT(CVT$$(A$,36%),1%)
        ELSE
              GOTO 5080
5082    PRINT FNPOS$(6,0);ES + 'J';FNPOS$(1,40);'= USING '; \
        PRINT FNOP$;
5083    PRINT FNPOS$(6,0);

5085    PRINT \
        PRINT 'DO YOU WISH TO LOAD ALPHA,DELTA.X, AND '; \
        PRINT FNOP$;
5086    PRINT ' FROM A DISK FILE <YES>'; \
        INPUT A$ \
        IF LEFT(CVT$$(A$,36%),1%)='N' GOTO 5100

5087    PRINT \
        INPUT 'DATA FILENAME';IFILE$ \
        OPEN IFILE$ FOR INPUT AS FILE 2%
5088    FOR X% = 1% TO 1000% \
              I% = X% \
              INPUT LINE #2%,A$\
              A$ = CVT$$(A$,6%)\
              A% = 0
5089          FOR J% = 1 UNTIL INSTR(A%,A$,',')=0
5090                IF J% = 1 THEN DELT.X(I%) = VAL ( LEFT ( A$ , INSTR ( 1, A$, ',')-1))\GOTO 5092
5091                IF J% = 2 THEN ALPHA(I%) = FND.R(VAL (MID(A$,A%,(INSTR(A%,A$,',')-A%)))
                                 ELSE H(I%,J%-2) = VAL(MID(A$,A%,(INSTR(A%,A$,','))-A%))
5092                A% = INSTR(A%,A$,',') + 1
5093          NEXT J%
              H(I%,J%-2)=VAL(RIGHT(A$,A%))
5094          IF I% = 1 THEN NS% = J%-2
                        PRINT'THE NUMBER OF SOILS FOUND WAS';NS%
5095    NEXT X%
5097    CLOSE 2% \
        NO.SLICES%=(I%-1)\
        PRINT 'THE NUMBER OF SOILS FOUND WAS';NO.SLICES%\
        SLEEP 2
5098    PRINT FNPOS$(6,0);ES + 'J';FNPOS$(2,40);'data from ';IFILE$;FNPOS$(6,0);
        PRINT #1%,'THE SLICE SIZE DATA FILE IS  ';IFILE$
5099    GOTO 6000

5100    INPUT 'NUMBER OF SOILS PLEASE';NS%
5101    FOR I% = 1% UNTIL LEFT(CVT$$(A$,36%),1%)='Y' \
              FLAG1% = 1 \ SAV% = I%\
              PRINT FNPOS$(6,0);ES + 'J'; \
              PRINT \
              PRINT 'SECTION';I% \
              INPUT 'ALPHA ___ ';ALPHA(I%) \
              ALPHA(I%) = FND.R(ALPHA(I%))\
              INPUT 'DELTA X _ ';DELT.X(I%)
5110          FOR J%= 1% TO NS% \
                    IF OP$='H' THEN
                          PRINT 'H';J%;'____ ';
                    ELSE
                          PRINT 'AREA';J%;'____ '; \
                          INPUT H(I%,J%) \
                    NEXT J%
5130          INPUT 'FINISH<no> ___ ';A$ \
              PRINT
5140    NEXT I%
        NO.SLICES%=I%-1% \ PRINT 'NUMBER OF SLICES IS';NO.SLICES%\SLEEP 2\
```

```
005     PRINT FNPOSS(6,0);ES + 'J'; \
        PRINT\
        INPUT 'SIGNIFICANCE RANGE <0.03> ___';RANGE \
        IF RANGE=0 THEN
                RANGE=0.03
006     INPUT 'Q ___ ';Q
007     IF Q = 0 THEN
                Q = 1
008     FOR I% = 1% TO NS% \
                PRINT 'GAMMA';I%;'___ '; \
                INPUT GAMMA(I%)
009     NEXT I%

40      PRINT
        INPUT 'DO YOU WISH TO LOAD COHESION, PHI, Z, INITIAL ALPHAT AND INITIAL HT FROM A DISK FILE <YES>';AS \
        IF LEFT(CVTSS(AS,36%),1%)='N' GOTO 6115
50      PRINT \
        INPUT 'DATA FILENAME';IFILES \
        OPEN IFILES FOR INPUT AS FILE 3%
55      FOR X% = 1% TO NO.SLICES% \
                I% = X% \
                INPUT LINE #3%,AS\
                AS = CVISS(AS,64)\
                A% = 0
60              FOR J% = 1 TO 5
65                      IF J% = 1 THEN COHES(I%) = VAL ( LEFT ( AS , INSTR ( 1, AS, ',')-1))
                                GOTO 6085
70                      IF J% = 2 THEN PHI(I%) = FND.R(VAL (MID(AS,A%,(INSTR(A%,AS,',',))-A%)))
                                GOTO 6085
75                      IF J% = 3 THEN Z(I%) = VAL (MID(AS,A%,(INSTR(A%,AS,',',))-A%))
                                GOTO 6085
80                      IF J% = 4 THEN ALPHAT(I%) = FND.R(VAL (MID(AS,A%,(INSTR(A%,AS,',',))-A%)))
82                      IF J% = 5 THEN HT(I%) = VAL (MID(AS,A%,(INSTR(A%,AS,',',))-A%))
85                      A% = INSTR(A%,AS,',') + 1
93              NEXT J%
94      NEXT X%
95      CLOSE 3%
96      IF (X% - NO.SLICES%) = 0 GOTO 6098
97      PRINT 'IDIOT!!!!! CHECK YOUR INPUT FILES.'\
        PRINT 'ARE YOU USING THE CORRECT NAMES?'\
        PRINT 'IF NOT YOUR 2 INPUT FILES ARE INCOMPATABLE.';CHR$(7)
                SLEEP 3
                GOTO 5085
3       PRINT 'DATA FILES COMPATABLE'
        SLEEP 2
)       PRINT FNPOSS(6,0);ES + 'LJ';FNPOSS(2,40);'data from ';IFILES;FNPOSS(6,0);
)       GOTO 6150


)       FOR X% = 1% TO NO.SLICES%
)               FLAG1% = 2 \ SAV% = X%\
                PRINT FNPOSS(8,0);ES + 'J'; \
                PRINT 'SECTION'; X%
)               INPUT 'COHESION ___ ';COHES(X%) \
                INPUT 'PHI ___ ';PHI(X%) \
                INPUT 'Z _______ ';Z(X%) \
                INPUT 'INITIAL ALPHAT';ALPHAT(X%) \
                INPUT 'INITIAL HT_____';HT(X%)
        PHI(X%) = FND.R(PHI(X%))
        ALPHAT(X%) = FND.R(ALPHAT(X%))
        NEXT X%
        PRINT FNPOSS(8,0);ES + 'J';'Please wait while I think'

0       GOSUB 14000
4       NO.TIMES = NO.TIMES - 1
5       PRINT \
        PRINT STRINGS(2%,7%);'THE FACTOR OF SAFETY IS';F;'AND WE ITERATED "F"';TOT.TIMES%;'TIMES'
)       GOSUB 12000
5       PRINT \
        PRINT
7       INPUT 'DO YOU WISH TO END THIS SESSION <YES>';a$
        IF CVISS(AS,36%) <>'N' GOTO 32700
)       INPUT 'DO YOU WISH TO CHANGE THE STRENGTH VALUES ONLY<no>';A$
)       IF LEFT(CVTSS(AS,36%),1%)='Y' GOTO 6000
)       PRINT \
        INPUT 'DO YOU WISH TO CHANGE THE SLICE SIZE DATA WITH PRESENT OUTPUT FILE BEING OVERWRITTEN<NO>';A$
)       IF LEFT(CVTSS(AS,36%),1%)='Y' GOTO 5080
)       PRINT \
        INPUT 'DO YOU WANT A NEW DATA FILE AND ALL NEW DATA?<NO>';A$
)       IF LEFT(CVTSS(AS,36%),1%)='Y' THEN GOTO 5000
)       GOTO 32700


)       ! print to output file section
)       ALPHA(I%) = FNR.D(ALPHA(I%))
.       PHI(I%) = FNR.D(PHI(I%))
        ALPHAT(I%) = FNR.D(ALPHAT(I%))
)       PRINT #1%,'CHRS(12%0;STRINGS(3,10)
        PRINT #1%,,TIES;STRINGS(2,10)
        HS = CVTSS(FNOPS,32%)
        PRINT #1%,'SLICE        HT        ALPHAT        COHESION      PHI          Z '
)       FOR I% = 1 TO NO.SLICES%
                PRINT #1%, USING ' ##         ###.###      ###.##      ',I%,HT(I%),ALPHAT(I%);
                PRINT #1%, USING ' #,###.#     ##          ##.#',COHES(I%),PHI(I%),Z(I%)
)       NEXT I%

)       FOR I% = 1 TO NO.SLICES%
                PRINT #1%,'GAMMA';I%;' = 'GAMMA(I%)'
        NEXT I%


)       PRINT #1%,STRINGS(2,10)
        PRINT #1%,'THE FACTOR OF SAFETY is';
        PRINT #1%, USING'###.######';F
)       PRINT #1%,STRINGS(3,10)
                'THE SLICE SIZE DATA FILE is  ';IFILES
```

```
1090    PRINT #1%,SIMILAR(2,10)"OF SAFETY IS";
        PRINT #1%,"THE FACTOR ";######";F
        PRINT #1%, USING"####.#####";F
1100    PRINT #1%,SIMILAR(1,10)
        PRINT #1%,"THE SLICE SIZE DATA FILE IS  ";IFILE$
1120    RETURN

3000    GOTO 32700

        !

3000    ! CALCULATE the f calculation loop

3100    F=1 \
        LAST.F=0 \
        SUM1=0 \
        SUM2=0 \
        STEP.F=0 \
        MAT DT = ZER\
        N = 0\
        TOT.TIMES% = 0
3102    VALUES = 'FALSE'
3150    FOR LOOP% = 1 UNTIL VALUES = 'TRUE'
3160    PRINT 'LAST.F                F  '
3200            FOR NO.TIMES%= 1 UNTIL ABS(LAST.F-F)<RANGE
3220                    IF NO.TIMES% <> 1 THEN
                                LAST.F = F
3300                    FOR SLICE% = 1% TO NO.SLICES%
3310                    J40=0 \
                        J42=0
3350                            IF OPS='A' THEN
                                        J40=J40 + (H(SLICE%,I%)*GAMMA(I%)) FOR I%= 1% TO NS% \
                                        J41= (J40 + DT(SLICE%))/DELT.X(SLICE%)
3400                            IF OPS='H' THEN
                                        J42=J42 + (H(SLICE%,I%) * GAMMA(I%)) FOR I% = 1% TO NS% \
                                        J41 = J42 + (DT(SLICE%)/DELT.X(SLICE%))
3420                            J43= J41 * DELT.X(SLICE%)
3440                            TAN.ALPHA = TAN(ALPHA(SLICE%))
3460                            U = Z(SLICE%) * 9.81
3480                            J44 = J41 - U
3500                            TAN.PHI = TAN(PHI(SLICE%))
3520                            J45 = J44 * TAN.PHI
3540                            J46 = COHES(SLICE%) + J45
3541                            J49 = (TAN.PHI * TAN.ALPHA) / F
3543                            J50 = 1 + J49
3545                            S = J46 / J50
3560                            J47 = S * DELT.X(SLICE%)
3565                            J70 = COS(ALPHA(SLICE%))
3566                            J71 = J70 * J70
3575                            SEC2.ALPHA = 1 / J71
3578                            J48 = J47 * SEC2.ALPHA
3586                            SUM1 = SUM1 + J48
3588                            J53 = J43 * TAN.ALPHA
3590                            SUM2 = SUM2 + J53
3600                    NEXT SLICE%
3660                    F = SUM1 / SUM2
3670                    PRINT LAST.F,F
3680                    SUM1=0 \
                        SUM2=0
3700            NEXT NO.TIMES%
3701            TOT.TIMES% = TOT.TIMES% + NO.TIMES%
3750            GOSUB 16000
3770    NEXT LOOP%
3799    RETURN



4100    !! CHECK STEP.F AND CALCULATE DT
4101    SLICE% = 1
4102    B=b+1
4103    SUM5 = 0
4104    SUM6 = 0
4111    PRINT 'STEP.F = ';STEP.F;'  F=  ';F
4120    IF ABS(STEP.F - F) < RANGE THEN
                VALUES = 'TRUE' \
                GOTO 16999
4140    VALUES = 'FALSE'
4200    FOR SLICE% = 1 TO NO.SLICES%
4205    J14 = 0
4206    J13 = 0
4210            IF OPS='A'THEN
                        J14 = J14 + (H(SLICE%,I%)*GAMMA(I%)) FOR I% = 1% TO NS% \
                        J15 = (J14 + DT(SLICE%)) / DELT.X(SLICE%)
4220            IF OPS='H'THEN
                        J13 = J13 + (H(SLICE%,I%)*GAMMA(I%)) FOR I% = 1% TO NS% \
                        J15 = J13 + (DT(SLICE%) / DELT.X(SLICE%))
4230            J16 = J15 * DELT.X(SLICE%)
4250            TAN.ALPHA = TAN(ALPHA(SLICE%))
4260            J22 = J16 * TAN.ALPHA
4280            U = Z(SLICE%) * 9.81
4290            J1 = J15 - U
4300            TAN.PHI = TAN(PHI(SLICE%))
4320            J2 = J1 * TAN.PHI
4340            J3 = COHES(SLICE%) + J2
4380            J8 = TAN.PHI * TAN.ALPHA
4400            J9 = J8 / F
4500            J10 = J9 + 1
4600            S2 = J3 / J10
4610            J23 = S2 * DELT.X(SLICE%)
4650            J24 = J23 / F
4680            J60 = COS(ALPHA(SLICE%))
4682            J61 = J60 * J60
4690            SEC2.ALPHA = 1 / J61
4700            J25 = J24 * SEC2.ALPHA
4750            DT(SLICE%) = J22 - J25
4850            IF SLICE% = 1 THEN
```

```
16340           J3 = COS(SLICE%) + J2
16380           J8 = TAN.PHI * TAN.ALPHA
16400           J9 = J8 / F
16500           J10 = J9 + 1
16600           S2 = J3 / J10
16610           J23 = S2 * DELT.X(SLICE%)
16650           J24 = J23 / F
16680           J60 = COS(ALPHA(SLICE%))
16682           J61 = J60 * J60
16690           SEC2.ALPHA = 1 / J61
16700           J25 = J24 * SEC2.ALPHA
16750           DE(SLICE%) = J22 - J25
16850           IF SLICE% = 1 THEN
                        E(SLICE%) = 0
                ELSE
                        E(SLICE%)= E(SLICE%-1) + DE(SLICE%-1)
16870           NEG1 = 0 - 1
16890           J26 = E(SLICE%) * NEG1
16895           IF B = 1 THEN
                        TAN.ALPHAT(SLICE%) = TAN(ALPHAT(SLICE%))
16905           J27 = J26 * TAN.ALPHAT(SLICE%)
16910           J28 = DE(SLICE%) / DELT.X(SLICE%)
16920           J29 = HT(SLICE%) * J28
16921           PRINT #1%, J29,J28,DE(SLICE%),HT(SLICE%),DELT.X(SLICE%),J22,J25
16930           T(SLICE%) = J27 + J29
16950           IF SLICE% = 1 THEN T(SLICE%) = 0 \ TAN.ALPHAT(SLICE%) = 0 \ GOTO 16990
16955           DT(SLICE% - 1) =T(SLICE%) - T(SLICE% - 1%)
16957           IF SLICE% = NO.SLICES% THEN DT(SLICE%) = (0 - T(SLICE%))
16960           TAN.ALPHAT(SLICE%) = T(SLICE%) / E(SLICE%)
16980           J50 = TAN(ALPHA(SLICE% - 1)) * DELT.X(SLICE% -1)
16981           J51 = TAN.ALPHAT(SLICE%) * DELT.X(SLICE% - 1)
16982           SUM5 = SUM5 + J50
16984           SUM6 = SUM6 + J51
16985           HT(SLICE%) = SUM5 - SUM6
16990   NEXT SLICE%
16995   STEP.F = F
16997   LAST.F = 0
16999   RETURN


17100   DEF FNPOS$(ROW,COL) = ES + 'Y' + CHR$(ROW + 32) + CHR$(COL + 32)


17200   DEF FND.R(A)
\       FND.R = A * (PI/180)
17220   FNEND

17300   DEF FNR.D(A)
\       FNR.D = A * (180/PI)
17320   FNEND

17400   DEF FNOP$
17401           IF OP$ = 'A' THEN FNOP$ = 'AREA'
                                ELSE FNOP$ = 'HEIGHT'
17402   FNEND


18000   !! CHECK INPUTED STRENGTH DATA
18020   IF FLAG1% = 1 THEN I% = SAV% \GOTO 5101
18040   IF FLAG1% = 2 THEN X% = SAV% \GOTO 6015


18999   GOTO 32700

19000   IF ERR=5% AND ERL = 5000% THEN
                RESUME 5020
19005   IF ERR = 5% AND ERL = 15020 THEN
                RESUME 15040
19010   IF ERR=5% AND ERL = 5090% THEN
                PRINT 'no such input file';CHR$(7%) \
                RESUME 5085
19040   IF ERR=50% AND ERL= 5094% THEN
                RESUME 5096
19060   IF ERR=50% AND ERL= 5096% THEN
                RESUME 5098
19080   IF ERR=11% AND ERL= 5088% THEN
                PRINT 'DATA READ IN SUCCESSFULLY' \
                X%=1000% \
                RESUME 5097%
19100   IF ERR=10% AND ERL=15020 THEN
                PRINT'PROTECTION VIOLATION -- IDIOT';STRING$(5%,7%) \
                SLEEP 2 \
                RESUME 15015
19120   IF ERR = 11% AND (ERL>5100 AND ERL<5140) OR (ERL>6008 AND ERL<6140)
        THEN RESUME 18000

19900   PRINT 'error';ERR;'at line'; \
        IF ERR=26% THEN
                PRINT LINE;
        ELSE
                PRINT ERL;
19920   PRINT CHR$(94)+'_______';RIGHT(SYS(CHR$(6%)+CHR$(9%)+CHR$(FRR)),3%)
19940   PRINT CHR$(7%) \
        SLEEP 3
19960   GOTO 32700


32700   ! end routine

32720   PRINT STRING$(24%,10%);STRING$(3%,9%);'bye -- bye';STRING$(10%,10%);STRING$(3%,7%)
32740   CLOSE 1%
32767   END
```

JOB = A Printed on 03-Apr-81 at 14:50 for User [45,9]
Copy 1 of 1 /Delete: YES File = SY :[45,9]JSITER.BAS
Record type: STREAM Format type: EMBEDDED

[[[<WAIKATO>#<WAIKATO>#<WAIKATO>#<WAIKATO>#<WAIKATO>#<WAIKATO>#<WAIKATO>#<WAIKATO>#<WAIKATO>#<WA
[[[<WAIKATO>#<WAIKATO>#<WAIKATO>#<WAIKATO>#<WAIKATO>#<WAIKATO>#<WAIKATO>#<WAIKATO>#<WAIKATO>#<WA

```
5       !!CALCULATES F USING JANBU SIMPLIFIED ANALYSIS. CAPACITY FOR 40 SOILS AND
!! 50 SLICES. OPTIONAL VARIABLES ARE GAMMA, Z, COHESION AND PHI. MUST RECORD MANUALLY
!! WHICH SLICES VARIABLES ARE ITERATED IN. WRITTEN BY G.BIRD 9/2/81.
10      EXTEND \
        ON ERROR GOTO 19000

20      DIM ALPHA(50),DELT.X(50),H(50,40),N(4,50)
23      DIM TERSE1%(30%)

50      ES=CHR$(155%)

1030    TERSET$ = SYS(CHR$(6%) + CHR$(16%) + CHR$(0%) + CHR$(255%)) \
        CHANGE TERSET$ TO TERSET%
1040    IF TERSET%(9%) = 255% AND (TERSET%(5%) = 81% OR TERSET%(5%) = 133%) THEN
                PRINT ES + '<';ES + '[?2l';
        ELSE            PRINT ES + '>';

5000    PRINT ES + 'H';ES + 'J';ES + '[' \
        INPUT 'output filename';OFILE$ \
        OPEN OFILE$ FOR INPUT AS FILE 1% \
        CLOSE 1% \
        PRINT 'the file already exists do you wish to overwrite <no>'; \
        INPUT A$ \
        IF LEFT(CVT$$(A$,36%),1%)<>'Y' GOTO 5000
5020    OPEN OFILE$ FOR OUTPUT AS FILE 1% \
        PRINT FNPOS$(1,0);ES + 'J';'output to ';OFILE$

5025    INPUT "PARAMETER OF INTEREST (NOMINATE ONE OF GAMMA, Z, C, PHI)"; A$
5026    PRINT #1, 'PARAMETER OF INTEREST IS '; A$

5060    PRINT FNPOS$(1,40);ES+'J';FNPOS$(3,0) \
        INPUT 'F0 ___ ';F0
5080    PRINT \
        INPUT 'DO YOU WISH TO USE "H" OR "AREA" __';A$ \
        IF LEFT(CVT$$(A$,36%),1%)='H' OR LEFT(CVT$$(A$,36%),1%)='A' THEN
                OP$ = LEFT(CVT$$(A$,36%),1%)
        ELSE GOTO 5080

5087    PRINT \
        INPUT 'DATA FILENAME';IFILE$ \
        OPEN IFILE$ FOR INPUT AS FILE 2%
5088    FOR X% = 1% TO 1000% \
                I%=X% \
                INPUT LINE #2%,A$\
                A$ = CVT$$(A$,8%)\
                A% = 0
5089            FOR J% = 1 UNTIL INSTR(A%,A$,',')=0
5090                    IF J% = 1 THEN DELT.X(I%) = VAL ( LEFT ( A$ , INSTR ( 1, A$, ',')-1))\ GOTO 5092
5091                    IF J% = 2 THEN ALPHA(I%) = FND.R(VAL ( MID(A$,A%,(INSTR(A%,A$,','))-A%)))
                        ELSE H(I%,J%-2) = VAL(MID(A$,A%,(INSTR(A%,A$,',')) - A%))
5092                    A% = INSTR(A%,A$,',') + 1
5093            NEXT J%
\               N(I%,J%-2)=VAL(RIGHT(A$,A%))
5094            IF I% = 1 THEN NS% = (J%-2)
\                               PRINT 'THE NUMBER OF SOILS FOUND WAS';NS%
5095    NEXT X%
5096    CLOSE 2% \
        NO.SLICES%=(I%-1)\
        PRINT 'THE NUMBER OF SLICES FOUND WAS';NO.SLICES%\
        SLEEP 2
5098    PRINT FNPOS$(0,0);ES + 'J';FNPOS$(2,40);'data from ';IFILE$;FNPOS$(6,0);

6110    FOR X% = 1% TO NO.SLICES% \
                FLAG1% = 2 \ SAV% = X%\
                PRINT FNPOS$(8,0);ES + 'J'; \
                PRINT 'SECTION'; X%
6111            INPUT 'cohesion ___ ';N(1,X%) \
                INPUT 'PHI ___ ';N(2,X%) \
                N(2,X%) = FND.R(N(2,X%))\
                INPUT 'Z _______ ';N(3,X%)
6112    NEXT X%

6120    PRINT FNPOS$(6,0);ES + 'J';
\       INPUT 'significance range <0.03> ___';RANGE \
        IF RANGE=0 THEN
                RANGE=0.03
6121    INPUT 'G ___ ';G

6122    FOR I% = 1 TO NS% \
                PRINT 'Gamma';I%;'___ ';\
                INPUT N(4,I%)
6123    NEXT I%
6124    PRINT #1%,,TIT$;STRING$(2,10)
\       H$ = CVT$$(FND$,32%)
\       PRINT #1%,'SLICE          COHESION      PHI          Z. '
6125    FOR I% = 1 TO NO.SLICES%
```

```
\       NEXT I%

6126    FOR I% = 1 TO NS%
\               PRINT #1%,'GAMMA';I%;' = 'N(4%,I%)'
\       NEXT I%


6150    PRINT '1 = COHESION   2 = PHI   3 = Z   4 = GAMMA'
\       INPUT 'DESIGNATE PARAMETER OF INTEREST'; SUB1%
6151    IF SUB1% = 3 GOTO 6190
6152    IF SUB1% = 4 GOTO 6201
6155    PRINT\INPUT 'START AT SLICE%';STPOINT%
\       INPUT 'END AT SLICE%';ENDPOINT%
\       IF ENDPOINT% < STPOINT% THEN PRINT 'IDIOT !!!!!!',CHR$(7)
\               GOTO 6155
6160    INPUT 'INITIAL VALUE OF PARAMETER';N(SUB1%,STPOINT%)
6170    INPUT 'INCREMENT TO PARAMETER'; SINC
6180    INPUT 'FINAL VALUE OF PARAMETER'; FINC
6181    IF SUB1% = 2 THEN N(SUB1%,STPOINT%) = FND.R(N(SUB1%,STPOINT%))
\                       SINC = FND.R(SINC)
\                       FINC = FND.R(FINC)
6182    N(SUB1%,SLICE%) = N(SUB1%,STPOINT%) FOR SLICE% = STPOINT% TO ENDPOINT%
6183    GOTO 6210

6190    PRINT\INPUT 'INCREMENT TO BE SUBTRACTED FROM Z';ZINC
\       STPOINT% = NO.SLICES%-1
6191    PRINT\INPUT 'NUMBER OF INCREMENTS';D
\       C=0
\       GOTO  6210
6192    PRINT #1%, E, '!' + SPACE$(XF%) + 'x' + SPACE$(80%-XF%) + '!      '; F
6194    C=C+1
\       E=C*ZINC
6195    FOR SLICE% = 1% TO NO.SLICES%
\               N(3,SLICE%)=N(3,SLICE%)-E
\               IF N(3,SLICE%)<0 THEN N(3,SLICE%)=0
\       NEXT SLICE%
6197    IF C<=D GOTO 6300
6200    GOTO 6600

6201    PRINT\INPUT 'INCREMENT AT SOIL ';STPOINT%
\       ENDPOINT% = STPOINT%
6202    PRINT\INPUT 'INITIAL VALUE OF GAMMA';N(SUB1%,STPOINT%)
6203    PRINT\INPUT 'VALUE OF INCREMENT';SINC
6204    PRINT\INPUT 'MAXIMUM VALUE OF GAMMA';FINC

6210    PRINT #1
6211    PRINT #1, 'VALUE OF PARAMETER                                        FACTOR OF SAFETY
ALUE OF F'
6212    PRINT #1, '              0                   1                   2                   3


6300    PRINT FNPOSS(8,0);ES + 'J';'PROCESSING'

6320    GOSUB 14000

6330    !!PRINTING SECTION
6331    XF = 20*F
6332    XF% = XF
\       IF SUB1% = 3 GOTO 6192
6333    PRINT #1, N(SUB1%,STPOINT%), '!' + SPACE$(XF%) + 'x' + SPACE$(80%-XF%) + '!           '; F
6510    LET N(SUB1%,SLICE%) = N(SUB1%,SLICE%) + SINC FOR SLICE% = STPOINT% TO ENDPOINT%
6520    IF N(SUB1%,SLICE%) <= FINC GO TO 6300
6600    CLOSE 1
6700    PRINT 'Computation completed'
6701    PRINT 'OUTPUT FILE IS ';OFILE$
6128    PRINT #1%,STRING$(3,10)
\       PRINT #1%,'THE SLICE SIZE DATA FILE IS ';IFILE$


11015   PRINT \
        PRINT
11017   INPUT 'Do you wish to end this session <yes>';a$
\       IF CVI$$(A$,36%) <> 'N' GOTO 32700
11020   PRINT\INPUT 'do you wish to change the cohesion,etc values<no>';A$
11040   IF LEFT$(CVI$$(A$,36%),1%)='Y' GOTO 6000
11060   PRINT \
        INPUT 'do you wish to change slice size data with output file unaltered <no>';A$
11080   IF LEFT$(CVI$$(A$,36%),1%)='Y' GOTO 5060
11140   PRINT \ input 'Do you wish to use another output file and new data<no>';a$
11160   IF LEFT$(CVI$$(A$,36%),1%)='Y' GOTO 5000

11999   GOTO 32700




14000   ! CALCULATE  the t calculation loop

14100   LAST.F=0 \
        SUM.1=0 \
        SUM.2=0 \
        F=1 \
        B = 1
14200   FOR NO.TIMES%= 1 UNTIL ABS(LAST.F-F)<RANGE
14220           IF B<>1 THEN
                        LAST.F=F
14300           FOR SLICE%= 1 TO NO.SLICES%
14310           A = 0
                P = 0
\               IF OP$ = 'A' THEN
                        W = W + (N(SLICE%,I%)*N(4,I%)) FOR I%= 1 TO NS%
\                       P = W / DELT.X(SLICE%)
14353           IF OP$ = 'M' THEN
                        P = P + (N(SLICE%,I%) * N(4,I%)) FOR  I% = 1 TO NS%
\                       A = P * DELT.X(SLICE%)
14360           U = N(3,SLICE%) * 9.81
```

```
            SUM.1=0 \
            SUM.2=0 \
            F=1 \
            B = 1
   14200    FOR NO.TIMES%= 1 UNTIL ABS(LAST.F-F)<RANGE \
   14220            IF B<>1 THEN
                            LAST.F=F
   14300            FOR SLICE%= 1 TO NO.SLICES%
   14310            W = 0
            \       P = 0
   14350            IF OP$ = 'A' THEN
                            W = W + (N(SLICE%,I%)*N(4,I%)) FOR I%= 1 TO NS%
            \               P = W / DELT.X(SLICE%)
   14353            IF OP$ = 'H' THEN
                            P = P + (N(SLICE%,I%) * N(4,I%)) FOR  I% = 1 TO NS%
            \               W = P * DELT.X(SLICE%)
   14360            U = N(3,SLICE%) * 9.81
   14400            J1 = P - U
   14450            J2 = J1 * TAN(N(2,SLICE%))
   14460            J3 = J2 + N(1,SLICE%)
   14480            J6 = (TAN(N(2,SLICE%))*TAN(ALPHA(SLICE%)))/F
   14500            J7 = J6 + 1
   14520            S = J3 / J7
   14550            J8 = S * DELT.X(SLICE%)
   14560            J50 = COS(ALPHA(SLICE%))
   14570            J51 = J50 * J50
   14580            SEC2.ALPHA = 1/J51
   14590            J9 = J8 * SEC2.ALPHA
   14600            SUM1 = SUM1 + J9
   14610            J11 = h * TAN(ALPHA(SLICE%))
   14620            SUM2 = SUM2 + J11
   14700            NEXT SLICE%
   14720            J12 = SUM2 + Q
   14740            J13 = SUM1 / J12
   14760            F = F0 * J13
   14780            SUM1=0 \
                    SUM2=0 \
                    B = B + 1
   14790            PRINT N(SUB1%,STPOINT%)
   14800    NEXT NO.TIMES%
   14999    RETURN


   17100    DEF FNPOS$(ROW,COL) = ES + 'Y' + CHR$(ROW + 32) + CHR$(COL + 32)

   17500    DEF FND.R(A)
            FND.R = A * (PI/180)
   17510    FNEND

   17600    DEF FNR.D(A)
            FNR.D = A * (180/PI)
   17610    FNEND

   18000    DEF FNOP$
   18001            IF OP$ = 'A' THEN FNOP$ = 'area'
                                 ELSE FNOP$ = 'height'
   18002    FNEND


   18003    !!CHECK INPUT STRENGTH DATA
   18020    IF FLAG1% = 1 THEN I% = SAV% \GOTO 5101
   18040    IF FLAG1% = 2 THEN I% = SAV% \GOTO 6110



   19000    IF ERR=5% AND ERL = 5000% THEN
                    RESUME 5020
   19005    IF ERR = 5% AND ERL = 15020 THEN
                    RESUME 15040
   19010    IF ERR=5% AND ERL = 5087% THEN
                    PRINT 'no such input file';CHR$(7%) \
                    RESUME 5085
   19080    IF ERR=11% AND ERL= 5088% THEN
                    PRINT 'DATA READ IN SUCCESSFULLY' \
                    A%=1000% \
                    RESUME 5096%
   19100    IF ERR=10% AND ERL=15020 THEN
                    PRINT'PROTECTION VIOLATION -- IDIOT';STRING$(5%,7%) \
                    SLEEP 2 \
                    RESUME 15015
   19120    IF ERR=11% AND (ERL>5100 AND ERL<5140) OR (ERL>6008 AND ERL<6140) THEN
                                RESUME 18003

   19900    PRINT 'error';ERR;'at line'; \
            IF ERR=28% THEN
                    PRINT LINE;
            ELSE
                    PRINT ERL;
   19920    PRINT CHR$(9%)+'_______';RIGHT(SYS(CHR$(6%)+CHR$(9%)+CHR$(ERR)),3%)
   19940    PRINT CHR$(7%) \
            SLEEP 3
   19960    GOTO 32700


   32700    ! end routine

   32720    PRINT STRING$(24%,10%);STRING$(3%,9%);'bye -- bye';STRING$(10%,10%);STRING$(3%,7%)
   32740    CLOSE 1%
   32767    END
```

REFERENCES

Akroyd, T.N.W. 1964: *Laboratory testing in soil engineering.* Soil Mechanics Ltd. 233p.

Aldridge, R.L. & Jackson, R.J. 1973: Interception of rainfall by hard beech (*Nothophagus truncata*) at Taita, New Zealand. *N.Z. Journal of Science*, 16(1), 185-198.

Anagnosti, P. 1967: Shear strength of soils other than clay. *Proceedings, Geotechnical Conference, Oslo*, Vol. 2, 73-76.

Arman, A.; Poplin, J.D. & Ahmad, N. 1975: Study of the vane shear. *Proceedings, Conference on in situ measurement of soil properties*, Vol. 1, 93-125. American Society of Civil Engineers.

A.S.C.E. 1960: *Proceedings, research conference on shear strength of cohesive soils, Boulder, Colorado.* Soil Mechanics and Foundations Division, American Society of Civil Engineers.

A.S.T.M. 1978: *Annual book of A.S.T.M. standards:* 19: *soil and rock; building stones; peats.* American Society for Testing and Materials, 560p.

Birrell, K.S. & Pullar, W.A. 1977: Weathering of the Rotoehu Ash in the Bay of Plenty district. *N.Z. Journal of Science*, 20, 303-310.

Bishop, A.W. 1955: The use of the slip circle in the stability analysis of slopes. *Geotechnique*, 5(1), 7-17.

Bishop, A.W. 1966: The strength of soils as engineering materials. Sixth Rankine lecture. *Geotechnique*, 16(2), 91-128.

Bishop, A.W. & Elden, G. 1950: Undrained triaxial tests on saturated sands and their significance in the general theory of shear strength. *Geotechnique*, 2(1), 13-21.

Bishop, A.W. & Henkel, D.J. 1962: *The measurement of soil properties in the triaxial test.* 2nd ed. Edward Arnold. 227p.

Blakeley, J.P. 1974: Determination of relevant information for the assessment of the stability of soil slopes. *Proceedings, Symposium on stability of slopes in natural ground.* N.Z. Institution of Engineers. Vol. 1(5).

Boutrup, E., Lovell, C.W. & Siegel, R.A. 1979: STABL2: A computer program for general slope stability analysis. *Proceedings, Third international conference on numerical methods in geomechanics, Aachen.* 747-57.

Boutrup, E. & Lovell, C.W. 1980: Searching techniques in slope stability analysis. *Engineering Geology*, 16(1/2), 51-61.

Bridson, J.D. 1981: *The effects of an extreme meteorological event on sediment production in a small steepland catchment, South Auckland, N.Z.* Unpublished thesis, held at University of Waikato, 148p.

Bromhead, E.N. 1978: Large landslides in London Clay at Herne Bay, Kent. *Quarterly Journal of Engineering Geology*, 11(4), 291-305.

Bromhead, E.N. 1979: Factors affecting the transition between the various types of mass movement in coastal cliffs consisting largely of over-consolidated clay, with special reference to southern England. *Quarterly Journal of Engineering Geology*, 12(4), 291-300.

Brothers, R.N. 1954: The relative Pleistocene chronology of the South Kaipara district, N.Z. *Transactions, Royal Society of N.Z.*, 82, 677-694.

Brown, E.H. & Waters, R.S. 1974: *Progress in geomorphology.* Institution of British Geographers. 255p.

Brunsden, D. & Jones, D.K.C. 1980: Relative time scales and formative events in coastal landslide systems. *Zeitschrift fur Geomorphologie. SB*34, 1-19.

Bryan, R.B. & Price, A-C. 1980: Recession of the Scarborough Bluffs, Ontario, Canada. *Zeitschrift fur Geomorphologie. SB*34, 48-62.

Capper, P.L. & Cassie, W.F. 1976: *The mechanics of engineering soils.* Spon. 376p.

Carson, M.A. & Kirkby, M.J. 1972: *Hillslope form and process.* Cambridge University Press. 475p.

Carter, R.K. 1971: *Computer oriented slope stability analysis by method of slices.* Unpublished thesis, held Purdue University, Indiana. 120p.

Chandler, M.P. & Rogers, N.W. 1978: *Triaxial and direct shear strength testing.* Unpublished Geomechanics Manual No. 1, University of Waikato, 73p.

Chappell, J. 1975: Upper Quaternary warping and uplift rates in the Bay of Plenty. *N.Z. Journal of Geology and Geophysics*, 18(1), 129-155.

Chorley, R.J. 1978: Bases for theory in geomorphology. *In* Embleton, C.; Brunsden, D. & Jones, D.K.C. (eds.) 1978: *Geomorphology: present problems and future prospects.* Oxford University Press. 281p.

Chowdhury, R.N. 1978: *Slope analysis.* Elsevier. 423p.

Coates, D.R. (ed.) 1976: *Geomorphology and engineering.* Dowden, Hutchinson & Ross. 360p.

Cooke, R.U. & Doornkamp, J.C. 1974: *Geomorphology in environmental management.* Clarenden Press. 413p.

Cotton, C.A. 1958: Fine Textured erosional relief in N.Z. *Zeitschrift fur Geomorphologie*, 2(3), 187-210.

Cotton, C.A. 1969: Marine cliffing according to Darwin's theory. *Transactions of the Royal Society of N.Z.*, 6(14), 187-208.

Cox, S.H. 1877: Report on the country between Opotoki and East Cape. *Reports on Geological Exploration, N.Z. Geological Survey (1876-77)* 10, 105-113.

Daji, M. 1979: *Landslides on recently deforested mudrock slopes in the Taumaranui County, N.Z.* Unpublished thesis, held University of Waikato. 146p.

Darwin, C. 1891: *Geological observations.* 3rd ed. Smith Elder. 664p.

Davidson, C.F. 1965: *Mass movement on the Gisborne coastline.* Unpublished thesis, held Canterbury University. 77p.

Davies-Colley, R.J. 1976: *Sediment dynamics of Tauranga Harbour and the Tauranga inlet.* Unpublished thesis, held University of Waikato. 148p.

de Lisle, J.F. 1962: Climate and Weather. *in National Resources Survey Part II: Bay of Plenty region.* Town & Country Planning Branch, Ministry of Works. 45-56.

Drost, H. & Pittams, R.J. 1973: Interim report. *in NWASCO hydrological research: Annual report 27.*

Duncan, J.M. & Wright, S.G. 1980: The accuracy of equilibrium methods of slope analysis. *Engineering Geology,* 16(1/2), 5-17.

East, G.R. 1974: Inclined plane slope failures in the Auckland Waitemata soils. *in Proceedings, symposium on the stability of slopes in natural ground.* N.Z. Institution of Engineers, 1(5), 5.17-5.35.

Embleton, C.; Brunsden, D. & Jones, D.K.C. 1978: *Geomorphology: present problems and future prospects.* Oxford University Press. 281p.

ESOPT 1974: *Proceedings, European symposium on penetration testing, Stockholm.* Vol. 1. ESOPT.

Folk, R.L.; Andrews. P.B. & Lewis, D.W. 1970: Detrital sedimentary rock classification and nomenclature for use in N.Z. *N.Z. Journal of Geology and Geophysics,* 13(4), 937-68.

Fredlund, D.G. & Krahn, J. 1977: Comparison of slope stability methods of analysis. *Canadian Geotechnical Journal,* 14, 429-39.

Gelinas, P.J. & Quigley, R.M. 1973: The influence of geology on erosion rates along the north shore of Lake Erie. *Proceedings, 16th conference on Great Lakes research,* 421-430.

Gibb, J.G. 1979: A coastal landslide. *Soil and Water, Oct. 1979,* 20-21.

Gibbs, H.S. & Pullar, W.A. 1961: Soils of the Bay of Plenty. *Proceedings, The N.Z. Grassland's Association conference,* 23, 1-12.

Green, P.A. & Ferguson, P.A.S. 1971: On liquefaction phenomena, by Professor A. Casagrande: Report of lecture. *Geotechnique*, 21(2), 197-202.

Gulliver, C.P. & Houghton, B.F. 1980: *Omokoroa Point land stability investigation.* Unpublished report prepared for Tauranga City Council by Tonkin and Taylor, consulting engineers.

Hails, J.R. (ed.) 1977: *Applied geomorphology.* Elsevier. 418p.

Harvey, D. 1969: *Explanation in geography.* Arnold. 521p.

Hawley, J.G. & Northey, R.D. 1981: Laboratory permeability tests with annular seals. Preprint, *International Society of Soil Mechanics and Foundation Engineering Conference.*

Healy, J.; Schofield, J.C. & Thompson, B.N. 1964: *Geological Map of N.Z.: Sheet 5, Rotorua.* 1:250,000. DSIR.

Healy, J.; Vucetich, C.G. & Pullar, W.A. 1964: Stratigraphy and chronology of late Quaternary volcanic ash in Taupo, Rotorua and Gisborne districts. *N.Z. Geological Survey bulletin 73 (n.s.).* 87p.

Healy, T.R.; Harray, K.G. & Richmond, B. 1977: Bay of Plenty coastal erosion survey. *Occasional report 3, University of Waikato, Department of Earth Sciences.* 22p.

Henderson, J. & Bartrum, J.A. 1913: The geology of the Aroha subdivision. *Geological Survey Bulletin 16 (n.s.).* 127p.

Hoek, E. & Bray , J.W. 1977: *Rock slope engineering. 2nd ed.* Institute of mining and metallurgy. 402p.

Hogg, A.G. 1979: Identification and correlation of thinly bedded late Quaternary tephras of Coromandel Peninsula, N.Z. *Unpublished thesis, held University of Waikato.* 333p.

Hovland, H.J. 1977: 3 dimensional slope stability analysis method. *ASCE Vol. 103, GT9,* 971-988.

Hutchinson, J.N. 1965: The stability of cliffs composed of soft rocks with particular reference to the coasts of south eastern England. *Unpublished thesis, held University of Cambridge.*

Huthinson, J.N. 1973: The response of London Clay cliffs to differing rates of toe erosion. *Geologica Applicata e Idrogeologia* 8, 221-239.

Hutchinson, J.N.; Bromhead, E.N. & Lupini, J.F. 1980: Additional observations on the Folkestone Warren landslides. *Quarterly Journal of Engineering Geology*, 13(1), 1-32.

Janbu, N.; Bjerrum, L. & Kjaernsli, B. 1956: Soil mechanics applied to some engineering problems. *Norwegian Geotechnical Institute publication 16.*

Johnson, D.W. 1919: *Shore processes and shoreline development.* Wiley. 602p.

Jones, D.K. 1980: British applied geomorphology: an appraisal. *Zeitschrift fur Geomorphologie SB*36, 48-73.

Kayes, T.J. 1974: Analysis of natural earth slope instability under static loading. *in Proceedings, symposium on stability of slopes in natural ground.* N.Z. Institution of Engineers, 1(5).

Kear, D. & Schofield, J.C. 1978: Geology of the Ngaruawahia Subdivision. *N.Z. Geological Survey Bulletin 88 (n.s.).* 168p.

Kear, D. & Waterhouse, B.C. 1961: Quaternary surfaces and sediments at Waihi Beach. *N.Z. Journal of Geology and Geophysics*, 4(4), 434-445.

Kear, D. & Waterhouse, B.C. 1971: Further comments: Waihi Terrace and Hamilton Ash ages. *Earth Science Journal*, 5(2), 114-115.

Keat, R. & Urry, J. 1975: *Social theory as science.* Routledge and Kegan Paul. 278p.

Keller, E.A. 1979: *Environmental geology.* 2nd ed. Merril. 548p.

Kezdi. A. 1980: *Handbook of soil mechanics: Volume 2: Soil testing.* Elsevier. 258p.

Kilgour, J.; Meloche, L. & Lalonde, F. 1976: Bluff erosion and instability. *Proceedings, 29th Canadian geotechnical conference.*

Kirkman, J.H. & Pullar, W.A. 1978: Halloysite in late Pleistocene rhyolitic tephra beds near Opotiki, coastal Bay of Plenty, North Island, N.Z. *Australian Journal of Soil Research*, 16(1), 1-8.

Kraft, V. 1953: *The Vienna circle.* Springer-Verlag. 168p.

Lambe, T.W. 1973: Up to date methods of investigating the strength and deformability of soils. *Proceedings, 8th international congress on soil mechanics and foundation engineering.* 3-43.

Lambe, T.W. & Whitman, R.V. 1979: *Soil mechanics; S.I. version.* Wiley. 553p.

Lapin, L.L. 1975: *Statistics: meaning and method.* Harcourt, Brace and Jovanovich. 591p.

Law, C.C. 1980: A geomechanical investigation into the origin of the amphitheatre basins in the Maungakawa range. *Unpublished thesis, held University of Waikato.*

Law, C.C. 1980: *Computer programs in geomechanics.* Unpublished Geomechanics Manual No. 5, University of Waikato.

Lohnes, R.A. & Handy, R.L. 1968: Slope angles in friable loess. *Journal of Geology*, 76, 247-258.

Mark, D.M. 1980: On scales of investigation in geomorphology. *Canadian Geographer*, 24(1), 81-2.

Mason, B. 1966: *Principles of geochemistry.* 3rd ed. Wiley. 329p.

McGreal, W.S. 1979: Factors promoting coastal slope instability in south-east County Down, Northern Ireland. *Zeitschrift fur Geomorphologie*, 23(1), 76-90.

McLean, R.F. & Davidson, C.F. 1968: The role of mass movement in shore platform development along the Gisborne coastline, N.Z. *Earth Science Journal.* 2(1), 15-25.

Mitchell, J.K. 1976: *Fundamentals of soil behaviour.* Wiley. 422p.

Nairn, I.A. 1972: Rotoehu Ash and the Rotoiti Breccia formation, Taupo volcanic zone, N.Z. *N.Z. Journal of Geology and Geophysics*, 15(2), 251-262.

Nash, D. 1980: Forms of bluffs degraded for different lengths of time in Emmet County, Michigan, USA. *Earth Surface Processes*, 5(4), 331-345.

Nelson, C.S. & Cochrane, R.H.A. 1970: A rapid X-ray method for the quantitative determination of selected minerals in fine grained and altered rocks. *Tane* (16), 151-162.

Norrman, J.P. 1980: Coastal erosion and slope development in Surtsey Island, Iceland. *Zeitschrift fur Geomorphologie, SB*34, 20-38.

Odenstad, S. 1951: The landslide at Sköttorp on the Lidan River. *Proceedings, Royal Swedish Geotechnical Institute, No. 4.*

Peck, R.B. 1967: Stability of natural slopes. *ASCE, Journal of the Soil Mechanics and Foundations Division*, 93(4), 419-436.

Pender, M.J. 1979: Probabilistic assessment of the stability of a cut slope.

Perrot, K.W.; Smith, B.F.L. & Inkson, R.H.E. 1976: The reaction of flouride with soils and soil minerals. *Journal of Soil Science*, 27(1), 58-67.

Petterson, K.E. 1955: The early history of circular sliding surfaces. *Geotechnique*, 5(1), 4-22.

Prior, D.B. & Ho, C. 1972: Coastal and mountain slope instability on the islands of St. Lucia and Barbados. *Engineering Geology*, 6(1), 1-10.

Prior, D.B. & Eve, R.M. 1973: Coastal landslide morphology at Røsnaes, Denmark. *Geografisk Tidsskrift*, 74, 12-20.

Prior, D.B. & Renwick, W.H. 1980. Landslide morphology and processes on some coastal slopes in Denmark and France. *Zeitschrift fur Geomorphologie, SB*34, 63-86.

Pullar, W.A. 1972: Thickness (metres) of cover deposits, Rotorua sheet, N.Z. *N.Z. Soil Bureau, map* 132/1.

Pullar, W.A. 1973: Age and distribution of basal tephra marker beds, Rotorua sheet, N.Z. *N.Z. Soil Bureau report 1, map* 131/1.

Pullar, W.A. & Cowie, J.D. 1967: Morphology of subfulvic and related soils in dunelands of Mt. Maunganui, Bay of Plenty. *N.Z. Journal of Science*, 10, 180-189.

Pullar, W.A. & Birrell, K.S. 1973: Age and distribution of late Quaternary pyroclastic and associated cover deposits of the Rotorua-Taupo area, North Island, N.Z. *N.Z. Soil Survey report 1, part 1.*

Pullar, W.A.; Birrell, K.S. and Heine, J.C. 1973: Named tephras and tephra formations occurring in the central North Island, with notes on derived soils and paleosols. *N.Z. Journal of Geology and Geophysics*, 16(3), 497-518.

Quigley, R.M. & Gelinas, P.J. 1976: Soil mechanics aspects of shoreline erosion. *Geoscience Canada*, 3(3), 169-173.

Quigley, R.M.; Gelinas, P.J.; Bou, W.T. & Packer, R.W. 1976: Cyclic erosion - instability relationship, Lake Erie, Canada. *in Proceedings, 29th Geotechnical Conference of Canada.* Part 2.

Quigley, R.M. & Di Nardo, L.R. 1980: Cyclic instability modes of eroding clay bluffs. *Zeitschrift fur Geomorphology, SB*34, 39-47.

Rogers, N.W. 1978: *The nature and causes of shallow translational landslides in the Hapuakohe Range, North Island, N.Z.* Unpublished thesis, held University of Waikato.

Roscoe, K.H. & Poorooshasb, H.B. 1963: Theoretical and experimental study of strains in triaxial compression tests on normally consolidated clays. *Geotechnique*, 13, 12-38.

Sauvigear, R.A. 1952: Some observations on slope development in South Wales. *Transactions, Institute of British Geographers*, 18, 31-52.

Schmertman, J.H. 1976: Measurement of *in situ* shear strength. *Proceedings, conference on in situ measurement of soil properties, Vol.* 2, 57-138.

Schofield, J.C. 1968: Dating of recent low sea level and Maori rock carvings, Ognari Point. *Earth Science Journal*, 2(2), 167-74.

Schuster, R.L. 1978: Introduction to landslides. *in* Schuster, R.L. & Krizek, R.J. (eds.) 1978: *Landslides: analysis and control.* National Academy of Sciences. 234p.

Schuster, R.L. & Krizek, R.J. (eds.) 1978: *Landslides: analysis and control.* National Academy of Sciences. 234p.

Schwartz, M.L. 1968: The scale of shore erosion. *Journal of Geology*, 26, 508-517.

Selby, M.J. 1966: Some slumps and boulderfields near Whitehall. *Journal of Hydrology* (N.Z.), 5(2), 35-44.

Selby, M.J.; Pullar, W.A. & McCraw, J.D. 1971: The age of Quaternary surfaces at Waihi Beach. *Earth Science Journal*, 5(2), 106-113.

Sharpe, C.F. 1950: *Landslides and related phenomena.* Columbia University Press. 137p.

Skempton, A.W. 1964: Long term stability of clay slopes. Fourth Rankine lecture. *Geotechnique*, 14(2), 75-101.

Skempton, A.W. & Bishop, A.W. 1950: The measurement of the shear strength of soils. *Geotechnique*, 2(2), 90-108.

Skempton, A.W. & Hutchinson, J.N. 1969: Stability of natural slopes and embankment foundations. *Proceedings, 7th international conference on soil mechanics and foundation engineering, Mexico City. State-of-the art volume*, 291-340.

Smalley, I.J. 1976: Factors relating to the landslide process in Canadian quickclays. *Earth Surface Processes*, 1, 163-172.

Smalley, I.J.; Ross, C.W. & Whitton, J.S. 1980: Clays from N.Z. support the inactive particle theory of soil sensitivity. *Nature*, 288 (576-7).

Söderblom, R. 1975: A new approach to the classification of quick clays. *Swedish Geotechnical Institute reprints and preliminary reports*, 55.

Sowers, G.B. & Sowers, G.F. 1961: *Introductory soil mechanics and foundations.* 2nd ed. Macmillan. 386p.

Spencer, E. 1967: A method of analysis for stability of embankments using parallel interslice forces. *Geotechnique*, 17(1). 11-26.

Spencer, E. 1973: The thrustline criterion in embankment stability analysis. *Geotechnique*, 23, 85-101.

Spörli, K.B. 1978: Mesozoic tectonics, North Island, N.Z. *Geological Society of America, Bulletin.* 89, 415-425.

Standards Association of N.Z. 1980: *Methods of testing soils for civil engineering purposes. Part 1; Soil classification and chemical tests.* SANZ. 91p.

Steel, R.G.D. & Torrie, J.H. 1960: *Principles and procedures of statistics.* McGraw-Hill. 481p.

Sunamura, T. 1973: Coastal cliff erosion due to waves: field investigations and laboratory experiments. *Journal of the Faculty of Engineering, University of Tokyo,* 32(1), 86.

Tauranga City Council 1979: *Report on damage caused by the March 19-21st storm, 1979.* Unpublished report, held T.C.C.

Tavenas, F.A. 1971: Discussion to de Mello (1971), *Fourth Pan American conference on soil mechanics and foundation engineering, Puerto Rico.* Vol. 3, 64-69.

Tavenas, F.; Trak, B. & Leroueil, S. 1980: Remarks on the validity of stability analyses. *Canadian Geotechnical Journal,* 17(1), 61-73.

Taylor, D.K.; Hawley, J.G. & Riddolls, B.W. 1977: Slope stability in urban development. *DSIR information series,* 122. 71p.

Terzaghi, K. 1944: Ends and means in soil mechanics. *Engineering Journal (Canada),* 27, 608-615.

Terzaghi, K. & Peck, R.B. 1967: *Soil mechanics in engineering practice.* Wiley. 729p.

Towner, G.D. 1973: An examination of the fall-cone method for the determination of some strength properties of remoulded agricultural soils. *Journal of Soil Science,* 24(4), 470-479.

Varnes, D.J. 1975: Slope movements in the western United States. *Mass Wasting, Geo Abstracts, Norwich,* 1-17.

Voight, B. (ed.) 1978: *Rockslides and avalanches, 1.* Elsevier. 833p.

Voight, B. (ed.) 1979: *Rockslides and avalanches, 2.* Elsevier. 850p.

Vucetich, C.G. and Kohn, B.P. 1980: Upper Quaternary tephra correlation, C 40 kyr to C 300 kyr. *Victoria University tephra workshop, preprint.*

Wallingford Hydraulics Research Station 1963: *Tauranga Harbour investigation, report on first stage.* Report EX20;. 69p.

Wellman, H.W. 1962: Holocene of the North Island of N.Z., a coastal reconnaissance. *Transactions, Royal Society of N.Z.*, 88, 29-99.

White, J. 1979: *Recent sediments of the Waikareao Estuary.* Unpublished thesis, held University of Waikato. 197p.

Whitman, R.V. & Bailey, W.A. 1967: Use of computers for slope stability analysis. *American Society of Civil Engineers*, 93, SM4, 475-498.

Wilun, Z. & Starzewski, K. 1972a: *Soil mechanics in foundation engineering; properties of soils and site investigations.* London Intertext Books, 1. 252p.

Wilun, Z. & Starzeuski, K. 1972b: *Soil mechanics in foundation engineering; theory and practice.* London Intertext Books, 2. 222p.

Wright, S.G. 1969: *A study of slope stability and the undrained shear strength of clay shales.* Unpublished thesis, held University of California, Berkely. 128p.

Wright, S.G. 1975: Evaluation of slope stability analysis procedures. *Proceedings, American Society of Civil Engineers national convention, Denver (Colorado).* 28p.

Wright, S.G.; Kulhawy, E.D. & Duncan, J.M. 1973: Accuracy of equilibrium slope stability analyses. *Journal of the soil mechanics and foundations division, American Society of Civil Engineers*, 99, SM10, 783-793.

Wroth, C.B. & Wood, O.M. 1978: Correlation of index properties with some basic engineering properties of soils. *Canadian Geotechnical Journal*, 15(2), 137-145.

Yong, R.N. & Warkentin, B.P. 1975: *Soil properties and behaviour.* Elsevier. 449p.

Zaruba, Q. & Mencl, V. 1969: *Landslides and their control.* Elsevier. 205p.

ADDENDUM

Kezdi, A. 1979: *Soil physics: selected topics*. Elsevier. 150p.